

UNIVERSIDAD DE GRANADA

PROGRAMA OFICIAL DE DOCTORADO

EN NUTRICIÓN HUMANA



International PhD Thesis:

Biological implications of insulin resistance signalling, inflammation and extracellular matrix genes in human adipose tissue-derived mesenchymal stem cell cultures

“Implicaciones biológicas de genes de vías de señalización de insulina, inflamación y matriz extracelular en cultivos de células madre mesenquimales derivadas de tejido adiposo humano”

Francisco Javier Ruiz Ojeda

Granada, 2016

Autor: Universidad de Granada. Tesis Doctorales

Editor: Francisco Javier Ruíz Ojeda

ISBN: 978-84-9163-034-0

URI: <http://hdl.handle.net/10481/44294>

UNIVERSIDAD DE GRANADA

DEPARTAMENTO DE BIOQUÍMICA Y BIOLOGÍA
MOLECULAR II FACULTAD DE FARMACIA

INSTITUTO DE NUTRICIÓN Y TECNOLOGÍA DE LOS
ALIMENTOS “JOSÉ MATAIX”

Implicaciones biológicas de genes de vías de señalización de insulina, inflamación y matriz extracelular en cultivos de células madre mesenquimales derivadas de tejido adiposo humano

Tesis Doctoral con Mención Internacional presentada por:

Francisco Javier Ruiz Ojeda

Bajo la dirección de los doctores:

Ángel Gil Hernández

Concepción M. Aguilera García



Bioquímica y
Biología Molecular



Granada, 2016

El doctorando Francisco Javier Ruiz Ojeda y los directores de la tesis Ángel Gil Hernández y Concepción María Aguilera García, garantizamos, al firmar esta tesis doctoral, que el trabajo ha sido realizado por el doctorando bajo la dirección de los directores de la tesis y hasta donde nuestro conocimiento alcanza, en la realización del trabajo, se han respetado los derechos de otros autores a ser citados, cuando se han utilizado sus resultados o publicaciones.

Granada,

Director/es de la Tesis

Doctorando

Fdo.:

Fdo.:

Ángel Gil Hernández

Francisco Javier Ruiz Ojeda

Concepción María Aguilera García

Ángel Gil Hernández, Catedrático del Departamento de Bioquímica y Biología Molecular II de la Universidad de Granada.

CERTIFICA

Que la Tesis Doctoral titulada “IMPLICACIONES BIOLÓGICAS DE GENES DE VÍAS DE SEÑALIZACIÓN DE INSULINA, INFLAMACIÓN Y MATRIZ EXTRACELULAR EN CULTIVOS DE CÉLULAS MADRE MESENQUIMALES DERIVADAS DE TEJIDO ADIPOSEO HUMANO”, de la que es autor Don Francisco Javier Ruiz Ojeda, ha sido realizada bajo mi dirección y asesoramiento y reúne las condiciones y calidad científica deseadas para ser presentada por el interesado para optar al grado de Doctor con mención internacional.

Y para que conste y surta los efectos oportunos, firmo el presente certificado en Granada,

Concepción María Aguilera García, Profesora titular del Departamento de Bioquímica y Biología Molecular II de la Universidad de Granada.

CERTIFICA

Que la Tesis Doctoral titulada “IMPLICACIONES BIOLÓGICAS DE GENES DE VÍAS DE SEÑALIZACIÓN DE INSULINA, INFLAMACIÓN Y MATRIZ EXTRACELULAR EN CULTIVOS DE CÉLULAS MADRE MESENQUIMALES DERIVADAS DE TEJIDO ADIPOSO HUMANO”, de la que es autor Don Francisco Javier Ruiz Ojeda, ha sido realizada bajo mi dirección y asesoramiento y reúne las condiciones y calidad científica deseadas para ser presentada por el interesado para optar al grado de Doctor con mención internacional.

Y para que conste y surta los efectos oportunos, firmo el presente certificado en Granada,

Alberto Vargas Morales, Catedrático y Director del Departamento de Bioquímica y Biología Molecular II de la Universidad de Granada

CERTIFICA

Que la Tesis Doctoral titulada “IMPLICACIONES BIOLÓGICAS DE GENES DE VÍAS DE SEÑALIZACIÓN DE INSULINA, INFLAMACIÓN Y MATRIZ EXTRACELULAR EN CULTIVOS DE CÉLULAS MADRE MESENQUIMALES DERIVADAS DE TEJIDO ADIPOSO HUMANO”, de la que es autor Don Francisco Javier Ruiz Ojeda ha sido realizado en las instalaciones del Instituto de Nutrición y Tecnología de los Alimentos, Centro de Investigación Biomédica, Universidad de Granada, donde están ubicados los laboratorios del grupo de investigación CTS-461 Bioquímica Nutricional: Implicaciones terapéuticas, perteneciente a este Departamento.

Y para que conste y surta los efectos oportunos, firmo el presente certificado en Granada,

Table of contents

Acknowledgments	1
Grants and fundings	5
List of publications and congress communications	7
Summary	11
Resumen	25
Introduction	37
Obesity prevalence	39
Etiology of obesity	41
Adipose tissue and adipocyte biology	43
Hyperplasic and hypertrophic adipocytes	45
Adipogenesis process	47
Obesity and natriuretic peptides	49
Obesity, oxidative stress and inflammation	52
Aims of the study	59
Background and justification	61
Hypothesis	63
Aims	63
General aim	63
Specific aims	64
Materials and methods	65
Materials	67
Cell culture	68
Oil Red O staining assay	68
Experiments for the study of NPR3 using C-ANP ₄₋₂₃ as synthetic ligand	69
Experiments for the study of CAT using the inhibitor 3-amine-1,2,4-triazole (3-AT)	70
Intracellular cAMP and cGMP level determination	71
Protein kinase A (PKA) determination	71
Lipolysis assay	71
Catalase activity assay	72

Intracellular H ₂ O ₂ determination	73
Superoxide dismutase and glutathione peroxidase activities assays	73
GSH/GSSG ratio detection assay	74
Quantitation of intracellular IL-6 protein levels	74
Glucose uptake assays	75
RNA isolation and qRT-PCR	75
Western blot assays	81
Statistical analysis	82
Results	83
Chapter 1. Literature review. Cell Models and Their Application for Studying Adipogenic Differentiation in Relation to Obesity: A Review	85
Abstract	87
Introduction	87
Methodology	88
Animal cell models	88
3T3-L1 mouse cell line	89
3T3-F442A mouse cell line	91
OP9 mouse cell line	92
C3H10T1/2 mouse cell line	93
Primary Mouse Embryonic Fibroblasts (MEFs)	93
Porcine primary preadipocytes	94
Feline primary preadipocytes	95
Human cell models	95
Adipose-derived stem cells (ASCs)	96
Primary preadipocytes	96
Brow/beige adipose cell lines	98
Primary cell models of browning	98
Brown/beige differentiated adipocytes	100
Cell lines representative of various diseases	100
Simpson-Golabi-Behemil Syndrome (SGBS) cells	100
LiSa-2 cells	101
Co-cultures and Three-Dimensional cultures (3D)	101

Conclusions	102
Acknowledgments	103
Author contributions	103
Conflicts of interest	103
References	103
Chapter 2. Results. An analogue of atrial natriuretic peptide (C-ANP₄₋₂₃) modulates glucose metabolism in human differentiated adipocytes	115
Abstract	115
Introduction	115
Material and Methods	116
Results	117
Discussion	118
Conflicts of interest	120
Acknowledgments	121
Supplementary data	122
References	122
Chapter 3. Results. Impact of 3-Amino-1,2,4-Triazole (3-AT)-Derived Increase in Hydrogen Peroxide Levels on Inflammation and Metabolism in Human Differentiated Adipocytes	123
Abstract	125
Introduction	126
Material and Methods	127
Results	131
Discussion	135
Conclusions	140
Limitations	140
Supporting information	140
Acknowledgments	141
Conflicts of interest	141
References	141
Discussion	147

Conclusions	159
Conclusiones	163
Future perspectives	167
References	171
Appendix	185
Supplementary data	187
Abbreviations	191
List of Figures and tables	194
Additional publication	195
<i>Curriculum vitae</i>	213

Acknowledgements

Han pasado ya cuatro años desde que empecé una de las etapas más importantes de mi carrera profesional y creo que es el momento de agradecer a todas aquellas personas que han formado parte de ello. En primer lugar, quiero dar las gracias a mi familia, en especial a mis padres y hermanos por todo el gran apoyo durante este tiempo y, también, a mis tíos y primos que sé que están ahí; así como a los que se fueron en el camino, a mi abuelo.

Queridos directores, es un orgullo llevar vuestro nombre como líderes de este trabajo. Chiqui, muchas gracias por confiar en mí desde el primer momento. Me alegro mucho de nuestra relación profesional y de amistad que hemos alcanzado. Sé que al principio no fue fácil, pero creo que nuestra sinceridad nos ha unido cada vez más y, a día de hoy, me siento muy orgulloso de que seas mi directora de tesis. Ángel, muchas gracias por ser cómo eres, por tu sabiduría, amabilidad, sencillez y por confiar en mí. Carolina, quiero agradecerte tu esfuerzo incondicional desde el primer momento. Aunque a nivel administrativo no pudieses formar parte de la dirección de la Tesis, eres y serás parte de ella, ya que sin tu ayuda no habría salido parte de éste trabajo, gracias. Por último y no menos importante, agradecer a Azahara su ayuda desde el primer día. Me ha encantado trabajar contigo, eres buena, eficaz, eficiente y me corriges el inglés jaja, muchas gracias por todo. Y, en general, muchas gracias al equipo excelencia que es el que ha formado la dirección del trabajo.

Quiero dar las gracias a todas aquellas personas que han formado parte de mi trabajo de tesis durante este tiempo, ya que muchas de ellas puede que sean de las personas con las que más horas al día he pasado:

A Mari Cruz, mi secretaria personal e intransferible, gracias por tu compañerismo y amistad, porque siempre estás ahí y me encanta llegar por las mañanas y charlar contigo diez minutos (y bien que lo sufrí en Canadá...). Belensita, relájate, que ya mismo acabas tu también...Me ha gustado mucho compartir esta etapa contigo, eres una buena compañera y amiga. Del mismo modo con Estefanía, por esos buenos momentos tanto en el centro como en los

congresos, espero que pronto salga todo adelante. Carolina, fue un placer volver a coincidir contigo en nuestra etapa predoctoral tras diez años conociéndonos en nuestra vida académica, ahora te deseo lo mejor en tu nueva etapa.

Julio, amigo, quiero agradecer toda tu ayuda incondicional mostrada hacia mí desde que me conoces. Ha sido un placer conocerte, integrarte en mi círculo, formar parte de tu boda con Belén y que las fiestas de mi pueblo te hayan dejado huella. A pesar de estar en dos líneas diferentes, hemos conseguido sin aparcarnos nuestras tareas, trabajar juntos.

Gracias a todos los compañeros del INYTA-CIBM (Luis, Cándido, María José Sáez, María Dolores Mesa, Susana, María José Soto, Miguel FINUT, Óscar, Josune, Jesús, Jerónimo, Casuso; y a los que también formaron parte en el pasado como Jesús Alcalá, Vivi, Laura, Belén y Miriam). Del mismo modo quiero agradecer a todo el Departamento de Bioquímica su amabilidad y compañerismo en todos los momentos que he pasado allí. En especial, gracias a Carmen por su buena gestión y amabilidad incondicional siempre. Gracias Marina por tus clases de bioquímica.

A Marieta por su amabilidad y compañerismo en un nuevo proyecto que nació durante mi doctorado y espero que dure mucho tiempo. Gracias también a Vicente por formar parte de ello.

I would like to thank to Chris Shannon and everyone from the School of Life Sciences, University of Nottingham. Thank you for your welcome me like one of you, and also, thank you Francis and Ian for your acceptance in your research group during my stay there. It was a great time in Nottingham! Aprovecho para dar las gracias a todas aquellas personas que tuve la oportunidad de conocer durante mi estancia en allí: Patri, Meri, Rubén, Paula, Ana, Víctor, Rosío y Carlo, amigos, espero veros pronto.

I would like also to acknowledge Prof. Spencer Proctor his acceptance in his research group during my short stay at the University of Alberta, Edmonton, Canada. In addition, thank you Stara, Sharon, Yosdel, Gayathri, Vijay and Randy for everything. Por supuesto, gracias a Antonio por enseñarme a

sobrevivir en *Deadmonton* y gracias al equipo aquí-Canadá: Sara, Laia y Vanni, por todas las cervezas y el gran viaje a Vancouver-Victoria en la autocaravana (*si te vas, yo también me voy...*).

Agradecer a uno de los grupos de amigos más importante desde que empecé mi vida en la Universidad. Hacen ya, exactamente, diez años que nos conocimos y seguimos como el primer día, todos juntos y organizando GHs con Andrés, Balta, Esteban, Lu, Marta, Paqui, Sara, Sensi, Silvia, Vero y Vicky.

A Meri, por formar parte de esta etapa en la que fue un gran apoyo personal. Gracias por todos los momentos en el zaidín y de viaje.

Quiero, por último, agradecer también a todos mis amigos con los que llevo compartiendo mucho tiempo, tanto de la Torre (Miguel, Dani, José, Paco, Antonio) como de Granada-Armilla (Manu Zuri, Pablo, Jesús, Mire, Lolo, Javi, Delia y Alberto). Gracias a todos.

Grants and fundings

The present work was financed through the following grants:

1. Instituto de Salud Carlos III, Fondo de Investigaciones Sanitarias (FIS). Ministerio de Salud: RD08/0072/0028 y RD12/0026/0015 “Red de Salud Materno Infantil SAMID”, Redes temáticas de investigación cooperativa RETIC.
2. Junta de Andalucía, Consejería de Innovación y Ciencia: P10-CTS-6770 Biological implications of insulin resistance signalling, inflammation and extracellular matrix genes human adipose tissue-derived mesenchymal stem cell cultures (*Implicaciones biológicas de genes de las vías de señalización de la insulina, inflamación y de la matriz extracelular en cultivos de células madre mesenquimales de tejido adiposo humano*).
3. Ministry of Education, Culture and Sport, Spanish Government: Francisco Javier Ruiz Ojeda is the recipient of a “*Formación de Profesorado Universitario, (FPU)*” stipend from 2013 to 2017 (Reference: AP2012-02068).
4. Ministry of Education, Culture and Sport, Spanish Government: Francisco Javier Ruiz Ojeda was the recipient of a short stay “*Estancias breves FPU 2013*” stipend for three months to be involved in a foreign Institution (B.O.E. 21 Nov 2013). The Ph. D. student visited the School of Life Sciences in Medical School, The University of Nottingham. Nottingham, United Kingdom. Supervisor: Prof. Dr. Ian A. Macdonald, (10 Sept 2014 – 10 Dec 2014).
5. Ministry of Education, Culture and Sport, Spanish Government: Francisco Javier Ruiz Ojeda was the recipient of a short stay “*Estancias breves FPU 2015*” stipend for three months to be involved in a foreign institution (B.O.E. 5 August 2015). The Ph. D. student visited the Li Ka Shing Centre for Health Innovation, University of Alberta, Edmonton, Alberta, Canada. Supervisor: Prof. Dr. Spencer Proctor, (10 May 2016 – 9 August 2016).

List of publications and congress communications

Publications

1. **Ruiz-Ojeda FJ**, Rupérez AI, Gomez-Llorente C, Gil A, Aguilera CM. Cell Models and Their Application for Studying Adipogenic Differentiation in Relation to Obesity: A Review. *Int. J. Mol. Sci.* 2016; 17(7), 1040.
2. **Ruiz-Ojeda FJ**, Aguilera CM, Rupérez AI, Gil Á, Gomez-Llorente C. An analogue of atrial natriuretic peptide (C-ANP₄₋₂₃) modulates glucose metabolism in human differentiated adipocytes. *Mol Cell Endocrinol.* 2016; 431:101-8.
3. **Ruiz-Ojeda FJ**, Gomez-Llorente C, Aguilera CM, Gil A, Rupérez AI. Impact of 3-Amino-1,2,4-Triazole (3-AT)-Derived Increase in Hydrogen Peroxide Levels on Inflammation and Metabolism in Human Differentiated Adipocytes. *PLoS One.* 2016; 11(3):e0152550.

Book Chapters

1. Chapter 4: RNA analyses. **Ruiz-Ojeda FJ**, Plaza-Diaz J, Gil A. Principles of Nutrigenetics and Nutrigenomics, International Society of Nutrigenetics/Nutrigenomics (ISNN), Elsevier (*Under review*).

Congress communications

International scope

1. **Francisco J. Ruiz-Ojeda**, Concepción Aguilera-García, Carolina Gómez-Llorente, Ángel Gil y Azahara I. Rupérez-Cano. Catalase: metabolic effects in adipocytes. SLAN (Sociedad Latinoamericana de Nutrición). Oral communication. Punta Cana, República Dominicana. 8 - 12 November 2015.
2. **Francisco J. Ruiz-Ojeda**, Concepción Aguilera-García, Azahara I. Rupérez-Cano, Ángel Gil y Carolina Gómez-Llorente. C-ANP₄₋₂₃ modulates gene expression associated with signaling pathway insulin and inflammation in human adipocytes. FENS (Federation of European Nutrition Societies). Poster communication. Berlin, Germany. 20 - 23 October 2015.

National scope

3. **Francisco J. Ruiz-Ojeda**, Concepción Aguilera-García, Carolina Gómez-Llorente, Ángel Gil y Azahara I. Rupérez-Cano. Efectos metabólicos de la catalasa en adipocitos diferenciados. Sociedad Española de Endocrinología Pediátrica (SEEP). Oral communication. Córdoba, Spain. 27 - 29 April 2016.
4. **Francisco J. Ruiz-Ojeda**, Azahara I. Rupérez-Cano, Ángel Gil, Concepción Aguilera-García y Carolina Gómez-Llorente. La activación del receptor 3 de los péptidos natriuréticos aumenta los niveles de adenosín monofosfato ciclado (AMPc) en adipocitos humanos. Federación Española de Sociedades de Nutrición, Alimentación y Dietética (FESNAD). Postercommunication. Sevilla, Spain. 5 - 7 March 2015.
5. **Francisco J. Ruiz-Ojeda**, Carolina Gómez-Llorente, Azahara I. Rupérez-Cano, Ángel Gil y Concepción Aguilera-García. Estudio de la expresión del gen Tenomodulina en adipocitos diferenciados de células mesenquimales derivadas de tejido adiposo humano. Sociedad Española de Nutrición (SEÑ). Poster communication. Pamplona, Spain. 3 - 5 July 2014.

Summary

Summary

Introduction

Obesity is an important public health problem and it is characterized by an excessive accumulation of fat in the adipose tissue, which can occur through an increase in adipocyte volume (hypertrophy), number (hyperplasia), or a combination of both (hypertrophy–hyperplasia). Moreover, obesity is associated with oxidative stress and low-grade inflammation in the adipose tissue; and it is a risk factor for insulin resistance (IR), diabetes type 2 and others co-morbidities (Morigny *et al.* 2016).

Adipose tissue is the main organ for energy storage. It contains adipocytes in addition to a wide population of cells, such as macrophages, fibroblasts, pericytes, blood cells, endothelial cells, smooth muscle cells, mesenchymal stem cells (MSCs) and adipose precursor cells. All of these cells are located in the stromal vascular fraction (SVF) and the cell composition and phenotype of the SVF are usually different depending on the location of the adipose tissue location and the adiposity (Wang *et al.* 2014). Adipogenesis is the process of cell differentiation by which preadipocytes become adipocytes and it has been intensively studied using different models of cellular differentiation. Adipose-derived stem cells (ADSCs) are a multipotent population found in adipose tissue capable to be plastic adherent, show trilineage differentiation potential and express different clusters of differentiation. Moreover, ADSCs can differentiate into several lineages, including the adipocytes (Volz *et al.* 2016). The main advantages of ADSCs are their high expansion capacity, their ability to be

passaged a number times, and their possibility of being cryopreserved for long periods of time (Lee *et al.* 2014). In the last years, the differentiation of fibroblast cell lines into adipocytes has been extensively studied (Wang *et al.* 2014) and different cell culture models and protocols have become available to study adipocyte biology (see *Chapter 1.Literature review* below).

On the other hand, three types of adipose depots exist in mammals, the white (WAT), the brown (BAT) and the beige or BRITE (bAT) adipose tissue. They have specificities related to cell composition, localization, pathways for homeostatic control, metabolic and endocrine capacities, responsiveness and roles (Lanthier *et al.* 2014). WAT is the principle site for safe energy storage, but it is also an endocrine organ that secretes cytokines and adipokines (Baraban *et al.* 2016). Among WAT, subcutaneous adipose tissue (SCAT) and visceral fat depots (VAT) depots represent 80% and 20% of total body fat storage, respectively. BAT is specialized in fat burning for heat generation and energy expenditure related to thermogenesis and to defend against cold and, eventually, obesity (Baraban *et al.* 2016). As brown adipocytes, beige adipocytes have numerous mitochondria and express high levels of UCP-1 and they only express the thermogenic genes (UCP-1 and others) in response to specific activation state (Harms *et al.* 2013).

Concerning to obesity and its co-morbidities, for the last two decades, it has been reported different molecules and hormones as mediators implicated in metabolic processes associated with obesity. In this sense, natriuretic peptides (NPs) are a family of peptide hormones that it has been described as mediators of those metabolic processes through the interaction with NPs receptors (NPRs): NPR1/NPR-A, NPR2/NPR-B and NPR3/NPR-C (Gruden *et al.* 2014). NPR3 has

been classically considered as a clearance receptor that is involved in the degradation of NPs (Schlueter *et al.* 2014). However, different studies revealed that NPR3 might be involved in some metabolic processes. In this regard, it has been described that obesity is associated with decreased circulating levels of atrial natriuretic peptide (ANP) and brain natriuretic peptide (BNP), and also, *NPR3* has been found to be up-regulated in WAT from obese adults and children (Gómez-Ambrosi *et al.* 2004, Aguilera *et al.* 2015). Additionally, it has been reported that NPR3 is coupled to the adenylate cyclase/cAMP system in various human tissues. Thus, it has been demonstrated its association with cAMP levels in different tissues, using the synthetic ligand C-ANP₄₋₂₃, a ring-deleted analogue of ANP which specifically interacts with NPR3 (Anand-Srivastava *et al.* 1990).

Regarding to oxidative stress, obesity leads to an excessive production of reactive oxygen species (ROS) in the adipose tissue, including hydrogen peroxide (H₂O₂), superoxide anion (O₂⁻) and the hydroxyl radical (OH[·]). In particular, H₂O₂ is one of the most abundant forms of ROS in adipocytes and the levels are regulated by different enzymes including catalase (CAT), glutathione peroxidases, superoxide dismutase and peroxiredoxins (Gough *et al.* 2011, Rupérez *et al.* 2014). Although H₂O₂ is an important signaling molecule at controlled levels, its increased production can determine metabolic alterations in adipocytes. Moreover, it is known that oxidative stress can activate the nuclear factor kappa-light-chain-enhancer of activated B cells (NF-κB) inflammation pathway (Sasaki *et al.* 2005). Additionally, ROS are also able to lower peroxisome proliferator-activated receptor-gamma (*PPAR-γ*) expression (Chen *et al.* 2006), which can itself regulate *CAT* expression in adipose tissue (Okuno *et al.* 2008).

CAT is one of the most important antioxidant enzymes in the cells, located in the peroxisomes. It degrades any H₂O₂ that exceeds the physiological levels. CAT expression was increased after caloric restriction in the adipose tissue of obese mice (Lijnen *et al.* 2012). However, its expression in mice hearts has also been observed to be increased after 30 weeks of high-fat feeding, possibly to compensate for the observed significant decrease in CAT-specific activity (Rindler *et al.* 2013). In humans, erythrocyte CAT activity has been shown to be decreased in obese adults (Amirkhizi *et al.* 2014) and was lower in children with insulin resistance and obesity (Rupérez *et al.* 2013).

Background and aims of the study

The research group “CTS-461-Nutritional Biochemistry. Therapeutic implications, BioNIT” focuses one of its research fields on obesity. First, the group reported some studies of the association of genetic variants with childhood obesity such as 11 β -hydroxysteroid dehydrogenase type 1 (*HSD11B1*), neuropeptide Y (*NPY*) and fat mass and obesity (*FTO*) genes (PhD defended by Olza J. 2011) (Olza J *et al.* 2012). Subsequently, the research group studied the potential implications of SNPs for antioxidant defense system-related genes in the risk of obesity and metabolic syndrome features in children; a PhD thesis on that subject was defended by Rupérez AI (2014) (Rupérez *et al.* 2013, Rupérez *et al.* 2014). Additionally, the group demonstrated that VAT exhibits a differential gene expression between obese and normal-weight prepuberal children (Aguilera *et al.* 2015). Consequently, we obtained a grant by Junta de Andalucía (project number CTS-6770), which allowed for selecting some genes that may affect obesity and its metabolic complications such as inflammation and insulin

resistance. Therefore, natriuretic peptide 3 (*NPR3*) and catalase (*CAT*) genes were selected among others to study the putative role on adipocyte metabolism and its possible association with obesity.

The present work was undertaken to determine the putative function of *NPR3* (Chapter 2) and *CAT* (Chapter 3) genes on adipocyte metabolism, as well to study the specific mechanisms which might contribute to metabolic alterations related to obesity in human differentiated adipocytes.

Material and methods

In the present study, a commercial cell line of ADSCs was purchased from Lonza. ADSCs were cultured, expanded and differentiated into adipocytes according to the manufacturer's recommendations (Lonza). Afterward, ADSCs were differentiated into mature adipocytes for 12 days and samples were taken at the different times (days 0, 5, 9 and 12), and adipogenesis was monitored and quantified via morphological examination of the cellular accumulation of lipid droplets at the different times (d0, d5, d9 and d12) by Oil Red O staining assay. Finally, all treatments were performed on differentiated adipocytes at day 10.

Experiments for the study of NPR3 using C-ANP₄₋₂₃ as synthetic ligand

The synthetic ligand C-ANP₄₋₂₃, an analogue peptide of the ANP and specific for NPR3, was first described by Maack *et al.* 1987. Since 1990 different studies have described the C-ANP₄₋₂₃ effects and its exclusive interaction with NPR3 in animal and human cells (Anand-Srivastava *et al.* 1990, Rutherford *et al.* 1994, Ortego *et al.* 1999, Sellitti *et al.* 2001, Zhang *et al.* 2005, Gower *et al.* 2006,

Li *et al.* 2012, Almeida *et al.* 2014; Li *et al.* 2014). As previously described, C-ANP₄₋₂₃ is capable to modify the cAMP levels in human cells (Sellitti *et al.* 2001). However, C-ANP₄₋₂₃ does not modify the cGMP levels and lipolysis (Anand Srivastava *et al.* 1990, Skowronska *et al.* 2010).

In order to test the appropriate concentration and incubation time of C-ANP₄₋₂₃, the cells were treated with different concentrations (50 nM, 1 μ M and 5 μ M) and incubation times (30 min, 4 h and 6 h) (Supplementary figure S3). The selected experimental conditions, based on the intracellular cAMP levels results, were 1 μ M of C-ANP₄₋₂₃ and 4 hours of incubation. Then, the cells were treated with 100 μ M SQ22536, which is an adenylate cyclase system inhibitor, for 30 min, in the presence or absence C-ANP₄₋₂₃, as described below. The intracellular cAMP, cGMP and protein kinase A (PKA) activity levels were determined by ELISA and gene and protein expression were determined by qRT-PCR and Western blot, respectively, in the presence or absence of C-ANP₄₋₂₃ in the human differentiated adipocytes. The levels of lipolysis and glucose uptake were also determined.

Experiments for the study of CAT using the inhibitor 3-amino-1,2,4-triazole (3-AT)

Human differentiated adipocytes were incubated with the irreversible CAT inhibitor 3-amino-1,2,4-triazole (3-AT) (Margoliash *et al.* 1960). 3-AT can produce both an immediate reversible inhibition of the enzyme at rather high concentrations of the inhibitor (Heim, Appleman & Pyfrom, 1956) and a slowly developing irreversible inhibition of catalytic activity in the presence of a low and

constant concentration of hydrogen peroxide (Margoliash & Novogrodsky, 1958). Thus, the differentiated adipocytes were incubated with 2 mM and 10 mM 3-AT (for 24 hours) to test their effect on catalase activity. Thus, 3-AT was able to significantly inhibit catalase activity in a dose-dependent manner producing an analogous increase in H₂O₂ levels. However, 10 mM 3-AT was able to generate a significantly higher increase in H₂O₂ than 2 mM 3-AT. According to these results, the final chosen condition for the following experiments was 10 mM 3-AT for 24 hours. The GPX and SOD activities were also determined. Gene expression of antioxidant enzymes, transcription factors, glucose and lipid metabolism were determined in the presence or absence of 3-AT in the human differentiated adipocytes. Moreover, NF-κB activation and increased tumor necrosis alpha (TNF-α) and interleukin (IL)-6 protein and gene expression levels were examined as main inflammation markers. Finally, glucose uptake and lipolysis assay were carried out in the presence or absence of 3-AT.

All experiments were repeated at least three times. In each independent experiment, two replicates were performed. Data are expressed as the mean ± standard error of the mean (SEM). Significant differences were determined using the non-parametric Mann-Whitney U test; statistical significance was defined as **P*<0.05; ***P*<0.01. Statistical analyses were performed using SPSS version 22, for Windows (SPSS, Chicago, IL, USA).

Results and discussion

Oil Red O staining assay showed that ADSCs were adequately differentiated into mature adipocytes, due to the significant increased of lipid

accumulation from d0 to d12. Additionally, leptin (*LEP*), adiponectin (*ADIPOQ*) and *PPAR-γ* gene expression were up-regulated during the adipogenic differentiation. As expected, we found that *NPR3* and *CAT* gene expression and protein levels were significantly up-regulated on d5, d9 and d12 compared with day 0 (Supplementary figure S1).

Regarding to *NPR3* study, C-ANP₄₋₂₃ treatment significantly increased the intracellular cAMP levels and the *GLUT4* and 5'-AMP-activated-kinase (*AMPK*) mRNA levels were up-regulated. Western blot showed a significant increase in *GLUT4* and phosphor-*AMPKα* levels in the C-ANP₄₋₂₃-treated adipocytes. Importantly, the adenylate cyclase inhibitor SQ22536 abolished these effects. Additionally, C-ANP₄₋₂₃ increased glucose uptake by 2-fold. Therefore, we have demonstrated that C-ANP₄₋₂₃ effects were mediated through cAMP increased levels enhancing glucose metabolism in human differentiated adipocytes (**Figure 1**).

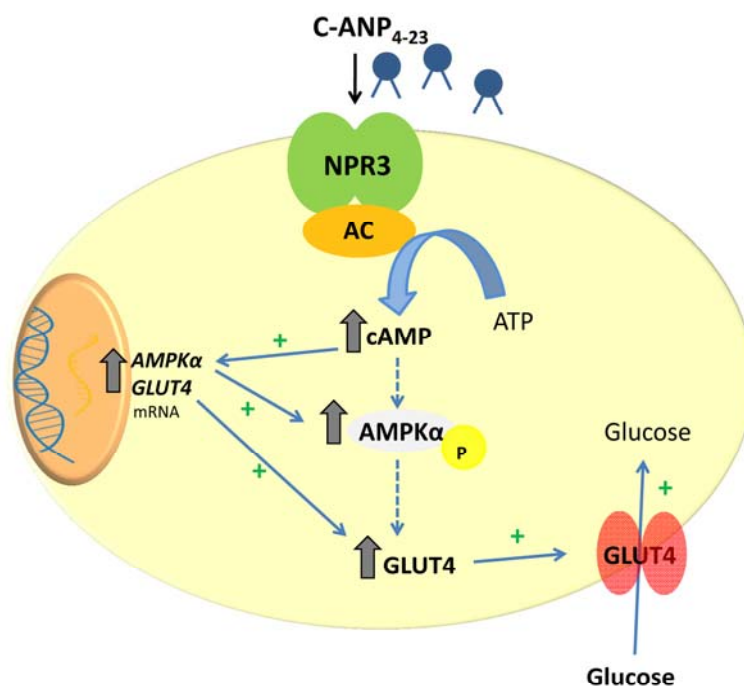


Figure 1. Conditions observed in the C-ANP₄₋₂₃-treated adipocytes (Chapter 2). AC, adenylylate cyclase; AMPK, AMP-activated kinase; ATP, adenosine triphosphate; cAMP, cyclic adenosine monophosphate; C-ANP₄₋₂₃, C-atrial natriuretic peptide (4-23); GLUT4, glucose transporter 4; NPR3, natriuretic peptide receptor. The black arrows indicate an increase or decrease in activity, expression or protein levels. The continuous blue lines indicate causal relationships between findings, and the dashed blue lines indicate potential relationships according to the revised literature.

Concerning to CAT study, the 3-AT treatment decreased CAT activity and increased intracellular H₂O₂ levels significantly. GPX activity was also reduced, and the gene expression levels of the antioxidant enzymes such as GPX and PRDXs were inhibited. Interestingly, this occurred along with lower mRNA levels of the transcription factors nuclear factor (erythroid 2-like 2) and forkhead box O 1 (FOXO1), which are involved in redox homeostasis. However, SOD activity and expression were increased. Moreover, 3-AT led to NF-κB activation and increased TNF-α and IL-6 protein and gene expression levels, while lowering PPAR-γ mRNA and protein levels. These alterations were accompanied by an altered

glucose and lipid metabolism. Indeed, adipocytes treated with 3-AT showed reduced basal glucose uptake, reduced GLUT4 gene and protein expression, reduced lipolysis, reduced AMPK activation and reduced gene expression of lipases. Therefore, the increased H_2O_2 levels caused by 3-AT treatment impair the antioxidant defense system and the adipocyte metabolism in human differentiated adipocytes (**Figure 2**).

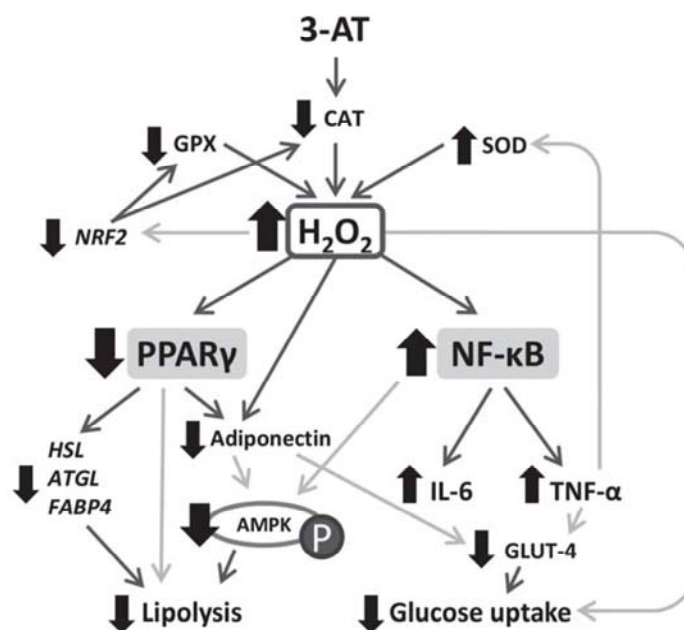


Figure 2. Conditions observed in the 3-AT-treated adipocytes (Chapter 3). AMPK: 5'-AMP-activated protein kinase; ATGL: adipose triglyceride lipase; CAT: catalase; FABP4: fatty-acid binding protein 4; GLUT4: glucose transporter type 4; GPX: glutathione peroxidase; HSL: hormone sensitive lipase; IL-6: interleukin 6; NRF2: nuclear factor, erythroid 2-like 2; NF-κB: nuclear factor of kappa light polypeptide gene enhancer in B-cells 2; P: enzyme phosphorylation; PPARγ: peroxisome proliferator-activated receptor gamma; SOD: superoxide dismutase; TNF-α: tumor necrosis factor alpha.

Conclusions

We found that *NPR3* and *CAT* genes are extensively involved in adipocyte metabolism. C-ANP₄₋₂₃ enhances glucose metabolism and might contribute to the

development of new peptide-based therapies for metabolic diseases. CAT activity plays a significant role in the metabolic and redox homeostasis of adipocytes as intracellular levels of H₂O₂ impairs the antioxidant defense system and initiates inflammation exerting complex signaling functions.

Limitations

The main limitation of the present study is the morphology of the differentiated adipocytes from human ADSCs. This was not completely identical to that of mature adipocytes that exists in the adipose tissue.

In relation to NPR3 study, the C-ANP₄₋₂₃ effects on glucose metabolism might be different between isolated adipocytes and adipose tissue.

Regarding to CAT, the degree to which we inhibited CAT (by approximately 70%) is higher than the inhibition of CAT activity observed in obese individuals (approximately 42%). Finally, the effects of 3-AT on the actions of insulin or other hormones upon other metabolic parameters and cellular responses was not fully elucidated in the present study, and thus, requires further research.

Resumen

Resumen

Introducción

La obesidad es un problema importante de salud pública y se caracteriza por una acumulación excesiva de grasa en el tejido adiposo, que puede ocurrir por un aumento del volumen del adipocito (hipertrofia), número de éstos (hiperplasia), o bien, una combinación de ambos (hipertrofia-hiperplasia). Además, la obesidad se asocia con un estrés oxidativo y una inflamación de bajo grado en el tejido adiposo; y ésto es un factor de riesgo para el síndrome de resistencia a la insulina (IR), diabetes tipo 2 y otras co-morbilidades (Morigny *et al.* 2016).

El tejido adiposo es el principal órgano de almacenamiento de energía. Contiene adipocitos y, además, una gran población de células como son los macrófagos, fibroblastos, pericitos, células sanguíneas, células endoteliales, células del músculo liso, células madre mesenquimales y células precursoras. Todas éstas células se encuentran localizadas en la fracción del estroma vascular (SVF) y la composición celular y fenotípica de las SVF son, normalmente, diferentes dependiendo de la localización y de la adiposidad corporal (Wang *et al.* 2014). La adipogénesis es el proceso de diferenciación celular mediante el cual los preadipocitos llegan a ser adipocitos y se ha estudiado intensamente, utilizando diferentes modelos de diferenciación celular. Las células madre mesenquimales derivadas del tejido adiposo (del inglés *Adipose-derived stem cells*, ADSCs) son una población multipotente encontrada en este tejido, capaces de ser adherentes, poseer un potencial trilineal de diferenciación y expresar diferentes marcadores

de diferenciación. Además, las ADSCs pueden diferenciarse hasta diferentes líneas celulares, incluyendo los adipocitos (Volz *et al.* 2016). La principal ventaja de las ADSCs son su alta capacidad de expansión, su capacidad para soportar un número elevado de pasajes y la posibilidad de ser congeladas durante largos períodos de tiempo (Lee *et al.* 2014). En los últimos años, se han estudiado muy a fondo el proceso de diferenciación de líneas celulares de fibroblastos hasta adipocitos (Wang *et al.* 2014) y se dispone de diferentes modelos de cultivo celular y protocolos con el objeto de estudiar la biología del adipocito (ver *Chapter 1.Literature review*, capítulo 1.Revisión bibliográfica más adelante).

Por otro lado, existen tres tipos de tejido adiposo en los mamíferos, el tejido adiposo blanco (del inglés *white adipose tissue*, WAT), el tejido adiposo marrón (del inglés *Brown adipose tissue*, BAT) y el tejido adiposo beige o *BRITE* (del inglés *beige adipose tissue*, bAT). Éstos tipos de tejido se diferencian según la composición celular, localización, vías de señalización y control homeostático, capacidades metabólica y endocrina, funciones y respuestas (Lanthier *et al.* 2014). El WAT es el principal lugar de reserva energética, pero es también un órgano endocrino que secreta citoquinas y adipocitoquinas (Baraban *et al.* 2016). Entre el WAT se distinguen el tejido adiposo subcutáneo (del inglés *subcutaneous adipose tissue*, SCAT) y depósitos viscerales representan el 80% y 20%, respectivamente, del almacenamiento de grasa del organismo. El BAT está especializado en el consumo de grasa para la generación de calor y aumentar el gasto energético, relacionado con la termogénesis y defensa contra el frío y, eventualmente, la obesidad (Baraban *et al.* 2016). Al igual que los adipocitos marrones, los adipocitos beige tienen numerosas mitocondrias y expresan altos

niveles de la proteína desacoplante UCP1 y solamente expresan genes termogénicos (UCP1 y otros) en respuesta a una activación específica (Harms *et al.* 2013).

En cuanto a las comorbilidades derivadas de la obesidad, en las últimas dos décadas, se han publicado diferentes moléculas y hormonas como mediadores implicados en procesos metabólicos asociados a dicha obesidad. En este sentido, los péptidos natriuréticos son una familia de hormonas peptídicas que han sido descritos como mediadores de esos procesos metabólicos, a través de la interacción con sus receptores (del inglés *natriuretic peptide receptors* NPRs): NPR1/NPR-A, NPR2/NPR-B y NPR3/NPR-C (Gruden *et al.* 2014). El receptor 3 de los péptidos natriuréticos (NPR3) se ha considerado, clásicamente, como un receptor de aclaramiento que se encuentra involucrado en la degradación de dichos péptidos (Schlueter *et al.* 2014). Sin embargo, diferentes estudios han demostrado que el NPR3 podría estar implicado en algunos procesos metabólicos. En este sentido, se ha descrito que la obesidad se asocia con un descenso de los niveles circulantes del péptido natriurético atrial (ANP) y del péptido natriurético cerebral (BNP), y además, se ha observado una sobreexpresión del gen *NPR3* en el WAT de personas con obesidad, tanto en adultos (Gómez-Ambrosi *et al.* 2004) como en niños (Aguilera *et al.* 2015). En este aspecto, diferentes estudios han demostrado que el NPR3 se encuentra acoplado al sistema adenilato ciclasa en varios tejidos humanos. Así, se ha asociado con los niveles de AMP cíclico (AMPC) en diferentes tejidos, utilizando un péptido sintético, el C-ANP₄₋₂₃, análogo al ANP que interacciona específicamente con el NPR3 (Anand-Srivastava *et al.* 1990).

En relación al estrés oxidativo, la obesidad conduce a una producción excesiva de especies reactivas de oxígeno (ROS) en el tejido adiposo, incluyendo el peróxido de hidrógeno (H_2O_2), el anión superóxido (O_2^-) y el radical hidroxilo ($OH\cdot$). En particular, el H_2O_2 es una de las formas más abundantes de los ROS en los adipocitos y los niveles están regulados por diferentes enzimas como son la catalasa (CAT), glutatión peroxidasa (GPX), superóxido dismutasa (SOD) y las peroxirredoxinas (PRDXs) (Gough *et al.* 2011, Rupérez *et al.* 2014). Aunque el H_2O_2 es una molécula de señalización importante a niveles controlados, un aumento en su producción puede determinar alteraciones metabólicas en los adipocitos. Además, se conoce que el estrés oxidativo puede activar la vía de inflamación del factor nuclear potenciador de las cadenas ligeras kappa de las células B activadas (NF- κ B) (Sasaki *et al.* 2005). Igualmente, los ROS pueden también disminuir la expresión del receptor activado por proliferador de los peroxisomas-gamma (*PPAR- γ*) (Chen *et al.* 2006), que, a su vez, puede regular la expresión de CAT en el tejido adiposo (Okuno *et al.* 2008). La CAT es una de las enzimas antioxidantes más importantes en las células. Se encuentra localizada en los peroxisomas y degrada el H_2O_2 que excede los niveles fisiológicos. Se ha observado que la expresión de CAT aumenta tras una restricción calórica en el tejido adiposo de ratones obesos (Lijnen *et al.* 2012). Sin embargo, su expresión se encuentra aumentada en el corazón de ratones que han sido alimentados durante 30 semanas con una dieta alta en grasa, posiblemente como mecanismo de compensación del descenso significativo observado en la actividad específica de CAT (Rindler *et al.* 2013). En humanos, se ha demostrado que la actividad de la CAT en los eritrocitos se encuentra disminuida en adultos obesos (Amirkhizi *et*

al. 2014) y, además, en niños con resistencia a la insulina y obesidad (Rupérez *et al.* 2013).

Antecedentes y objetivos del estudio

El grupo de investigación “CTS-461 Bioquímica de la nutrición. Implicaciones terapéuticas, BioNIT” centra una de sus principales líneas de investigación en el estudio de la obesidad. En principio, el grupo llevó a cabo algunos estudios de asociación de variantes genéticas (del inglés *single nucleotide polymorphism*, SNPs) con el riesgo de desarrollar obesidad infantil como son los genes 11 β -hidroxiesteroide deshidrogenasa tipo 1 (*HSD11B1*), neuropéptido Y (*NPY*) y el gen asociado a la obesidad y masa grasa (del inglés *fat mass and obesity associated*, *FTO*) (Tesis doctoral defendida por Olza J. 2011) (Olza *et al.* 2012). Posteriormente, el grupo de investigación estudió las implicaciones potenciales de algunos SNPs de genes relacionados con el sistema de defensa antioxidante, el riesgo de obesidad y algunas características del síndrome metabólico en niños; tesis defendida por Rupérez AI (2014) (Rupérez *et al.* 2013, Rupérez *et al.* 2014). Además, el grupo de investigación demostró que el tejido adiposo visceral muestra una expresión génica diferencial entre niños obesos y niños normopeso prepúberes (Aguilera *et al.* 2015). Consecutivamente, el grupo obtuvo un proyecto de la Junta de Andalucía (proyecto número CTS-6770), que permitió estudiar algunos genes seleccionados que pueden afectar a la obesidad y sus complicaciones metabólicas como son la inflamación y la resistencia a la insulina. De esta forma, se seleccionaron los genes *NPR3* y *CAT*, entre otros, para estudiar su posible función en el metabolismo del adipocito y su asociación con la obesidad.

El presente trabajo fue diseñado para determinar la posible función de los genes *NPR3* (Capítulo 2) y *CAT* (Capítulo 3) en el metabolismo del adipocito, además para estudiar el mecanismo específico por el cual podrían contribuir a las alteraciones metabólicas asociadas a la obesidad en adipocitos humanos diferenciados.

Material y métodos

En el presente estudio, se adquirió una línea celular comercial de células madre mesenquimales derivadas de tejido adiposo humano (ADSCs) de la firma Lonza. Las ADSCs se cultivaron, expandieron y diferenciaron hasta adipocitos siguiendo las recomendaciones del fabricante (Lonza). A continuación, las ADSCs se diferenciaron hasta adipocitos maduros durante 12 días y las muestras se recolectaron en diferentes tiempos (día 0, 5, 9 y 12) y la adipogénesis se comprobó y cuantificó mediante el ensayo de tinción con un colorante lipídico “*Oil Red O*”, examinando morfológicamente la acumulación de gotas de lípidos en las células a diferentes tiempos (d0, d5, d9 y d12). Finalmente, todos los tratamientos *a posteriori* se realizaron en los adipocitos a día 10.

Experimentos para el estudio del NPR3 mediante el ligando sintético C-ANP₄₋₂₃

El ligando sintético C-ANP₄₋₂₃, un péptido análogo del ANP y específico para NPR3, fue el primero en ser publicado por Maack et al. 1987. Desde 1990 diferentes estudios han descrito los efectos del C-ANP₄₋₂₃ y su interacción exclusiva con el NPR3, tanto en células humanas como de animales (Anand-Srivastava et al. 1990, Rutherford et al. 1994, Ortego et al. 1999, Sellitti et al.

2001, Zhang *et al.* 2005, Gower *et al.* 2006, Li *et al.* 2012, Almeida *et al.* 2014; Li *et al.* 2014). Como se ha explicado anteriormente, el C-ANP₄₋₂₃ es capaz de modificar los niveles de AMPc en células humanas (Sellitti *et al.* 2001). Sin embargo, el C-ANP₄₋₂₃ no modifica los niveles de GMPc ni de lipólisis (Anand Srivastava *et al.* 1990, Skowronska *et al.* 2010).

Con el objeto de conocer la concentración apropiada y el tiempo de incubación del C-ANP₄₋₂₃, las células fueron tratadas con diferentes concentraciones (50 nM, 1 μ M and 5 μ M) y tiempos (30 min, 4 h y 6 h) (Figura suplementaria S3). Las condiciones experimentales seleccionadas, basadas en los resultados de los niveles de AMPc, fueron 1 μ M de C-ANP₄₋₂₃ y 4 h de incubación. Seguidamente, las células se trataron con 100 μ M de SQ22536, que es un inhibidor del sistema adenilato ciclasa, durante 30 minutos, en presencia y ausencia del C-ANP₄₋₂₃, como se ha descrito anteriormente. Los niveles intracelulares de AMPc, GMPc y actividad de la proteína quinasa A (PKA) se determinaron mediante kits de ELISA y las evaluaciones de la expresión génica y proteica de algunos genes se llevaron a cabo mediante qRT-PCR y Western blot, respectivamente, en presencia o ausencia del C-ANP₄₋₂₃ en adipocitos humanos diferenciados. Los niveles de lipólisis y captación de glucosa también se determinaron en dichas condiciones.

Experimentos para el estudio de CAT utilizando el inhibidor 3-amino-1,2,4-triazol (3-AT)

Los adipocitos humanos diferenciados se incubaron con el inhibidor irreversible de la actividad de CAT 3-amino-1,2,4-triazol (3-AT) (Margoliash *et al.*

1960). El 3-AT puede producir tanto una inhibición reversible rápida de la enzima a concentraciones bastante altas del inhibidor (Heim, Appleman & Pyfrom, 1956), como una inhibición irreversible de desarrollo lento de la actividad catalítica a baja concentración y constante de peróxido de hidrógeno (Margoliash & Novogrodsky, 1958). Con el objeto de determinar la concentración apropiada, los adipocitos diferenciados se incubaron con 2 mM y 10 mM de 3-AT (durante 24 h) y se determinó la actividad de la CAT. Así, el 3-AT inhibió de forma significativa la actividad enzimática de manera dosis-dependiente produciendo un aumento en los niveles de H₂O₂. Sin embargo, a 10 mM generó un aumento significativamente más alto de H₂O₂ que a 2 mM. De acuerdo con estos resultados, la condición finalmente elegida para el desarrollo de los experimentos fue la de 10 mM de 3-AT durante 24 horas.

Se determinó también la actividad de la GPX y SOD. La expresión génica de enzimas antioxidantes, factores de transcripción, metabolismo glucídico y lipídico se determinaron en presencia y ausencia del 3-AT en adipocitos humanos diferenciados. Además, se determinó la activación del NF-κB y los niveles de expresión génica y proteica del factor de necrosis tumoral alpha (TNF-α) e interleucina 6 (IL-6). Finalmente, se llevaron a cabo ensayos de lipólisis y captación de glucosa en presencia y ausencia del 3-AT.

Todos los experimentos fueron repetidos al menos tres veces. En cada experimento independiente, se realizaron dos réplicas. Los datos están expresados como la media ± error estándar de la media (E.E.M.). Las diferencias significativas entre medias se determinaron mediante el test no paramétrico de U de Mann-Whitney. La significancia estadística se definió como * $P < 0.05$; ** $P < 0.01$.

Los análisis estadísticos se llevaron a cabo mediante el programa SPSS versión 22, para Windows (SPSS, Chicago, IL, EEUU).

Resultados y discusión

El ensayo de tinción con *Oil Red O* mostró que las células ADSCs se diferenciaron correctamente hasta adipocitos maduros, debido al aumento significativo de la acumulación lipídica desde el d0 hasta el d12. Además, los genes leptina (*LEP*), adiponectina (*ADIPOQ*) y de *PPAR-γ* fueron sobreexpresados durante la diferenciación adipogénica. Como se esperaba, se encontró que la expresión génica y proteica de *NPR3* y *CAT* fue significativamente más alta durante los días d5, d9 y d12 comparados con el día 0 (Figura suplementaria S1).

En cuanto al estudio del *NPR3*, el tratamiento con C-ANP₄₋₂₃ aumentó de forma significativa los niveles intracelulares de AMPc y los niveles de expresión génica de GLUT4 y AMPK fueron más altos. Los resultados del Western blot mostraron un aumento significativo en los niveles de GLUT4 y phospho-AMPK-α en los adipocitos tratados con C-ANP₄₋₂₃. Todos estos efectos no se observaron en presencia del inhibidor de la adenilato ciclasa SQ22536. Además, C-ANP₄₋₂₃ aumentó la captación de glucosa dos veces (**Figura 1**). En definitiva, hemos demostrado que los efectos de C-ANP₄₋₂₃ fueron mediados a través del aumento de los niveles de AMPc, mejorando el metabolismo glucídico en adipocitos humanos diferenciados.

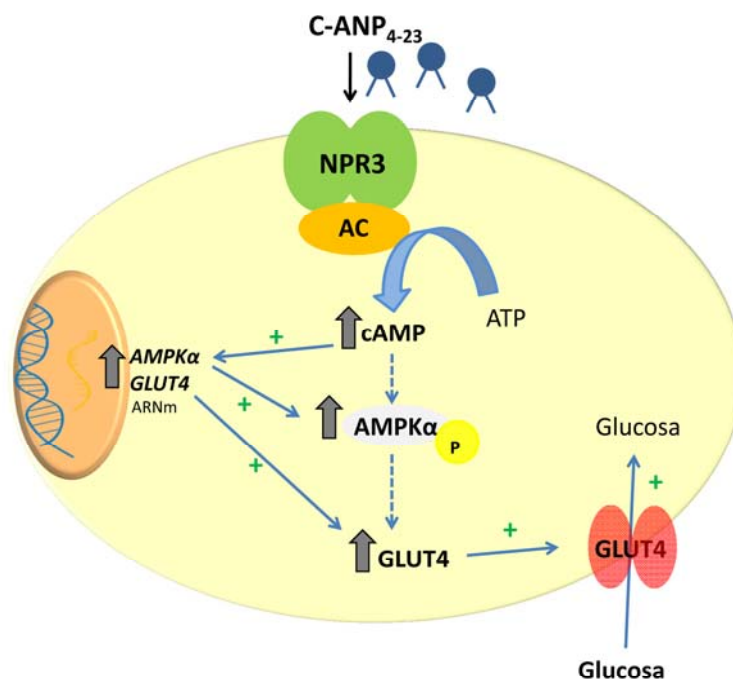


Figura 1. Condiciones observadas en los adipocitos tratados con C-ANP₄₋₂₃ (Capítulo 2). AC, adenilato ciclasa; AMPK, proteína quinasa activada por AMP; ATP, adenosin trifosfato; cAMP, adenosín monofosfato cíclico; C-ANP₄₋₂₃, C-péptido natriurético atrial (4-23); GLUT4, transportador de glucosa 4; NPR3, receptor 3 de los péptidos natriuréticos. Las flechas negras indicant un aumento o disminución en la actividad, expresión o niveles proteicos. Las líneas azules contínuas indicant una relación directa encontrada entre los hallazgos, y las líneas azules discontinúas indican la relación potencial existente de acuerdo a lo revisado en bibliografía.

En cuanto al estudio de CAT, el tratamiento con 3-AT disminuyó la actividad catalasa y aumentó los niveles de H₂O₂ de forma significativa. La actividad de la GPX también se redujo y la expresión de los genes de enzimas antioxidantes como la GPX y PRDXs disminuyó. Curiosamente, esto ocurrió junto con niveles bajos de mRNA del factor de transcripción Nrf2 y FOXO1, que están involucrados en la homeostasis redox. Sin embargo, la actividad y expresión de la SOD aumentaron. Además, el 3-AT produjo una activación del NF-κB y aumento de los niveles de expresión génica y proteica de TNF-α y IL-6, mientras disminuyó los de PPAR-γ. Estas alteraciones se acompañaron por una alteración

en el metabolismo glucídico y lipídico. De hecho, los adipocitos tratados con el 3-AT mostraron una reducción basal en la captación de glucosa, una expresión génica y proteica de GLUT4 disminuida, menor lipólisis, menor activación de la AMPK y reducción de la expresión génica de lipasas (**Figura 2**). En definitiva, el aumento de los niveles de H_2O_2 causado por el tratamiento con 3-AT produjo un daño en el sistema de defensa antioxidante y en el metabolismo de los adipocitos humanos diferenciados.

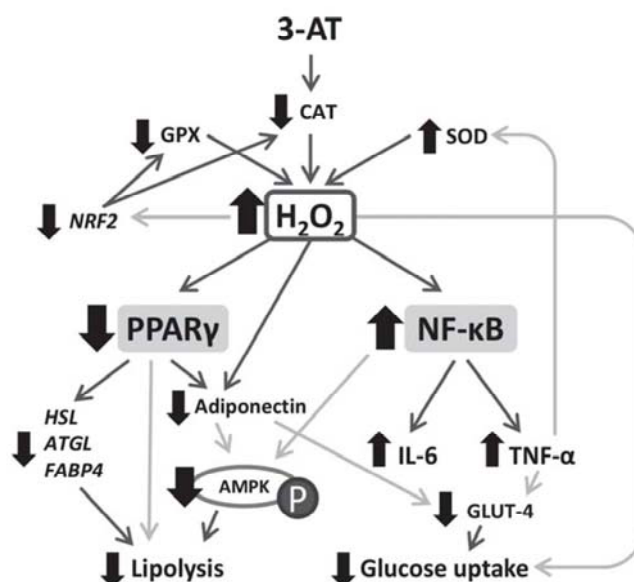


Figura 2. Condiciones observadas en los adipocitos tratados con 3-AT (Capítulo 3). AMPK: 5'-proteín kinasa activada por AMP; ATGL: lipasa de triglicéridos; CAT: catalasa; FABP4: proteína de unión a ácidos grasos 4; GLUT4: transportador de glucosa 4; GPX: glutatión peroxidasa; HSL: lipasa sensible a las hormonas; IL-6: interleucina 6; NRF2: nuclear factor, factor nuclear eritroide-tipo2; NF-κB: factor nuclear potenciador de las cadenas ligeras kappa de las células B activas; P: fosforilación de enzima; PPARγ: receptor activado por proliferador de los peroxisomas gamma; SOD: superóxido dismutasa; TNF-α: factor de necrosis tumoral alpha.

Conclusiones

Los genes *NPR3* y *CAT* están ampliamente involucrados en el metabolismo del adipocito. El C-ANP₄₋₂₃ mejora el metabolismo glucídico y podría contribuir al

desarrollo de nuevas terapias basadas en péptidos para enfermedades metabólicas. La actividad de la CAT juega un papel importante en la homeostasis metabólica y redox de los adipocitos, de tal forma que los niveles altos de H₂O₂ alteran el sistema de defensa antioxidante e inicia una inflamación ejerciendo funciones de señalización complejas.

Limitaciones

La principal limitación del presente estudio es la morfología de los adipocitos diferenciados a partir de las células ADSCs humanas. Estas no son completamente idénticas a los adipocitos maduros que existen en el propio tejido adiposo.

En relación al estudio del NPR3, los efectos del C-ANP₄₋₂₃ sobre el metabolismo glucídico podrían ser diferentes entre los adipocitos aislados y el tejido adiposo.

En cuanto a la CAT, el grado mediante el cual la actividad CAT fue inhibida (aproximadamente un 70 %) es más alta que la inhibición de la actividad de CAT observada en individuos obesos (aproximadamente un 42 %). Finalmente, los efectos del 3-AT en las acciones de la insulina y otras hormonas bajo otros parámetros metabólicos y respuestas celulares, no fueron completamente clarificados en el presente estudio, y por tanto, se precisa de más investigación.

Introduction

Introduction

1.1. Obesity prevalence

Obesity is one of the most important public health burdens both in developed and developing countries. According to the World Health Organization (WHO) obesity and overweight are defined as “abnormal or excessive fat accumulation that may impair health”. An increased consumption of highly caloric foods, without an equal increase in energy expenditure, mainly by physical activity, leads to an unhealthy increase in weight; and also, decreased levels of physical activity will result in an energy imbalance and lead to weight gain (WHO 2016). In fact, obesity is a disease with worldwide continually increasing prevalence and independently of age group, material status or origin (Lewandowska *et al.* 2016).

Worldwide obesity has more than doubled since 1980. In 2014, more than 1.9 billion adults, 18 years and older, were overweight and of these over 600 million were obese. Thus, 30 % of adults aged 18 years and over were overweight in 2014, and 13 % were obese (**Figure 1**). In addition, 41 million children under the age of 5 were overweight or obese in 2014 (WHO 2016).

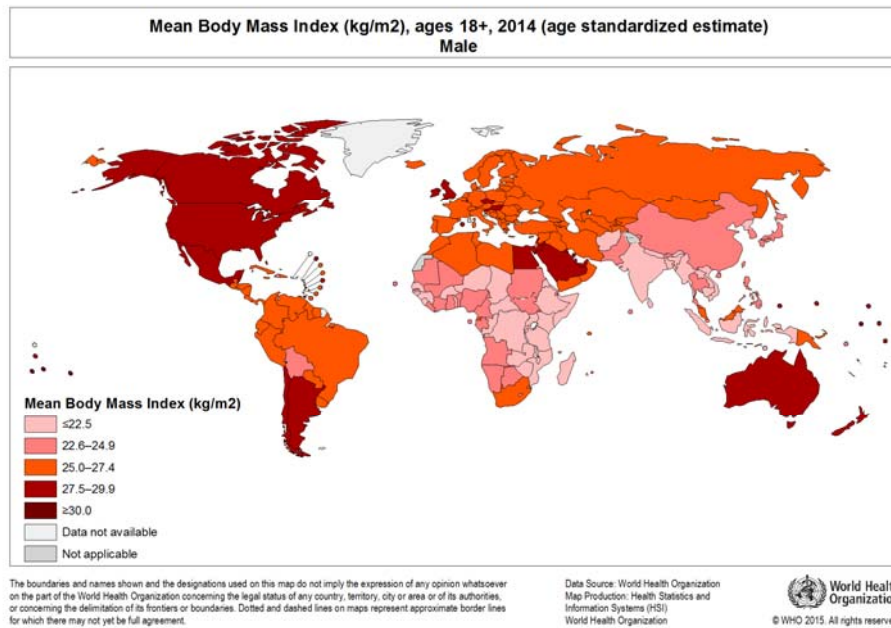


Figure 1A. World map of obesity prevalence in male. Data are presented as mean Body Mass Index (kg/m²), ages +18 (age standardized estimate), 2014; World Health Organization (WHO).

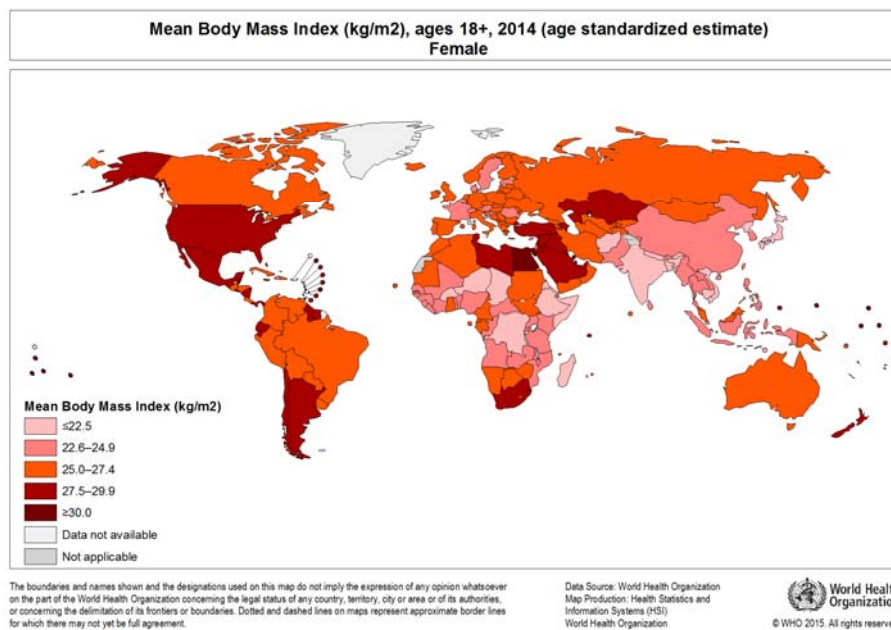


Figure 1B. World map of obesity prevalence in female. Data are presented as mean Body Mass Index (kg/m²), ages +18 (age standardized estimate), 2014; World Health Organization (WHO).

Additionally, obesity is a risk factor for insulin resistance (IR) and development of type 2 diabetes, and also, diabetes is associated with complications such as cardiovascular diseases, non-alcoholic fatty liver disease (NAFLD), retinopathy, angiopathy and nephropathy, with consequently leads to higher mortality risks (Morigny *et al.* 2016).

1.2. Etiology of obesity

Obesity is the result of genetic, behavioral, environmental, physiological, social and cultural factors that result in energy imbalance and promote excessive fat deposition. The relative contribution of each of these factors has been studied extensively, and although genes play an important role in the regulation of body weight, the WHO on obesity concluded that behavioral and environmental factors (i.e. sedentary lifestyles combined with excess energy intake) are primarily responsible for the dramatic increase in obesity during the past two decades. Consequently, obesity and its co-associated metabolic diseases results from a complex interaction between environmental and genetic factors. Thus, people with obesity have more cardiovascular and metabolic risk factors than people with normal weight. However, in the past few years, controversy has surrounded the idea that some individuals with obesity can be considered healthy with regards to their metabolic and cardiorespiratory fitness, which has been termed the ‘obesity paradox’ (Lavie *et al.* 2016).

The inter-individual variations of genetic information such as the study of single-nucleotide polymorphisms (SNPs) and structural variants determine the patterns of DNA sequence associated with obesity. Furthermore, these SNPs can condition the metabolic response to nutritional events, which are studied by

nutrigenetics. Thus, different SNPs have been reported by genetic variations such as fat mass and obesity-associated (*FTO*), neuropeptide FF receptor 2 (*NPF2*) or melanocortin 4 receptor (*MC4R*) (Hunt *et al.* 2011, Cordero *et al.* 2015). Recently, a study by Wheeler *et al.*, 2013 on paediatric obesity found new genetic variants involved in the early onset of obesity: leptin receptor (*LEPR*) and protein kinase C (*PRKCH*) (Wheeler *et al.* 2013). Technical development of high-throughput techniques for massive approaches, such as genetic wide association studies (GWAS), provides valuable information for the understanding of obesity and associated co-morbidities on a genetic basis (Fall *et al.* 2014). GWAS for adiposity traits and obesity risk have identified at least 160 loci that contribute to body weight and fat distribution in adults and children of diverse ancestry. Shungin *et al.* (2015) identified 49 loci (33 new) associated with waist-to-hip ratio adjusted for body mass index (BMI), and an additional 19 loci newly associated with related waist and hip circumference measures (Locke *et al.* 2015, Shungin *et al.* 2015) Recently, Lu *et al.* 2016 have described new loci for body fat percentage that reveal a link between adiposity and cardiovascular disease risk. A meta-analysis of data from more than 100,000 individuals identified 12 loci significantly associated with body fat %. Particularly striking is that two of the 12 loci harbour genes (*IRS1*, *GRB14*) that influence insulin receptor signalling, and two other loci contain genes (*IGF2BP1*, *PICK1*) that are involved in the GH/IGF1 pathway, that in turn also relates to insulin receptor signalling (Lu *et al.* 2016).

Although gene code contains the information that could define the individual phenotype, there seems to be parallel translation machinery regulating the

expression of the information stored in the genome. The proposed molecular mechanism that could mediate this control is epigenetic (Cordero *et al.* 2015). Hence new approaches researching the epigenetic are laying the groundwork for the knowledge of the etiology of the obesity.

1.3. Adipose tissue and adipocyte biology

Adipose tissue has been recognized as an active endocrine organ and a main energy store of the body (Kershaw *et al.* 2004). Excess adiposity and adipocyte dysfunction result in dysregulation of a wide range of adipose tissue-derived secretory factors, referred to as adipokines, which may contribute to the development of various metabolic diseases via altered glucose and lipid homeostasis as well as inflammatory responses. Additionally, excess fat accumulation promotes the release of free fatty acids (FFA) into the circulation from adipocytes, which may be a critical factor in modulating insulin sensitivity (Jung *et al.* 2015).

Adipose tissue contains adipocytes in addition to a wide population of cells, such as macrophages, fibroblasts, pericytes, blood cells, endothelial cells, smooth muscle cells, mesenchymal stem cells (MSCs) and adipose precursor cells. All of these cells are located in the SVF and the cell composition and phenotype of the SVF are usually different depending on the location of the adipose tissue location and the adiposity (Wang *et al.* 2014).

Adipose tissues secrete various hormones, cytokines, and metabolites such as adipokines that control systemic energy balance by regulating appetitive signals from the central nerve system as well as metabolic activity in peripheral tissues (Choe *et al.* 2016). Three types of adipose depots exist in mammals, commonly

classified following their colour appearance: the white (WAT), the brown (BAT) and the beige or BRITE (bAT) adipose tissue. They have specificities related to cell composition, localization, pathways for homeostatic control, metabolic and endocrine capacities, responsiveness and roles (Lanthier *et al.* 2014). WAT is the principle site for safe energy storage, but it is also an endocrine organ that secretes cytokines and adipokines (Baraban *et al.* 2016). Among WAT, subcutaneous adipose tissue (SCAT) and visceral fat depots (VAT) depots represent 80% and 20% of total body fat storage, respectively. VAT is drained directly to the liver through the portal vein. As a result, FFA, adipokines and cytokines have a hepatic first pass and reach the liver at high concentration. Moreover, adipogenesis is relatively restrained and accommodation of excess fat depends on adipocyte hypertrophy, a form of storage rather associated with higher metabolic alterations and inflammation (Ibrahim *et al.* 2010, Lanthier *et al.* 2014). On the other hand, the enhanced capacity to store lipids subcutaneously by stimulation of adipogenesis rather than by hypertrophy does not cause inflammation and may protect against fat deposition in visceral locations and ectopic tissues. In addition, compared to SCAT, VAT is metabolically more active, with an increased lipolytic activity (Ibrahim *et al.* 2010) and protein secretion. However, the majority of the studies on obesity and adipose tissue inflammation in humans, authors analyze the SCAT and not the VAT, because it is more readily accessible (Bradley *et al.* 2012, Lanthier *et al.* 2014).

Brown adipose tissue (BAT) is specialized in fat burning for heat generation and energy expenditure related to thermogenesis and to defend against cold and,

eventually, obesity. Brown adipocytes promote energy expenditure via mitochondrial uncoupling protein 1 (UCP-1). An intermediate type of adipocytes that expresses UCP-1 has also been described. This type of adipocyte is referred to as beige or “*BRITE*” (brown in white) adipocytes and regarded as a non-classical/inducible brown adipocyte (Wu *et al.* 2012, Xu *et al.* 2015). As brown adipocytes, beige adipocytes have numerous mitochondria and express high levels of UCP-1. However, they do not originate from the same precursors than BAT and they only express the thermogenic genes (UCP-1 and others) in response to specific activation, while BAT expresses those genes in the basal state (Harms *et al.* 2013). Chronic cold exposure, agonists of the β -adrenergic receptor or peroxisome proliferator active receptor gamma (PPAR- γ) stimulates white to beige transformation (Lanthier *et al.* 2014).

1.4. Hyperplastic and hypertrophic adipocytes

The excessive accumulation of fat mass in WAT can occur through an increase in adipocyte volume (hypertrophy), number (hyperplasia), or a combination of both (hypertrophy–hyperplasia) (**Figure 2**). Adipocyte hypertrophy and hyperplasia are regulated by environmental and genetic factors (Spiegelman *et al.* 2001).

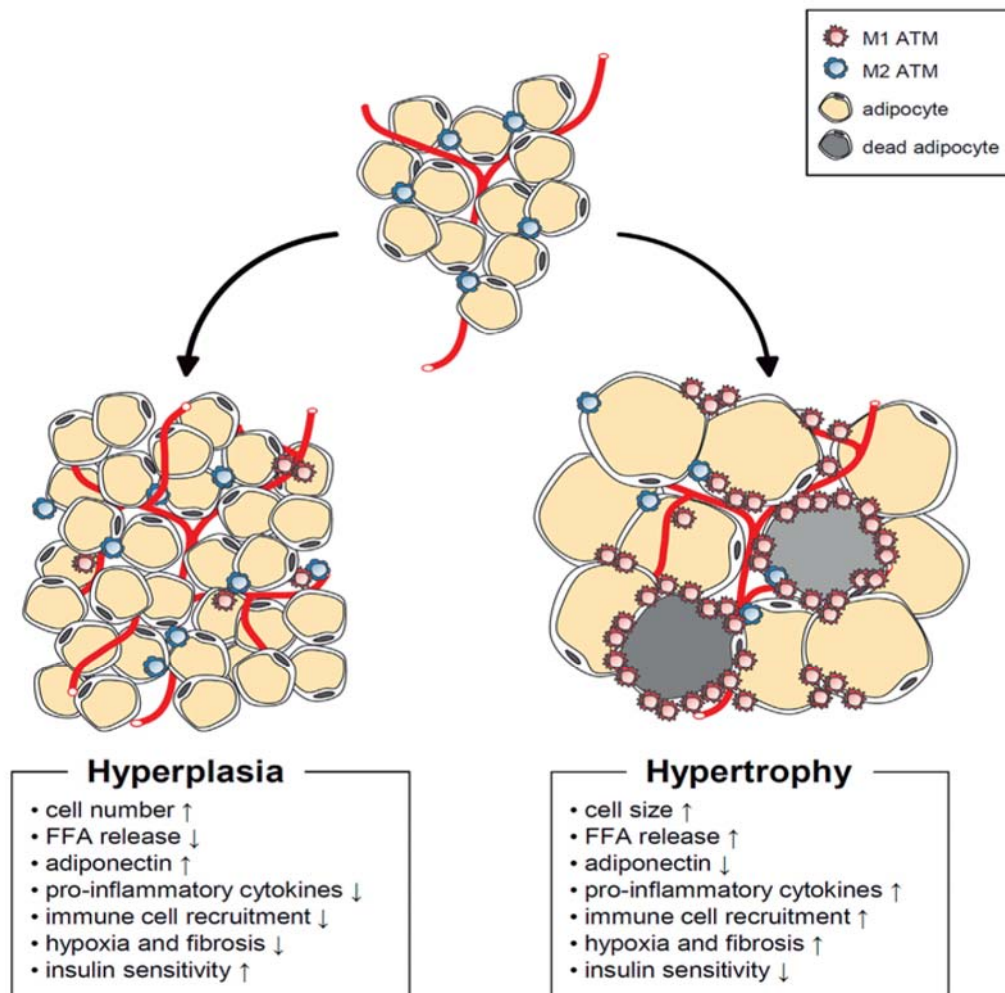


Figure 2. Characteristics of hypertrophic and hyperplastic adipocytes in obesity (Choe *et al.* 2016). FFA: Free fatty acids.

Recently, it has been suggested that adipocyte hypertrophy *per se* results in abnormal adipocyte function and leads to IR (Kim *et al.* 2015). WAT from people with obesity, hypertrophic adipocytes show necrotic-like abnormalities. An increase of dead adipocytes in obesity will impede adipose tissue function and induce inflammation by secreting of pro-inflammatory cytokines such as tumor necrosis factor α (TNF α), inter-leukin (IL)-6, IL-8, and monocyte chemoattractant

protein-1 (MCP-1) (Jernas *et al.* 2006). This elevation of pro-inflammatory cytokines leads to serine phosphorylation of insulin receptor substrate-1 (IRS-1) via NF- κ B and Jun N-terminal kinase signaling, resulting in the development of IR (Hirosumi *et al.* 2002). Additionally, adipocyte hypertrophy induces local adipose tissue hypoxia due to a relative deficiency of vasculature and the expression levels of angiogenic factors and inflammatory response-associated genes are up-regulated (Trayhurn *et al.* 2012). On the other hand, lipolysis is elevated in hypertrophic adipocytes, increasing the leakage of FFA. Large amounts of FFA released from the obese adipose tissue are taken up by other tissues, such as the liver and muscle, which can cause ectopic lipid accumulation and lipotoxicity (Rutkowski *et al.* 2015). Moreover, adipocyte hypertrophy also impairs insulin-dependent glucose uptake because of a defect in glucose transport 4 (GLUT4) trafficking (Kim *et al.* 2015, Choe *et al.* 2016).

Regarding to hyperplasia expansion of adipose tissue, adipocyte precursor cells must differentiate into adipocytes through the adipogenesis process. Several studies suggest that *de novo* differentiation of small adipocyte could ameliorate IR in obesity by providing additional capacity to store excess energy. Although the implications of adipocyte hyperplasia in the adipose tissue function are not fully understood, the regulation of hyperplastic adipocytes may exert beneficial effects against adipocyte hypertrophy and subsequent IR (Choe *et al.* 2016).

1.5. Adipogenesis process

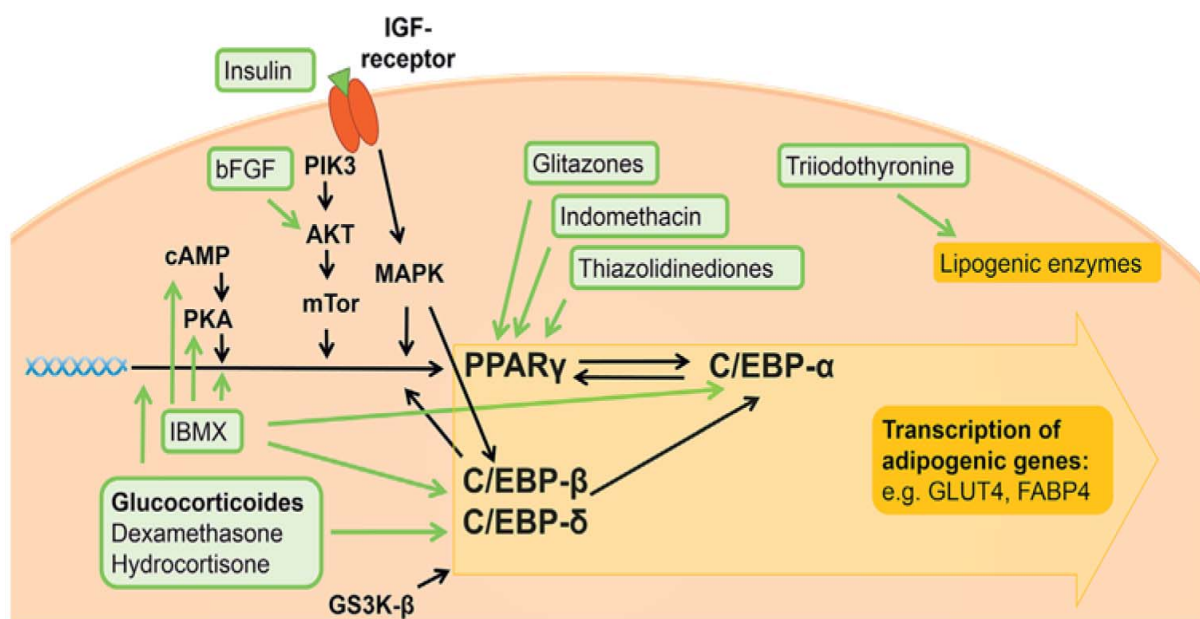
Adipogenesis is the process of cell differentiation by which preadipocytes become adipocytes and it has been one of the most intensively studied models of cellular differentiation. WAT is capable of massive expansion and contraction in

response to chronic alterations in energy balance, accounting for as little as 5% body mass in extremely lean athletes or as much as 60% body mass in morbidly obese individuals. On a cellular level, WAT expansion is driven by both hypertrophy and hyperplasia of adipocytes, as it was described above (Cawthorn *et al.* 2012).

Adipose-derived stem cells (ADSCs) are a population of mesenchymal stem cells (MSCs) found in adipose tissue. MSCs are defined by the Minimal Criteria of the International Society for Cellular Therapy whereafter these cells have to be plastic adherent, show trilineage differentiation potential and express cluster of differentiation (CD) 73, CD90 and CD105 (Dominici *et al.* 2006, Volz *et al.* 2016). Up to date, different methods for ADSCs isolation exists such as the purification of the SFV, from endothelial and hematopoietic cells by fluorescent-activated cell sorting (FACs) or magnetic-activated cell sorting (MACs) and exclusion of CD31 and CD45-positive cells. Most of researcher directly plate the SVF assuming the target cells to been riched by plastic adherence for 6 hours and following culture adherence 6 hours and following culture (Volz *et al.* 2016).

Moreover, ADSCs are multipotent and can be differentiated into several lineages, like the adipogenic, chondrogenic and osteogenic lineage. The *in vitro* adipogenic differentiation of MSCs has been discovered before the existence of stem cells in adipose tissue was shown. It is well understood at the molecular level and initiated by various partly interdependent differentiation factors. Thus, PPAR- γ and CCAAT-enhancer binding protein alpha (C/EBP- α) are considered as the central regulators of adipogenesis and are induced early in the differentiation process (Rosen *et al.* 2000). The transcription of PPAR- γ and C/EBP- α is in turn

activated by the factors C/EBP- β and δ which are mediating the transcription of adipogenic genes like GLUT4 or fatty acid binding protein 4 (FABP4) consecutive to adipogenic stimuli (Petersen *et al.* 2008). C/EBP- β is known to be activated via mitogen activated protein kinases (MAPK), glycogen synthase 3- β as well as through cyclic adenosine monophosphate (cAMP). The latter is additionally able to activate PPAR- γ via protein kinase A (PKA) (Zhang *et al.* 2004, Volz *et al.* 2016) (**Figure 3**). Furthermore, sterol regulatory element-binding transcription factor 1c (SREBP1c) is another key transcription factor that stimulates the expression of lipogenic genes, including acetyl-CoA carboxylase, fatty acid synthase, and saturated fatty acid dehydrogenase. It has



been reported that activation of SREBP1c provides endogenous PPAR- γ ligands and consequently increases adipogenesis (Choe *et al.* 2016).

Figure 3. Molecular mechanism of adipogenesis and its common in vitro inducers.

PPAR- γ and C/EBP- α are the main modulators of adipogenesis and their activation finally results in the transcription of adipogenic genes (Volz *et al.* 2016). AKT, PKB protein kinase B; cAMP, cyclic adenosine monophosphate; CEBP, CCAAT-enhancer binding protein alpha; FABP4. Fatty

acid binding protein 4; GLUT4, glucose transporter 4; GS3K- β , glycogen synthase kinase 3 beta; IBMX, 3-isobutyl-1-methylxanthine; IGF, insulin-like growth factor-1; MAPK, mitogen-activated protein kinase; PIK3, phosphatidylinositol 3 kinase; PKA, protein kinase A; PPAR γ , peroxisome proliferator-activated receptor gamma.

1.6. Obesity and natriuretic peptides

Natriuretic peptides (NPs) have been revealed to be key mediators of metabolic processes and have been implicated in the development of diabetes. NPs are a family of peptide hormones that are predominantly secreted from the heart and that exert a variety of physiological functions by interacting with NP receptors (NPRs) (Gruden *et al.* 2014, Li *et al.* 2014, Schlueter *et al.* 2014) (**Figure 4**). The NP family comprises three members, atrial natriuretic peptide (ANP), brain natriuretic peptide (BNP), and C-type natriuretic peptide (CNP). These peptides are secreted as pro-hormones and are then cleaved by proteases into their biologically active forms and corresponding inactive peptides at equimolar ratios; and ANP and BNP are predominantly secreted by cardiomyocytes, whereas CNP is mainly produced by the central nervous system, the endothelium, the bone, and the reproductive system (Gruden *et al.* 2014).

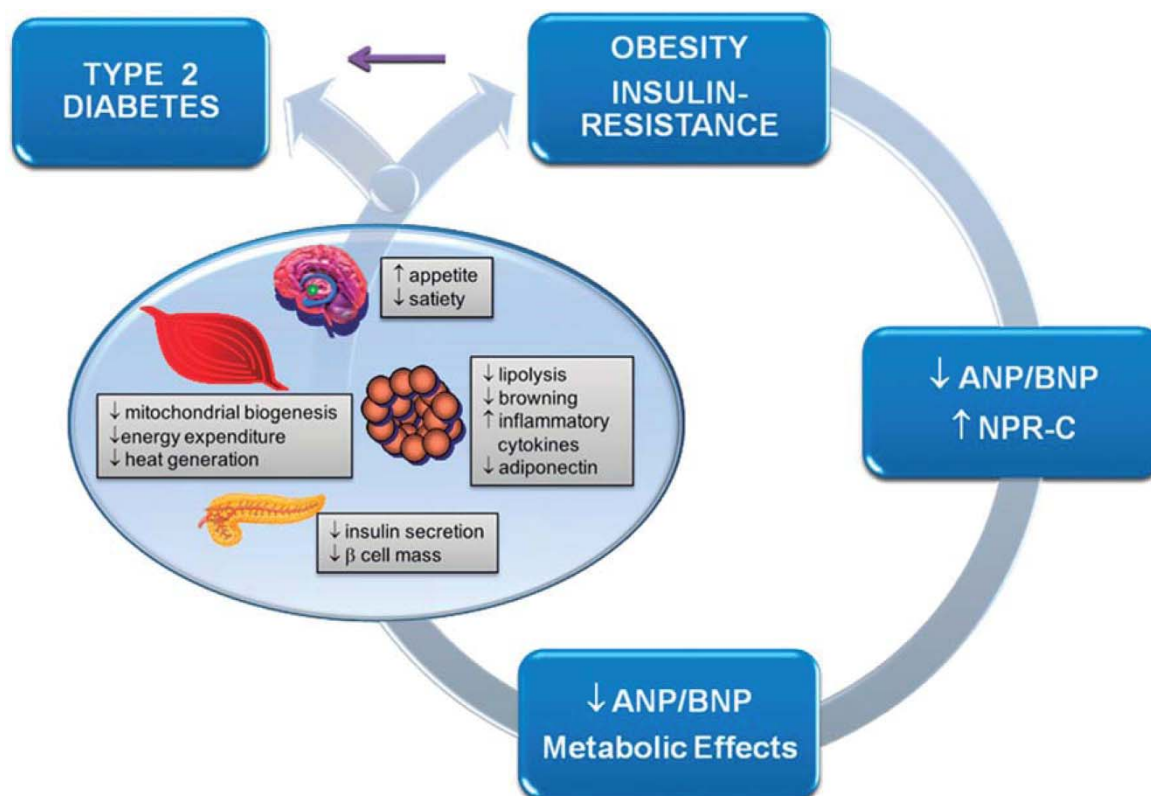


Figure 4. Potential link between NPs, obesity, insulin resistance, and diabetes. Obesity and insulin resistance are associated with both impaired ANP and BNP cardiac release and overexpression of the clearance NPR-C or NPR3, leading to reduced NP-mediated beneficial effects on target organs of metabolism (Grunden et al. 2014). ANP, atrial natriuretic peptide; BNP, brain natriuretic peptide; NPR-C, natriuretic peptide receptor C.

There are three NPRs: NPR1 or NPR-A and NPR2 or NPR-B are membrane guanylyl cyclase receptors that are primarily responsible for the metabolic activity of NPs; and, NPR3 or NPR-C has been classically considered as a clearance receptor that is involved in the degradation of NPs (Schlueter *et al.* 2014). NPR3 can bind to all NPs; it displays the highest affinity for ANP and the lowest affinity for BNP (Potter *et al.* 2006) (**Figure 5**).

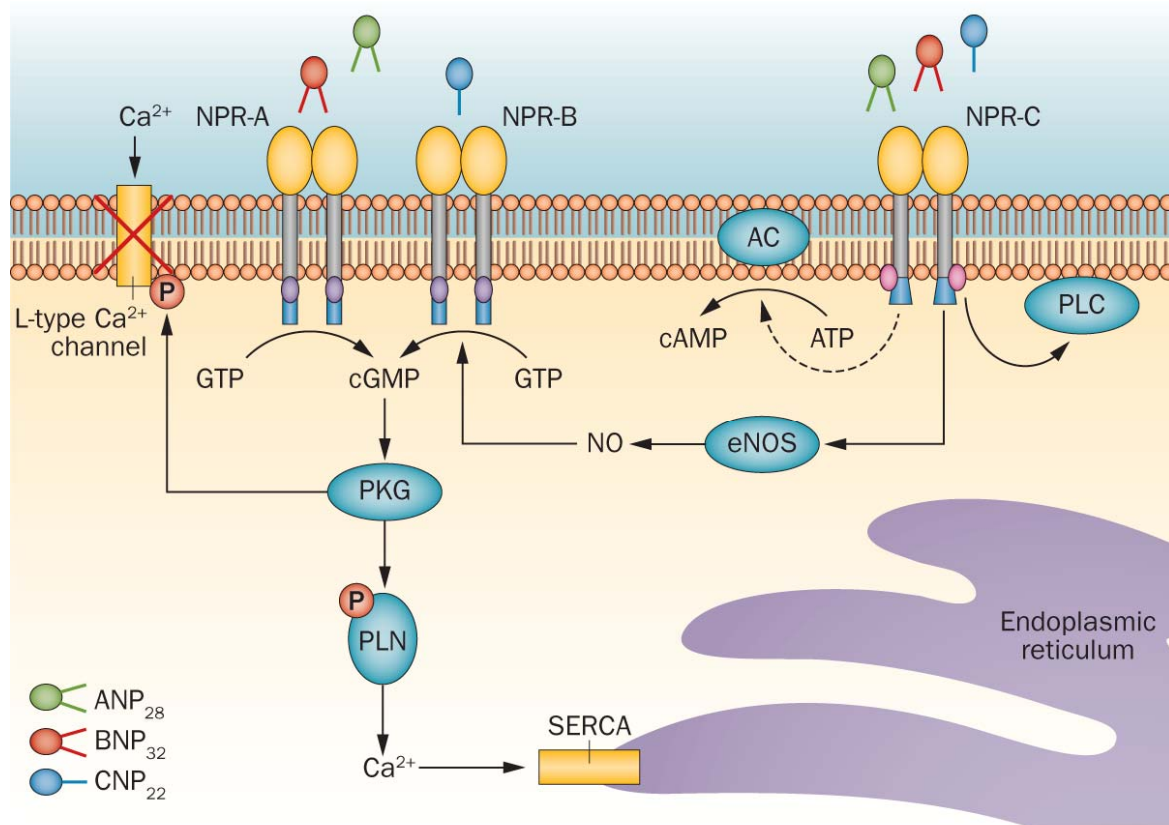


Figure 5. The natriuretic peptides exert their effects through transmembrane receptors: NPR-A/NPR1, NPR-B/NPR2, and NPR-C/BNPR3. NPR-A and NPR-B are guanylyl cyclases, which catalyse the synthesis of cGMP from GTP. The NPR-C/NPR3 lacks guanylyl cyclase activity; instead, receptor activation is coupled to AC or PLC (Zois *et al.* 2014). AC, adenylate cyclase; ANP, atrial natriuretic peptide; ATP, adenosine triphosphate; BNP, brain natriuretic peptide; cAMP, cyclic adenosine monophosphate ; cGMP, cyclic guanosine monophosphate; CNP, C-type natriuretic peptide; eNOS, endothelial nitric oxide synthase; GTP, guanosine triphosphate; NO, nitric oxide; NPR-A, natriuretic peptide receptor A; NPR-B, natriuretic peptide receptor B; NPR-C, natriuretic peptide receptor C; P, phosphorylation; PKG, protein kinase G; PLC, phospholipase C; PLN, perilipin.

Obesity is associated with decreased circulating levels of ANP and BNP, and a negative linear relationship between BMI and NP plasma values has been consistently reported in epidemiological studies (Gruden *et al.* 2014). NPRs are expressed in different human tissues, including adipose tissue, where NPs can stimulate lipolysis, modulate adipokine secretion, and promote white adipocyte browning (Gruden *et al.* 2014, Sarzani *et al.* 1996, Moro *et al.* 2013, Bordicchia *et al.* 2012). Additionally, the expression levels of *NPR3* in adipose tissue have been

observed to be considerably increased in obese adults (Gómez-Ambrosi *et al.* 2004, Baranova *et al.* 2005) and obese children (Aguilera *et al.* 2015). Moreover, insulin increases *NPR3* expression in subcutaneous adipose tissue in subjects with moderate obesity and normal glucose tolerance (Pivovarova *et al.* 2012). Several studies have revealed that the plasma levels of NPs are decreased in patients with obesity or type 2 diabetes (Moro *et al.* 2013, Wang *et al.* 2007) and this decrease may be primarily due to impaired NP release (Omar *et al.* 2009). Another possible explanation is that the up-regulation of *NPR3* increases NP clearance from the circulation (Dessi-Fulgheri *et al.* 1997) although the ablation of *NPR3* in mice did not affect the circulating levels of NPs (Pivovarova *et al.* 2012 and Matsukawa *et al.* 1999). It has been reported that NPR3 is coupled to the adenylate cyclase/cAMP system through a 37-amino acid intracellular region of NPR3 that is expressed in various human tissues (Schenk *et al.* 1987, Sengenès *et al.* 2005). Studies using the synthetic ligand C-ANP₄₋₂₃, a ring-deleted analogue of ANP, which specifically interacts with NPR3, have shown decreased cAMP levels in the anterior pituitary, the aorta, the brain striatum, and the adrenal cortex, as well as in rat vascular smooth muscle cells and cultured adipocytes (Anand-Srivastava *et al.* 1990, Crilley *et al.* 1997). However, incubation in C-ANP₄₋₂₃ increased the cAMP levels in human thyrocytes (Sellitti *et al.* 2001). In addition, in cultured adipocytes, molecules that increase the intracellular cAMP levels have been demonstrated to increase the activity of 5' adenosine monophosphate (AMP)-activated protein kinase (AMPK), a critical regulator of energy homeostasis and a therapeutic target for the treatment of type 2 diabetes (Yin *et al.* 2003, Hutchinson *et al.* 2005).

1.7. *Obesity, oxidative stress and inflammation*

As it has been previously described, obesity leads to an excessive accumulation of fat in the adipose tissue, accompanied by low-grade inflammation, hypoxia and oxidative stress. Oxidative stress is defined as an imbalance between the reactive oxygen species (ROS) scavenging and producing systems in the organism. ROS include molecules, such as hydrogen peroxide (H_2O_2), superoxide anion (O_2^-) and the hydroxyl radical ($\text{OH}\cdot$). The controlled production of these molecules is known to help protect against microorganisms during infections processes, as well as contribute to normal function in the cell, including proliferation, differentiation and signaling. Nevertheless, a non-physiological increase in ROS levels from excessive caloric intake, inflammation or hypoxia, or a decrease in the antioxidant capacity of the organism can lead to the aforementioned alterations. In particular, one of the most abundant forms of ROS in adipocytes is H_2O_2 , the levels of which are heavily regulated by different enzymes that include catalase (CAT), glutathione peroxidases (GPX), superoxide dismutase (SOD) and peroxiredoxins (PRDXs) (**Figure 6**). Although H_2O_2 is an important signaling molecule at controlled levels, its increased production can determine metabolic alterations in adipocytes (Gough *et al.* 2011, Rupérez *et al.* 2014).

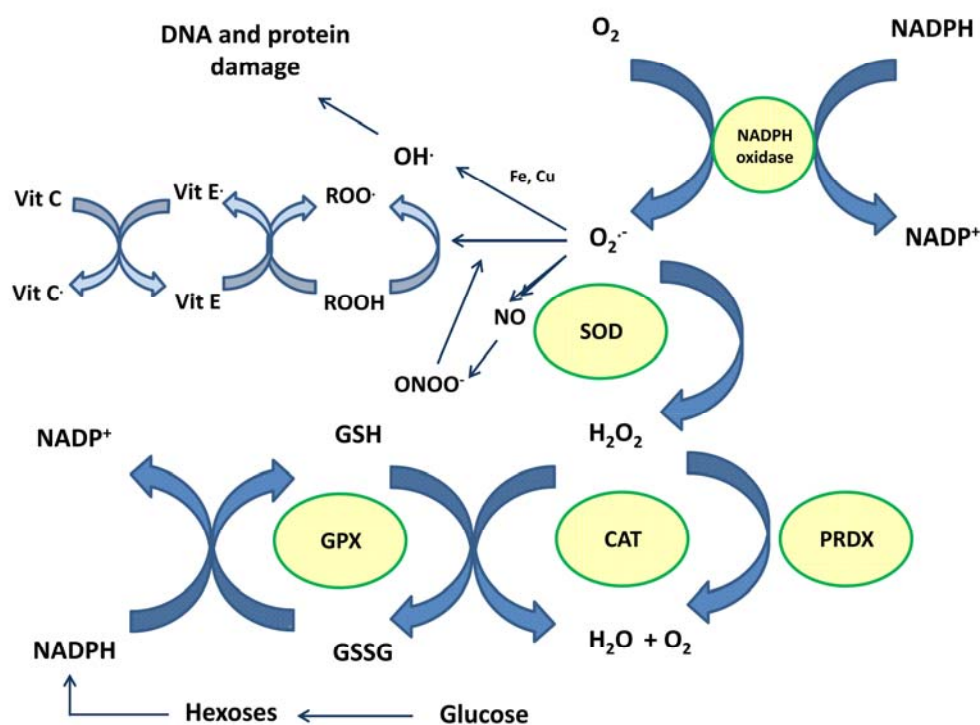


Figure 6. Effects of different antioxidant enzymes on oxidative metabolism in adipocytes. CAT, catalase; GPX, glutathione peroxidase; GSH, glutathione; GSSG, glutathione disulfide; H_2O_2 , peroxide of hydrogen; NADPH, nicotinamide adenine dinucleotide phosphate; PRDX, peroxiredoxin; SOD, superoxide dismutase; vit, vitamine.

Concerning to inflammation, it is known that oxidative stress can activate the NF- κ B inflammation pathway. Serine phosphorylation at various sites of the NF- κ B p65 subunit has been shown to be important for the transcription of various inflammatory mediators, including TNF- α and IL-6 (Sasaki *et al.* 2005). Additionally, ROS are also able to lower *PPAR- γ* expression (Chen *et al.* 2006), which can itself regulate *CAT* expression in adipose tissue (Okuno *et al.* 2008). In fact, in obese individuals, treatment with rosiglitazone, a *PPAR- γ* agonist, increased *CAT* protein levels in adipose tissues (Ahmed *et al.* 2010). Along with this finding, it has been observed that oxidative stress can lead to a down-

regulation of adiponectin and *GLUT4* gene expressions in adipose tissue (Furukawa *et al.* 2004, Anderson *et al.* 2009, Rudich *et al.* 1998).

On the other hand, H₂O₂ has been shown to inhibit AMP-stimulated protein kinase A (PKA) activity, thus reducing lipolysis in adipocytes (Vázquez-Meza *et al.* 2013). Regarding AMPK, it has been shown to be activated as a consequence of lipolysis, in parallel with an increase in oxidative stress (Gauthier *et al.* 2008). Furthermore, oxidative stress can inhibit the expression of lipase genes by activating inflammation and reducing *PPAR-γ* expression.

The cellular responses to oxidative stress, nuclear factor (erythroid 2-like 2) (Nrf2) and forkhead box O (FOXO1) play important roles in maintaining intracellular redox homeostasis by inducing the expression of antioxidant enzymes (Kim *et al.* 2010, Higuchi *et al.* 2013). Moreover, it has been reported that ROS can modulate the Wnt/β-catenin pathway and that low levels of oxidative stress favor the interaction of β-catenin with FOXO1 to protect the cell against oxidative damage (Korswagen *et al.* 2006). Among antioxidant enzymes, CAT is one of the most important in the cells and it is located in the peroxisomes. It degrades any H₂O₂ that exceeds the physiological levels. CAT expression was increased after caloric restriction in the adipose tissue of obese mice. However, its expression in mice hearts has also been observed to be increased after 30 weeks of high-fat feeding, possibly to compensate for the observed significant decrease in CAT-specific activity (Rindler *et al.* 2013). Similarly, a high-fat diet significantly decreased the expression of CAT in adipose tissue from mice (Coate *et al.* 2010). In humans, it has been reported that erythrocyte CAT activity has

been shown to be decreased in obese adults (Amirkhizi *et al.* 2014). Likewise, Ahmed *et al.* (2010) observed a higher CAT protein levels after rosiglitazone treatment, a drug to increase insulin sensitivity, for 14 days in adipose tissue from obese adults (Ahmed *et al.* 2010). On the other hand, it has been demonstrated that CAT erythrocyte activity was lower in children with insulin resistance and obesity (Rupérez *et al.* 2013).

Aims of the study

Aims of the study

Background and justification

The research group “CTS-461-Nutritional Biochemistry. Therapeutic implications, BioNIT” focuses one of its research fields on childhood obesity through different approaches. The first approach in the study of genetic variants affecting childhood obesity risk was to observe SNPs from obesity-related genes associated with childhood obesity such as 11 β -hydroxysteroid dehydrogenase type 1 (*HSD11B1*), neuropeptide Y (*NPY*), fat mass and obesity (*FTO*) (PhD thesis defended by Olza J. 2011) (Olza J *et al.* 2012). Afterward, the research group studied the potential implications of SNPs for antioxidant defense system-related genes in the risk of obesity and metabolic syndrome features in children, a PhD thesis was defended by Rupérez A.I. (2014) (Rupérez *et al.* 2013, Rupérez *et al.* 2014).

Additionally, the CTS-461 group demonstrated that visceral adipose tissue (VAT) exhibits a differential gene expression between obese and normal-weight prepubertal children. A total of fifteen obese and sixteen normal-weight children undergoing abdominal elective surgery were selected. RNA was extracted from VAT biopsies, microarrays experiments were performed (six obese and five normal-weight samples) and a validation by quantitative PCR (qPCR) was carried out on an additional ten obese and ten normal-weight VAT samples. As validated by qPCR, expression was up-regulated in genes involved in lipid and amino acid metabolism (*CES1*, *NPR3* and *BHMT2*), oxidative stress an

extracellular matrix regulation (*TNMD* and *NQO1*), adipogenesis (*CRYAB* and *AFF1*) and inflammation (*ANXA1*); by contrast, only *CALCRL* gene expression was confirmed to be down-regulated. This study demonstrates that some genes influence the pathogenesis of childhood obesity, as well as that may be candidate genes in the etiology of obesity (Aguilera *et al.* 2015).

Subsequently, the research group obtained a grant by Junta de Andalucía (project number CTS-6770; Secretaría General de Universidades, Investigación y Tecnología. Consejería de Economía, Innovación y Ciencia) to study the role of some genes related to insulin resistance signalling, inflammation and extracellular matrix in cultured human adipose tissue-derived mesenchymal stem cells (*Implicaciones biológicas de genes de las vías de señalización de la insulina, inflamación y matriz extracelular en cultivos de células madre mesenquimales de tejido adiposo humano*). The present PhD thesis derives from that research project, which allowed for selecting some candidate genes that may affect obesity and its metabolic complications, such as inflammation and IR. Therefore, natriuretic peptide 3 (*NPR3*) and catalase (*CAT*) genes were selected to study their putative role on adipocyte metabolism and its possible association with obesity.

The expression levels of *NPR3* in adipose tissue have been observed to be considerably up-regulated in obese children (Aguilera *et al.* 2015), which may have an antilipolytic effect through receptor inhibition of lipolysis mediated by natriuretic peptides. Moreover, several studies have revealed that the plasma levels of NPs are decreased in patients with obesity or type 2 diabetes (Moro *et al.*

2013, Wang *et al.* 2007) and this decrease may be primarily due to impaired NP release.

CAT activity is responsible for the degradation of excessive amounts of H₂O₂, has been shown to be decreased in obese adults (Amirkhizi *et al.* 2014) as well as in children with obesity and insulin resistance (Rupérez *et al.* 2013, Shin *et al.* 2006). Moreover, obese and type 2 diabetic mice have lower *CAT* expression and higher H₂O₂ levels in adipose tissue; and, in addition to its genetic variation, has traditionally been studied for diseases other than obesity. Due to this fact, our group recently published a study conducted on obese children that showed the association of some SNPs located in the *CAT* promoter with obesity (Rupérez *et al.* 2013).

Hypothesis

The initial hypothesis was that *NPR3* and *CAT* genes could be implicated in the development of obesity and its complications. Furthermore, we hypothesized that *NPR3* gene could be involved on glucose metabolism in adipocytes; and *CAT* gene might contribute to mechanism by which catalase activity contributes to the deleterious effects of oxidative stress and inflammation in adipose tissue.

Aims

General aim

The present work was undertaken to determine the putative function of *NPR3* and *CAT* genes on adipocyte metabolism, as well to study the specific mechanism

for which they could contribute to metabolic alterations related to obesity in human differentiated adipocytes.

Specific aims

1. To review the literature to update the different human cell culture models available for studying the *in vitro* adipogenic differentiation process related to obesity and its co-morbidities in the last five years.
2. To acquire a suitable commercial cell model human adipose-derived stem cells (ADSCs) and to carry out properly the adipogenic differentiation according to the manufacture protocols.
3. To test the adipogenic differentiation of ADSC into adipocytes through the well known oil red O staining assay at the different times (d0, d5, d9 and d12).
4. To determine *NPR3* and *CAT* gene and protein expression during the adipogenic differentiation at the different times (d0, d5, d9 and d12).
5. To study the mechanism by which *NPR3* and *CAT* genes might contribute to metabolic alterations such as inflammation, insulin resistance or oxidative stress.
6. To study the role of the synthetic ligand C-ANP₄₋₂₃, a ring-deleted analogue of ANP and which specifically interacts with NPR3, on glucose metabolism in human differentiated adipocytes.
7. To study the contribution of catalase activity to the protection against the progression of inflammation, oxidative stress and adipocyte metabolism dysfunction by using the irreversible CAT inhibitor 3-amino-1,2,4-triazole (3-AT) in human differentiated adipocytes.

Materials and methods

Materials and methods

Materials

ADSCs were purchased directly from Lonza (Poietics™ Normal ADSCs, Lonza, *PT-5006*, Lot 0F4505, Switzerland). These commercially available ADSCs are isolated from normal (non-diabetic) adult subcutaneous lipoaspirates collected during elective surgical liposuction procedures. ADSCs have been reported to differentiate into many different lineages, including chondrogenic, osteogenic, adipogenic and neural lineages. Adipogenesis media and reagents were also obtained from Lonza. Oil Red O was acquired from Sigma (234117, Sigma-Aldrich, St. Louis, MO, USA). C-ANP₄₋₂₃ (H3134), ANP (H2095) and CNP-22 (H1296) were purchased from Peninsula Laboratories (Bachem AG, Switzerland). An adenylate cyclase inhibitor (SQ22536, T2678), adenosine 3',5'-cyclic monophosphate (cAMP) (A9501) and 3-amino-1,2,4-triazole (3-AT) (A8056) were acquired from Sigma (Sigma-Aldrich, St. Louis, MO, USA). The rabbit anti-GLUT4 antibody (H-61) and TNF- α antibody (SC-52746) were acquired from Santa Cruz Biotechnology (Santa Cruz, CA, USA); the goat anti-adiponectin antibody (AF1065) was obtained from R&D Systems (R&D, Inc. USA), the rabbit anti-PPAR- γ (D69), phosphor-NF-kB p65 (Ser536), the rabbit anti-total AMPK α (D5A2) and rabbit anti-phospho-AMPK α (Thr172) antibodies were acquired from Cell Signaling Technologies (Beverly, MA, USA), and the mouse anti- α -tubulin antibody (T5158) and horseradish

peroxidase-conjugated immunoglobulin were purchased from Sigma. Unless otherwise indicated, all other chemicals were purchased from Sigma.

Cell culture

ADSCs were cultured, expanded and differentiated into adipocytes according to the manufacturer's recommendations (Lonza). Briefly, ADSCs were grown and expanded in appropriate sterile plastic dishes in complete Advanced-Dulbecco's modified eagle medium (DMEM) (Gibco, Life Technologies, Spain) supplemented with 2 mM L-glutamine (25030, Gibco), 10 % fetal bovine serum (FBS, PT-9000 H, Lonza), 100 U ml⁻¹ of penicillin and 100 µg ml⁻¹ of streptomycin (10378-016, Gibco). The cells were incubated at 37°C in a humidified atmosphere containing 5 % CO₂. The cell culture medium was replaced twice per week, and the cells were passaged a maximum of 6 times. To induce differentiation, the cells were seeded in 35-mm dishes at a density of 30 000 cells/cm² and cultured in preadipocyte growth medium (PGM) consisting of Preadipocyte Basal Medium-2 (PT-8002, Lonza) supplemented with 10 % FBS, 2 mM L-Glutamine (PT-9001 H, Lonza) and 0.1 µg ml⁻¹ Gentamicin Sulfate Amphotericin-B (PT-4504, Lonza). At 90 % confluency, the growth medium was replaced with differentiation medium (PGM supplemented with dexamethasone (DEX), 3-isobutyl-1-methylxanthine (IBMX), indomethacin and h-insulin, PT-9502, Lonza). ADSCs were differentiated for 12 days and samples were taken at the different times (days 0, 5, 9 and 12).

Oil Red O staining assay

Adipogenesis was monitored and quantified via morphological examination of the cellular accumulation of lipid droplets at the different times (d0, d5, d9 and d12) by Oil Red O staining assay. Oil Red O stock was prepared by dissolving 500 mg Oil Red O in 100 mL of isopropanol at room temperature and subsequently filtered with a filter paper. For a working solution, the stock was diluted in distilled water (3:2, v/v). Cells were washed twice with phosphate buffer saline (PBS) and fixed with 4% formaldehyde in PBS for 30 min. Subsequently, the cells were washed once with PBS and then twice with 60% isopropanol. When cells were completely dried, they were incubated with Oil Red O working solution at room temperature for 10 min, after which they were washed thrice with PBS and imaged using a light microscopy. To yield a quantitative measure of lipid accumulation, the optical density of the eluted Oil-Red O stain was quantified with 100 % isopropanol, and the optical density at 550 nm were measured using a microplate reader (BioTek HTX, Fischer Scientific, USA).

Experiments for the study of NPR3 using C-ANP₄₋₂₃ as synthetic ligand

In order to test the appropriate concentration and incubation time of C-ANP₄₋₂₃, the cells were treated with different concentrations (50 nM, 1 μ M and 5 μ M) and incubation times (30 min, 4h and 6h) (Supplementary figure S3). The selected experimental conditions, based on the intracellular cAMP levels results, were 1 μ M of C-ANP₄₋₂₃ and 4 hours of incubation. Subsequently, the cells were treated with 100 μ M SQ22536 for 30 min, in the presence or absence C-ANP₄₋₂₃, as described below. The appropriate

concentration and incubation time of SQ22536 were obtained from the available literature (Santangelo *et al.* 2011). All treatments were performed on differentiated adipocytes at day 10.

Experiments for the study of CAT using the inhibitor 3-amino-1,2,4-triazole (3-AT)

In relation to characterize the toxicity of 3-AT in human differentiated adipocytes, we monitored the cellular viability in adipocytes exposed for 24 h to increasing concentrations of 3-AT (0, 2, 6, 10, 50 and 100 mM) using a Neubauer chamber and trypan blue (4%), and no toxicity was observed for the tested range of 3-AT (Supplementary figure S6). Then, taking into consideration this information as well as the available literature (Mukherjee *et al.* 1982, May *et al.* 1982, Kumar *et al.* 2010), we chose the concentrations of 2 mM and 10 mM 3-AT to test their effect on catalase activity in human differentiated adipocytes. 3-AT was able to significantly inhibit catalase activity in a dose-dependent manner producing an analogous increase in H₂O₂ levels (Results section, chapter 3). However, 10 mM 3-AT was able to generate a significantly higher increase in H₂O₂ than 2 mM 3-AT. According to these results, the final chosen condition for the following experiments was 10 mM 3-AT for 24 hours.

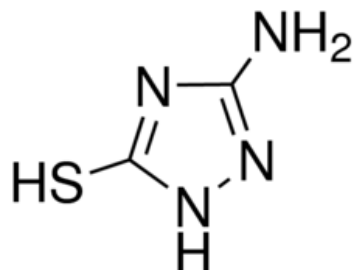


Figure 7.3-amino-1,2,4-triazole (3-AT) chemical structure.

Intracellular cAMP and cGMP level determination

Human differentiated adipocytes were incubated in the presence or absence of C-ANP₄₋₂₃, and the intracellular cAMP and cGMP levels were determined using the commercial cAMP (ADI-900-163, Enzo Life Science, Switzerland) and cGMP (ADI-900-164, Enzo Life Science, Switzerland) ELISA kits. In additional experiments, the cells were incubated in SQ22536 prior to treatment with or without C-ANP₄₋₂₃, followed by determination of the intracellular cAMP levels using the aforementioned kit.

Protein kinase A (PKA) activity assay

Human differentiated adipocytes were incubated in the presence or absence of C-ANP₄₋₂₃, and Protein kinase A (PKA) activity was determined using the PKA kinase activity kit (ADI-EKS-390A, Enzo Life Science, Switzerland). Moreover, the cells were incubated in SQ22536 prior to treatment with or without C-ANP₄₋₂₃, followed by determination of PKA activity using the aforementioned kit.

Additionally, human differentiated adipocytes were incubated in the presence or absence of 10 mM 3-AT for 24 hours and cell lysates were obtained with PLB as previously described. Then, Protein kinase A (PKA) activity was determined after incubating the cell lysates with or without cAMP (0.1 mM) for 15 min.

Lipolysis assay

The total level of glycerol, the final product of lipolysis, was measured in cell supernatants using a colorimetric assay (Free Glycerol Reagent, F6428, Sigma-Aldrich, St. Louis, MO, USA). In the study of C-ANP₄₋₂₃, the cells were treated with 1 μ M C-ANP₄₋₂₃ and with 1 μ M ANP as a positive control during 4 hours, and the cell supernatants were harvested. Similarly, the cells were treated with 3-AT (10 mM) for 24 h and the cell supernatants were harvested. Then, the cell supernatants were incubated in the reagent at room temperature for 15 min in a 96-well plate, and the optical density was measured using a microplate reader (BioTek HTX) at 550 nm.

Catalase activity assay

Human differentiated adipocytes were incubated in the presence or absence of 3-AT (2 mM and 10 mM) for 24 hours, and the catalase activity was determined in cell lysates using a colorimetric assay (K033-H1, Arbor assays, Michigan, USA). Briefly, the cells were harvested lysed with protein lysis buffer (PLB) containing 10 mM Tris-HCl (pH 7.5), 150 mM NaCl, 2 mM EDTA, 1% Triton X-100, 10% glycerol and protease inhibitor cocktail (Thermo Scientific, Massachusetts, USA) and placed on ice for 20 min. Then, the cell lysate was centrifuged (30 min, 13000 $\times g$, 4°C), and the supernatant was used to determine the protein concentration with the Protein Assay Kit II (Bio-Rad Laboratories, California, USA), performed according to the manufacturer's instructions. A bovine catalase standard was used to generate a standard curve for the assay. Next, hydrogen peroxide was added to the supernatant and incubated at room temperature for 30 minutes. The HRP reacts with the substrate in the presence of hydrogen peroxide to

convert the colorless substrate into a pink-colored product. All samples were read off from the standard curve and the activity of catalase in each sample was calculated after making the appropriate corrections for dilutions, using the software available with the plate reader. The results were presented as units of catalase activity per mg protein. Sensitivity was determined as 0.052 U/mL and the limit of detection was determined as 0.062 U/mL.

Intracellular H₂O₂ determination

The generation of intracellular H₂O₂ in the presence or absence of 3-AT (2 mM and 10 mM) for 24 hours by adipocytes was measured in cell lysates using the OxiSelect fluorometric assay (Cell Biolabs, San Diego, CA, USA). Cell lysates were incubated, and the fluorescence was measured with a microplate reader in standard 96-well fluorescence black microtiter plates using an excitation wavelength of 530 nm and a detection wavelength of 590 nm. Intracellular H₂O₂ results were expressed as μ M of H₂O₂.

Superoxide dismutase and glutathione peroxidase activities assays

SOD and GPX activities were determined spectrophotometrically in cell lysates of adipocytes in the presence or absence of 3-AT (10 mM) for 24 hours, using two commercial kits (K028-H1 for SOD, Arbor assays, Michigan, USA; 703102 for GPX, Cayman Chemical, Michigan, USA). Samples were harvested with PLB, diluted in the buffer diluents and then added to the wells with the rest of the reagents. The SOD activity assay was performed according to the manufacturer's instructions. The absorbance was measured at 450 nm and the results were expressed in terms of the

units of SOD activity per mg protein. Sensitivity was determined as 0.044 U/mL and the limit of detection was determined as 0.0625 U/mL. GPX activity was measured indirectly by a coupled reaction with glutathione reductase (GR). Oxidized glutathione (GSSG), produced upon reduction of cumene hydroperoxide by GPX, and is recycled to its reduced state by GR and NADPH. The oxidation of NADPH to NADP⁺ is accompanied by a decrease in absorbance at 340 nm. Thus, the rate of decrease is directly proportional to the GPX activity in the sample. The results were expressed in nmol/min/mg protein. Sensitivity was determined as 0.02 of decreased absorbance per minute and the limit of detection was determined as 50 nmol/min/mL.

GSH/GSSG ratio detection assay

Reduced and oxidized glutathione GSH/GSSG ratio of cell lysates was measured with a fluorometric kit (ab138881, Abcam, Cambridge, UK). GSH and total glutathione were determined by changes in fluorescence intensity, and GSSG concentration was calculated using total glutathione – GSH. The results were expressed as GSH/GSSG ratios in the presence or absence of 3-AT (10 mM) for 24 h in human differentiated adipocytes.

Quantitation of intracellular IL-6 protein levels

The intracellular IL-6 levels were determined in cell lysates in the presence or absence of 10 mM 3-AT for 24 hours. Samples were harvested with PLB, diluted in the buffer diluents and then added to the wells with the rest of the reagents. IL-6 was determined using a MILLIplex™ kit

(HADK2MAG-61K-05), with the Luminex 200 multiplex assay system built on xMAP technology (Millipore, USA). Results were calculated as pg per mg protein and, the bars were represented as units of IL-6 adjusted to control, taken as %.

Glucose uptake assays

Glucose uptake was determined using a colorimetric assay kit (MAK083, Sigma-Aldrich). Briefly, ADSCs were differentiated in 12-well plates as described above. Differentiated adipocytes were washed twice with PBS and then starved in serum-free medium overnight. Then, the cells were washed 3 times with PBS and glucose-starved via incubation in KRPH buffer (5 mM Na₂HPO₄, 20 mM HEPES, pH 7.4, 1 mM MgSO₄, 1 mM CaCl₂, 137 mM NaCl and 4.7 mM KCl) containing 2 % BSA for 40 min. Glucose uptake was assessed in the presence or absence of C-ANP₄₋₂₃ with 1 mM 2-deoxy-D-glucose in KRPH for 20 min at 37 °C and 5 % CO₂. As a positive control, the cells were stimulated with insulin (1 μM) for 20 min. Moreover, glucose uptake assay was assessed in the presence or absence of 3-AT for the CAT study. The results are expressed in pmol/well.

RNA isolation and qRT-PCR

Total RNA was extracted from cells using the PeqGOLD HP Total RNA kit (Peqlab, Germany). Isolated RNA was treated with Turbo DNase (Ambion, Life Technologies, Carlsbad, CA, USA). The final RNA concentration and quality were determined using a NanoDrop2000 device (NanoDrop Technologies, Winooski, Vermont, USA). Total RNA (500 ng)

was transcribed into cDNA using the iScript cDNA Synthesis Kit (Bio-Rad Laboratories, California, USA). Differential gene expression of natriuretic peptide receptor 3 (*NPR3*), peroxisome proliferator-activated receptor gamma (*PPAR γ*), leptin (*LEP*), adiponectin (*ADIPOQ*), catalase (*CAT*), hormone sensitive lipase (*HSL*), adipose triglyceride lipase (*ATGL*), adipocyte fatty acid-binding protein (*FABP4*), perilipin (*PLIN*) and uncoupled protein 1 (*UCP1*) expression levels were determined via qPCR using glyceraldehyde 3-phosphate dehydrogenase (*GAPDH*) as a reference gene, and the quantification was performed using the Pfaffl method (Pfaffl *et al.* 2001). The specific primers for *NPR3*, *PPAR γ* , *LEP*, *ADIPOQ*, *CAT*, *HSL*, *ATGL*, *FABP4*, *PLIN*, *UCP1* and *GAPDH* were designed using Primer3 (<http://bioinfo.ut.ee/primer3-0.4.0/>) (Table 1). Hypoxanthine-guanine phosphoribosyltransferase-1 (*HPRT1*) was used for 3-AT treatment experiments, as *GAPDH* is not a suitable reference gene when glucose metabolism is altered. Primers for *GLUT4*, *IL-6*, *TNF- α* , *NFKB2* and tumor necrosis factor receptor superfamily, member 1A (*TNFRSF1A*), glutathione peroxidase 4 (*GPX4*), peroxiredoxin 1 (*PRDX1*), peroxiredoxin 3 (*PRDX3*), peroxiredoxin 5 (*PRDX5*), catenin beta 1 (*CTNNB1*), *FOXO1*, Nrf2 (*NFE2L2*), superoxide dismutase 1, soluble (*SOD1*), natriuretic peptide receptor 1 (*NPR1*) and natriuretic peptide receptor 2 (*NPR2*) were acquired from Bio-Rad Laboratories, California, USA. The qPCR was performed with an ABI Prism 7900 instrument (Applied Biosystems, Foster City, CA, USA) using SYBR Green PCR Master Mix (Applied Biosystems, Foster City, CA, USA). Quantification was performed using the Pfaffl method (Pfaffl *et al.*

2001). Results are expressed as fold changes calculated using the $2^{-\Delta\Delta Ct}$ method.

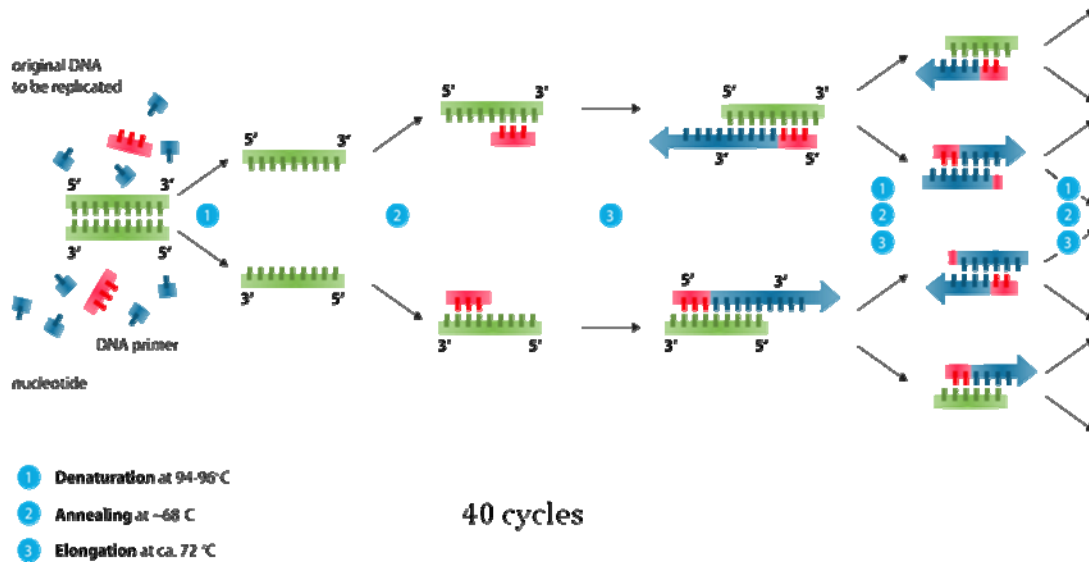


Figure 8. Diagram of polymerase chain reaction (PCR). The PCR process generally consists of a series of temperature changes that are repeated 40 times. These cycles normally consist of three stages: the first, at around 95 °C, allows the separation of the nucleic acids double chain; the second, at a temperature of around 50-60 °C, allows the binding of the primers with the DNA template; the third, at between 68 - 72 °C, facilitates the polymerization carried out by the DNA polymerase. Due to the small size of the fragments the last step is usually omitted in this type of PCR as the enzyme is able to increase either number during the change between the alignment stage and the denaturing stage.

Differential gene expression in human differentiated adipocytes after incubation in C-ANP₄₋₂₃ was determined via Human PCR Arrays (Bio-Rad Laboratories, California, USA). Each array comprised primer pairs that were specific to nineteen selected genes related to the insulin, inflammation, adipogenesis and lipolytic signalling pathways. *GAPDH* and *HPRT1* were used as reference genes. qPCR was performed in an ABI-7500H (Applied Biosystems, University of Granada, Spain). The data were analysed using PrimePCR analysis software, version 1.0 (Bio-Rad Laboratories, California,

USA). Bio-Rad's PrimePCR assays make the minimum information for publication of quantitative real-time-PCR experiments (MIQE) compliance easy. Statistical validation of reference genes stability was calculated in each sample. Bio-Rad recommends using a <0.5 value, which is the most stable expression in the tested samples. The results are expressed as the fold-change in expression and were calculated using the $2^{-\Delta\Delta C_t}$ method.

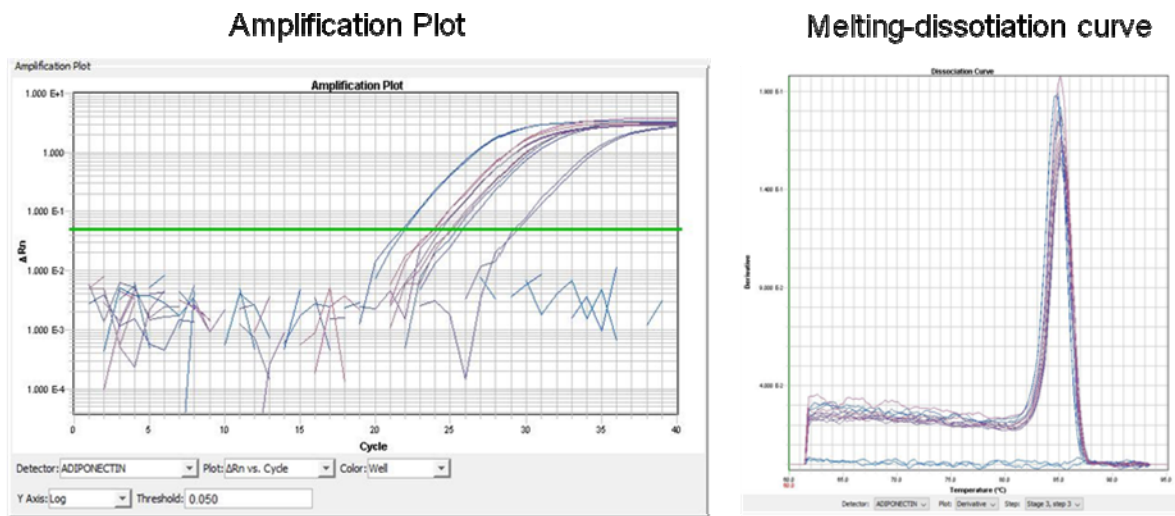


Figure 9. Amplification plot and melting-dissociation curve of a real-time PCR by using Sybr green in a ABI-7900HT instrument. The temperatures and the timings used for each cycle depend on a wide variety of parameters, such as: the enzyme used to synthesize the DNA, the concentration of divalent ions and deoxyribonucleotides (dNTPs) in the reaction and the bonding temperature of the primers.

Table 1. Forward and reverse primer sequences used in the qPCR assays.

Gene	Primer sequence		Size (bp)
	Forward	Reverse	
<i>CAT</i>	5'-GCCTGGGACCCAATTATCTT-3'	5'-GAATCTCCGCACTTCTCCAG-3'	203
<i>HSL</i>	5'CTTCTGGAAAGCCTTCTGGAACATCACCGA-3'	5'-CTGAGCTCCTCACTGTCCTGTCCTTCAC-3'	249
<i>ATGL</i>	5'-GACGAGCTCATCCAGGCCAATGTCTG-3'	5'-GATGGTGTTCCTTAAGCTCATAGAGTGGCAGG-3'	141
<i>PPARγ</i>	5'-CTCGAGGACACCGGAGAGG-3'	5'-CACGGAGCTGATCCCAAAGT-3'	121
<i>FABP4</i>	5'-GCTTTTGTAGGTACCTGGAAACTT-3'	5'-ACACTGATGATCATGTTAGGTTTGG-3'	125
<i>PLIN</i>	5'-CTCTCGATACACCGTGCAGA-3'	5'-TGGTCCTCATGATCCTCCTC-3'	207
<i>GAPDH</i>	5'GAGTCAACGGATTTGGTCGT-3'	5'-TTGATTTTGGAGGGATCTCG-3'	238

HPRT1 5'GAGATGGGAGGCCATCACATTGTAGCCCTC-3' 5'CTCCACCAATTACTTTTATGTCCCCTGTTGACTGGTC3'

NPR3 5'-GGAGACCGATATGGGGATTT-3' 5'-CACTGCCGATTCTTCTAGGC-3'

LEP 5'-GTTGCAAGGCCCAAGAAGCCCA-3' 5'-CAGTGTCTGGTCCATCTTGGATAAGGTCAGG-3'

ADIPOQ 5'-GGCCGTGATGGCAGAGAT-3' 5'-CCTTCAGCCCGGGTACT--3'

UCP1 5'-TGGAATAGCGGCGTGCTTG-3' 5'-CTCATCAGATTGGGAGTAG-3'

CAT, Catalase; HSL, Hormone sensitive lipase; ATGL, Adipose triglyceride lipase; PPAR γ , Peroxisome proliferator-activated receptor gamma; FABP4, Fatty acid binding protein 4, adipocyte; PLIN, Perilipin; GAPDH, Glyceraldehyde 3-phosphate dehydrogenase; HPRT1, Hypoxanthine-guanine phosphoribosyltransferase-1; LEP, Leptin; ADIPOQ, Adiponectin; UCP1, Uncoupled protein 1.

Western blot assays

The cells were harvested in 10 mM Tris-HCl (pH 7.5), 150 mM NaCl, 2 mM EDTA, 1 % Triton X-100, 10 % glycerol and protease inhibitor cocktail (Thermo Scientific) and were placed on ice for 20 min. After centrifugation (30 min, 13 000 g, 4°C), the protein content in the supernatant was determined using the Protein Assay Kit II (Bio-Rad Laboratories, California, USA). Samples containing 2.5 µg of protein were mixed with 3X SDS-PAGE sample buffer (100 mM Tris-HCl, pH 6.8, 25% SDS, 0.4 % bromophenol blue, 10 % β-mercaptoethanol and 2 % glycerol), separated via SDS-PAGE using a TGX Any kD gel (Bio-Rad Laboratories, California, USA) and transferred to a nitrocellulose membrane (Bio-Rad Laboratories, California, USA) (**Figure 9**). After incubation in blocking buffer (5 % non-fat milk and 1 % Tween 20 in Tris-buffered saline (TBS), the membranes were probed with the following antibodies: anti-GLUT4 (1:100 in 5 % non-fat milk), anti-total AMPKα, anti-phosphorylated AMPKα (phospho-AMPKα T172) (both 1:1000 in 5 % BSA), anti-catalase (1:2000 in 5% non-fat milk), anti-adiponectin (1:500 in 5% bovine serum albumin, BSA), anti-PPAR-γ (1:1000 in 5% BSA), anti-TNFα (1:100 in 5% BSA), anti-phospho-NF-kB p65 (Ser536) (1:500 in 5% BSA) and anti-α-tubulin (internal control; 1:4000 in 5 % non-fat milk). Immunoreactive signals were detected via enhanced chemiluminescence (SuperSignal West Dura Chemiluminescent Substrate, 34075, Thermo Scientific, Europe), and the membranes were digitally imaged and analysed using ImageJ software for densitometric analysis. The results are expressed as the fold-change in expression relative to the control.



Figure 10. Western blot equipment from Bio-rad

Statistical analysis

All experiments were repeated at least three times. In each independent experiment, two replicates were performed. Data are expressed as the mean \pm standard error of the mean (SEM). Significant differences in the levels of gene and protein expressions, intracellular cAMP, catalase activity, intracellular H₂O₂, SOD activity, GPX activity, gene and protein expression, lipolysis and glucose uptake were determined using the non-parametric Mann-Whitney U test; statistical significance was defined as * $P < 0.05$; ** $P < 0.01$. Statistical analyses were performed using SPSS version 22, for Windows (SPSS, Chicago, IL, USA).

Results

Chapter 1:

Literature Review

Cell Models and Their Application for Studying Adipogenic Differentiation in Relation to Obesity: A Review.

Ruiz-Ojeda FJ, Rupérez AI, Gomez-Llorente C, Gil A,
Aguilera CM.

International Journal of Molecular Sciences. **2016**; 17(7),
1040

Impact Factor 2015: **3,257**



Review

Cell Models and Their Application for Studying Adipogenic Differentiation in Relation to Obesity: A Review

Francisco Javier Ruiz-Ojeda^{1,2}, Azahara Iris Rupérez¹, Carolina Gomez-Llorente^{1,2,3}, Angel Gil^{1,2,3} and Concepción María Aguilera^{1,2,3,*}

- ¹ Department of Biochemistry and Molecular Biology II, School of Pharmacy, Campus de Cartuja s/n, 18071, Institute of Nutrition and Food Technology “José Mataix”, Center of Biomedical Research, Avenida del Conocimiento s/n, 18016, University of Granada, Granada 18071, Spain; fruizojeda@ugr.es (F.J.R.-O.); azahararuperez@ugr.es (A.I.R.); gomezll@ugr.es (C.G.-L.); agil@ugr.es (A.G.)
- ² Instituto de Investigación Biosanitaria ibs, Complejo Hospitalario Universitario de Granada/Universidad de Granada, Granada 18014, Spain
- ³ CIBEROBN (Physiopathology of Obesity and Nutrition CB12/03/30038), Instituto de Salud Carlos III (ISCIII), Madrid 28029, Spain
- * Correspondence: caguiler@ugr.es; Tel.: +34-958-241-000 (ext. 20314)

Academic Editor: Toshiro Arai

Received: 24 May 2016; Accepted: 24 June 2016; Published: 30 June 2016

Abstract: Over the last several years, the increasing prevalence of obesity has favored an intense study of adipose tissue biology and the precise mechanisms involved in adipocyte differentiation and adipogenesis. Adipocyte commitment and differentiation are complex processes, which can be investigated thanks to the development of diverse in vitro cell models and molecular biology techniques that allow for a better understanding of adipogenesis and adipocyte dysfunction associated with obesity. The aim of the present work was to update the different animal and human cell culture models available for studying the in vitro adipogenic differentiation process related to obesity and its co-morbidities. The main characteristics, new protocols, and applications of the cell models used to study the adipogenesis in the last five years have been extensively revised. Moreover, we depict co-cultures and three-dimensional cultures, given their utility to understand the connections between adipocytes and their surrounding cells in adipose tissue.

Keywords: adipocytes; beige cells; brown adipose tissue; cell culture techniques; cell differentiation; in vitro techniques; obesity; white adipose tissue

1. Introduction

Obesity is one of the most important public health burdens both in developed and developing countries. It is characterized by an excessive accumulation of fat mass in white adipose tissue (WAT), which can occur through an increase in adipocyte volume (hypertrophy), number (hyperplasia), or a combination of both (hypertrophy–hyperplasia) [1].

Adipose tissue contains adipocytes in addition to a wide population of cells, such as macrophages, fibroblasts, pericytes, blood cells, endothelial cells, smooth muscle cells, mesenchymal stem cells (MSCs), and adipose precursor cells. All of these cells are located in the stromal vascular fraction (SVF), and the cell composition and phenotype of the SVF are usually different depending on the location of the adipose tissue and the adiposity [1,2].

Two types of adipose tissue, “white” and “brown”, have been described [1]. WAT is the principle site for safe energy storage, but it is also an endocrine organ that secretes cytokines and adipokines [3,4]. In the context of obesity, WAT is characterized by the presence of inflammation

and oxidative stress associated with insulin resistance, which leads to systemic alterations such as metabolic syndrome [5,6]. In contrast, brown adipose tissue (BAT) is specialized in fat burning for heat generation and energy expenditure related to thermogenesis and to defend against cold and, eventually, obesity. Brown adipocytes promote energy expenditure via mitochondrial uncoupling protein 1 (UCP-1). An intermediate type of adipocytes that expresses UCP-1 has also been described. This type of adipocyte is referred to as beige or “*brite*” (brown in white) adipocytes and regarded as a non-classical/inducible brown adipocyte [7,8].

Adipocytes are derived from MSCs, which differentiate into lipoblasts, then into preadipocytes, and finally into mature adipocytes [9]. Adipocyte differentiation is a complex and multi-step process involving a cascade of transcription factors for key proteins that induce gene expression and lead to adipocyte development. During adipogenesis, fibroblast-like preadipocytes differentiate into lipid-laden and insulin-responsive adipocytes [10]. It is well known that peroxisome proliferator-activated receptor gamma (PPAR- γ), CCAAT/enhancer-binding proteins (C/EBPs), and sterol regulatory element binding protein (SREBP) transcription factors are the major determinants of adipocyte fate [11]. Interestingly, it has been reported that the isoform-2 of PPAR- γ (PPAR- γ 2) is implicated in metabolic alterations such as obesity, insulin resistance, type 2 diabetes, and dyslipidemia. The PPAR- γ 2 isoform is highly present in adipose tissue and functions to promote adipocyte differentiation and triacylglycerols storage [12].

Since the 1970s, the differentiation of fibroblast cell lines into adipocytes has been extensively studied [1]. The ability to study this process in a tissue culture dish has enabled the exploration of general cellular mechanisms. In the last few years, different cell culture models and protocols have become available to study adipocyte biology [13–15] as revised by Armani et al. [16] and Poulos et al. [17]. Mature adipocytes, MSCs, and preadipocytes can be easily isolated from adipose tissue homogenates and used for research purposes. Moreover, adipocytes may also be allowed to dedifferentiate into lipid-free multipotent cells, referred to as dedifferentiated fat (DFAT) cells.

The aim of the present work was to update the different animal and human cell culture models available for studying the *in vitro* adipogenic differentiation process as it is related to obesity and its co-morbidities. The main advantages, disadvantages, new protocols, and applications of the cell models used to study adipogenesis in the last five years have been extensively revised. Moreover, we depict co-cultures and three-dimensional cultures given their utility to understand the connections between adipocytes and their surrounding cells in adipose tissue.

2. Methodology

A comprehensive search of the relevant literature was performed in electronic databases: MEDLINE through PubMed (U.S. National Library of Medicine and the NIH). The following phrases were included in the search of the literature over the last five years (PubMed): differentiat* and adipocyte* and obesity and adipogen* and (“cell culture techniques” (MeSH) OR “cell line” (MeSH) OR preadipocyte* OR primary OR “adipocyte progenitor” OR “adipocyte precursor”). A total of 628 results in English were obtained, from which 568 articles were selected and categorized as works conducted with animal cell models and human cell models. Inclusion was based upon the use of cellular *in vitro* models to study the adipogenesis process related to obesity and its co-morbidities. Then, articles were classified according to the different cell types and applications. Additionally, previous original articles and reviews focusing on different cell lines useful for the study of adipogenesis in the context of obesity were carefully examined.

3. Animal Cell Models

Preadipose cells and mature adipocytes from different animals have been studied over the last several years. The most commonly used cells have traditionally been from rodents, although feline or porcine cells have also been used to a lesser extent. Although studies in animal models of obesity and

related metabolic diseases offer significant insights, their applicability to humans is actually limited by the existing differences in their metabolism and physiology [18].

Primary preadipocytes are fibroblast-shaped cells that, under the appropriate conditions, can differentiate into mature adipocytes. Adipogenesis can be divided in two main phases: commitment and terminal differentiation. Adipogenic stimuli induce the differentiation in committed preadipocytes to an adipocyte phenotype prior to expressing some markers that include the PPAR γ and C/EBP family of regulators. Once preadipocytes have committed to the adipogenesis program, a transcriptional cascade is activated that induces the expression of metabolic genes and adipokines associated with the adipocyte phenotypes, such as fatty acid-binding protein 4 (FABP4, also known as AP2), glucose transporter 4 (GLUT4, also known as SLC2A4), leptin, and adiponectin [19]. Murine preadipocytes have been commonly used to study various aspects of adipocyte biology and adipogenesis. Several major advantages of primary cultures are that they can be derived from various locations or depots and from animals of different ages to examine depot- or age-dependent adipogenic or secretory mechanisms, whereas preadipocyte cell lines are incapable of addressing these aspects [20]. Nevertheless, these models have several limitations such as they do not propagate in culture; they are more difficult to transfect with DNA; they have a huge triacylglycerol store that interferes with biochemical and microscopy analyses; they vary as a result of the genetics and conditions of the animals from which they are isolated; and the isolation procedure is tedious [21]. Additionally, differences exist between bovine, porcine, human, rat, and mouse preadipocytes such as 3T3-L1, 3T3-F442A, and C3H10T1/2 stromal cells (Table 1 and Figure 1).

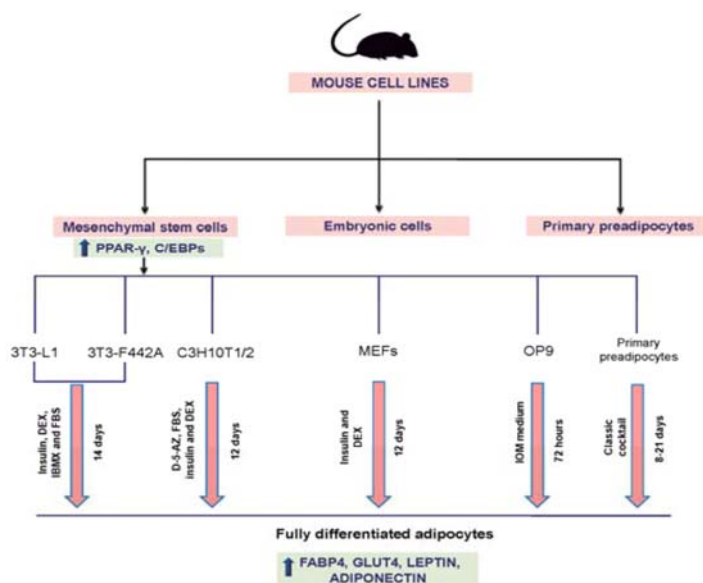


Figure 1. Mouse cell lines to study the adipogenesis process. DEX, dexamethasone; FBS, fetalbovineserum; IBMX, 3-isobutyl-1-methylxanthine; D-5-AZ, demethylating agent 5-azacytidine; IOMmedium, 10% FBS, 175 nM Insulin, 0.25 m MDEX, 0.5 m MIBMX, 2 mM L-glutamine, 100 U/mL penicillin, and 100 mg/mL streptomycin.

3.1. 3T3-L1 Mouse Cell Line

The 3T3-L1 cell line is a well-established preadipose cell line that was developed from murine Swiss 3T3 cells [22]. The 3T3-L1 cells are derived from disaggregated 17- to 19-day-old Swiss 3T3 mouse embryos, which display a fibroblast-like morphology that, under appropriate conditions, can acquire an adipocyte-like phenotype [16,22,23]. Indeed, close to a third of the published articles in the last five years have described the use of 3T3-L1 cells for the study of adipogenesis and obesity-related characteristics.

Table 1. Mouse cell lines to study the adipogenesis process.

Cell Model	Source	Differentiation Time	Characteristics	Differentiation Cocktail	Articles in the Last 5 Years
3T3-L1	Murine Swiss 3T3 cells from embryos	14 days	Easier and less costly to use than freshly isolated cells Stand a high number of passages Homogenous response to treatments and experiments	Insulin, DEX, IBMX and FBS (Green and Meuth 1974 [22]) DEX and troglitazone (Vishwanath et al. [24]) Rosiglitazone (Zebisch et al. [25])	392
3T3-F442A	Murine Swiss 3T3 cells	14 days	More advanced commitment towards adipocyte differentiation than 3T3-L1 cells	Insulin, DEX, IBMX and FBS (Green and Kehinde [23])	7
C3H10T1/2	Mouse embryonic stem cell precursor	12 days	Homogeneous population of multipotent cells More commitment of stem cells towards the adipocyte lineage	Demethylating agent 5-azacytidine and 10% FBS, insulin and DEX (Reznikoff et al. [26])	13
OP9	Mouse stromal cell	72 h	Fast adipogenic differentiation (72 h) Confluent after many passages Long periods in culture suitable for high-throughput screening	IOM medium (Wolins et al. [21])	6
MEFs	Mouse embryonic fibroblasts	14–15 days	Unlimited, undifferentiated proliferation in vitro	Fei medium (Fei et al. [27]) Petrov medium and Bauters medium [28]	9

Abbreviations: Bauters medium, 1.7 μ M insulin, 1 μ M DEX, 0.5 mM IBMX, and 5 μ M rosiglitazone; DEX, dexamethasone; FBS, fetal bovine serum; Fei medium, 0.5 mM IBMX, 1 μ M DEX, 10 μ g/mL insulin, 10 μ M troglitazone, and 10% FBS; IBMX, 3-isobutyl-1-methylxanthine; IOM medium, 10% FBS, 175 nM insulin, 0.25 mM DEX, 0.5 mM IBMX, 2 mM L-glutamine, 100 U/mL penicillin, and 100 mg/mL streptomycin; Petrov medium, 1 μ mol/L DEX, 0.5 mmol/L IBMX, 5 μ g/mL insulin, and 0.5 μ mol/L rosiglitazone.

Generally, to convert 3T3-L1 cells from their fibroblast phenotype into adipocytes, it is necessary to treat them with adipogenic agents, such as insulin, dexamethasone (DEX), and 3-isobutyl-1-methylxanthine (IBMX), which elevates the intracellular cAMP levels in the presence of fetal bovine serum (FBS) [29], at concentrations of 1 $\mu\text{g}/\text{mL}$, 0.25 μM , and 0.5 mM, respectively. Zebisch et al. reported that 3T3-L1 cells can differentiate within 10 to 12 days and persist for at least up to cell culture passage 10 using rosiglitazone (2 μM) as an additional adipogenic agent [25]. Moreover, Vishwanath et al. published a new method that promoted the differentiation of 3T3-L1 preadipocytes over a shorter span of time using a combination of DEX and troglitazone over fewer days compared to the combination of IBMX and DEX with the standard protocol. Moreover, by using DEX and troglitazone, the lipid droplet accumulation increased by 112%, and glucose transporter 4 (GLUT4) mediated a 137% higher glucose uptake compared to cells that were differentiated using the traditional method [24].

One of the main advantages of this cell line is that it is easier to culture and less costly to use than freshly isolated cells, such as mature adipocytes, even though freshly isolated cells allow for various comparisons, such as the *in vitro* evaluation of different *in vivo* conditions. Moreover, they can tolerate an increased number of passages and are homogeneous in terms of the cell population. Therefore, these cells provide a homogenous response following treatments and changes in experimental conditions [17].

Because of this, 3T3-L1 cells have been extensively over the last five years to evaluate the effects of compounds or nutrients on adipogenesis, to establish the underlying molecular mechanisms of adipogenesis and to evaluate the potential application of various compounds and nutrients in the treatment of obesity [30–32]. Particularly, compounds such as quercetin [33,34] and resveratrol [35,36] inhibit adipogenesis in 3T3-L1 adipocytes. Moreover, these cells have been used to describe the effect of melatonin [37], reactive oxygen species (ROS), or antioxidants [38] on adipogenic differentiation [39], and also, the role of some androgens such as testosterone that inhibit the adipogenic differentiation by activation of androgen receptor/ β -catenin/T-cell factor 4 interaction in 3T3-L1 adipocytes [40]. Apart from that, 3T3-L1 cells have been useful to study the mechanisms of action during the differentiation process of several compounds or nutrients that have previously been shown *in vivo* to inhibit obesity [41]. Additionally, several endocrine disruptors and obesogenic compounds have also been evaluated during the differentiation of 3T3-L1 cells [42].

Furthermore, different gene silencing techniques such as siRNA and shRNA, together with different transfection procedures (adenovirus, lentivirus transfection, and plasmid electroporation) have been applied to study the function of different genes associated with adipogenesis in 3T3-L1 cells. In particular, inflammatory pathways, adipokine synthesis, and secretion of study enzyme's function have been investigated through gene silencing in adipocytes [43–47]. These cells have also been useful for deciphering the biological role of several miRNAs, such as miRNA-195a, which plays an essential role in various cellular processes including proliferation and differentiation [48].

Finally, this cell line is useful in the study of co-cultures and three-dimensional cell cultures, as well as diverse studies of high-throughput screening of compounds [49,50].

However, the 3T3-L1 model has several limitations such as the time of initial subculture, in addition to the fact that adipogenic differentiation requires at least two weeks [51]. Moreover, when 3T3-L1 cells become confluent or they have been passaged extensively, they no longer differentiate into adipocytes; they are difficult to transfect; and because this cell line originated from a single clone, it fails to recapitulate the characteristics of primary cell culture models [21].

3.2. 3T3-F442A Mouse Cell Line

Another important cell line derived from murine Swiss 3T3 cells is the 3T3-F442A cell line, which displays a more advanced commitment in the adipocyte lineage than 3T3-L1 due to its isolation from a third selection of clones that converts into fat cells clusters of increased size and at a higher frequency. Thus, 3T3-F442A cells are capable of accumulating more fat than the 3T3-L1 cells, and

an early exposure to glucocorticoids is not necessary to initiate the adipogenic differentiation of the 3T3-F442A cells [9,23]. Regarding in vitro adipogenic differentiation studies, this cell line has been significantly used less than the 3T3-L1 cells, despite the minimal differences between the differentiation protocols of both cell lines. Nevertheless, 3T3-F442A cells have also been used to study the effects of compounds during the differentiation process. Moreover, gene silencing through siRNA has been carried out to study the role of alkaline phosphatase in lipid metabolism and gene expression as well as the secretion of adipokines [52]. Additionally, this cell line has been used to study the effects of some drugs on adipocyte differentiation [53]. Finally, others have reported the effects of a variety of receptors and transcription factors during adipogenic differentiation [54].

In summary, 3T3-L1 and 3T3-F442A cell lines have been well established as good models for studying various aspects of adipogenesis in vitro since 1974, in spite of the described disadvantages of the 3T3-L1 cell line such as adipogenic differentiation time or the difficulty in transfecting these cells.

3.3. OP9 Mouse Cell Line

The OP9 mouse stromal cell line is a new adipocyte cell culture model that provides a tractable alternative for adipogenesis studies. This cell line was established from the calvaria of newborn mice genetically deficient in functional macrophage colony-stimulating factor. OP9 cells are mouse bone marrow-derived stromal cells that accumulate large triacylglycerol filled droplets after only seventy-two hours of adipogenic stimuli, making them a suitable model for high-throughput screening [21,55]. OP9 adipogenic differentiation is a PPAR- γ dependent process, and differentiated cells express PPAR- γ , CEBP α , CEBP β , perilipin 1 (PLIN1), and PLIN4 proteins similar to other adipocyte models [55]. These cells have also been used in co-culture to support hematopoietic cell differentiation from embryonic stem cells [21,56]. Unlike 3T3-L1 cells, OP9 cells are able to differentiate into adipocytes after reaching confluence and are also able to be passaged for long periods of time in culture. Furthermore, they can be differentiated rapidly enough to detect protein expressed from transiently transfected DNA in fully differentiated adipocytes [21].

Three methods can be used to differentiate OP9 preadipocytes into adipocytes: the serum replacement method (SR), the insulin/oleate method (IOM), and the adipogenic cocktail method (AC). In the SR method, the cells are grown to confluence and then cultured for two additional days in OP9 propagation medium containing α -minimum essential medium eagle (α -MEM), FBS, L-glutamine, penicillin, and streptomycin. Then, cells are cultured up to four more days in serum replacement medium containing α -MEM, penicillin, and streptomycin. In the IOM method, when the adherent cells become confluent, the medium is replaced with insulin/oleate medium containing FBS, insulin, DEX, IBMX, L-glutamine, penicillin, and streptomycin. Finally, the AC method is very similar to that of the 3T3-L1 cells where the differentiation medium contains DMEM, FBS, L-glutamine, penicillin, streptomycin, insulin, DEX, and IBMX and the process lasts two days. Differentiated OP9 cells are maintained in OP9 propagation medium [57].

Regarding its applicability in recent studies, the OP9 cell line has been used to evaluate the effects of compounds or nutrients on the adipogenesis process. To this end, Seo et al. explored the mechanisms responsible for the anti-adipogenic activity of quercetin, and its' effects on lipolysis in OP9 cells [58]. Similarly, Kim et al. investigated the inhibitory effects of *Pericarpium zanthoxyli* extract on the adipogenic differentiation of OP9 cells [59]. Another study showed that ascorbic acid, which has been demonstrated to be an adenylate cyclase inhibitor, inhibits adipogenesis in the OP9 cell line [60].

This cell line has also been used to study the role of oxidative stress on the adipogenesis process. The fullerene effects on adipogenesis-accompanying oxidative stress and inflammatory changes were also examined. Xiao et al. [61] demonstrated that hydrogen peroxide stimulates lipid accumulation in 3T3-L1 preadipocytes and that lipid uptake causes ROS generation in OP9 preadipocytes, both of which were then markedly suppressed with fullerene. Additionally, Saitoh et al. [62] investigated the effects of a novel polyhydroxylated fullerene derivate C₆₀(OH)₄₄, which is water-soluble with antioxidant

properties, on intracellular lipid accumulation, intracellular ROS generation, lipid composition, and the protein expression of PPAR- γ in OP9 preadipocytes.

Conversely, Lane et al. investigated the feasibility of OP9 clonal derived cells as a model for rapid drug screening and the effect of gene knockdown on adipogenesis. They established a clonal population of OP9 cells, OP9-K, which differentiate rapidly, robustly, and reproducibly and compared the transcriptome of differentiating OP9-K cells with other models of adipogenesis. The transfection efficiency was 80% in OP9-K cells, and the cells differentiated rapidly and reproducibly into adipocytes. Moreover, they validated the OP9-K cells as an adipocyte model system for microarray analysis of the differentiating transcriptome [55]. One limitation of OP9 cells is that not every protocol may be optimized for adipocyte differentiation and manipulation, and also, that, when maintained at low cell density, OP9 cells adopt a spindly morphology and differentiate into adipocytes poorly.

In summary, the OP9 cell line has a clear potential use as a new model for the study of adipogenesis, and it could be useful for fast high-throughput studies.

3.4. C3H10T1/2 Mouse Cell Line

The C3H10T1/2 cell line was established in 1973 from 14- to 17-day-old C3H mouse embryonic stem cell precursors and has the capacity to differentiate into mesodermal cell types such as adipocytes, chondrocytes, osteoblasts, and myocytes. This cell line displays a fibroblast morphology similar to multipotent MSCs. Adipogenic differentiation can be induced by treatment with the demethylating agent 5'-azacytidine [9,26].

In the last five years, the main applications of C3H10T1/2 cells have focused on evaluating the effects of different compounds on adipogenesis and on investigating the molecular mechanisms related to adipogenic differentiation associated with obesity [63,64]. Specifically, as in the 3T3-L1 cell line, the role of miR-195a as regulator of adipocyte differentiation was studied in C3H10T1/2 cells [48]. Additionally, this cell line has been used for studying food contaminants such as tributyltin, which is an endocrine disrupting compound that promotes adipogenic differentiation in vitro [65]; some androgens, such as testosterone, inhibit adipogenesis in the C3H10T1/2 cell line through an androgen receptor-mediated pathway and β -catenin complex/T-cell factor-4 [40], and the androgen action activated a number of WNT target genes, including the Follistatin (*Fst*) gene (which binds and antagonizes native ligands of the TGF- β /Smad pathway) and cross communication with the Smad signaling pathway [66]; or in gene silencing studies by using shRNA [67]. Finally, the role that bone morphogenetic proteins (BMPs) play on adipogenesis was elucidated by Xue et al. [68] who performed an in vitro study using the C3H10T1/2 cells to investigate BMP4 and BMP7.

3.5. Primary Mouse Embryonic Fibroblasts (MEFs)

Primary mouse embryonic fibroblasts (MEFs) are derived from totipotent cells of early mouse mammalian embryos and are capable of differentiating into adipocytes with variable efficiency (usually 10%–70%), whereas most immortalized MEF lines do not differentiate unless a pro-adipogenic transcription factor such as PPAR- γ or C/EBP α is introduced [69]. MEFs present a number of properties that make them an attractive cell culture model. These cells are easy to establish and maintain, proliferate rapidly, and large numbers of cells can be produced from a single embryo within several days following explantation. Moreover, MEFs can be expanded through several passages. Similar to the primary cultures, MEFs have certain limitations as a consequence of their origin. Therefore, because of the cellular heterogeneity of embryonic tissue, the culture of these cells is often difficult, although steps can be taken to ensure a greater degree of homogeneity. Additionally, primary cultures of MEFs tend to reach senescence around passage 12 [28]. However, the adipogenesis of MEFs cells can be induced for eight days with a standard differentiation induction medium containing 0.5 mM IBMX, 1 μ M DEX, 10 μ g/mL insulin, 10 μ M troglitazone, and 10% (*v/v*) FBS [27].

Recently, MEFs have been used to study adipogenesis in vitro as well as mechanisms related to obesity such as genes or transcription factor implicated in the adipogenesis process, signaling pathways

in adipocytes, or the known fat mass and obesity-associated (*FTO*) gene. In this sense, MEFs derived from *FTO* overexpressing mice exhibited an increased potential for adipogenic differentiation, while MEFs derived from *FTO* knockout mice showed a reduced adipogenesis. Thus, fat pads from *FTO* mice fed a high-fat diet showed an increased number of adipocytes [70]. Conversely, Han et al. studied the role of the unfolded protein response (UPR), a protein associated with oxidative stress, in adipogenesis because UPR is expressed in adipose tissue [71]. Similarly, the role of deadenylase nocturnin (Noc), a protein found to regulate lipid metabolism and to control preadipocyte differentiation, in modulating early adipogenesis was studied in MEFs derived from 13.5-days-old embryos by Hee et al. [72]. Another study performed by Kim et al. [73] using MEFs to study the role of Makorin Ring Finger Protein 1 (MKRN1), which is a negative regulator of PPAR- γ 2 in obesity, indicated that MKRN1 is a potential new therapeutic target in PPAR- γ related diseases. Recently, Braga et al. reported a novel role of *Fst* in regulation of energy/lipid metabolism and modulation of brown adipocytes and MEFs. In differentiated MEFs from *Fst*-KO mice, the induction of brown adipocyte proteins was attenuated, suggesting that *Fst* produced by adipocytes may act in a paracrine manner [74].

In summary, MEF cell lines appear to be a good model to study adipogenesis in vitro because it presents many advantages. However, as with all animal models, the main limitation is the origin (mouse embryos) and the particular physiological characteristics, which differ in a number of aspects from those of human adipocytes.

3.6. Porcine Primary Preadipocytes

Porcine preadipocytes are a much better model for the study of adipogenesis and obesity-related diseases compared to rodent cell models because of their higher similarity to human cells [75]. In porcine cell cultures, lipid-free preadipocytes are recruited during an early DEX period, and then, in the second period, insulin stimulates lipid accretion in the recruited preadipocytes. Although FBS was used for differentiation, it was eventually removed from differentiation medium of porcine cell cultures because it was shown to inhibit differentiation [19].

Porcine preadipocytes have been used as an adipocyte model to study the effects of different effectors on adipocyte dysfunction and metabolism. In this regard, Shu et al. described the role of phloretin, which promotes the differentiation of 3T3-L1 adipocytes, and demonstrated that phloretin enhances the lipid accumulation in a time-dependent manner in porcine primary adipocytes [76]. In another study, primary cultures of pig SVF cells were differentiated to study the effect of temperature on proliferation and differentiation [77]. Furthermore, retinol binding protein 4 (RBP-4) was observed to significantly suppress differentiation in porcine preadipocytes by decreasing the activation of insulin signaling pathways [78]. Pang et al. [79] studied the effects of Akt2 and sirtuin 1 (SIRT-1) on lipogenesis in porcine preadipocytes and its regulatory mechanisms.

This cell model has also been used to study the role of miRNAs. miR-125a, which promoted the differentiation of porcine preadipocytes upon inhibition, may provide new insights into pork quality improvement and obesity control [80]. In contrast, miR-199a, which is highly expressed in porcine subcutaneous fat deposits compared to several other tissue types, was observed to promote cell proliferation while attenuating the lipid deposition in porcine adipocytes [81]. Furthermore, miR-181a overexpression regulates adipogenesis by repressing the tumor necrosis factor- α in porcine preadipocytes, and it may become a new therapeutic target for anti-obesity drugs [82].

Conversely, porcine preadipocytes have been used to study different genes and mechanisms that inhibit adipogenesis. In this sense, Mai et al. described that BMP and activin membrane-bound inhibitor (BAMBI), inhibit adipogenesis through the wntless (Wnt)/ β -catenin pathway in porcine preadipocytes [83]. Additionally, Pang et al. showed that forkhead box-1 (FOXO-1) and its regulation, through C/EBP β and the phosphatidylinositol 3-kinase/glycogen synthase kinase 3- β (PI3K/GSK3 β) signaling pathway, inhibited adipogenesis in porcine preadipocytes isolated from Bamei pigs (an obese breed) and large white pigs (a lean breed) [79].

3.7. Feline Primary Preadipocytes

Similar to porcine preadipocytes, feline preadipocytes have also been used to study adipogenesis *in vitro*. Adipogenesis can be induced in feline preadipocytes with preadipocyte medium containing insulin, DEX, biotin, pantothenate, IBMX, and a PPAR- γ agonist. After seven days, three-fifths of the medium is exchanged with adipocyte medium (lacking IBMX and the PPAR- γ agonist) [84]. Riedel et al. [84] investigated the presence of selected renin-angiotensin system (RAS) components in isolated feline adipocytes. Their results showed the existence of a potentially functional local RAS in feline adipose tissue that is differentially regulated during adipogenesis and dependent on the fat tissue depot and nutritional status. These findings could also be relevant for the understanding of the path-mechanisms in obese cats and dogs and could provide new approaches for the prevention and treatment of obesity-related diseases in cats.

In summary, animal cell models have been widely used to understand adipogenesis *in vitro* over the last several years because they are easier to isolate, less costly, and there are well-established differentiation protocols for the cell lines.

4. Human Cell Models

Although animal cell models have traditionally been the most frequently used for adipogenesis studies, human cells have been rapidly developed and are gaining importance in *in vitro* studies. It is clear that results obtained with human cells are far more reliable than those from animal models because of their applicability towards human diseases such as obesity and its derived metabolic disturbances. In fact, human fat is the origin of these cell models, and it is derived from the SVF, which is formed by a mix of cells including preadipocytes, stem cells, endothelial cells, as well as immunological cells such as macrophages, neutrophils, and lymphocytes [85] (Figure 2).

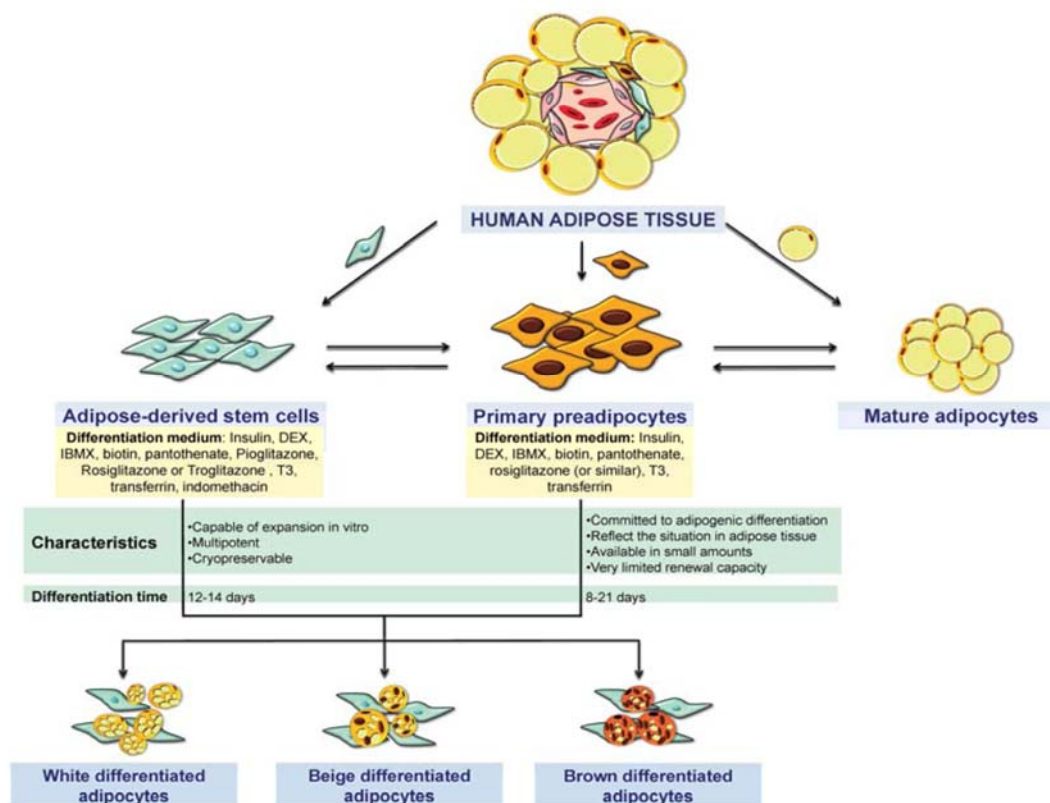


Figure 2. Human models to study the adipogenesis process. DEX, dexamethasone; IBMX, 3-isobutyl-1-methylxanthine; T3, triiodothyronine.

4.1. Adipose-Derived Stem Cells (ASCs)

One of the most important cell types present in the SVF of adipose tissue is adipose-derived stem cells (ADSCs). Different names have been designated to describe this cell population isolated from adipose tissue: Adipose-Derived Stem/Stromal Cells (ASCs), Adipose Derived Adult Stem (ADAS) Cells, Adipose Derived Adult Stromal Cells (ADASC), Adipose Derived Stromal Cells (ADSC), Adipose Stromal Cells (ASC), Adipose Mesenchymal Stem Cells (AdMSC), Lipoblasts, Pericytes, Pre-Adipocytes, and Processed Lipoaspirate (PLA) Cells. Thus, the diverse nomenclature has led to significant confusion in the literature. To address this issue, the International Fat Applied Technology Society reached a consensus to adopt the term “Adipose-Derived Stem Cells” (ASCs) to identify the isolated, plastic adherent, multipotent cell population [86].

The presence of these perivascular cells in adipose tissue was discovered in the last century, when de novo fat formation was first observed [87]. Since then, strong research has been undertaken to characterize the nature of these multipotent stem cells, including their potential to differentiate into numerous cell types (adipocytes, chondrocytes, osteocytes, and myocytes) [86,88], as well as the best method for their isolation, culture, cryopreservation, and expansion [18,89,90]. Finally, ASCs have been distinguished from adherent bone marrow adult stem cells, which are known as MSCs and, recently, multipotent mesenchymal stromal cells (MMSCs) [89].

The main advantages of ASCs are their multipotency, their high expansion capacity, their ability to be passaged a number of times, and their possibility of being cryopreserved for long periods of time [18]. Moreover, they reflect donor- and depot-specific characteristics, which is useful for assessing adipose tissue differences in proliferation or differentiation capacity.

Once differentiated into adipocytes, ASCs display phenotypic characteristics of genuine adipocytes; that is, freshly isolated ones. Specifically, they respond to physiologically relevant concentrations of hormones, including insulin and β -adrenergic agonists. Adipogenic differentiation of ASCs can be induced using culture medium supplemented with 0.5 mM IBMX, 50 μ M indomethacin, and 0.5 μ M DEX. The adipocyte medium needs to be changed every three days until mature adipocytes are obtained after 12–14 days of differentiation [89,91]. Interestingly, it has been proven critical to use a cAMP-elevating agent such as IBMX to obtain a correct adipogenic differentiation of ASCs [92], unlike in murine preadipocyte cell lines, where PPAR- γ agonists, DEX, and insulin are enough to promote adipogenesis.

In the last five years, ASCs have been used to study the effect of different compounds on adipogenesis [93,94]. This cellular model has also been used for the characterization of molecules and cellular processes involved in adipogenesis [95–98]. Moreover, ASCs have served as a tool to investigate the role of different genes associated with adipocyte metabolism [99,100]. Finally, ASCs have also been used for the study of miRNAs [1,101] and browning, because they are capable of converting from white to brown adipocytes [102], which enables the study of the differential effect of certain molecules in white and brown adipogenesis such as p53 [103].

4.2. Primary Preadipocytes

Among the SVF cells, preadipocytes have proven to be an excellent model for the study of adipogenesis and fat cell biology. They can be easily obtained from adipose tissue and, under the appropriate conditions, differentiate into mature adipocytes.

ASCs and preadipocytes share many characteristics such as surface markers and have been used interchangeably in many studies where mixed preadipose cells obtained from the SVF are induced for adipogenesis. However, ASCs and preadipocytes also show some important differences. First, ASCs are Lin⁺/CD29⁺/Sca-1⁺/CD140a⁺, and committed preadipocytes are Lin[–]/CD29⁺/CD34⁺/Sca-1⁺/CD105[–]/CD117[–]/CD24⁺/CD140a[–]. Moreover, as Cawthorn et al. [86] explain in an excellent review, one of the main differences between both cell types is the expression of PPAR- γ by preadipocytes. Moreover, unlike ASCs, which retain a high proliferative and

multiline-age-differentiation capacity, preadipocytes from the SVF are already committed to adipogenic differentiation, meaning that they can only differentiate into adipocytes.

Human primary preadipocytes are an excellent model for the study of adipocyte-related biology and obesity-related alterations because they reflect a situation close to that of adipose tissue. This is due to the presence of depot-specific properties, such as differences in the adipogenic capacity of visceral and subcutaneous preadipocytes, which may involve the existence of additional properties from the depot of origin. Indeed, the fact that they reflect characteristics from their donor makes them useful in studies assessing differences between individuals (obesity, weight-loss, age, etc.) [104–108]. Moreover, human preadipocytes do not require extensive proliferation *in vitro* to differentiate, suggesting that they may have already reached the necessary cell division state *in vivo*. Additionally, the fact that primary preadipocytes successfully differentiate in serum-free conditions allows for the study of specific compounds on adipogenesis, which could be inhibited by highly variable serum components [16].

Despite these advantages, human preadipocytes are usually available in small amounts and have a very limited renewal capacity. In an attempt to overcome this drawback, Darimont et al. [109] expanded the proliferative capacity of human SVF preadipocytes by adding telomerase activity through the co-expression of the h-TERT and E7 oncoprotein from the human papillomavirus type 16 (HPV-E7). It must be taken into account that a higher proliferative capacity is accompanied by a decline in the adipogenic potential as the number of passages increases. Thus, immortalized human preadipocytes require the addition of PPAR- γ agonists to properly accumulate lipids [110].

Preadipocyte adipogenic differentiation protocols are generally divided into an induction period and a maintenance period. The induction period usually lasts three to seven days and is characterized by the presence of insulin, IBMX, a PPAR- γ agonist or indomethacin, and DEX or cortisol (glucocorticoids that activate the glucocorticoid receptor GR). Interestingly, by prolonging the induction period from three to seven days, Lee et al. [111], found a significantly higher proportion of cells with adipocyte morphology together with higher adipogenic marker expression and improved metabolic phenotypes. Lee et al. [111] also studied the impact of 3% FBS on adipogenesis, which was inhibited in a dose-dependent manner, as were the responses to β -adrenergic-stimulated lipolysis. However, the rates of insulin-stimulated glucose uptake were higher in differentiated adipocytes with 3% FBS, whereas the sensitivity to insulin was almost unaltered.

Induction of gene expression in primary human preadipocytes has been achieved by different methods: lentiviral gene transfection [112], adenoviral delivery [113], or plasmid transfection [114]. Conversely, gene silencing has been generally achieved by siRNA delivery [115].

In the last five years, human preadipocytes have been used for many purposes. They have been proven useful for the study of precursor cell commitment and differentiation, a key process that has been found to be altered in hypertrophic obesity [105,113,114]. This cell culture model has also been widely used for the characterization of regulatory molecules implicated in the adipogenic differentiation process [116,117], including depot and disease-dependent differences in adipogenic capacity [104,106,108,118], as already mentioned above. Primary preadipocytes have also been employed to define differences and elucidate the origin and mechanisms behind alterations found in obesity [107–120]. The function of miRNAs on adipogenic differentiation and proliferation [101,121–124] has also been widely investigated in human preadipocytes.

In addition, the mechanisms by which endocrine disruptors increase adipogenesis and obesity has been explored with this cell model [125,126]. In contrast, the effects of different extracts and compounds inhibiting adipogenic differentiation have also been studied in primary human preadipocytes, suggesting potential treatments against obesity-related diseases [127,128].

Finally, primary human preadipocytes have also been used to validate [129] or refute findings from animal adipocyte models [130,131]. These studies imply that findings from studies in adipocyte cell models are extremely dependent on the exact model that is used. Thus, studies with the aim

of elucidating human obesity-related disorders must always validate their findings using human cell models.

5. Brown/Beige Adipose Cell Lines

The interest in brown and beige adipocytes has been centered on the potential of these cell types to be used for the study of metabolic diseases such as obesity and its co-morbidities.

The major BAT depots in rodents are in the interscapular region embedded in and around deep back muscles. The interscapular BAT depots have also been found in human infants, which may decrease with age [132,133]. However, the presence of a metabolically highly active BAT in adult humans has been demonstrated [134]. Moreover, subsequent investigations have shown an inverse association between obesity and type 2 diabetes mellitus and the presence of active BAT [132,135]. Most brown fat cells originate from precursor cells in the embryonic mesoderm that also give rise to skeletal muscle cells and a subpopulation of white adipocytes. These precursors transiently express *Myf5* and *Pax7*, two genes that were previously thought to selectively mark skeletal myogenic cells in the mesoderm. The main activators described for the development of these cells are cold, thiazolidinedione's, natriuretic peptides, thyroid hormone, fibroblast growth factor-21 (FGF-21), BMP7, BMP8b, and orexin. Beige adipocytes are located in the supraclavicular regions in humans and are interspersed within WAT subcutaneous fat in both mice and humans. Moreover, beige adipocytes do not have a history of *Myf5* expression, at least in the subcutaneous depot. It remains unknown whether beige adipocytes come from white adipocytes through trans-differentiation or if they arise from de novo differentiation and maturation of precursors [135]. The main activators described for these cells are the same as BAT activators, plus irisin and other myokines and cytokines, which display a selective action on beige adipocytes [135,136]. Within those myokines, a new small molecule, β -aminoisobutyric acid, has been identified as a critical substance involved in the browning process of WAT [137].

Brown and beige adipogenic differentiation of a variety of animal and human cells can be achieved using specific medium containing supplements such as insulin, DEX, IBMX, rosiglitazone, and triiodothyronine (T3) in different concentrations [102,138–142] (Table 2).

Next, the main brown/beige preadipocytes and adipocytes from animals and humans developed over the last several years as adipocyte models to study the effects of different effectors in brown adipogenesis and some aspects related to obesity and browning in vitro are reviewed.

5.1. Primary Cell Models of Browning

Murine primary brown preadipocytes are primarily isolated from interscapular BAT from mice. These preadipose cells have been useful for studying the effects of compounds on BAT development by promoting brown adipogenesis [143]. In addition, the role of thermogenic genes or transcription factors capable of stimulating brown adipocyte differentiation has also been investigated [144,145].

As for human primary cells, they have also been useful for studying brown fat differentiation, with the primary advantage that human cells are used and, therefore, the results are more reliable. Additionally, there are other sources of primary adipocytes such as the progenitors isolated from human cervical fat, which were used by Lee et al. [146]. They reported that these cells were able to differentiate into adipocytes with either a brown adipocyte-like or white adipocyte phenotype and investigated the role of FGF-21. FGF-21, which is a cold-induced beige adipokine capable of promoting a brown fat-like thermogenic program in WAT, could provide metabolic benefits of therapeutic relevance through browning of white adipose tissue.

Table 2. Brown/beige adipogenic differentiation cocktails.

	Elsen et al [138]	Than et al. [139]	Li et al. [140]	Pisani et al. [102]	Hiroki et al. [141]	Gburcik et al. [142]
Cells	hASC (Subcutaneous AT)	Rat Primary Preadipocytes	Mice Primary Cultures of White and Brown Adipocytes	hMADS	3T3-L1	Brown Adipocytes (3129/Sv Strain of Mice)
<i>Adipogenic induction</i>						
Insulin	66 nM	860 nM	850 nM	850 nM	1.72 nM	2.4 nM
Dexamethasone	5.1 nM	1 nM	1 mM	1 μ M	0.25 μ M	
Indomethacin	125 μ M		125 nM			
IBMX	0.5 mM	0.5 mM	0.5 mM	0.5 mM	0.5 mM	
Rosiglitazone	0.5 μ M	1 mM	1 μ M	0.1 μ M	1 μ M	1 μ M
FBS	10%	10%				10%
T3	1 nM	1 nM	1 nM	0.2 nM	50 nM	
Cortisol	100 nM					
Transferrin				10 μ g/mL		
Apo-transferrin	10 mg/mL					
Gentamycin	50 mg/mL					
Troglitazone	5 μ M					
Ascorbate						
L-Glutamine						25 g/mL
Differentiation Days	14	8	7	14–16	8	4 mM 6

FBS, fetal bovine serum; hASC, human adipose-derived stem cells; hMADS, human mesenchymal adipose-derived stem cells; IBMX, 3-isobutyl-1-methylxanthine; T3, triiodothyronine.

5.2. Brown/Beige Differentiated Adipocytes

Brown adipocytes, like white adipocytes, are derived from multipotent stem cells. Similar to white adipogenic differentiation of different cell models such as 3T3-L1, 3T3-F442A, MSCs, human ASCs, SVF from WAT, and other cell lines, brown/beige adipogenic differentiation of these cell models has also been extensively reported over the last several years. Indeed, 3T3-L1 cells can differentiate into beige adipocytes with the appropriate differentiation cocktail that contains insulin, DEX, IBMX, rosiglitazone, and T3 [141,147–149]. In a similar way, the pluripotent C3H10T1/2 cells have served as a model for the study of the brown adipocyte developmental program by investigating the role of secreted frizzled-related protein 5 (SFRP5), which is a WNT protein inhibitor, in adipogenesis of white and brown adipocytes [150]. Moreover, C3H10T1/2 cells have been used to study the putative role of BMP4 in the differentiation of brown fat-like adipocytes [68]. Murine MSCs are also suitable candidates for BAT formation *de novo*. Sheyn et al., 2013 demonstrated that the transient overexpression of *PPAR- γ 2* and *C/EBP- α* induces BAT because it mediates adipogenic differentiation [151].

Another murine cell line is the H1B-1B brown preadipocyte developed by Spiegelman (Harvard Medical School). The H1B-1B, which is a cell line derived from a brown fat tumor of a transgenic mouse, was the first established brown adipocyte cell line capable of expressing the brown fat-specific mitochondrial protein UCP-1 [152]. Kim et al. [153] studied the role of MKP3 as important factor in the regulation of brown adipocyte differentiation using H1B-1B cells.

As for human models, clones of brown and white preadipocytes from human neck fat have been characterized for their adipogenic and thermogenic differentiation capacity. Xue et al. [154] demonstrated the role of the positive UCP-1 regulators, PREX1 (phosphatidylinositol-3,4,5-triphosphate dependent Rac exchange factor 1) and EDNRB (endothelin receptor type B) for brown differentiation. Additionally, human ASCs are also able to differentiate into functional brown-like adipocytes upon the appropriate stimuli. ASCs from subcutaneous adipose tissue have been able to differentiate into “*brite*” adipocytes for the study of BMP4 on the browning process [138]. Similarly, MSCs from human bone marrow are also able to differentiate into white or brown adipocytes. Huang et al., 2011 investigated the role of PGC-1 α (PPARG coactivator 1 alpha) in brown adipose differentiation. They reported that PGC-1 α could mediate the differentiation of MSCs into brown adipocytes, which was accompanied by an increase in mitochondrial biogenesis and the up-regulation of UCP-1 expression. Because MSCs are multipotent stem cells, they demonstrated that PGC-1 α inhibited the differentiation of MSCs into osteocytes under osteogenic conditions [155].

6. Cell Lines Representative of Various Diseases

6.1. Simpson-Golabi-Behemil Syndrome (SGBS) Cells

Simpson-Golabi-Behemil syndrome (SGBS) is an X-linked congenital overgrowth disease, characterized by macroglossia, macrosomia, renal and skeletal abnormalities, and an increased risk of embryonal cancer [156]. A preadipocyte cell strain was isolated from the stromal cells fraction of subcutaneous adipose tissue of an infant with SGBS. It is important to highlight that, technically, these cells are the only described, fully inducible preadipocyte cell line derived from humans. One of the main advantages of SGBS cells is that they can be considered as an unbounded source of homogenous and fully inducible cells [157,158]. Induction of differentiation from SGBS cells to adipocytes is performed in the presence of insulin, T3, cortisol, and the *PPAR- γ* agonist BRL49653 [157]. Moreover, adipogenic differentiation is carried out in a serum- and albumin-free medium [159].

SGBS cells have the capacity for adipogenic differentiation and, once differentiated, show a gene expression profile comparable to that of mature human fat cells [157]. Fully differentiated SGBS cells present a more similar morphology, transcript level, and biochemical function to primary omental adipocytes than 3T3-L1 cells. Moreover, co-culture of the esophageal adenocarcinoma cell line (OE33) cells with SGBS or primary omental adipocytes induced the differential expression of genes involved in adhesion, angiogenesis, and invasion and metastasis [160]. In addition, using SGBS

cells as preadipocyte and adipocyte models has allowed for the development of a novel high-content analysis procedure for direct visualization and quantification of adipogenesis and adipopoapoptosis by laser scanning cytometry [161].

Recently, the link between the metabolic and gene regulatory networks has been studied using the SGBS cell line and endothelial cells using experimental and computational analyses. Their results reveal the convergence of miRNAs and transcription factors within the branched amino acid metabolic pathway, which provides a possible explanation for its down-regulation in obese and diabetic conditions [162].

In conclusion, the SGBS cell line can be considered as an appropriate model for the study of various aspects of adipocyte differentiation in humans. However, we need to bear in mind that they are derived from a specific syndrome that appears to arise as a result of either deletions or point mutations within the *glypican 3 (GPC3)* genes or by mutations in another currently unknown genes [159].

6.2. LiSa-2 Cells

Another cell model that might serve as a tool to investigate the effects of chemical or food compounds on adipogenesis is the LiSa-2 cell line, a stable cell line derived from a poorly differentiated, pleomorphic liposarcoma. This cell line retains the potential to undergo adipose differentiation [163]. Differentiated LiSa-2 cells display multiple small lipid droplets [164]. Only a few studies have used this cell line. Two studies were focused on the effect of HIV-protease inhibitors and catalase function [165,166]. In addition, another study using these cells described that knockdown of the COP9 signalosome (CNS) elevates the C/EBP homologous protein, which retards adipogenesis [88].

Differences in gene expression between isolated adipocytes and LiSa-2 cells have been observed, particularly in genes involved in fatty acid metabolism. These differences may be explained by the inability of LiSa-2 cells to develop into fully unilocular adipocytes, to their immortality, which may be the cause of the continuous cell growth that is observed during their differentiation and to the lack of essential factors such as nutrients or signaling molecules that are present in vivo and missing in vitro [164].

7. Co-Cultures and Three-Dimensional Cultures (3D)

Co-cultures and three-dimensional (3D) cultures of adipocytes with other cell types (i.e., endothelial cells, macrophages, and muscle cells) are crucial tools for understanding the multiple metabolic connections between fat and other tissues. These studies provide a more real insight into the factors and pathways that may be the target of new pharmacological interventions against obesity and its co-morbidities [16].

Most co-culture studies using adipocytes have been designed to investigate the relationship between obesity and insulin resistance or inflammation. This can be evaluated by co-culturing macrophages and adipocytes because the direct cell-cell contact is capable of inducing an inflammatory response in adipocytes. Accordingly, a co-culture of 3T3-L1 adipocytes and macrophages developed by Huang et al. [49] suggested that phloretin (PT) and phlorizin (PZ), which are natural drugs used to treat diabetes and inhibit adipocyte differentiation, increased lipolysis in adipocytes, and also, suppressed the macrophage inflammatory response that is stimulated by conditioned medium from 3T3-L1 cells. Similarly, Kim et al. [165] carried out a study of the role of esculetin, an anti-inflammatory compound isolated from natural plants, in a co-culture with 3T3-L1 adipocytes and macrophages. This study demonstrated that esculetin exhibited anti-inflammatory properties by inhibiting the production of some cytokines such as TNF- α and MCP-1 in the interaction between adipocytes and macrophages through hemoxygenase-1.

Additionally, an established human model system that combines the THP-1 monocytic cell line, which originates from an acute monocytic leukemia, and the preadipocyte cell strain SGBS was proposed as a useful model to study adipose inflammation in vitro. This co-culture model represents an

inexpensive, highly reproducible human adipose tissue inflammation system, which can be extended for use with primary human macrophages and fat cells [166].

Trying to better resemble the adipose tissue cell plasticity, Chazenbalk et al., 2011 carried out an in vitro co-culture with ASCs and adipose tissue macrophages (ATMs) resulting in a robust proliferation of preadipocytes. Moreover, these new preadipocytes were observed to rapidly turn into adipocytes. They demonstrated that the co-culture of adipocytes with ATMs and ASCs increased the formation of new preadipocytes, increased lipid accumulation, and C/EBP α and PPAR- γ gene expression [167]. Regarding the adipogenesis process, it has been reported a co-culture method of preadipocytes with primary subcutaneous and visceral adipocytes to identify molecules that regulate adipocyte differentiation, such as Slc27a1 (Solute Carrier Family 27 (Fatty Acid Transporter), Member 1), vimentin, Ceruloplasmin and Ecm1 (extracellular matrix protein 1) promoted adipocyte differentiation, whereas Got2 (a known cell-surface fatty acid transporter) or Interleukin-1 receptor like 1 decreased the differentiation. These findings demonstrated a regulation of adipocyte differentiation through positive or negative and autocrine feedback loop mechanisms [168].

The biological significance of 3D cell culture in understanding cellular behavior and function is highlighted by studies with various cell types. Consequently, 3D adipocyte cultures have been developed to better understand the role of adipocytes in adipogenesis and the treatment of obesity over the last several years. Regarding inflammation, a 3D spheroid organization of adipose cells was reproduced by culturing 3T3-L1 preadipocytes on an elastin-like polyethyleneimine (ELP-PEI)-coated surface. This work investigated the cellular responses to a pro-inflammatory stimulus, indicating a more differentiated phenotype in 3D spheroid cultures relative to two-dimensional (2D) monolayer analogs. Therefore, this 3D spheroid model with enhanced adipogenic differentiation features a platform for elucidating the key phenotypic responses that occur in pro-inflammatory microenvironments that characterize obesogenic states [169].

Recently, significant efforts have been made to understand the biology of BAT and its potential as a new therapeutic target for obesity. In this sense, Unser et al. [170] created "brown-fat-in-microstands" by encapsulating brown preadipocytes and pluripotent stem cells in 3D alginate hydrogel microstrands and directly differentiating them into functional brown adipocytes. Accordingly, they used mouse embryonic stem cells, which were used as the model to test the feasibility of 3D brown adipogenesis in alginate microstrands. The microstrands expressed the brown adipocyte-defining marker UCP-1 and exhibited characteristics of brown adipocyte activation in response to β -adrenergic agonists.

Finally, some efforts have been made to provide the cells with a more physiologically relevant environment by using surface-structure and 3D culture systems. Thus, Brännmark et al. [171] investigated the effect of using aligned and randomly oriented polycaprolactone fibers matrices for large cell populations of ASCs differentiated into adipocytes by measuring proliferation, glucose uptake, gene expression, and lipolysis. Moreover, those results were compared with human primary mature adipocytes demonstrating an increased maturity of this adipocyte cell model using ASCs differentiation on aligned polycaprolactone fiber matrices compared to classic cultured cells.

8. Conclusions

The present review focuses on the available cellular models useful for evaluating the adipogenesis process and adipocyte differentiation in vitro related to obesity and adipocyte dysfunction. Recently, new cell lines and protocols have appeared to improve adipocyte culture, such as the OP9 cell line and other models to study the brown/beige adipocytes. However, the 3T3-L1 cells remain to be the most commonly used cell model for studying adipogenesis in vitro because the protocols for these cells are highly developed and standardized. In contrast, results arising from these studies are not as useful for applications on human health as human cell lines, given the physiological and metabolic differences between species. In particular, human preadipocytes and ASCs have become excellent models for studying adipogenesis and obesity-related metabolic alterations as well as for studying adipocyte renewal and expansion and donor and depot-specific differences. Finally, co-cultures and

3D cultures are essential for the better understanding of the connections between adipocytes and their surrounding cells in both health and disease situations. The main limitation of the current models is the great diversity of protocols for some cell lines, such as, for instance, the precise concentration of the compounds needed in the adipogenic differentiation cocktail.

Acknowledgments: This work was supported by Junta de Andalucía (project number CTS-6770; Secretaría General de Universidades, Investigación y Tecnología. Consejería de Economía, Innovación y Ciencia. Implicaciones biológicas de genes de las vías de señalización de la insulina, inflamación y de la matriz extracelular en cultivos de células madre mesenquimales de tejido adiposo humano). Francisco Javier Ruiz-Ojedawas funded by a Formación de Profesorado Universitario (FPU) stipend from the Ministry of Education and Science of the Spanish Government (AP2012-02068). This paper will be part of Francisco Javier Ruiz-Ojeda's doctorate, which is being completed as part of the "Nutrition and Food Sciences Program" at the University of Granada, Spain.

Author Contributions: Francisco Javier Ruiz-Ojeda, Azahara Iris Rupérez, Carolina Gomez-Llorente, Angel Gil and Concepción María Aguilera contributed to the planning of the literature search, designed the analysis and presentation of the results, created the tool for assessing the quality of the articles, and were involved in the analyses of the articles. Francisco Javier Ruiz-Ojeda and Azahara Iris Rupérez wrote the manuscript. All authors discussed and revised drafts and approved the final manuscript.

Conflicts of Interest: The authors declare no conflict of interest.

References

1. Wang, Q.A.; Scherer, P.E.; Gupta, R.K. Improved methodologies for the study of adipose biology: Insights gained and opportunities ahead. *J. Lipid Res.* **2014**, *55*, 605–624. [[CrossRef](#)] [[PubMed](#)]
2. Li, G.; Yao, W.; Jiang, H. Short-chain fatty acids enhance adipocyte differentiation in the stromal vascular fraction of porcine adipose tissue. *J. Nutr.* **2014**, *144*, 1887–1895. [[CrossRef](#)] [[PubMed](#)]
3. Ouchi, N.; Parker, J.L.; Lugus, J.J.; Walsh, K. Adipokines in inflammation and metabolic disease. *Nat. Rev. Immunol.* **2011**, *11*, 85–97. [[CrossRef](#)] [[PubMed](#)]
4. Baraban, E.; Chavakis, T.; Hamilton, B.S.; Sales, S.; Wabitsch, M.; Bornstein, S.R.; Ehrhart-Bornstein, M. Anti-inflammatory properties of bone morphogenetic protein 4 in human adipocytes. *Int. J. Obes.* **2016**, *40*, 319–327. [[CrossRef](#)] [[PubMed](#)]
5. Wensveen, F.M.; Valentić, S.; Šestan, M.; TurkWensveen, T.; Polić, B. The "Big Bang" in obese fat: Events initiating obesity-induced adipose tissue inflammation. *Eur. J. Immunol.* **2015**, *45*, 2446–2456. [[CrossRef](#)] [[PubMed](#)]
6. Boyer, W.R.; Johnson, T.M.; Fitzhugh, E.C.; Richardson, M.R.; Churilla, J.R. The associations between increasing degrees of homeostatic model assessment for insulin resistance and muscular strengthening activities among euglycaemic US adults. *Diabetes Vasc. Dis. Res.* **2015**, *12*, 420–427. [[CrossRef](#)] [[PubMed](#)]
7. Wu, J.; Boström, P.; Sparks, L.M.; Ye, L.; Choi, J.H.; Giang, A.H.; Khandekar, M.; Virtanen, K.A.; Nuutila, P.; Schaart, G.; et al. Beige adipocytes are a distinct type of thermogenic fat cell in mouse and human. *Cell* **2012**, *150*, 366–376. [[CrossRef](#)] [[PubMed](#)]
8. Xu, S.; Chen, P.; Sun, L. Regulatory networks of non-coding RNAs in brown/beige adipogenesis. *Biosci. Rep.* **2015**, *35*. [[CrossRef](#)] [[PubMed](#)]
9. Gregoire, F.M.; Smas, C.M.; Sul, H.S. Understanding adipocyte differentiation. *Physiol. Rev.* **1998**, *78*, 783–809. [[PubMed](#)]
10. Lefterova, M.I.; Lazar, M.A. New developments in adipogenesis. *Cell* **2009**, *20*, 107–114. [[CrossRef](#)] [[PubMed](#)]
11. Moseti, D.; Regassa, A.; Kim, W.K. Molecular Regulation of Adipogenesis and Potential Anti-Adipogenic Bioactive Molecules. *Int. J. Mol. Sci.* **2016**, *17*. [[CrossRef](#)] [[PubMed](#)]
12. Saraf, N.; Sharma, P.K.; Mondal, S.C.; Vipin, K.G.; Singh, A.K. Role of PPARγ2 transcription factor in thiazolidinedione-induced insulin sensitization. *J. Pharm. Pharmacol.* **2012**, *64*, 161–171. [[CrossRef](#)] [[PubMed](#)]
13. Klein, J.; Fasshauer, M.; Klein, H.H.; Benito, M.; Kahn, C.R. Novel adipocyte lines from brown fat: A model system for the study of differentiation, energy metabolism, and insulin action. *Bioessays* **2002**, *24*, 382–388. [[CrossRef](#)] [[PubMed](#)]
14. Sorisky, A. From preadipocyte to adipocyte: Differentiation-directed signals of insulin from the cell surface to the nucleus. *Crit. Rev. Clin. Lab. Sci.* **1999**, *36*, 1–34. [[CrossRef](#)] [[PubMed](#)]

15. Dodson, M.V.; Vierck, J.L.; Hossner, K.L.; Byrne, K.; McNamara, J.P. The development and utility of a defined muscle and fat co-culture system. *Tissue Cell* **1997**, *29*, 517–524. [[CrossRef](#)]
16. Armani, A.; Mammi, C.; Marzolla, V.; Calanchini, M.; Antelmi, A.; Rosano, G.M.; Fabbri, A.; Caprio, M. Cellular models for understanding adipogenesis, adipose dysfunction, and obesity. *J. Cell. Biochem.* **2010**, *110*, 564–572. [[CrossRef](#)] [[PubMed](#)]
17. Poulos, S.P.; Dodson, M.V.; Hausman, G.J. Cell line models for differentiation: Preadipocytes and adipocytes. *Exp. Biol. Med.* **2010**, *35*, 1185–1193. [[CrossRef](#)] [[PubMed](#)]
18. Lee, M.J.; Fried, S.K. Optimal Protocol for the Differentiation and Metabolic Analysis of Human Adipose Stromal Cells. *Methods Enzymol.* **2014**, *538*, 49–65. [[PubMed](#)]
19. Cristancho, A.G.; Lazar, M.A. Forming functional fat: A growing understanding of adipocyte differentiation. *Nat. Rev. Mol. Cell Biol.* **2011**, *12*, 722–734. [[CrossRef](#)] [[PubMed](#)]
20. Hausman, G.J.; Basu, U.; Wei, S.; Hausman, D.B.; Dodson, M.V. Preadipocyte and Adipose Tissue Differentiation in Meat Animals: Influence of Species and Anatomical Location *Annu. Rev. Anim. Biosci.* **2014**, *2*, 323–351. [[CrossRef](#)] [[PubMed](#)]
21. Wolins, N.E.; Quaynor, B.K.; Skinne, J.R. OP9 mouse stromal cells rapidly differentiate into adipocytes: Characterization of a useful new model of adipogenesis. *J. Lipid Res.* **2006**, *47*, 450–460. [[CrossRef](#)] [[PubMed](#)]
22. Green, H.; Meuth, M. An established pre-adipose cell line and its differentiation in culture. *Cell* **1974**, *3*, 127–133. [[CrossRef](#)]
23. Green, H.; Kehinde, O. Spontaneous heritable changes leading to increased adipose conversion in 3T3 cells. *Cell* **1976**, *7*, 105–113. [[CrossRef](#)]
24. Vishwanath, D.; Srinivasan, H.; Patil, M.S.; Seetarama, S.; Kumar, S.A.; Dixit, M.N. Novel method to differentiate 3T3 L1 cells in vitro to produce highly sensitive adipocytes for a GLUT4 mediated glucose uptake using fluorescent glucose analog. *J. Cell Commun. Signal.* **2013**, *7*, 129–140. [[CrossRef](#)] [[PubMed](#)]
25. Zebisch, K.; Voigt, V.; Wabitsch, M.; Brandsch, M. Protocol for effective differentiation of 3T3-L1 cells to adipocytes. *Anal. Biochem.* **2012**, *425*, 88–90. [[CrossRef](#)] [[PubMed](#)]
26. Reznikoff, C.A.; Brankow, D.W.; Heidelberger, C. Establishment and characterization of a cloned line of C3H mouse embryo cells sensitive to post confluence inhibition of division. *Cancer Res.* **1973**, *33*, 3231–3238. [[PubMed](#)]
27. Fei, Z.; Bera, T.K.; Liu, X.; Xiang, L.; Pastan, I. *Ankrd26* Gene Disruption Enhances Adipogenesis of Mouse Embryonic Fibroblasts. *J. Biol. Chem.* **2011**, *286*, 27761–27768. [[CrossRef](#)] [[PubMed](#)]
28. Garfield, A.S. Derivation of Primary Mouse Embryonic Fibroblast (PMEF) Cultures. *Methods Mol. Biol.* **2010**, *633*, 19–27. [[PubMed](#)]
29. Caprio, M.; Fève, B.; Claës, A.; Viengchareun, S.; Lombès, M.; Zennaro, M.C. Pivotal role of the mineralocorticoid receptor in corticosteroid-induced adipogenesis. *FASEB J.* **2007**, *21*, 2185–2194. [[CrossRef](#)] [[PubMed](#)]
30. Lai, C.S.; Chen, Y.Y.; Lee, P.S.; Kalyanam, N.; Ho, C.T.; Liou, W.S. Bisdemethoxycurcumin Inhibits Adipogenesis in 3T3-L1 Preadipocytes and Suppresses Obesity in High-Fat Diet-Fed C57BL/6 Mice. *J. Agric. Food Chem.* **2016**, *64*, 821–830. [[CrossRef](#)] [[PubMed](#)]
31. Kang, M.C.; Kang, N.; Ko, S.C.; Kim, Y.B.; Jeon, Y.J. Anti-obesity effects of seaweeds of Jeju Island on the differentiation of 3T3-L1 preadipocytes and obese mice fed a high-fat diet. *Food Chem. Toxicol.* **2016**, *90*, 36–44. [[CrossRef](#)] [[PubMed](#)]
32. Tutino, V.; Orlando, A.; Russo, F.; Notarnicola, M. Hydroxytyrosol Inhibits Cannabinoid CB1 Receptor Gene Expression in 3T3-L1 Preadipocyte Cell Line. *J. Cell. Physiol.* **2016**, *231*, 483–489. [[CrossRef](#)] [[PubMed](#)]
33. Okabe, Y.; Shimada, T.; Horikawa, T.; Kinoshita, K.; Koyama, K.; Ichinose, K.; Aburada, M.; Takahashi, K. Suppression of adipocyte hypertrophy by polymethoxyflavonoids isolated from *Kaempferia parviflora*. *Phytomedicine* **2014**, *21*, 800–806. [[CrossRef](#)] [[PubMed](#)]
34. Eseberri, I.; Miranda, J.; Lasa, A.; Churruga, I.; Portillo, M.P. Doses of Quercetin in the Range of Serum Concentrations Exert Delipidating Effects in 3T3-L1 Preadipocytes by Acting on Different Stages of Adipogenesis, but Not in Mature Adipocytes. *Oxid. Med. Cell. Longev.* **2015**, *2015*, 480943. [[CrossRef](#)] [[PubMed](#)]
35. Patel, R.; Apostolatos, A.; Carter, G.; Ajmo, J.; Gali, M.; Cooper, D.R.; You, M.; Bisht, K.S.; Patel, N.A. Protein kinase C δ (PKC δ) splice variants modulate apoptosis pathway in 3T3L1 cells during adipogenesis: Identification of PKC δ II inhibitor. *J. Biol. Chem.* **2013**, *288*, 26834–26846. [[CrossRef](#)] [[PubMed](#)]

36. Chang, C.C.; Lin, K.Y.; Peng, K.Y.; Day, Y.J.; Hung, L.M. Resveratrol exerts anti-obesity effects in high-fat diet obese mice and displays differential dosage effects on cytotoxicity, differentiation, and lipolysis in 3T3-L1 cells. *Endocr. J.* **2015**, *63*, 169–178. [[CrossRef](#)] [[PubMed](#)]
37. Kato, H.; Tanaka, G.; Masuda, S.; Ogasawara, J.; Sakurai, T.; Kizaki, T. Melatonin promotes adipogenesis and mitochondrial biogenesis in 3T3-L1 preadipocytes. *J. Pineal. Res.* **2015**, *59*, 267–275. [[CrossRef](#)] [[PubMed](#)]
38. Calzadilla, P.; Gómez-Serrano, M.; García-Santos, E.; Schiappacasse, A.; Abalde, Y.; Calvo, J.C.; Peral, B.; Guerra, L.N. N-Acetylcysteine affects obesity-related protein expression in 3T3-L1 adipocytes. *Redox. Rep.* **2013**, *18*, 210–218. [[CrossRef](#)] [[PubMed](#)]
39. Matsuo, H.; Kondo, Y.; Kawasaki, T.; Imamura, N. Cineromycin B isolated from *Streptomyces cineromycetorum* inhibits adipocyte differentiation of 3T3-L1 cells via Krüppel-like factors 2 and 3. *Life Sci.* **2015**, *135*, 35–42. [[CrossRef](#)] [[PubMed](#)]
40. Singh, R.; Artaza, J.N.; Taylor, W.E.; Gonzalez-Cadavid, N.F.; Bhasin, S. Androgens stimulate myogenic differentiation and inhibit adipogenesis in C3H10T1/2 pluripotent cells through an androgen receptor-mediated pathway. *Endocrinology* **2003**, *144*, 5081–5088. [[CrossRef](#)] [[PubMed](#)]
41. Mammi, C.; Marzolla, V.; Armani, A.; Feraco, A.; Antelmi, A.; Maslak, E. A novel combined glucocorticoid-mineralocorticoid receptor selective modulator markedly prevents weight gain and fat mass expansion in mice fed a high-fat diet. *Int. J. Obes.* **2016**. [[CrossRef](#)] [[PubMed](#)]
42. Regnier, S.M.; El-Hashani, E.; Kamau, W.; Zhang, X.; Massad, N.L.; Sargis, R.M. Tributyltin differentially promotes development of a phenotypically distinct adipocyte. *Obesity* **2015**, *23*, 1864–1871. [[CrossRef](#)] [[PubMed](#)]
43. Abdesselem, H.; Madani, A.; Hani, A.; Al-Noubi, M.; Goswami, N.; Ben Hamidane, H.; Billing, A.M.; Pasquier, J.; Bonkowski, M.S.; Halabi, N.; et al. SIRT1 Limits Adipocyte Hyperplasia through c-Myc Inhibition. *J. Biol. Chem.* **2016**, *291*, 2119–2135. [[CrossRef](#)] [[PubMed](#)]
44. Ma, X.; Ding, W.; Wang, J.; Wu, G.; Zhang, H.; Yin, J.; Zhou, L.; Li, D. LOC66273 isoform 2, a novel protein highly expressed in white adipose tissue, induces adipogenesis in 3T3-L1 cells. *J. Nutr.* **2012**, *142*, 448–455. [[CrossRef](#)] [[PubMed](#)]
45. Lien, C.C.; Jiang, J.L.; Jian, D.Y.; Kwok, C.F.; Ho, L.T.; Juan, C.C. Chronic endothelin-1 infusion causes adipocyte hyperplasia in rats. *Obesity* **2016**, *24*, 643–653. [[CrossRef](#)] [[PubMed](#)]
46. Lee da, S.; Choi, H.; Han, B.S.; Kim, W.K.; Lee, S.C.; Oh, K.J. c-Jun regulates adipocyte differentiation via the KLF15-mediated mode. *Biochem. Biophys. Res. Commun.* **2016**, *469*, 552–558. [[CrossRef](#)] [[PubMed](#)]
47. An, L.; Pang, Y.W.; Gao, H.M.; Tao, L.; Miao, K.; Wu, Z.H.; Tian, J.H. Heterologous expression of *C. elegans* Fat-1 decreases the N-6/N-3 fatty acid ratio and inhibits adipogenesis in 3T3-L1 cells. *Biochem. Biophys. Res. Commun.* **2012**, *428*, 405–410. [[CrossRef](#)] [[PubMed](#)]
48. Yun, U.J.; Song, N.J.; Yang, D.K.; Kwon, S.M.; Kim, K.; Kim, S. miR-195a inhibits adipocyte differentiation by targeting the preadipogenic determinant Zfp423. *J. Cell. Biochem.* **2015**, *116*, 2589–2597. [[CrossRef](#)] [[PubMed](#)]
49. Huang, W.C.; Chang, W.T.; Wu, S.J.; Xu, P.Y.; Ting, N.C.; Liou, C.J. Phloretin and phlorizin promote lipolysis and inhibit inflammation in mouse 3T3-L1 cells and in macrophage-adipocyte co-cultures. *Mol. Nutr. Food Res.* **2013**, *57*, 1803–1813. [[CrossRef](#)] [[PubMed](#)]
50. Turner, P.A.; Tang, Y.; Weiss, S.J.; Janorkar, A.V. Three-dimensional spheroid cell model of in vitro adipocyte inflammation. *Tissue Eng. Part A* **2015**, *21*, 1837–1847. [[CrossRef](#)] [[PubMed](#)]
51. Student, A.K.; Hsu, R.Y.; Lane, M.D. Induction of fatty acid synthetase synthesis in differentiating 3T3-L1 preadipocytes. *J. Biol. Chem.* **1980**, *255*, 4745–4750. [[PubMed](#)]
52. Hernández-Mosqueira, C.; Velez-delValle, C.; Kuri-Harcuch, W. Tissue alkaline phosphatase is involved in lipid metabolism and gene expression and secretion of adipokines in adipocytes. *Biochim. Biophys. Acta* **2015**, *1850*, 2485–2496. [[CrossRef](#)] [[PubMed](#)]
53. Desarzens, S.; Liao, W.H.; Mammi, C.; Caprio, M.; Faresse, N. Hsp90 blockers inhibit adipocyte differentiation and fat mass accumulation. *PLoS ONE* **2014**, *9*, e94127. [[CrossRef](#)] [[PubMed](#)]
54. Scroyen, I.; Bauters, D.; Vranckx, C.; Lijnen, H.R. The Anti-Adipogenic Potential of COUP-TFII is Mediated by down regulation of the Notch Target Gene Hey1. *PLoS ONE* **2015**, *10*, e0145608. [[CrossRef](#)] [[PubMed](#)]
55. Lane, J.M.; Doyle, J.R.; Fortin, J.P.; Kopin, A.S.; Ordovás, J.M. Development of an OP9 derived cell line as a robust model to rapidly study adipocyte differentiation. *PLoS ONE* **2014**, *9*, e112123. [[CrossRef](#)] [[PubMed](#)]

56. Nakano, T.; Kodama, H.; Honjo, T. Generation of lymphohematopoietic cells from embryonic stem cells in culture. *Science* **1994**, *265*, 1098–1101. [[CrossRef](#)] [[PubMed](#)]
57. Gerhard Vogel, H. *Drug Discovery and Evaluation Pharmacological Assays*, 3rd ed.; Springer Verlag Berlin: Heidelberg, Germany, 2008; pp. 1379–1381.
58. Seo, Y.S.; Kang, O.H.; Kim, S.B.; Mun, S.H.; Kang, D.H.; Yang, D.W.; Choi, J.G.; Lee, Y.M.; Kang, D.K.; Lee, H.S.; et al. Quercetin prevents adipogenesis by regulation of transcriptional factors and lipases in OP9 cells. *Int. J. Mol. Med.* **2015**, *35*, 1779–1785. [[CrossRef](#)] [[PubMed](#)]
59. Kim, H.R.; Kim, J.M.; Kim, M.S.; Hwang, J.K.; Yang, S.H.; Kim, H.J.; Lee, D.S.; Oh, H.; Kim, Y.C.; Ryu, D.G.; et al. Inhibitory effects of *Pericarpium zanthoxyli* extract on adipocyte differentiation. *Int. J. Mol. Med.* **2014**, *33*, 1140–1146. [[CrossRef](#)] [[PubMed](#)]
60. Rahman, F.; Al Frouh, F.; Bordignon, B.; Fraterno, M.; Landrier, J.F.; Peiretti, F.; Fontes, M. Ascorbic acid is a dose-dependent inhibitor of adipocyte differentiation, probably by reducing cAMP pool. *Front. Cell Dev. Biol.* **2014**, *7*, 2–29. [[CrossRef](#)] [[PubMed](#)]
61. Xiao, L.; Aoshima, H.; Saitoh, Y.; Miwa, N. Highly hydroxylated fullerene localizes at the cytoskeleton and inhibits oxidative stress in adipocytes and a subcutaneous adipose-tissue equivalent. *Free. Radic. Biol. Med.* **2011**, *51*, 1376–1389. [[CrossRef](#)] [[PubMed](#)]
62. Saitoh, Y.; Mizuno, H.; Xiao, L.; Hyoudou, S.; Kokubo, K.; Miwa, N. Polyhydroxylated fullerene C(OH) suppresses intracellular lipid accumulation together with repression of intracellular superoxide anion radicals and subsequent PPAR γ 2 expression during spontaneous differentiation of OP9preadipocytes into adipocytes. *Mol. Cell. Biochem.* **2012**, *366*, 191–200. [[CrossRef](#)] [[PubMed](#)]
63. Lee, N.; Kim, I.; Park, S.; Han, D.; Ha, S.; Kwon, M. Creatine inhibits adipogenesis by downregulating insulin-induced activation of the phosphatidylinositol 3-kinase signaling pathway. *Stem Cells Dev.* **2015**, *24*, 983–994. [[CrossRef](#)] [[PubMed](#)]
64. Beg, M.; Chauhan, P.; Varshney, S.; Shankar, K.; Rajan, S.; Saini, D. A withanolide coagulin-L inhibits adipogenesis modulating Wnt/ β -catenin pathway and cell cycle in mitotic clonal expansion. *Phytomedicine* **2014**, *21*, 406–414. [[CrossRef](#)] [[PubMed](#)]
65. Biemann, R.; Fischer, B.; Blüher, M.; Navarrete Santos, A. Tributyltin affects adipogenic cell fate commitment in mesenchymal stem cells by a PPAR γ independent mechanism. *Chem. Biol. Interact.* **2014**, *214*, 1–9. [[CrossRef](#)] [[PubMed](#)]
66. Singh, R.; Bhasin, S.; Braga, M.; Artaza, J.N.; Pervin, S.; Taylor, W.E.; Krishnan, V.; Sinha, S.K.; Rajavashisth, T.B.; Jasuja, R. Regulation of myogenic differentiation by androgens: Cross talk between androgen receptor/ β -catenin and follistatin/transforming growth factor- β signaling pathways. *Endocrinology* **2009**, *150*, 1259–1268. [[CrossRef](#)] [[PubMed](#)]
67. Guo, B.; Chatterjee, S.; Li, L.; Kim, J.M.; Lee, J.; Yechoor, V.K. The clock gene, brain and muscle Arnt-like 1, regulates adipogenesis via Wnt signaling pathway. *FASEB J.* **2012**, *26*, 3453–3463. [[CrossRef](#)] [[PubMed](#)]
68. Xue, R.; Wan, Y.; Zhang, S.; Zhang, Q.; Ye, H.; Li, Y. Role of bone morphogenetic protein 4 in the differentiation of brown fat-like adipocytes. *Am. J. Physiol. Endocrinol. Metab.* **2014**, *306*, 363–372. [[CrossRef](#)] [[PubMed](#)]
69. Rosen, E.D.; MacDougald, O.A. Adipocyte differentiation from the inside out. *Nat. Rev. Mol. Cell Biol.* **2006**, *7*, 885–896. [[CrossRef](#)] [[PubMed](#)]
70. Merkestein, M.; Laber, S.; McMurray, F.; Andrew, D.; Sachse, G.; Sanderson, J.; Li, M.; Usher, S.; Sellayah, D.; Ashcroft, F.M.; et al. *FTO* influences adipogenesis by regulating mitotic clonal expansion. *Nat. Commun.* **2015**, *6*, 6792. [[CrossRef](#)] [[PubMed](#)]
71. Han, J.; Murthy, R.; Wood, B.; Song, B.; Wang, S.; Sun, B.; Malhi, H.; Kaufman, R.J. ER stress signaling through eIF2 α and CHOP, but not IRE1 α , attenuates adipogenesis in mice. *Diabetologia* **2013**, *56*, 911–924. [[CrossRef](#)] [[PubMed](#)]
72. Hee, S.W.; Tsai, S.H.; Chang, Y.C.; Chang, C.J.; Yu, I.S.; Lee, P.C.; Lee, W.J.; Yun-Chia Chang, E.; Chuang, L.M. The role of nocturnin in early adipogenesis and modulation of systemic insulin resistance in human. *Obesity* **2012**, *20*, 1558–1565. [[CrossRef](#)] [[PubMed](#)]
73. Kim, J.H.; Park, K.W.; Lee, E.W.; Jang, W.S.; Seo, J.; Shin, S.; Hwang, K.A.; Song, J. Suppression of PPAR γ through MKRN1-mediated ubiquitination and degradation prevents adipocyte differentiation. *Cell. Death Differ.* **2014**, *21*, 594–603. [[CrossRef](#)] [[PubMed](#)]

74. Braga, M.; Reddy, S.T.; Vergnes, L.; Pervin, S.; Grijalva, V.; Stout, D.; David, J.; Li, X.; Tomasian, V.; Reid, C.B. Follistatin promotes adipocyte differentiation, browning, and energy metabolism. *J. Lipid Res.* **2014**, *55*, 375–384. [CrossRef] [PubMed]
75. Pang, W.; Wang, Y.; Wei, N.; Xu, R.; Xiong, Y.; Wang, P.; Shen, Q.; Yang, G. Sirt1 inhibits Akt2-mediated porcine adipogenesis potentially by direct protein-protein interaction. *PLoS ONE* **2013**, *8*, e71576. [CrossRef] [PubMed]
76. Shu, G.; Lu, N.S.; Zhu, X.T.; Xu, Y.; Du, M.Q.; Xie, Q.P.; Zhu, C.J.; Xu, Q.; Wang, S.B.; Wang, L.N.; et al. Phloretin promotes adipocyte differentiation in vitro and improves glucose homeostasis in vivo. *J. Nutr. Biochem.* **2014**, *25*, 1296–1308. [CrossRef] [PubMed]
77. Bohan, A.E.; Purvis, K.N.; Bartosh, J.L.; Brandebourg, T.D. The proliferation and differentiation of primary pig preadipocytes is suppressed when cultures are incubated at 37° Celsius compared to euthermic conditions in pigs. *Adipocyte* **2014**, *3*, 322–332. [CrossRef] [PubMed]
78. Cheng, J.; Song, Z.Y.; Pu, L.; Yang, H.; Zheng, J.M.; Zhang, Z.Y.; Shi, X.E.; Yang, G.S. Retinol binding protein 4 affects the adipogenesis of porcine preadipocytes through insulin signaling pathways. *Biochem. Cell Biol.* **2013**, *91*, 236–243. [CrossRef] [PubMed]
79. Pang, W.J.; Wei, N.; Wang, Y.; Xiong, Y.; Chen, F.F.; Wu, W.J.; Zhao, C.Z.; Sun, S.D.; Yang, G.S. Obese and lean porcine difference of FoxO1 and its regulation through C/EBP β and PI3K/GSK3 β signaling pathway. *J. Anim. Sci.* **2014**, *92*, 1968–1979. [CrossRef] [PubMed]
80. Ji, H.L.; Song, C.C.; Li, Y.F.; He, J.J.; Li, Y.L.; Zheng, X.L.; Yang, G.S. miR-125a inhibits porcine preadipocytes differentiation by targeting ERK α . *Mol. Cell. Biochem.* **2014**, *395*, 155–165. [CrossRef] [PubMed]
81. Shi, X.E.; Li, Y.F.; Jia, L.; Ji, H.L.; Song, Z.Y.; Cheng, J.; Wu, G.F.; Song, C.C.; Zhang, Q.L.; Zhu, J.Y.; et al. MicroRNA-199a-5p affects porcine preadipocyte proliferation and differentiation. *Int. J. Mol. Sci.* **2014**, *15*, 8526–8538. [CrossRef] [PubMed]
82. Li, H.; Chen, X.; Guan, L.; Qi, Q.; Shu, G.; Jiang, Q.; Yuan, L.; Xi, Q.; Zhang, Y. MiRNA-181a regulates adipogenesis by targeting tumor necrosis factor- α (TNF- α) in the porcine model. *PLoS ONE* **2013**, *8*, e71568.
83. Mai, Y.; Zhang, Z.; Yang, H.; Dong, P.; Chu, G.; Yang, G.; Sun, S. BMP and activin membrane-bound inhibitor (BAMBI) inhibits the adipogenesis of porcine preadipocytes through Wnt/ β -catenin signaling pathway. *Biochem. Cell Biol.* **2014**, *92*, 172–182. [CrossRef] [PubMed]
84. Riedel, J.; Badewien-Rentzsch, B.; Kohn, B.; Hoeke, L.; Einspanier, R. Characterization of key genes of the renin-angiotensin system in mature feline adipocytes and during in vitro adipogenesis. *J. Anim. Physiol. Anim. Nutr.* **2015**. [CrossRef] [PubMed]
85. Esteve Ràfols, M. Adipose tissue: Cell heterogeneity and functional diversity. *Endocrinol. Nutr.* **2014**, *61*, 100–112. [CrossRef] [PubMed]
86. Cawthorn, W.P.; Scheller, E.L.; MacDougald, O.A. Adipose tissue stem cells meet preadipocyte commitment: Going back to the future. *J. Lipid Res.* **2012**, *53*, 227–246. [CrossRef] [PubMed]
87. Clark, E.R.; Clark, E.L. Microscopic studies of the new formation of fat in living adult rabbits. *Am. J. Anat.* **1940**, *67*, 255–285. [CrossRef]
88. Huang, X.; Ordemann, J.; Müller, J.M.; Dubiel, W. The COP9 signalosome, cullin 3 and Keap1 super complex regulates CHOP stability and adipogenesis. *Biol. Open* **2012**, *1*, 705–710. [CrossRef] [PubMed]
89. Bunnell, B.A.; Flaate, M.; Gagliardi, C.; Patel, B.; Ripoll, C. Adipose-derived Stem Cells: Isolation, Expansion and Differentiation. *Methods* **2008**, *45*, 115–120. [CrossRef] [PubMed]
90. Yong, K.W.; Pingguan-Murphy, B.; Xu, F.; Abas, W.A.; Choi, J.R.; Omar, S.Z.; Azmi, M.A.; Chua, K.H.; Wan Safwani, W.K. Phenotypic and functional characterization of long-term cryopreserved human adipose-derived stem cells. *Sci. Rep.* **2015**, *5*. [CrossRef] [PubMed]
91. Diascro, D.D., Jr.; Vogel, R.L.; Johnson, T.E.; Witherup, K.M.; Pitzenberger, S.M.; Rutledge, S.J.; Prescott, D.J.; Rodan, G.A.; Schmidt, A. High fatty acid content in rabbit serum is responsible for the differentiation of osteoblasts into adipocyte-like cells. *J. Bone Miner. Res.* **1998**, *13*, 96–106. [CrossRef] [PubMed]
92. Jia, B.; Madsen, L.; Petersen, R.K.; Techer, N.; Kopperud, R.; Ma, T.; Døskeland, S.O.; Ailhaud, G.; Wang, J.; Amri, E.Z.; et al. Activation of protein kinase A and exchange protein directly activated by cAMP promotes adipocyte differentiation of human mesenchymal stem cells. *PLoS ONE* **2012**, *7*, e34114. [CrossRef] [PubMed]
93. Kang, I.; Kim, Y.; Tomás-Barberán, F.A.; Espín, J.C.; Chung, S. 1-Urolithin A, C and D, but not iso-Urolithin A and Urolithin B, attenuate triglyceride accumulation in human cultures of adipocytes and hepatocytes. *Mol. Nutr. Food Res.* **2016**, *60*, 1129–1138. [CrossRef] [PubMed]

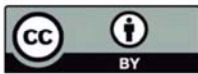
94. Zhao, L.; Yagiz, Y.; Xu, C.; Lu, J.; Chung, S.; Marshall, M.R. Muscadine grape seed oil as a novel source of tocotrienols to reduce adipogenesis and adipocyte inflammation. *Food Funct.* **2015**, *6*, 2293–2302. [[CrossRef](#)] [[PubMed](#)]
95. Xu, Y.; Gu, Y.; Liu, G.; Zhang, F.; Li, J.; Liu, F.; Zhang, Z.; Ye, J.; Li, Q. Cidec promotes the differentiation of human adipocytes by degradation of AMPK α through ubiquitin-proteasome pathway. *Biochim. Biophys. Acta* **2015**, *1850*, 2552–2562. [[CrossRef](#)] [[PubMed](#)]
96. Roca-Rodríguez, M.M.; El Bekay, R.; Garrido-Sánchez, L.; Gómez-Serrano, M.; Coin-Aragüez, L.; Oliva-Olivera, W.; Lhamyani, S.; Clemente-Postigo, M.; García-Santos, E.; de Luna Diaz, R.; et al. Parathyroid Hormone-Related Protein, Human Adipose-Derived Stem Cells Adipogenic Capacity and Healthy Obesity. *J. Clin. Endocrinol. Metab.* **2015**, *100*, 826–835. [[CrossRef](#)] [[PubMed](#)]
97. Narvaez, C.J.; Simmons, K.M.; Brunton, J.; Salinero, A.; Chittur, S.V.; Welsh, J.E. Induction of STEAP4 correlates with 1,25-dihydroxyvitamin D3 stimulation of adipogenesis in mesenchymal progenitor cells derived from human adipose tissue. *J. Cell. Physiol.* **2013**, *228*, 2024–2036. [[CrossRef](#)] [[PubMed](#)]
98. Higuchi, M.; Dusting, G.J.; Peshavariya, H.; Jiang, F.; Hsiao, S.T.; Chan, E.C.; Liu, G.S. Differentiation of human adipose-derived stem cells into fat involves reactive oxygen species and Forkhead box O1 mediated upregulation of antioxidant enzymes. *Stem Cells Dev.* **2013**, *22*, 878–888. [[CrossRef](#)] [[PubMed](#)]
99. Ruiz-Ojeda, F.J.; Gomez-Llorente, C.; Aguilera, C.M.; Gil, A.; Rupérez, A.I. Impact of 3 Amino-1,2,4-Triazole (3-AT)-Derived Increase in Hydrogen Peroxide Levels on Inflammation and Metabolism in Human Differentiated Adipocytes. *PLoS ONE* **2016**, *11*, e0152550. [[CrossRef](#)] [[PubMed](#)]
100. Ruiz-Ojeda, F.J.; Aguilera, C.M.; Rupérez, A.I.; Gil, A.; Gomez-Llorente, C. An analogue of atrial natriuretic peptide (C-ANP₄₋₂₃) modulates glucose metabolism in human differentiated adipocytes. *Mol. Cell. Endocrinol.* **2016**, *431*, 101–108. [[CrossRef](#)] [[PubMed](#)]
101. Yang, L.; Shi, C.M.; Chen, L.; Pang, L.X.; Xu, G.F.; Gu, N.; Zhu, L.J.; Guo, X.R.; Ni, Y.H.; Ji, C.B. The biological effects of hsa-miR-1908 in human adipocytes. *Mol. Biol. Rep.* **2015**, *42*, 927–935. [[CrossRef](#)] [[PubMed](#)]
102. Pisani, D.F.; Djedaini, M.; Beranger, G.E.; Elabd, C.; Scheideler, M.; Ailhaud, G.; Amri, E.Z. Differentiation of Human Adipose-Derived Stem Cells into “Brite” (Brown-in-White) Adipocytes. *Front. Endocrinol.* **2011**, *2*. [[CrossRef](#)] [[PubMed](#)]
103. Molchadsky, A.; Ezra, O.; Amendola, P.G.; Krantz, D.; Kogan-Sakin, I.; Buganim, Y.; Rivlin, N.; Goldfinger, N.; Folgiero, V.; Falcioni, R.; et al. p53 is required for brown adipogenic differentiation and has a protective role against diet-induced obesity. *Cell Death. Differ.* **2013**, *20*, 774–783. [[CrossRef](#)] [[PubMed](#)]
104. Lessard, J.; Laforest, S.; Pelletier, M.; Leboeuf, M.; Blackburn, L.; Tchernof, A. Low abdominal subcutaneous preadipocyte adipogenesis is associated with visceral obesity, visceral adipocyte hypertrophy, and a dysmetabolic state. *Adipocyte* **2014**, *3*, 197–205. [[CrossRef](#)] [[PubMed](#)]
105. Michaud, A.; Lacroix-Pépin, N.; Pelletier, M.; Daris, M.; Biertho, L.; Fortier, M.A.; Tchernof, A. Expression of genes related to prostaglandin synthesis or signaling in human subcutaneous and omental adipose tissue: Depot differences and modulation by adipogenesis. *Mediators Inflamm.* **2014**, *2014*. [[CrossRef](#)] [[PubMed](#)]
106. Park, H.T.; Lee, E.S.; Cheon, Y.P.; Lee, D.R.; Yang, K.S.; Kim, Y.T.; Hur, J.Y.; Kim, S.H.; Lee, K.W.; Kim, T. The relationship between fat depot-specific preadipocyte differentiation and metabolic syndrome in obese women. *Clin. Endocrinol.* **2012**, *76*, 59–66. [[CrossRef](#)] [[PubMed](#)]
107. Carey, A.L.; Vorlander, C.; Reddy-Luthmoodoo, M.; Natoli, A.K.; Formosa, M.F.; Bertovic, D.A.; Anderson, M.J.; Duffy, S.J.; Kingwell, B.A. Reduced UCP-1 content in in vitro differentiated beige/brite adipocytes derived from preadipocytes of human subcutaneous white adipose tissues in obesity. *PLoS ONE* **2014**, *9*, e91997. [[CrossRef](#)] [[PubMed](#)]
108. Rossmeislová, L.; Malisová, L.; Kracmerová, J.; Tencerová, M.; Kováčová, Z.; Koc, M.; Siklová-Vítková, M.; Viquerie, N.; Langin, D.; Stich, V. Weight loss improves the adipogenic capacity of human preadipocytes and modulates their secretory profile. *Diabetes* **2013**, *62*, 1990–1995. [[CrossRef](#)] [[PubMed](#)]
109. Darimont, C.; Macé, K. immortalization of human preadipocytes. *Biochimie* **2003**, *85*, 1231–1233. [[CrossRef](#)] [[PubMed](#)]
110. Church, C.; Brown, M.; Rodeheffer, M.S. Conditional immortalization of primary adipocyte precursor cells. *Adipocyte* **2015**, *4*, 203–211. [[CrossRef](#)] [[PubMed](#)]
111. Lee, M.J.; Wu, Y.; Fried, S.K. A modified protocol to maximize differentiation of human preadipocytes and improve metabolic phenotypes. *Obesity* **2012**, *20*, 2334–2340. [[CrossRef](#)] [[PubMed](#)]

112. Divoux, A.; Karastergiou, K.; Xie, H.; Guo, W.; Perera, R.J.; Fried, S.K.; Smith, S.R. Identification of a novel lncRNA in gluteal adipose tissue and evidence for its positive effect on preadipocyte differentiation. *Obesity* **2014**, *22*, 1781–1785. [[CrossRef](#)] [[PubMed](#)]
113. Fenech, M.; Gavrilovic, J.; Turner, J. Effect of tissue inhibitor of metalloproteinases 3 on DLK1 shedding in cultured human pre-adipocytes and implications for adipose tissue remodelling. *Lancet* **2015**, *385*, S35. [[CrossRef](#)]
114. Gustafson, B.; Hammarstedt, A.; Hedjazifar, S.; Hoffmann, J.M.; Svensson, P.A.; Grimsby, J.; Rondinone, C.; Smith, U. BMP4 and BMP Antagonists Regulate Human White and Beige Adipogenesis. *Diabetes* **2015**, *64*, 1670–1681. [[CrossRef](#)] [[PubMed](#)]
115. Lee, M.J.; Pickering, R.T.; Puri, V. Prolonged efficiency of siRNA-mediated gene silencing in primary cultures of human preadipocytes and adipocytes. *Obesity* **2014**, *22*, 1064–1069. [[CrossRef](#)] [[PubMed](#)]
116. Moreno-Navarrete, J.M.; Serrano, M.; Sabater, M.; Ortega, F.; Serino, M.; Pueyo, N.; Luche, E.; Waget, A.; Rodriguez-Hermosa, J.I.; Ricart, W. Study of lactoferrin gene expression in human and mouse adipose tissue, human preadipocytes and mouse 3T3-L1 fibroblasts. Association with adipogenic and inflammatory markers. *J. Nutr. Biochem.* **2013**, *24*, 1266–1275. [[CrossRef](#)] [[PubMed](#)]
117. Söhle, J.; Machuy, N.; Smailbegovic, E.; Holtzmann, U.; Grönniger, E.; Wenck, H.; Stüb, F.; Winnefeld, M. Identification of new genes involved in human adipogenesis and fat storage. *PLoS ONE* **2012**, *7*, e31193. [[CrossRef](#)] [[PubMed](#)]
118. Veilleux, A.; Côté, J.A.; Blouin, K.; Nadeau, M.; Pelletier, M.; Marceau, P.; Laberge, P.Y.; Luu-The, V.; Tchernof, A. Glucocorticoid-induced androgen inactivation by aldo-keto reductase 1C2 promotes adipogenesis in human preadipocytes. *Am. J. Physiol. Endocrinol. Metab.* **2012**, *302*, E941–E949. [[CrossRef](#)] [[PubMed](#)]
119. Berti, L.; Irmeler, M.; Zdichavsky, M.; Meile, T.; Böhm, A.; Stefan, N.; Fritsche, A.; Beckers, J.; Königsrainer, A.; Häring, H.U.; et al. Fibroblast growth factor 21 is elevated in metabolically unhealthy obesity and affects lipid deposition, adipogenesis, and adipokine secretion of human abdominal subcutaneous adipocytes. *Mol. Metab.* **2015**, *4*, 519–527. [[CrossRef](#)] [[PubMed](#)]
120. Famulla, S.; Schlich, R.; Sell, H.; Eckel, J. Differentiation of human adipocytes at physiological oxygen levels results in increased adiponectin secretion and isoproterenol-stimulated lipolysis. *Adipocyte* **2012**, *1*, 132–181. [[CrossRef](#)] [[PubMed](#)]
121. Xu, G.; Ji, C.; Song, G.; Shi, C.; Shen, Y.; Chen, L.; Yang, L.; Zhao, Y.; Guo, X. Obesity-associated microRNA-26b regulates the proliferation of human preadipocytes via arrest of the G1/S transition. *Mol. Med. Rep.* **2015**, *12*, 3648–3654. [[CrossRef](#)] [[PubMed](#)]
122. Song, G.; Xu, G.; Ji, C.; Shi, C.; Shen, Y.; Chen, L.; Zhu, L.; Yang, L.; Zhao, Y.; Guo, X. The role of microRNA-26b in human adipocyte differentiation and proliferation. *Gene* **2014**, *533*, 481–487. [[CrossRef](#)] [[PubMed](#)]
123. Chen, L.; Dai, Y.M.; Ji, C.B.; Yang, L.; Shi, C.M.; Xu, G.F.; Pang, L.X.; Huang, F.Y.; Zhang, C.M.; Guo, X.R. MiR-146b is a regulator of human visceral preadipocyte proliferation and differentiation and its expression is altered in human obesity. *Mol. Cell. Endocrinol.* **2014**, *393*, 65–74. [[CrossRef](#)] [[PubMed](#)]
124. Zhu, Y.; Zhang, X.; Ding, X.; Wang, H.; Chen, X.; Zhao, H.; Jia, Y.; Liu, S.; Liu, Y. miR-27 inhibits adipocyte differentiation via suppressing CREB expression. *Acta Biochim. Biophys.* **2014**, *46*, 590–596. [[CrossRef](#)] [[PubMed](#)]
125. Boucher, J.G.; Boudreau, A.; Atlas, E. Bisphenol A induces differentiation of human preadipocytes in the absence of glucocorticoid and is inhibited by an estrogen-receptor antagonist. *Nutr. Diabetes* **2014**, *4*, e102. [[CrossRef](#)] [[PubMed](#)]
126. Ellero-Simatos, S.; Claus, S.P.; Benelli, C.; Forest, C.; Letourneur, F.; Cagnard, N.; Beaune, P.H.; de Waziers, I. Combined transcriptomic-(1)H NMR metabolomic study reveals that monoethylhexyl phthalate stimulates adipogenesis and glyceroneogenesis in human adipocytes. *J. Proteome Res.* **2011**, *10*, 5493–5502. [[CrossRef](#)] [[PubMed](#)]
127. You, J.S.; Lee, Y.J.; Kim, K.S.; Kim, S.H.; Chang, K.J. Anti-obesity and hypolipidaemic effects of *Nelumbo nucifera* seed ethanol extract in human pre-adipocytes and rats fed a high-fat diet. *J. Sci. Food Agric.* **2014**, *94*, 568–575. [[CrossRef](#)] [[PubMed](#)]
128. Zhong, S.; Leong, J.; Ye, W.; Xu, P.; Lin, S.H.; Liu, J.Y.; Lin, Y.C. (–)-Gossypol-enriched cottonseed oil inhibits proliferation and adipogenesis of human breast pre-adipocytes. *Anticancer Res.* **2013**, *33*, 949–955. [[PubMed](#)]

129. Todoric, J.; Strobl, B.; Jais, A.; Boucheron, N.; Bayer, M.; Amann, S.; Lindroos, J.; Teperino, R.; Prager, G.; Bilban, M. Cross-talk between interferon- γ and hedgehog signaling regulates adipogenesis. *Diabetes* **2011**, *60*, 1668–1676. [[CrossRef](#)] [[PubMed](#)]
130. Gagnon, A.; Foster, C.; Landry, A.; Sorisky, A. The role of interleukin 1 β in the anti-adipogenic action of macrophages on human preadipocytes. *J. Endocrinol.* **2013**, *217*, 197–206. [[CrossRef](#)] [[PubMed](#)]
131. Dewulf, E.M.; Ge, Q.; Bindels, L.B.; Sohet, F.M.; Cani, P.D.; Brichard, S.M.; Delzenne, N.M. Evaluation of the relationship between GPR43 and adiposity in human. *Nutr. Metab.* **2013**, *10*, 11. [[CrossRef](#)] [[PubMed](#)]
132. Lidell, M.E.; Betz, M.J.; Dahlqvist Leinhard, O.; Heglind, M.; Elander, L.; Slawik, M.; Mussack, T.; Nilsson, D.; Romu, T.; Nuutila, P.; et al. Evidence for two types of brown adipose tissue in humans. *Nat. Med.* **2013**, *19*, 631–634. [[CrossRef](#)] [[PubMed](#)]
133. Pfannenberger, C.; Werner, M.K.; Ripkens, S.; Stef, I.; Deckert, A.; Schmadl, M.; Reimold, M.; Häring, H.U.; Claussen, C.D.; Stefan, N. Impact of age on the relationships of brown adipose tissue with sex and adiposity in humans. *Diabetes* **2010**, *59*, 1789–1793. [[CrossRef](#)] [[PubMed](#)]
134. Nedergaard, J.; Bengtsson, T.; Cannon, B. Unexpected evidence for active brown adipose tissue in adult humans. *Am. J. Physiol. Endocrinol. Metab.* **2007**, *293*, E444–E452. [[CrossRef](#)] [[PubMed](#)]
135. Harms, M.; Seale, P. Brown and beige fat: Development, function and therapeutic potential. *Nat. Med.* **2013**, *19*, 1252–1263. [[CrossRef](#)] [[PubMed](#)]
136. Boström, P.; Wu, J.; Jedrychowski, M.P.; Korde, A.; Ye, L.; Lo, J.C.; Rasbach, K.A.; Boström, E.A.; Choi, J.H.; Long, J.Z. A PGC1- α -dependent myokine that drives brown-fat-like development of white fat and thermogenesis. *Nature* **2012**, *481*, 463–468. [[CrossRef](#)] [[PubMed](#)]
137. Roberts, L.D.; Boström, P.; O’Sullivan, J.F.; Schinzel, R.T.; Lewis, G.D.; Dejam, A.; Lee, Y.K.; Palma, M.J.; Calhoun, S.; Georgiadi, A.; et al. β -Aminoisobutyric acid induces browning of white fat and hepatic β -oxidation and is inversely correlated with cardiometabolic risk factors. *Cell Metab.* **2014**, *19*, 96–108. [[CrossRef](#)] [[PubMed](#)]
138. Elsen, M.; Raschke, S.; Eckel, J. Browning of white fat: Does irisin play a role in humans? *J. Endocrinol.* **2014**, *222*, R25–R38. [[CrossRef](#)] [[PubMed](#)]
139. Than, A.; He, H.L.; Chua, S.H.; Xu, D.; Sun, L.; Leow, M.K.; Chen, P. Apelin enhances brown adipogenesis and browning of white adipocytes. *J. Biol. Chem.* **2015**, *290*, 14679–14691. [[CrossRef](#)] [[PubMed](#)]
140. Li, Y.; Bolze, F.; Fromme, T.; Klingenspor, M. Intrinsic differences in BRITE adipogenesis of primary adipocytes from two different mouse strains. *Biochim. Biophys. Acta* **2014**, *1841*, 1345–1352. [[CrossRef](#)] [[PubMed](#)]
141. Hiroki, A.; Yohei, K.; Satoshi, H.; Takayuki, N.; Ken, K.; Tohru, M.; Masayuki, F. Induction of Beige-Like Adipocytes in 3T3-L1 Cells. *J. Vet. Med. Sci.* **2014**, *76*, 57–64.
142. Gburcik, V.; Cawthorn, W.P.; Nedergaard, J.; Timmons, J.A.; Cannon, B. An essential role for Tbx15 in the differentiation of brown and “brite” but not white adipocytes. *Am. J. Physiol. Endocrinol. Metab.* **2012**, *303*, E1053–E1060. [[CrossRef](#)] [[PubMed](#)]
143. Nam, D.; Chatterjee, S.; Yin, H.; Liu, R.; Lee, J.; Yechoor, V.K.; Ma, K. Novel Function of Rev-erb α in Promoting Brown Adipogenesis. *Sci. Rep.* **2015**, *5*, 11239. [[CrossRef](#)] [[PubMed](#)]
144. Jeong, M.Y.; Kim, H.L.; Park, J.; Jung, Y.; Youn, D.H.; Lee, J.H.; Jin, J.S.; So, H.S.; Park, R.; Kim, S.H.; et al. *Rubi Fructus* (*Rubus coreanus*) activates the expression of thermogenic genes in vivo and in vitro. *Int. J. Obes. (Lond.)* **2015**, *39*, 456–464. [[CrossRef](#)] [[PubMed](#)]
145. Federico, L.; Ren, H.; Mueller, P.A.; Wu, T.; Liu, S.; Popovic, J.; Blalock, E.M.; Sunkara, M.; Ovaas, H.; Albers, H.M.; et al. Autotaxin and its product lysophosphatidic acid suppress brown adipose differentiation and promote diet-induced obesity in mice. *Mol. Endocrinol.* **2012**, *26*, 786–797. [[CrossRef](#)] [[PubMed](#)]
146. Lee, P.; Werner, C.D.; Kebebew, E.; Celi, F.S. Functional thermogenic beige adipogenesis is inducible in human neck fat. *Int. J. Obes.* **2014**, *38*, 170–176. [[CrossRef](#)] [[PubMed](#)]
147. Zhong, X.J.; Shen, X.D.; Wen, J.B.; Kong, Y.; Chu, J.J.; Yan, G.Q.; Li, T.; Liu, D.; Wu, M.Q.; Zeng, G.H.; et al. Osteopontin-induced brown adipogenesis from white preadipocytes through a PI3K-AKT dependent signaling. *Biochem. Biophys. Res. Commun.* **2015**, *459*, 553–559. [[CrossRef](#)] [[PubMed](#)]
148. Sjölund, J.; Pelorosso, F.G.; Quigley, D.A.; Del Rosario, R.; Balmain, A. Identification of Hipk2 as an essential regulator of white fat development. *Proc. Natl. Acad. Sci. USA.* **2014**, *111*, 7373–7378. [[CrossRef](#)] [[PubMed](#)]
149. Baboota, R.K.; Singh, D.P.; Sarma, S.M.; Kaur, J.; Sandhir, R.; Boparai, R.K.; Kondepudi, K.K.; Bishnoi, M. Capsaicin induces “brite” phenotype in differentiating 3T3-L1 preadipocytes. *PLoS ONE* **2014**, *9*, e103093. [[CrossRef](#)] [[PubMed](#)]

150. Wang, R.; Hong, J.; Liu, R.; Chen, M.; Xu, M.; Gu, W.; Zhang, Y.; Ma, Q.; Wang, F.; Shi, J. SFRP5 acts as a mature adipocyte marker but not as a regulator in adipogenesis. *J. Mol. Endocrinol.* **2014**, *53*, 405–415. [CrossRef] [PubMed]
151. Sheyn, D.; Pelled, G.; Tawackoli, W.; Su, S.; Ben-David, S.; Gazit, D.; Gazit, Z. Transient overexpression of Pparg2 and C/ebp α in mesenchymal stem cells induces brown adipose tissue formation. *Regen. Med.* **2013**, *8*, 295–308. [CrossRef] [PubMed]
152. Klaus, S.; Choy, L.; Cham, O. Characterization of the novel brown adipocyte cell line HIB 1B. Adrenergic pathways involved in regulation of uncoupling protein gene expression. *J. Cell Sci.* **1994**, *107*, 313–319. [PubMed]
153. Kim, W.K.; Oh, K.J.; Choi, H.R.; Park, A.; Han, B.S.; Chi, S.W.; Kim, S.J.; Bae, K.H.; Lee, S.C. MAP kinase phosphatase 3 inhibits brown adipocyte differentiation via regulation of Erk phosphorylation. *Mol. Cell. Endocrinol.* **2015**, *416*, 70–76. [CrossRef] [PubMed]
154. Xue, R.; Lynes, M.D.; Dreyfuss, J.M.; Shamsi, F.; Schulz, T.J.; Zhang, H.; Huang, T.L.; Townsend, K.L.; Li, Y.; Takahashi, H.; et al. Clonal analyses and gene profiling identify genetic biomarkers of the thermogenic potential of human brown and white preadipocytes. *Nat. Med.* **2015**, *21*, 760–768. [CrossRef] [PubMed]
155. Huang, P.I.; Chen, Y.C.; Chen, L.H.; Juan, C.C.; Ku, H.H.; Wang, S.T.; Chiou, S.H.; Chiou, G.Y.; Chi, C.W.; Hsu, C.C. PGC-1 α mediates differentiation of mesenchymal stem cells to brown adipose cells. *J. Atheroscler. Thromb.* **2011**, *18*, 966–980. [CrossRef] [PubMed]
156. Golabi, M.; Leung, A.; Lopez, C. *Simpson-Golabi-Behmel Syndrome Type 1*. *Gene. Reviews*; University of Washington: Seattle, DC, USA, 2006; pp. 1993–2016.
157. Wabitsch, M.; Brenner, R.E.; Melzner, I.; Braun, M.; Möller, P.; Heinze, E.; Debatin, K.M.; Hauner, H. Characterization of a human preadipocyte cell strain with high capacity for adipose differentiation. *Int. J. Obes. Relat. Metab. Disord.* **2001**, *25*, 8–15. [CrossRef] [PubMed]
158. Ludewig, A.H.; Klapper, M.; Wabitsch, M.; Döring, F.; Nitz, I. Differential expression of alternative Acyl-CoA binding protein (ACBP) transcripts in an inducible human preadipocyte cell line. *Horm. Metab. Res.* **2011**, *43*, 440–442. [CrossRef] [PubMed]
159. Fischer-Posovszky, P.; Newell, F.S.; Wabitsch, M.; Tornqvist, H.E. Human SGBS cells—A unique tool for studies of human fat cell biology. *Obes. Facts* **2008**, *1*, 184–189. [CrossRef] [PubMed]
160. Allott, E.H.; Oliver, E.; Lysaght, J.; Gray, S.G.; Reynolds, J.V.; Roche, H.M.; Pidgeon, G.P. The SGBS cell strain as a model for the in vitro study of obesity and cancer. *Clin. Transl. Oncol.* **2012**, *14*, 774–782. [CrossRef] [PubMed]
161. Doan-Xuan, Q.M.; Sarvari, A.K.; Fischer-Posovszky, P.; Wabitsch, M.; Balajthy, Z.; Fesus, L.; Bacso, Z. High content analysis of differentiation and cell death in human adipocytes. *Cytometry A* **2013**, *83*, 933–943. [PubMed]
162. Galhardo, M.; Sinkkonen, L.; Berninger, P.; Lin, J.; Sauter, T.; Heinäniemi. Integrated analysis of transcript-level regulation of metabolism reveal as disease-relevant nodes of the human metabolic network. *Nucleic Acids Res.* **2014**, *42*, 1474–1496. [CrossRef] [PubMed]
163. Wabitsch, M.; Brüderlein, S.; Melzner, I.; Braun, M.; Mechttersheimer, G.; Möller, P. LiSa-2, a novel human liposarcoma cell line with a high capacity for terminal adipose differentiation. *Int. J. Cancer.* **2000**, *88*, 889–894. [CrossRef]
164. Van Beek, E.A.; Bakker, A.H.; Kruyt, P.M.; Vink, C.; Saris, W.H.; Franssen-van Hal, N.L.; Keijer, J. Comparative expression analysis of isolated human adipocytes and the human adipose cell lines LiSa-2 and PAZ6. *Int. J. Obes.* **2008**, *32*, 912–921. [CrossRef] [PubMed]
165. Kim, Y.; Park, Y.; Namkoong, S.; Lee, J. Esculetin inhibits the inflammatory response by inducing heme oxygenase-1 in cocultured macrophages and adipocytes. *Food Funct.* **2014**, *5*, 2371–2377. [CrossRef] [PubMed]
166. Keuper, M.; Dzyakanchuk, A.; Amrein, K.E.; Wabitsch, M.; Fischer-Posovszky, P. THP-1 Macrophages and SGBS Adipocytes—A New Human in vitro Model System of Inflamed Adipose Tissue. *Front. Endocrinol.* **2011**, *2*. [CrossRef] [PubMed]
167. Chazenbalk, G.; Bertolotto, C.; Heneidi, S.; Jumabay, M.; Trivax, B.; Aronowitz, J.; Yoshimura, K.; Simmons, C.F.; Dumesic, D.A.; Azziz, R. Novel pathway of adipogenesis through cross-talk between adipose tissue macrophages, adipose stem cells and adipocytes: Evidence of cell plasticity. *PLoS ONE* **2011**, *6*, e17834. [CrossRef] [PubMed]

168. Challa, T.D.; Straub, L.G.; Balaz, M.; Kiehlmann, E.; Donze, O.; Rudofsky, G.; Ukropec, J.; Ukropcova, B.; Wolfrum, C. Regulation of de novo Adipocyte Differentiation through Cross Talk between Adipocytes and Preadipocytes. *Diabetes* **2015**, *64*, 4075–4087. [[CrossRef](#)] [[PubMed](#)]
169. Turner, P.A.; Tang, Y.; Weiss, S.J.; Janorkar, A.V. Three-Dimensional Spheroid Cell Model of in vitro Adipocyte Inflammation. *Tissue Eng.* **2015**, *21*, 11–12.
170. Unser, A.M.; Mooney, B.; Corr, D.T.; Tseng, Y.H.; Xie, Y. 3D brown adipogenesis to create Brown-Fat-in-Microstrands. *Biomaterials*. **2016**, *75*, 123–134. [[CrossRef](#)] [[PubMed](#)]
171. Brännmark, C.; Paul, A.; Ribeiro, D.; Magnusson, B.; Brolén, G.; Enejder, A.; Forslöw, A. Increased adipogenesis of human adipose-derived stem cells on polycaprolactone fiber matrices. *PLoS ONE* **2014**, *9*, e113620. [[CrossRef](#)] [[PubMed](#)]



© 2016 by the authors; licensee MDPI, Basel, Switzerland. This article is an open access article distributed under the terms and conditions of the Creative Commons Attribution (CC-BY) license (<http://creativecommons.org/licenses/by/4.0/>).

Chapter 2:

Results

An analogue of atrial natriuretic peptide (C-ANP₄₋₂₃) modulates glucose metabolism in human differentiated adipocytes.

Ruiz-Ojeda FJ, Aguilera CM, Rupérez AI, Gil Á, Gomez-Llorente C.

Molecular and Cellular Endocrinology.**2016**; 431:101-8.

Impact Factor 2015: **3,859**



Contents lists available at ScienceDirect

Molecular and Cellular Endocrinology

journal homepage: www.elsevier.com/locate/mce

An analogue of atrial natriuretic peptide (C-ANP₄₋₂₃) modulates glucose metabolism in human differentiated adipocytes



Francisco Javier Ruiz-Ojeda^{a, b, c}, Concepción María Aguilera^{a, b, c, d},
Azahara Iris Rupérez^{a, b}, Ángel Gil^{a, b, c, d}, Carolina Gomez-Llorente^{a, b, c, d, *}

^a Department of Biochemistry and Molecular Biology II, School of Pharmacy, University of Granada, Campus de Cartuja s/n, 18071 Granada, Spain

^b Institute of Nutrition and Food Technology "José Mataix", Center of Biomedical Research, University of Granada, Avda. del Conocimiento s/n, 18016 Armilla, Granada, Spain

^c Instituto de Investigación Biosanitaria ibs, Granada, Spain

^d CIBER Fisiopatología de la Obesidad y la Nutrición (CIBEROBN), Madrid, Spain

ARTICLE INFO

Article history:

Received 19 January 2016

Received in revised form

27 April 2016

Accepted 10 May 2016

Available online 13 May 2016

Keywords:

Obesity

Adipocytes

Natriuretic peptide

Natriuretic peptide receptor 3

ABSTRACT

The present study was undertaken to investigate the effects of C-atrial natriuretic peptide (C-ANP₄₋₂₃) in human adipose-derived stem cells differentiated into adipocytes over 10 days (1 μM for 4 h). The intracellular cAMP, cGMP and protein kinase A levels were determined by ELISA and gene and protein expression were determined by qRT-PCR and Western blot, respectively, in the presence or absence of C-ANP₄₋₂₃. The levels of lipolysis and glucose uptake were also determined. C-ANP₄₋₂₃ treatment significantly increased the intracellular cAMP levels and the gene expression of *glucose transporter type 4* (GLUT4) and *protein kinase, AMP-activated, alpha 1 catalytic subunit* (AMPK). Western blot showed a significant increase in GLUT4 and phosphor-AMPK α levels. Importantly, the adenylate cyclase inhibitor SQ22536 abolished these effects. Additionally, C-ANP₄₋₂₃ increased glucose uptake by 2-fold. Our results show that C-ANP₄₋₂₃ enhances glucose metabolism and might contribute to the development of new peptide-based therapies for metabolic diseases.

© 2016 Elsevier Ireland Ltd. All rights reserved.

1. Introduction

Obesity and its comorbidities, specifically metabolic syndrome and type 2 diabetes, have reached epidemic proportions, especially in developed countries. Natriuretic peptides (NPs) have been revealed to be key mediators of metabolic processes and have been implicated in the development of diabetes (Gurden et al., 2014). NPs are a family of peptide hormones that are predominantly

secreted from the heart and that exert a variety of physiological functions by interacting with NP receptors (NPRs) (Li et al., 2014; Schlueter et al., 2014). The NP family comprises three members, atrial natriuretic peptide (ANP), brain natriuretic peptide (BNP), and C-type natriuretic peptide (CNP). These peptides are secreted as pro-hormones and are then cleaved by proteases into their biologically active forms and corresponding inactive peptides at equimolar ratios. There are three NPRs: NPR1 and NPR2 are membrane guanylyl cyclase receptors that are primarily responsible for the metabolic activity of NPs, and NPR3, a non-guanylyl cyclase-coupled receptor (Levin, 1993), has been classically considered as a clearance receptor that is involved in the degradation of NPs (Schlueter et al., 2014). NPR3 can bind to all NPs; it displays the highest affinity for ANP and the lowest affinity for BNP (Potter et al., 2006).

NPRs are expressed in different human tissues, including adipose tissue, where NPs can stimulate lipolysis, modulate adipokine secretion, and promote white adipocyte browning (Gurden et al., 2014; Sarzani et al., 1996; Moro and Lafontan, 2013; Bordicchia et al., 2012). Additionally, the expression levels of NPR3 in

Abbreviations: AMPK, AMP-activated kinase; BSA, bovine serum albumin; CASP1, caspase 1; C-ANP₄₋₂₃, C-atrial natriuretic peptide (4-23); cAMP, cyclic adenosine monophosphate; CNP-22, C-type natriuretic peptide-22; cGMP, cyclic guanosine monophosphate; DMEM, Dulbecco's modified Eagle's medium; FBS, foetal bovine serum; GAPDH, glyceraldehyde 3-phosphate dehydrogenase; GLUT4, glucose transporter type 4; HPRT1, hypoxanthine-guanine phosphoribosyl-transferase-1; IL1 β , interleukin 1, beta; NPR3, natriuretic peptide receptor 3; PKA, protein kinase A.

* Corresponding author. Department of Biochemistry and Molecular Biology II, Institute of Nutrition and Food Technology "José Mataix", Center of Biomedical Research, University of Granada, Avda. del Conocimiento s/n, 18016 Armilla, Granada, Spain.

E-mail address: gomezll@ugr.es (C. Gomez-Llorente).

<http://dx.doi.org/10.1016/j.mce.2016.05.011>

0303-7207/© 2016 Elsevier Ireland Ltd. All rights reserved.

adipose tissue have been observed to be considerably increased in obese adults (Gómez-Ambrosi et al., 2004; Baranova et al., 2005) and obese children (Aguilera et al., 2015). Moreover, insulin increases NPR3 expression in subcutaneous adipose tissue in subjects with moderate obesity and normal glucose tolerance (Pivovarov et al., 2012). Several studies have revealed that the plasma levels of NPs are decreased in patients with obesity or type 2 diabetes (Moro and Lafontan, 2013; Wang et al., 2007) and this decrease may be primarily due to impaired NP release (Omar et al., 2009). Another possible explanation is that the up-regulation of NPR3 increases NP clearance from the circulation (Dessi-Fulgheri et al., 1997) although the ablation of NPR3 in mice did not affect the circulating levels of NPs (Pivovarov et al., 2012; Matsukawa et al., 1999). It has been reported that NPR3 is coupled to the adenylate cyclase/cAMP system through a 37-amino acid intracellular region of NPR3 that is expressed in various human tissues (Schenk et al., 1987; Sengenès et al., 2005). Studies using the synthetic ligand C-ANP_{4–23}, a ring-deleted analogue of ANP, that specifically interacts with NPR3, have shown decreased cAMP levels in the anterior pituitary, the aorta, the brain striatum, and the adrenal cortex, as well as in rat vascular smooth muscle cells and cultured adipocytes (Anand-Srivastava et al., 1990; Crilley and Garcia, 1997). However, incubation in C-ANP_{4–23} increased the cAMP levels in human thyrocytes (Sellitti et al., 2001). In addition, in cultured adipocytes, molecules that increase the intracellular cAMP levels have been demonstrated to increase the activity of AMP-activated protein kinase (AMPK), a critical regulator of energy homeostasis and a therapeutic target for the treatment of type 2 diabetes (Yin et al., 2003; Hutchinson et al., 2005). In human adipocytes, the modulation of the cAMP levels by C-ANP_{4–23} has not been reported. Consequently, the present study was undertaken to determine whether the C-ANP_{4–23} treatment alters glucose metabolism via AMPK in human adipocytes and to explore whether this effect is mediated by the adenylate cyclase system.

2. Material and methods

2.1. Materials

Commercially available adipose derived-stem cells (ADSCs) were purchased directly from Lonza (Poietics™ Normal ADSCs, Lonza, PT-5006, Lot 0F4505, Switzerland). ADSCs are isolated from normal (non-diabetic) adult lipoaspirates collected during elective surgical liposuction procedures (from subcutaneous adipose tissue). ADSCs have been reported to differentiate down many different lineages including chondrogenic, osteogenic, adipogenic and neural. ADSCs have been cryopreserved at primary passage. Adipogenesis media were obtained from Lonza. Oil Red O was acquired from Sigma (234117, Sigma-Aldrich, St. Louis, MO, USA). C-ANP_{4–23} (H3134), ANP (H2095) and CNP-22 (H1296) were purchased from Peninsula Laboratories (Bachem AG, Switzerland). An adenylate cyclase inhibitor (SQ22536, T2678) was acquired from Sigma (Sigma-Aldrich, St. Louis, MO, USA). The rabbit anti-glucose transporter type 4 (GLUT4) antibody (H-61) was acquired from Santa Cruz Biotechnology (Santa Cruz, CA, USA); the rabbit anti-total AMPK α (D5A2) and rabbit anti-phospho-AMPK α (Thr172) antibodies were obtained from Cell Signalling Technologies (Beverly, MA, USA), and the mouse anti- α -tubulin antibody (T5158) and horseradish peroxidase-conjugated immunoglobulin were purchased from Sigma. Unless otherwise indicated, all other chemicals were purchased from Sigma.

2.2. Cell culture and incubation

ADSCs were cultured, expanded and differentiated into

adipocytes according to the manufacturer's recommendations (Lonza). Briefly, ADSCs were grown and expanded in appropriate sterile plastic dishes in complete Advanced-DMEM (Gibco, Life Technologies, Spain) supplemented with 2 mM L-glutamine (25030, Gibco), 10% foetal bovine serum (FBS, PT-9000 H, Lonza), 100 U ml⁻¹ of penicillin and 100 μ g ml⁻¹ of streptomycin (10378-016, Gibco). The cells were incubated at 37 °C in a humidified atmosphere containing 5% CO₂. The cell culture medium was replaced twice per week, and the cells were passaged a maximum of 6 times. To induce differentiation, the cells were seeded in 35-mm dishes at a density of 30,000 cells/cm² and cultured in preadipocyte growth medium (PGM) consisting of Preadipocyte Basal Medium-2 (PT-8002, Lonza) supplemented with 10% FBS, 2 mM L-Glutamine (PT-9001 H, Lonza) and 0.1 μ g ml⁻¹ Gentamicin Sulfate Amphotericin-B (PT-4504, Lonza). At 90% confluency, the growth medium was replaced with differentiation medium (PGM supplemented with dexamethasone, 3-isobutyl-1-methylxanthine (IBMX), indomethacin and h-insulin, PT-9502, Lonza). ADSCs were differentiated for 10 days. Finally, the cells were washed twice with PBS, and the differentiation medium was replaced with PGM and IBMX (0.1 mM) overnight. All treatments were performed on differentiated adipocytes at day 10.

In order to test the appropriate concentration and incubation time of C-ANP_{4–23}, the cells were treated with different concentrations (50 nM, 1 μ M and 5 μ M) and incubation times (30 min, 4 h and 6 h). The selected experimental conditions, based on the intracellular cAMP levels results, were 1 μ M of C-ANP_{4–23} and 4 h of incubation (Supplementary Fig. S3). Subsequently, the cells were treated with 100 μ M SQ22536 for 30 min, in the presence or absence C-ANP_{4–23}, as described below. The appropriate concentration and incubation time of SQ22536 were obtained from the available literature (Santangelo et al., 2011).

2.3. Intracellular cAMP and cGMP level determination

Human differentiated adipocytes were incubated in the presence or absence of C-ANP_{4–23}, ANP (1 μ M, 4 h) or CNP-22 (1 μ M, 4 h), and the intracellular cAMP and cGMP levels were determined using the commercial cAMP (ADI-900-163, Enzo Life Science, Switzerland) and cGMP (ADI-900-164, Enzo Life Science, Switzerland) ELISA kits. In additional experiments, the cells were incubated in SQ22536 prior to treatment with or without C-ANP_{4–23}, followed by determination of the intracellular cAMP levels using the aforementioned kit.

2.4. Protein kinase A (PKA) activity assay

Human differentiated adipocytes were incubated in the presence or absence of C-ANP_{4–23}, and Protein kinase A (PKA) activity was determined using the PKA kinase activity kit (ADI-EKS-390A, Enzo Life Science, Switzerland). Additionally, the cells were incubated in SQ22536 prior to treatment with or without C-ANP_{4–23}, followed by determination of PKA activity using the aforementioned kit.

2.5. Lipolysis assay

The total level of glycerol, the final product of lipolysis, was measured in cell supernatants using a colorimetric assay (Free Glycerol Reagent, F6428, Sigma-Aldrich, St. Louis, MO, USA). The cells were treated with 1 μ M C-ANP_{4–23} and with 1 μ M ANP as a positive control or with CNP-22 (1 μ M) during 4 h, and the cell supernatants were harvested. Then, the cell supernatants were incubated in the reagent at room temperature for 15 min in a 96-well plate, and the optical density was measured using a

microplate reader (BioTek HTX) at 550 nm.

2.6. RNA isolation and qRT-PCR

Total RNA was extracted from cells using the PeqGOLD HP Total RNA kit (Peqlab, Germany). Isolated RNA was then treated with Turbo DNase (Ambion, Life Technologies, Spain). The final RNA concentration and quality were determined using a NanoDrop 1000 (NanoDrop Technologies, Winooski, Vermont, USA). Total RNA (500 ng) was transcribed into cDNA using the iScript cDNA Synthesis Kit (Bio-Rad Laboratories, California, USA). The *NPR3*, *peroxisome proliferator-activated receptor gamma (PPARG)*, *leptin (LEP)* and *adiponectin (ADIPOQ)* expression levels were determined via qPCR using *glyceraldehyde 3-phosphate dehydrogenase (GAPDH)* as a reference gene, and the quantification was performed using the Pfaffl method (Pfaffl, 2001). The specific primers for *NPR3*, *PPARG*, *LEP*, *ADIPOQ*, *uncoupled protein 1 (UCP1)* and *GAPDH* were designed using Primer3 (<http://bioinfo.ut.ee/primer3-0.4.0/>). The primer sequences were as follows: *NPR3* forward primer, 5'-GGA-GACCGATATGGGATTT-3', and reverse primer, 5'-CACTGCC-GATTCTCTAGGC-3'; *GAPDH* forward primer, 5'-GAGTCAACGGATTGGTCGT-3', and reverse primer, 5'-TTGATTTG-GAGGGATCTCG-3'; *PPARG* forward primer, 5'-CTCGAGGA-CACCGGAGAGG-3', and reverse primer, 5'-CACGGAGCTGATCCCAAAGT-3'; *LEP* forward primer, 5'-GTTGCAAGGCCCAAGAAGCCCA-3', and reverse primer, 5'-CAGTGTCTGGTCCATCTTGATAAGGTCAGG-3'; *ADIPOQ* forward primer, 5'-GGCCGTGATGCCAGAGAT-3', and reverse primer, 5'-CCTTCAGCCCGGTACT-3'; *UCP1* forward primer, 5'-TGGAA-TAGCCGGCTGCTTG-3', and reverse primer, 5'-CTCATCA-GATTGGGAGTAG-3'. *Natriuretic peptide receptor 1 (NPR1)* and *Natriuretic peptide receptor 2 (NPR2)* primers were acquired from Bio-Rad Laboratories (Bio-Rad Laboratories, California, USA). qPCR was performed in an ABI Prism 7900 instrument (Applied Biosystems, Foster City, CA, USA) using SYBR Green PCR Master Mix (Applied Biosystems).

Differential gene expression in human differentiated adipocytes after incubation in C-ANP₄₋₂₃ was determined via Human PCR Arrays (Bio-Rad Laboratories, California, USA). Each array comprised primer pairs that were specific to nineteen selected genes related to the insulin, inflammation, adipogenesis and lipolytic signalling pathways. *GAPDH* and *hypoxanthine-guanine phosphoribosyl-transferase-1 (HPRT1)* were used as reference genes. qPCR was performed in an ABI-7500H (Applied Biosystems, University of Granada, Spain). The data were analysed using PrimePCR analysis software, version 1.0 (Bio-Rad Laboratories, California, USA). Bio-Rad's PrimePCR assays make the minimum information for publication of quantitative real-time-PCR experiments (MIQE) compliance easy. Statistical validation of reference genes stability was calculated in each sample. Bio-Rad recommends using a <0.5 value, which is the most stable expression in the tested samples. The results are expressed as the fold-change in expression and were calculated using the $2^{-\Delta\Delta Ct}$ method.

2.7. Western blot assays

The cells were harvested in 10 mM Tris-HCl (pH 7.5), 150 mM NaCl, 2 mM EDTA, 1% Triton X-100, 10% glycerol and protease inhibitor cocktail (Thermo Scientific) and were placed on ice for 20 min. After centrifugation (30 min, 13,000 g, 4 °C), the protein content in the supernatant was determined using the Protein Assay Kit II (Bio-Rad Laboratories, California, USA). Samples containing 2.5 µg of protein were mixed with 3× SDS-PAGE sample buffer (100 mM Tris-HCl, pH 6.8, 25% SDS, 0.4% bromophenol blue, 10% β-mercaptoethanol and 2% glycerol), separated via SDS-PAGE using a

TGX Any kD gel (Bio-Rad Laboratories, California, USA) and transferred to a nitrocellulose membrane (Bio-Rad Laboratories, California, USA). After incubation in blocking buffer 5% non-fat milk and 1% Tween 20 in Tris-buffered saline (TBS), the membranes were probed with the following antibodies: anti-GLUT4 (1:100 in 5% non-fat milk), anti-total AMPKα, anti-phosphorylated AMPKα (phospho-AMPKα T172) (both 1:1000 in 5% BSA) and anti-α-tubulin (internal control; 1:4000 in 5% non-fat milk). Immunoreactive signals were detected via enhanced chemiluminescence (Super-Signal West Dura Chemiluminescent Substrate, 34075, Thermo Scientific, Europe), and the membranes were digitally imaged and analysed using ImageJ software for densitometric analysis. The results are expressed as the fold-change in expression relative to the control.

2.8. Glucose uptake assays

Glucose uptake was determined using a colorimetric assay kit (MAK083, Sigma-Aldrich). Briefly, ADSCs were differentiated in 12-well plates as described above. Differentiated adipocytes were washed twice with PBS and then starved in serum-free medium overnight. Then, the cells were washed 3 times with PBS and glucose-starved via incubation in KRPH buffer (5 mM Na₂HPO₄, 20 mM HEPES, pH 7.4, 1 mM MgSO₄, 1 mM CaCl₂, 137 mM NaCl and 4.7 mM KCl) containing 2% BSA for 40 min. Glucose uptake was assessed in the presence or absence of C-ANP₄₋₂₃ with 1 mM 2-deoxy-D-glucose in KRPH for 20 min at 37 °C and 5% CO₂. As a positive control, the cells were stimulated with insulin (1 µM) for 20 min. The results are expressed in pmol/well.

2.9. Statistical analysis

All experiments were repeated at least three times. In each experiment two replicates were performed. Data are expressed as the mean ± standard error of the mean (s.e.m.). Significant differences in the levels of gene and protein expressions, intracellular cAMP, lipolysis and glucose uptake were determined using the non-parametric Mann-Whitney *U* test; statistical significance was defined as **P* < 0.05, ***P* < 0.01. Statistical analyses were performed using SPSS version 22, for Windows (SPSS, Chicago, IL, USA).

3. Results

3.1. Adipogenic characterization of ADSCs

Adipogenesis was monitored via morphological examination of the cellular accumulation of lipid droplets by staining with Oil Red O (Supplementary Fig. S1) and via gene expression of *LEP*, *ADIPOQ* and *PPARG* adipogenic genes during differentiation (Supplementary Fig. S1). In agreement with previous results (Wu et al., 1999, Vater et al., 2011), we observed an increase of *LEP*, *ADIPOQ* and *PPARG* expression from day 0 to day 10.

3.2. NPR1, NPR2 and NPR3 expression in human adipocytes

We found that *NPR1*, *NPR2* and *NPR3* expression levels significantly increased during adipogenic differentiation (Supplementary Fig. S2). However, *NPR1* showed higher expression levels than *NPR2* or *NPR3*.

3.3. The effects of C-ANP₄₋₂₃ treatment on lipolysis

To determine the effects of C-ANP₄₋₂₃ on lipolysis, we measured the total glycerol levels in the cell supernatants. C-ANP₄₋₂₃ did not have any effect on lipolysis, whereas 1 µM ANP, a well-known

lipolysis activator through NPR1, increased glycerol levels (Fig. 1c).

3.4. C-ANP₄₋₂₃ incubation increased the cAMP levels in adipocytes

Human differentiated adipocytes were treated with C-ANP₄₋₂₃ to evaluate the effects of NPR3 activation on the intracellular cAMP levels. We observed increased intracellular cAMP levels in cells treated with C-ANP₄₋₂₃ ($P = 0.046$; Fig. 1a). However, the intracellular cGMP levels did not change after C-ANP₄₋₂₃ treatment (three separate experiments, in each experiment three replicates were performed) (Supplementary Fig. S3b). Finally, C-ANP₄₋₂₃ did not modify PKA activity in the adipocytes (Fig. 1b).

To test the effects of C-ANP₄₋₂₃ on the adenylate cyclase system, adipocytes were incubated with the adenylate cyclase inhibitor SQ22536 prior to C-ANP₄₋₂₃ treatment. As expected, we did not find any change on the intracellular cAMP levels when the adenylate cyclase system was inhibited (Fig. 1a).

3.5. Gene expression profile after the treatment of human adipocytes with C-ANP₄₋₂₃

Table 1 shows the expression of the nineteen evaluated genes expressed as the relative to no treatment fold-change. The PCR array revealed the up-regulation of AMPK and GLUT4 after C-ANP₄₋₂₃ treatment ($P = 0.0001$ and $P = 0.0046$, respectively), whereas the gene expression of interleukin 1, beta (IL1B) and caspase 1 (CASP1) was down-regulated ($P = 0.0188$ and $P = 0.0014$, respectively). Additionally, the UCP1 mRNA levels were not modified by C-ANP₄₋₂₃.

3.6. Effects of C-ANP₄₋₂₃ on GLUT4 and phosphor-AMPK α protein expression levels

We determined the intracellular protein levels of GLUT4, total AMPK α (catalytic subunit alpha) and phosphorylated AMPK α by Western blot analysis. As shown in Fig. 2a, GLUT4 levels were significantly higher after C-ANP₄₋₂₃ treatment (fold-change, 5.69; $P = 0.006$). However, we did not observe any change when the adenylate cyclase was inhibited. Although the total AMPK α levels did not change after treatment with C-ANP₄₋₂₃ (Fig. 3a), the levels of phosphor-AMPK α (which is required for AMPK activation) were significantly higher after this treatment (fold-change, 1.72; $P = 0.037$; Fig. 3b). Therefore, the ratio phosphor-AMPK α to total AMPK α levels was also significantly higher in the C-ANP₄₋₂₃ treated cells (fold-change, 1.65; $P = 0.04$; Fig. 3c). However, we did not observe any change when the adenylate cyclase was inhibited.

3.7. Glucose uptake in human adipocytes treated with C-ANP₄₋₂₃

We also determined whether the up-regulation of GLUT4 in adipocytes resulted in increased glucose uptake using insulin as a positive control. Glucose uptake was significantly 2-fold higher in human differentiated adipocytes after treatment with C-ANP₄₋₂₃ ($P = 0.0001$; in five different experiments, in each experiments two replicates were performed; Fig. 2b).

4. Discussion

In the present study we demonstrate that the synthetic ligand C-ANP₄₋₂₃ increases the intracellular cAMP levels in human

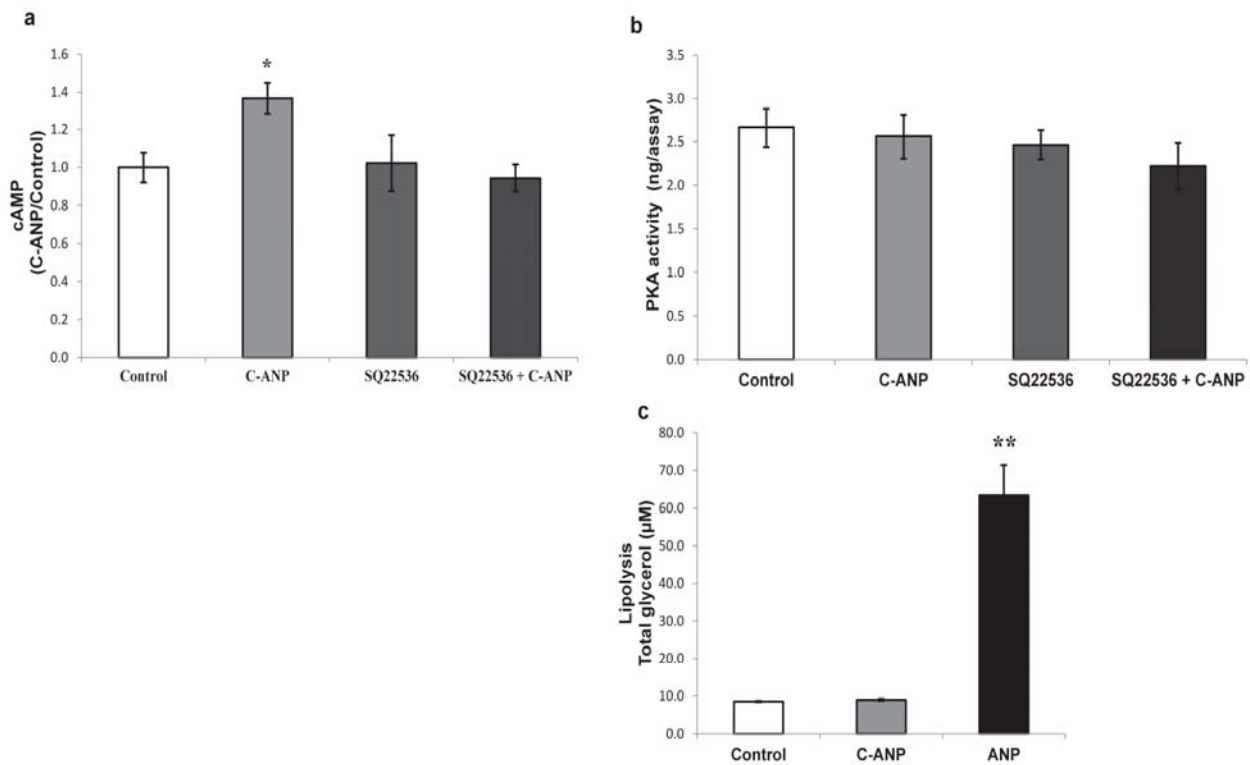


Fig. 1. Effects of C-atrial natriuretic peptide (C-ANP₄₋₂₃) on the intracellular cyclic adenosine monophosphate (cAMP), protein kinase A (PKA) activity and total glycerol levels in human differentiated adipocytes. (a) Intracellular cAMP levels after treatment with C-ANP₄₋₂₃ (1 μ M, 4 h) alone ($n = 9$) or in the presence of adenylate cyclase system inhibitor SQ22536 ($n = 4$) (100 μ M for 30 min). The normalised data are presented as the means C-ANP/control \pm s.e.m. (b) PKA activity levels (ng/assay) after treatment with C-ANP₄₋₂₃ (1 μ M, 4 h) alone or in the presence of adenylate cyclase system inhibitor SQ22536 (100 μ M for 30 min). The data are presented as the means \pm s.e.m of five independent experiments. (c) Glycerol levels (μ M) in total cell supernatants after treatment with C-ANP₄₋₂₃ (1 μ M, 4 h) or ANP (1 μ M, 4 h) as a positive control. The data are presented as the means \pm s.e.m of three independent experiments. Significant differences were analysed using the Mann-Whitney U test; * $P < 0.05$, ** $P < 0.01$.

Table 1
Gene expression in adipocytes after the treatment with C-ANP₄₋₂₃ by real-time PCR.

Gene symbol	Gene name	Real-time PCR		
		Probe set ID	Fold change	P value
SLC2A4	Solute carrier family 2 (facilitated glucose transporter), member 4	Hs.380691	14.504	^a 0.0046
IL1B	Interleukin 1, beta	Hs.126256	0.084	^a 0.0188
PRKAA1	protein kinase, AMP-activated, alpha 1 catalytic subunit	Hs.43322	9.695	^a 0.0001
CASP1	Caspase 1	Hs.2490	0.266	^a 0.0014
PTEN	Phosphatase and tensin homolog	Hs.500466	0.402	0.7041
GNAI2	Guanine nucleotide binding protein, alpha inhibiting activity polypeptide 2	Hs.77269	0.463	0.8050
PPARGC1A	Peroxisome proliferator-activated receptor gamma, coactivator 1 alpha	Hs.527078	2.022	0.0268
NFKB2	Nuclear factor of kappa light polypeptide gene enhancer in B-cells 2 (p49/p100)	Hs.73090	1.355	0.0002
NOS3	Nitric oxide synthase 3	Hs.647092	1.272	0.3952
NOS2	nitric oxide synthase 2, inducible	Hs.709191	1.272	0.3952
TOLLIP	toll interacting protein	Hs.368527	1.269	0.1647
GNAS	GNAS complex locus	Hs.125898	1.196	0.1191
PLCG1	phospholipase C, gamma 1	Hs.268177	1.182	0.2086
TNFRSF1A	tumour necrosis factor receptor superfamily, member 1A	Hs.279594	1.172	0.3372
TIMP1	TIMP metalloproteinase inhibitor 1	Hs.522632	1.139	0.0346
IRAK4	interleukin-1 receptor-associated kinase 4	Hs.138499	1.129	0.1684
IRS1	insulin receptor substrate 1	Hs.471508	1.117	0.4828
PIK3R1	phosphoinositide-3-kinase, regulatory subunit 1 (alpha)	Hs.132225	0.881	0.4822
CCND1	cyclin D1	Hs.523852	1.088	0.5583

^a Δ Ct values were compared differentiated adipocytes and differentiated adipocytes incubated with C-ANP₄₋₂₃ using the ($P < 0.05$).

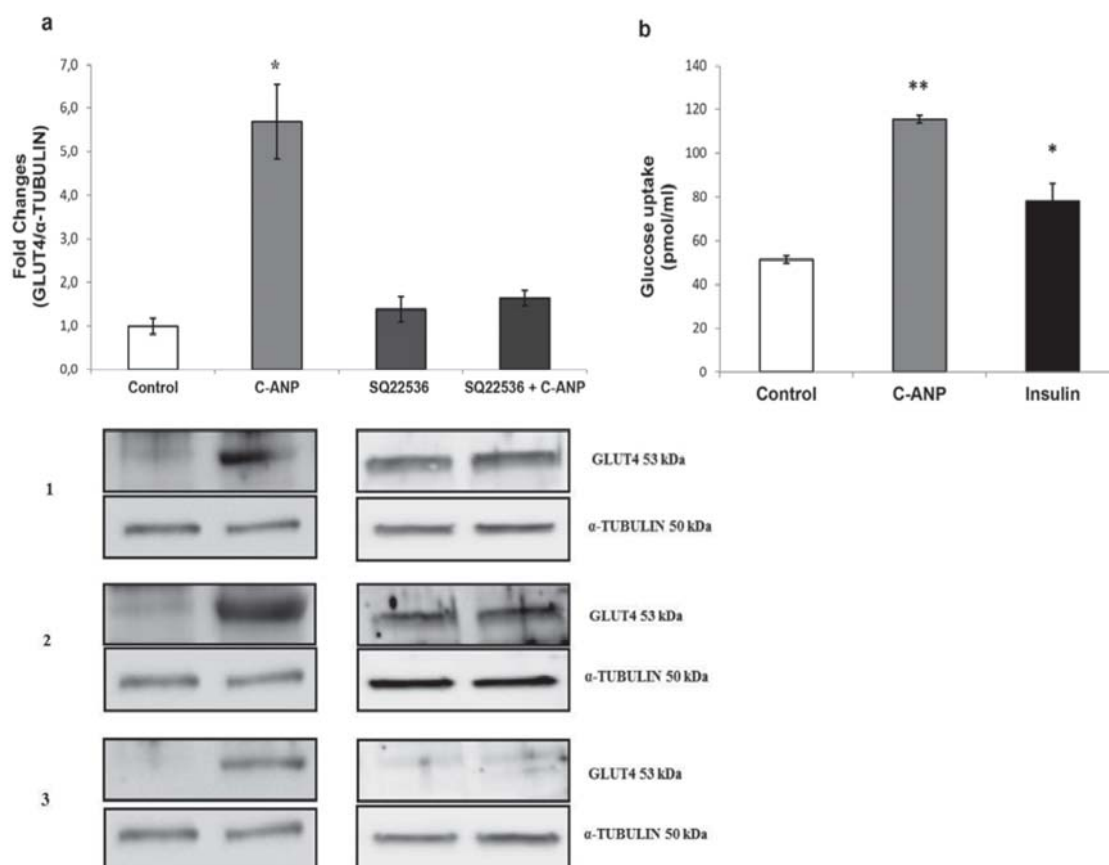


Fig. 2. Effect of C-atrial natriuretic peptide (C-ANP₄₋₂₃) treatment on glucose metabolism in human differentiated adipocytes. **(a)** Glucose transporter 4 (GLUT4) protein levels after treatment with C-ANP₄₋₂₃ (1 μ M, 4 h) alone or in the presence of adenylyl cyclase system inhibitor SQ22536 (100 μ M, 30 min). The cell lysates were prepared and then analysed by Western blot using a specific antibody against GLUT4 as described in the Methods section. The data are presented as the relative to no treatment fold-change, and the bars represent the means \pm s.e.m. of three separate experiments. Significant differences were analysed using the Mann-Whitney *U* test; * $P < 0.05$. **(b)** Glucose uptake levels in human differentiated adipocytes after treatment with C-ANP₄₋₂₃ (1 μ M, 4 h) or insulin (1 μ M, 30 min) as a positive control. The data are presented as the means \pm s.e.m. of five separate experiments. Significant differences were analysed using the Mann-Whitney *U* test; ** $P < 0.001$, control vs C-ANP; * $P < 0.01$, control vs Insulin and C-ANP vs Insulin.

differentiated adipocytes. Furthermore, C-ANP₄₋₂₃ up-regulates the gene and protein expression of GLUT4 and enhances glucose uptake, and this effect appears to be mediated by AMPK activation. To

the best of our knowledge, this is the first description of a putative role of C-ANP₄₋₂₃ in glucose metabolism in human adipocytes.

Maack et al., 1987 was the first to describe C-ANP₄₋₂₃ as an

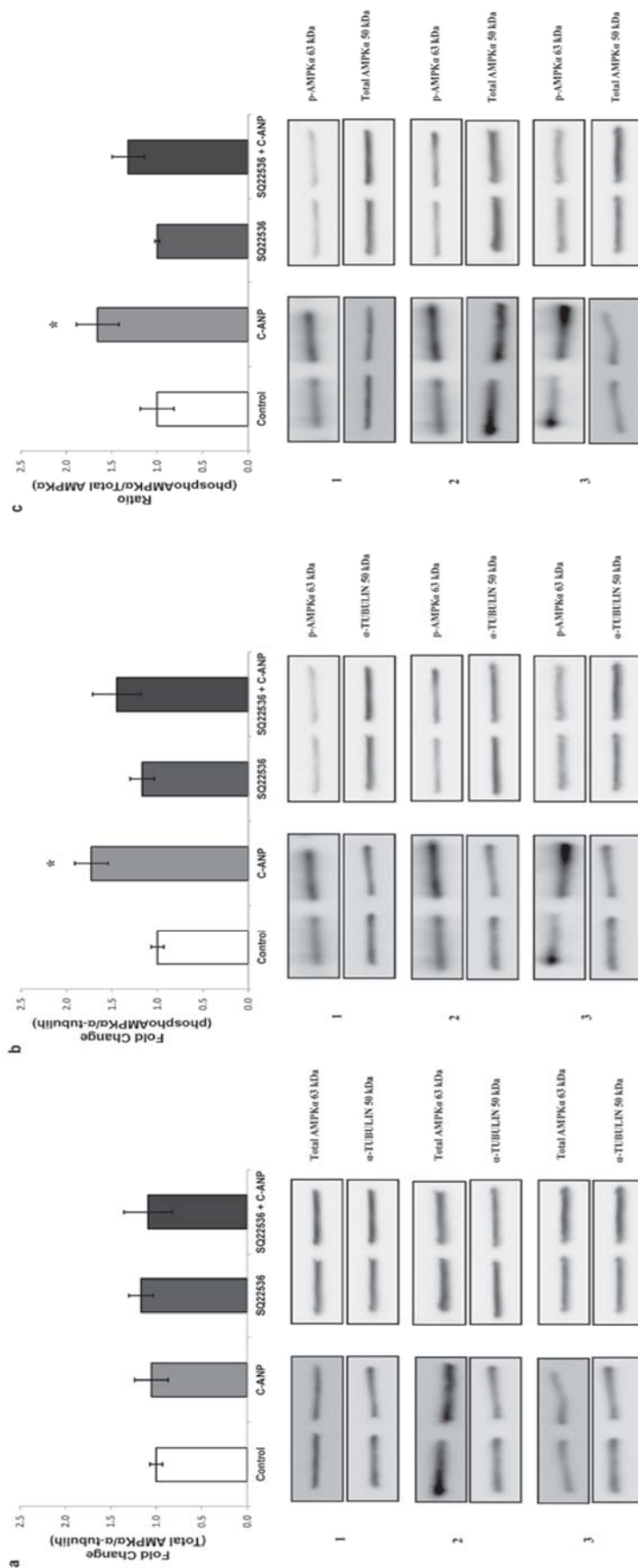


Fig. 3. Effect of C-atrial natriuretic peptide (C-ANP₄₋₂₃) treatment on 5'AMP-activated protein kinase subunit alpha (AMPK α) expression in human differentiated adipocytes. **(a, b)** Protein levels after treatment with C-ANP₄₋₂₃ (1 μ M, 4 h) alone or in the presence of adenylyl cyclase system inhibitor SQ22536 (100 μ M for 30 min). The cell lysates were prepared and then analysed by Western blot using specific antibodies against total AMPK α **(a)** and phospho-AMPK α (Thr172) **(b)** as described in the Methods section. **(c)** Ratio phospho-AMPK α /total-AMPK α . The data are presented as the relative to no treatment fold-change, and the bars represent the means \pm s.e.m. of three separate experiments. Significant differences were analysed using the Mann-Whitney U test; * $P < 0.05$.

agonist peptide for NPR3 with no affinity for NPR1 or NPR2 (Maack et al., 1987; Li et al., 2014). Since then, numerous studies have described its exclusive interaction with NPR3 in animal (Anand-Srivastava et al., 1987; 1990; Nishikimi et al., 2009; Li et al., 2012, 2014; Almeida et al., 2014) and human cells (Rutherford et al., 1994; Ortego and Coca-Prados, 1999; Sellitti et al., 2001; Zhang et al., 2005; Gower et al., 2006; Skowrońska et al., 2010). To this date, the main reported relevance of C-ANP₄₋₂₃ has been the improvement of endothelial migration, proliferation and angiogenesis in bovine and human endothelial cells (Almeida et al., 2014; Li et al., 2014). In 1984, Anand-Srivastava et al. showed that NPR3 was coupled to adenylyl cyclase activity via inhibitory guanine nucleotide regulatory proteins (Gi) (Anand-Srivastava 2005). Two different subtypes of NPR3 with molecular mass of 67 and 77 kDa have been identified. The 77-kDa protein is implicated in ligand internalization as a clearance receptor, endocytosis and degradation; whereas the 67-kDa protein is coupled to adenylyl cyclase system (Anand-Srivastava et al., 1987; Anand-Srivastava et al., 1990). Anand-Srivastava demonstrated the inhibition of adenylyl cyclase by C-ANP₄₋₂₃ in rat cells (1990). However, Sellitti et al. (2001) reported the possibility that the binding of C-ANP₄₋₂₃ to NPR3 activates rather than inhibits the adenylyl cyclase system. This was explained by the hypothesis that NPR3 coupling to adenylyl cyclase (inhibition vs stimulation) might be restricted to certain cell types, possibly because some cells express enzymes (e.g., kinases) that are capable of modifying the intracellular NPR3 domain (Sellitti et al., 2001). Our results show that the intracellular cAMP levels increase rather than decrease in human adipocytes after treatment with C-ANP₄₋₂₃. Indeed, the adenylyl cyclase inhibitor SQ22536 suppressed the C-ANP₄₋₂₃-induced increase in the cAMP levels, which confirms the implication of the adenylyl cyclase system in NPR3 function.

On one hand, it has been demonstrated that elevated intracellular cAMP levels in rat cultured adipocytes stimulate AMPK activity, which plays an important role in the regulation of glucose uptake (Omar et al., 2009; Bolsoni-lopes et al., 2014). Upon activation, AMPK promotes GLUT4 expression and translocation to the plasma membrane and glucose uptake independent of insulin (Govers, 2014; Bolsoni-lopes et al., 2014). Correspondingly, we observed significantly higher levels of activated AMPK (phospho-AMPK α -Thr172) after treatment with C-ANP₄₋₂₃. Indeed, we have found that C-ANP₄₋₂₃ increases glucose uptake by 2-fold in adipocytes and up-regulates GLUT4 gene and protein expression. Importantly, such increase in GLUT4 protein expression and activation of AMPK induced by C-ANP₄₋₂₃, was prevented by inhibition of adenylyl cyclase systems with SQ22536. Although many of the downstream effects of cAMP are mediated by PKA, exchange proteins directly activated by cAMP have been shown to mediate signals downstream of cAMP independent of PKA (Omar et al., 2009). The exact mechanism by which C-ANP₄₋₂₃ increases glucose uptake in human differentiated adipocytes was not completely elucidated here, however, our findings suggested that this effect is mediated by cAMP/AMPK activation.

On the other hand, it has been reported that catecholamines stimulate the adenylyl cyclase system/cAMP and inhibit glucose uptake in adipocytes through the dissociation of mTOR complex (Mullins et al., 2014). However, this fact is due to products of lipolysis which inhibit glucose uptake (Mullins et al., 2014). As we have shown, incubation with C-ANP₄₋₂₃ did not increase the lipolysis levels in adipocytes neither the intracellular cGMP levels, in agreement with previous studies showing that C-ANP₄₋₂₃ does not increase cGMP levels (Anand-Srivastava et al., 1990; Skowrońska et al., 2010). In contrast with ANP, which increases cGMP and lipolysis levels acting via NPR1 (Potter et al., 2006; Moro and Lafontan, 2013; Kumar et al., 1997; Pandey 2005). As for the

biological natriuretic peptide (CNP-22), it has been described that it could have similar effects to the synthetic ligand C-ANP₄₋₂₃ through its binding to NPR3 (Sellitti et al., 2001; Matsukawa et al., 1999; Pandey 2014). However, we did not find differences in cAMP and GMP levels, lipolysis, GLUT4 and AMPK-stimulated PKA activity between control and CNP-22-treated adipocytes (Supplementary Fig. S4).

Additionally, a relationship between NPs and inflammation in adipose tissue has been reported. Adipocytes secrete adipokines and cytokines that are implicated in the chronic low-grade inflammation and insulin resistance associated with obesity, and ANP inhibits the secretion of factors involved in inflammation (Moro et al., 2006). We explored whether C-ANP₄₋₂₃ affects the inflammatory pathway in human adipocytes by analysing the expression of different genes involved in the inflammatory system, such as *IL1B*, *CASP1*, *nuclear factor of kappa light polypeptide gene enhancer in B-cells 2 (p49/p100) (NFkB2)*, *Toll interacting protein (TOLLIP2)*, *tumour necrosis factor receptor superfamily, member 1A (TNFRSF1A)* and *interleukin-1 receptor-associated kinase 4 (IRAK4)*. We found that *IL1B* and *CASP1* were significantly down-regulated after C-ANP₄₋₂₃ treatment. However, we were unable to determine the protein levels of these two genes in the cell lysates. The NLRP3 inflammasome controls the activation of *CASP1* and promotes the maturation of IL-1 β (Haneklaus and O'Neill, 2015; Schroder and Tschopp, 2010). Therefore, C-ANP₄₋₂₃ might be involved in the inflammatory process independent of glucose metabolism by inhibiting the inflammasome in adipocytes. Further studies are needed to fully characterise the role of C-ANP₄₋₂₃ in the inflammatory process in adipocytes.

We are aware of several limitations to the present study; in particular, the morphology of the differentiated adipocytes from human ADSCs was not completely identical to that of mature adipocytes. Thus, the putative role of C-ANP₄₋₂₃ in glucose metabolism might be different between isolated adipocytes and adipose tissue.

In summary, this study demonstrates for the first time that the synthetic ligand C-ANP₄₋₂₃ exerts modifications in glucose metabolism through an increase in intracellular cAMP levels, AMPK activation, and GLUT4 levels; and enhances glucose uptake in human differentiated adipocytes. Based on these findings, C-ANP₄₋₂₃ may have a potential use in the development of new peptide-based therapies for obesity associated metabolic diseases such as insulin resistance and type 2 diabetes. Further research is needed to clarify the specific mechanism of action of C-ANP₄₋₂₃, including interventional studies that investigate the effects of this peptide *in vivo*.

Conflicts of interest

The authors declare no conflicts of interest.

Acknowledgements

This work was supported by Junta de Andalucía (project number CTS-6770; Secretaría General de Universidades, Investigación y Tecnología. Consejería de Economía, Innovación y Ciencia. Implicaciones biológicas de genes de las vías de señalización de la insulina, inflamación y de la matriz extracelular en cultivos de células madre mesenquimales de tejido adiposo humano). Ruiz-Ojeda FJ was funded by a Formación de Profesorado Universitario (FPU) stipend from the Ministry of Education and Science of the Spanish Government (AP2012-02068). CG-L is a recipient of a fellowship from Plan Propio UGR. This paper will be part of Francisco Javier Ruiz-Ojeda's doctorate, which is being performed within the "Nutrition and Food Sciences Program" at the University of Granada.

Appendix A. Supplementary data

Supplementary data related to this article can be found at <http://dx.doi.org/10.1016/j.mce.2016.05.011>.

References

- Aguilera, C., Gomez-Llorente, C., Tofe, I., Gil-Campos, M., Cañete, R., Gil Á, 2015. Genome-wide expression in visceral adipose tissue from obese prepubertal children. *Int. J. Mol. Sci.* 16, 7723–7737.
- Almeida, S.A., Cardoso, C.C., Orellano, L.A., Reis, A.M., Barcelos, L.S., Andrade, S.P., 2014. Natriuretic peptide clearance receptor ligand (C-ANP4–23) attenuates angiogenesis in a murine sponge implant model. *Clin. Exp. Pharmacol. Physiol.* 41, 691–697.
- Anand-Srivastava, M.B., Srivastava, A.K., Cantin, M., 1987. Pertussis-toxin attenuates atrial natriuretic factor-mediated inhibition of adenylate cyclase. Involvement of inhibitory guanine nucleotide regulatory protein. *J. Biol. Chem.* 262, 4931–4934.
- Anand-Srivastava, M.B., Sairam, M.R., Cantin, M., 1990. Ring-deleted analogs of atrial natriuretic factor inhibit adenylate cyclase/cAMP system. Possible coupling of clearance atrial natriuretic factor receptors to adenylate cyclase/cAMP signal transduction system. *J. Biol. Chem.* 265, 8566–8572.
- Anand-Srivastava, M.B., 2005. Natriuretic peptide receptor-C signaling and regulation. *Peptides* 26, 1044–1059.
- Baranova, A., Collantes, R., Gowder, S.J., Elariny, H., Schlauch, K., Younoszai, A., et al., 2005. Obesity-related differential gene expression in the visceral adipose tissue. *Obes. Surg.* 15, 758–765.
- Bolsoni-Lopes, A., Festuccia, W.T., Chimin, P., Farias, T.S., Torres-Leal, F.L., Cruz, M.M., et al., 2014. Palmitoleic acid (n-7) increases white adipocytes GLUT4 content and glucose uptake in association with AMPK activation. *Lipids Health Dis.* 13, 199. <http://dx.doi.org/10.1186/1476-511X-13-199>.
- Bordicchia, M., Liu, D., Amri, E.Z., Ailhaud, G., Dessi-Fulgheri, P., Zhang, C., et al., 2012. Cardiac natriuretic peptides act via p38 MAPK to induce the brown fat thermogenic program in mouse and human adipocytes. *J. Clin. Invest.* 122, 1022–1036.
- Crilly, C., Garcia, R., 1997. Effects of atrial natriuretic factor on glucose metabolism in isolated adipocytes. *Regul. Pept.* 68, 125–130.
- Dessi-Fulgheri, P., Sarzani, R., Tamburrini, P., Moraca, A., Espinosa, E., Cola, G., et al., 1997. Plasma atrial natriuretic peptide and natriuretic peptide receptor gene expression in adipose tissue of normotensive and hypertensive obese patients. *J. Hypertens.* 15, 1695–1699.
- Gómez-Ambrosi, J., Catalán, V., Díez-Caballero, A., Martínez-Cruz, L.A., Gil, M.J., García-Foncillas, J., et al., 2004. Gene expression profile of omental adipose tissue in human obesity. *FASEB J.* 18, 215–217.
- Govers, R., 2014. Molecular mechanisms of GLUT4 regulation in adipocytes. *Diabetes Metab.* 40, 400–410.
- Gower Jr., W.R., Carter, G.M., McAfee, Q., Solivan, S.M., 2006. Identification, regulation and anti-proliferative role of the NPR-C receptor in gastric epithelial cells. *Mol. Cell Biochem.* 293 (1–2), 103–118.
- Gruden, G., Landi, A., Bruno, G., 2014. Natriuretic peptides, heart, and adipose tissue: new findings and future developments for diabetes research. *Diabetes Care* 37, 2899–2908.
- Haneklaus, M., O'Neill, L.A., 2015. NLRP3 at the interface of metabolism and inflammation. *Immunol. Rev.* 265, 53–62.
- Hutchinson, D.S., Chernogubova, E., Dallner, O.S., Cannon, B., Bengtsson, T., 2005. Beta-adrenoceptors, but not alpha-adrenoceptors, stimulate AMP-activated protein kinase in brown adipocytes independently of uncoupling protein-1. *Diabetologia* 48, 2386–2395.
- Kumar, R., Cartledge, W.A., Lincoln, T.M., Pandey, K.N., 1997. Expression of guanylyl cyclase-A/atrial natriuretic peptide receptor blocks the activation of protein kinase C in vascular smooth muscle cells. Role of cGMP and cGMP-dependent protein kinase. *Hypertension* 29, 414–421.
- Levin, E.R., 1993. Natriuretic peptide C-receptor: more than a clearance receptor. *Am. J. Physiol.* 264 (4 Pt 1), E483–E489.
- Li, Y., Madiraju, P., Anand-Srivastava, M.B., 2012. Knockdown of natriuretic peptide receptor-A enhances receptor C expression and signalling in vascular smooth muscle cells. *Cardiovasc. Res.* 93, 350–359.
- Li, Y., Sarkar, O., Brochu, M., Anand-Srivastava, M.B., 2014. Natriuretic peptide receptor-C attenuates hypertension in spontaneously hypertensive rats: role of nitrooxidative stress and Gi proteins. *Hypertension* 63, 846–855.
- Maack, T., Suzuki, M., Almeida, F.A., Nussenzweig, D., Scarborough, R.M., McEnroe, G.A., et al., 1987. Physiological role of silent receptors of atrial natriuretic factor. *Science* 238, 675–678.
- Matsukawa, N., Grzesik, W.J., Takahashi, N., Pandey, K.N., Pang, S., Yamauchi, M., et al., 1999. The natriuretic peptide clearance receptor locally modulates the physiological effects of the natriuretic peptide system. *Proc. Natl. Acad. Sci. U. S. A.* 96, 7403–7408.
- Moro, C., Lafontan, M., 2013. Natriuretic peptides and cGMP signaling control of energy homeostasis. *Am. J. Physiol. Heart Circ. Physiol.* 304, H358–H368.
- Moro, C., Polak, J., Hejnova, J., Klimcakova, E., Crampes, F., Stich, V., et al., 2006. Atrial natriuretic peptide stimulates lipid mobilization during repeated bouts of endurance exercise. *Am. J. Physiol. Endocrinol. Metab.* 290, E864–E869.
- Mullins, G.R., Wang, L., Rajea, V., Sherwooda, S.G., Rebecca, C., 2014. Catecholamine-induced lipolysis causes mTOR complex dissociation and inhibits glucose uptake in adipocytes. *PNAS* 111, 17450–17455.
- Nishikimi, T., Iemura-Inaba, C., Akimoto, K., Ishikawa, K., Koshikawa, S., Matsuoka, H., 2009. Stimulatory and inhibitory regulation of lipolysis by the NPR-A/cGMP/PKG and NPR-C/Gi pathways in rat cultured adipocytes. *Regul. Pept.* 153, 56–63.
- Omar, B., Zmuda-Trzebiatowska, E., Manganiello, V., Göransson, O., Degerman, E., 2009. Regulation of AMP-activated protein kinase by cAMP in adipocytes: roles for phosphodiesterases, protein kinase B, protein kinase A, Epac and lipolysis. *Cell Sig.* 21, 760–766.
- Ortego, J., Coca-Prados, M., 1999. Functional expression of components of the natriuretic peptide system in human ocular nonpigmented ciliary epithelial cells. *Biochem. Biophys. Res. Commun.* 258 (1), 21–28.
- Pandey, K.N., 2005. Biology of natriuretic peptides and their receptors. *Peptides* 26, 901–932.
- Pandey, K.N., 2014. Guanylyl cyclase/natriuretic peptide receptor-A signaling antagonizes phosphoinositide hydrolysis, Ca(2+) release, and activation of protein kinase C. *Front. Mol. Neurosci.* 22 (7), 7–75.
- Pfaffl, M.W., 2001. A new mathematical model for relative quantification in real-time RT-PCR. *Nucleic Acids Res.* 29, e45.
- Pivovarov, O., Gögebakan, Ö., Klötting, N., Sparwasser, A., Weickert, M.O., Haddad, I., et al., 2012. Insulin up-regulates natriuretic peptide clearance receptor expression in the subcutaneous fat depot in obese subjects: a missing link between CVD risk and obesity? *J. Clin. Endocrinol. Metab.* 97, 731–739.
- Potter, L.R., Abbey-Hosch, S., Dickey, D.M., 2006. Natriuretic peptides, their receptors, and cyclic guanosine monophosphate-dependent signaling functions. *Endocr. Rev.* 27, 47–72.
- Rutherford, R.A., Matsuda, Y., Wilkins, M.R., Polak, J.M., Wharton, J., 1994. Identification of renal natriuretic peptide receptor subpopulations by use of the non-peptide antagonist, HS-142–1. *Br. J. Pharmacol.* 113 (3), 931–939.
- Santangelo, C., Vari, R., Scazzocchio, B., Filesi, C., D'Archivio, M., Giovanni, C., et al., 2011. CCAAT/enhancer-binding protein-β participates in oxidized LDL-enhanced proliferation in 3T3-L1 cells. *Biochimie* 93, 1510–1519.
- Sarzani, R., Dessi-Fulgheri, P., Paci, V.M., Espinosa, E., Rappelli, A., 1996. Expression of natriuretic peptide receptors in human adipose and other tissues. *J. Endocrinol. Invest.* 19, 581–585.
- Schenk, D.B., Phelps, M.N., Porter, J.G., Fuller, F., Cordell, B., Lewicki, J.A., 1987. Purification and subunit composition of atrial natriuretic peptide receptor. *Proc. Natl. Acad. Sci. U. S. A.* 84, 1521–1525.
- Schlueter, N., de Sterke, A., Willmes, D.M., Spranger, J., Jordan, J., Birkenfeld, A., 2014. Metabolic actions of natriuretic peptides and therapeutic potential in the metabolic syndrome. *Pharmacol. Ther.* 144, 12–27.
- Schroder, K., Tschopp, J., 2010. The inflammasomes. *Cell* 140, 821–832.
- Sellitti, D.F., Perrella, G., Doi, S.Q., Curcio, F., 2001. Natriuretic peptides increase cAMP production in human thyrocytes via the natriuretic peptide clearance receptor (NPR-C). *Regul. Pept.* 97, 103–109.
- Sengenès, C., Moro, C., Galitzky, J., Berlan, M., Lafontan, M., 2005. Natriuretic peptides: a new lipolytic pathway in human fat cells. *Med. Sci. Paris* 21, 29–33.
- Skowronska, M., Zielińska, M., Albrecht, J., 2010. Stimulation of natriuretic peptide receptor C attenuates accumulation of reactive oxygen species and nitric oxide synthesis in ammonia-treated astrocytes. *J. Neurochem.* 115 (4), 1068–1076.
- Vater, C., Kasten, P., Stiehler, M., 2011. Culture media for the differentiation of mesenchymal stromal cells. *Acta Biomater.* 7, 463–477.
- Wang, T.J., Larson, M.G., Keyes, M.J., Levy, D., Benjamin, E.J., Vasan, R.S., 2007. Association of plasma natriuretic peptide levels with metabolic risk factors in ambulatory individuals. *Circulation* 115, 1345–1353.
- Wu, Z., Rosen, E.D., Brun, R., Hauser, S., Adelmant, G., Troy, A.E., et al., 1999. Crossregulation of C/EBPβ and PPARγ controls the transcriptional pathway of adipogenesis and insulin sensitivity. *Mol. Cell.* (3), 151–158.
- Yin, W., Mu, J., Birnbaum, M.J., 2003. Role of AMP-activated protein kinase in cyclic AMP-dependent lipolysis in 3T3-L1 adipocytes. *J. Biol. Chem.* 278, 43074–43080.
- Zhang, M., Tang, H., Shen, G., Zhou, B., Wu, Z., Peng, Z., et al., 2005. Atrial natriuretic peptide induces an acrosome reaction in giant panda spermatozoa and enhances their penetration of salt-stored porcine oocytes. *Theriogenology* 64 (6), 1297–1308.

Chapter 3: *Results*

Impact of 3-Amino-1,2,4-Triazole (3-AT)-Derived Increase in Hydrogen Peroxide Levels on Inflammation and Metabolism in Human Differentiated Adipocytes.

Ruiz-Ojeda FJ, Gomez-Llorente C, Aguilera CM, Gil A,
Rupérez AI.

PLoS One.**2016**; 11(3):e0152550.

Impact Factor 2015: **3,234**

RESEARCH ARTICLE

Impact of 3-Amino-1,2,4-Triazole (3-AT)-Derived Increase in Hydrogen Peroxide Levels on Inflammation and Metabolism in Human Differentiated Adipocytes

Francisco Javier Ruiz-Ojeda¹, Carolina Gomez-Llorente^{1,2,3}, Concepción María Aguilera^{1,2,3}, Angel Gil^{1,2,3}, Azahara Iris Rupérez^{1*}

1 Department of Biochemistry and Molecular Biology II, Institute of Nutrition and Food Technology "José Mataix", Center of Biomedical Research, University of Granada, Avda. del Conocimiento s/n., Armilla, Granada, 18016, Spain, **2** Instituto de Investigación Biosanitaria IBS.GRANADA, Granada, Spain, **3** CIBER Fisiopatología de la Obesidad y la Nutrición (CIBEROBN), Madrid, Spain

* azahararuperez@ugr.es


 OPEN ACCESS

Citation: Ruiz-Ojeda FJ, Gomez-Llorente C, Aguilera CM, Gil A, Rupérez AI (2016) Impact of 3-Amino-1,2,4-Triazole (3-AT)-Derived Increase in Hydrogen Peroxide Levels on Inflammation and Metabolism in Human Differentiated Adipocytes. PLoS ONE 11(3): e0152550. doi:10.1371/journal.pone.0152550

Editor: Makoto Kanzaki, Tohoku University, JAPAN

Received: November 5, 2015

Accepted: March 16, 2016

Published: March 29, 2016

Copyright: © 2016 Ruiz-Ojeda et al. This is an open access article distributed under the terms of the [Creative Commons Attribution License](https://creativecommons.org/licenses/by/4.0/), which permits unrestricted use, distribution, and reproduction in any medium, provided the original author and source are credited.

Data Availability Statement: Data are available at <https://figshare.com/s/73efef6a8cad6a4fe501>.

Funding: This work was supported by Junta de Andalucía (Project number CTS-6770; Secretaría General de Universidades, Investigación y Tecnología, Consejería de Economía, Innovación y Ciencia), and Instituto de Salud Carlos III, Fondo de Investigaciones Sanitarias, Redes temáticas de investigación cooperativa RETIC (Red SAMID RD08/0072/0028). FJRO was funded by a Formación de Profesorado Universitario stipend from the Ministry of Education and Science of the Spanish Government (AP2012-02068). CGL and AIR are recipients of

Abstract

Obesity is characterized by an excessive accumulation of fat in adipose tissue, which is associated with oxidative stress and chronic inflammation. Excessive H₂O₂ levels are degraded by catalase (CAT), the activity of which is decreased in obesity. We investigated the effects of inhibition of catalase activity on metabolism and inflammation by incubating human differentiated adipocytes with 10 mM 3-amino-1,2,4-triazole (3-AT) for 24 h. As expected, the treatment decreased CAT activity and increased intracellular H₂O₂ levels significantly. Glutathione peroxidase (GPX) activity was also reduced, and the gene expression levels of the antioxidant enzymes *GPX4* and peroxiredoxins (1, 3 and 5) were inhibited. Interestingly, this occurred along with lower mRNA levels of the transcription factors nuclear factor (erythroid 2-like 2) and forkhead box O, which are involved in redox homeostasis. However, superoxide dismutase activity and expression were increased. Moreover, 3-AT led to nuclear factor kappa-light-chain-enhancer of activated B cells (NF-κB) activation and increased tumor necrosis alpha and interleukin 6 protein and gene expression levels, while lowering peroxisome proliferator-activated receptor gamma (*PPARγ*) mRNA and protein levels. These alterations were accompanied by an altered glucose and lipid metabolism. Indeed, adipocytes treated with 3-AT showed reduced basal glucose uptake, reduced glucose transporter type 4 gene and protein expression, reduced lipolysis, reduced AMP-activated protein kinase activation and reduced gene expression of lipases. Our results indicate that increased H₂O₂ levels caused by 3-AT treatment impair the antioxidant defense system, lower *PPARγ* expression and initiate inflammation, thus affecting glucose and lipid metabolism in human differentiated adipocytes.

fellowships from the University of Granada Plan Propio. The funders had no role in study design, data collection and analysis, decision to publish, or preparation of the manuscript.

Competing Interests: The authors have declared that no competing interests exist.

Introduction

Obesity is a global concern for societies and healthcare systems [1], and its prevalence worldwide needs to be decreased. In obese adipose tissue, the adipokine secretion profile is altered, there is low-grade inflammation and lipid and glucose metabolism are affected [2,3]. In addition, obese adipose tissue has also been characterized by an excessive production of reactive oxygen species (ROS) [4].

An imbalance between ROS production and scavenging mechanisms leads to the development of oxidative stress in adipose tissue, which is associated with the previously mentioned metabolic alterations [4,5,6]. In particular, one of the most abundant forms of ROS in adipocytes is hydrogen peroxide (H_2O_2), the levels of which are heavily regulated by different enzymes that include catalase (CAT), glutathione peroxidases (GPX), superoxide dismutase (SOD) and peroxiredoxins (PRDXs) [7]. Although H_2O_2 is an important signaling molecule at controlled levels [8,9], its increased production can determine metabolic alterations in adipocytes [10].

Interestingly, catalase activity, which is responsible for the degradation of excessive amounts of H_2O_2 , has been shown to be decreased in obese adults [11] as well as in children with obesity and insulin resistance [12,13]. Moreover, obese and type 2 diabetic mice have lower CAT expression and higher H_2O_2 levels in adipose tissue [4,14].

It is known that oxidative stress can activate the nuclear factor kappa-light-chain-enhancer of activated B cells (NF- κ B) inflammation pathway. Serine phosphorylation at various sites of the NF- κ B p65 subunit has been shown to be important for the transcription of various inflammatory mediators, including tumor necrosis factor alpha (TNF- α) and interleukin 6 (IL-6) [15,16]. TNF- α is a potent cytokine with many adverse effects such as insulin resistance [17] and activation of lipolysis [18].

Additionally, ROS are also able to lower peroxisome proliferator-activated receptor gamma (PPAR γ) expression [19], which can itself regulate CAT expression in adipose tissue [20]. In fact, in obese individuals, treatment with rosiglitazone, a PPAR γ agonist, increased CAT protein levels in adipose tissues [21]. Along with this finding, it has been observed that oxidative stress can lead to a down-regulation of adiponectin (ADIPOQ) and glucose transporter 4 (GLUT4) gene expression in adipose tissue [4,6].

Regarding the effects of oxidative stress on lipid metabolism, H_2O_2 has been shown to inhibit cAMP-stimulated protein kinase A (PKA) activity, thus reducing lipolysis in adipocytes [14]. Regarding 5'-AMP-activated protein kinase (AMPK), it has been shown to be activated as a consequence of lipolysis, in parallel with an increase in oxidative stress [22]. Furthermore, oxidative stress can inhibit the expression of lipase genes by activating inflammation and reducing PPAR γ expression.

Regarding the cellular responses to oxidative stress, nuclear factor (erythroid 2-like 2) (Nrf2) and forkhead box O (FOXO1) play important roles in maintaining intracellular redox homeostasis by inducing the expression of antioxidant enzymes [23,24]. Moreover, it has been reported that ROS can modulate the Wnt/ β -catenin pathway and that low levels of oxidative stress favor the interaction of β -catenin with FOXO1 to protect the cell against oxidative damage [25].

Although these facts make it clear that oxidative stress is associated with inflammation, insulin resistance and altered lipid metabolism, the exact contribution of catalase activity to the protection against the progression of these metabolic alterations is not clear. Thus, by using the irreversible CAT inhibitor 3-amino-1,2,4-triazole (3-AT) [26] in human differentiated adipocytes, we investigated the mechanism by which catalase activity contributes to the deleterious effects of oxidative stress in adipose tissue.

Materials and Methods

Materials

Adipose derived-stem cells (ADSCs) were purchased directly from Lonza (Poietics™ Normal ADSCs, Lonza, PT-5006, Lot 0F4505, Switzerland). These commercially available ADSCs are isolated from normal (non-diabetic) adult subcutaneous lipoaspirates collected during elective surgical liposuction procedures. ADSCs have been reported to differentiate into many different lineages, including chondrogenic, osteogenic, adipogenic and neural lineages. Adipogenesis media and reagents were obtained from Lonza, and 3-AT was purchased from Sigma (Sigma-Aldrich, St. Louis, MO, USA). Adenosine 3',5'-cyclic monophosphate (cAMP) was acquired from Sigma (A9501). The rabbit anti-GLUT4 antibody (H-61) and TNF- α antibody (SC-52746) were acquired from Santa Cruz Biotechnology (Santa Cruz, CA, USA). The goat anti-adiponectin antibody (AF1065) was obtained from R&D Systems (R&D, Inc. USA). The rabbit anti-PPAR γ (D69), phosphor-NF-kB p65 (Ser536), rabbit anti-total AMPK α (D5A2) and rabbit anti-phospho-AMPK α (Thr172) antibodies were acquired from Cell Signaling Technologies (Beverly, MA, USA). The mouse anti- α -tubulin antibody (T5158) and horseradish peroxidase-conjugated immunoglobulin were purchased from Sigma. Unless otherwise indicated, all other chemicals were purchased from Sigma.

Cell culture and incubation

The ADSCs were cultured, expanded and differentiated into adipocytes according to the manufacturer's recommendations. Briefly, ADSCs were grown and expanded in appropriate sterile plastic dishes in complete Advanced-DMEM medium (Gibco, Life Technologies, Carlsbad, CA, USA) supplemented with 2 mM L-glutamine (25030, Gibco, Life Technologies, Carlsbad, CA, USA), 10% fetal bovine serum (FBS, PT-9000 H, Lonza, Basel, Switzerland), 100 U ml⁻¹ penicillin and 100 μ g ml⁻¹ streptomycin (10378-016, Gibco, Life Technologies, Carlsbad, CA, USA). Cells were incubated at 37°C in a humidified atmosphere containing 5% CO₂. The cell culture medium was replaced twice per week, and cells were passaged up to a maximum of 6 times. To induce differentiation, cells were seeded in 35-mm dishes at a density of 30,000 cells/cm² and cultured in preadipocyte growth medium (PGM) consisting of Preadipocyte Basal Medium-2 (PT-8002, Lonza) supplemented with 10% FBS, 2 mM L-Glutamine (PT-9001 H, Lonza) and 0.1 μ g/ml gentamicin sulfate/amphotericin-B (PT-4504, Lonza). At 90% confluency, the growth medium was replaced with differentiation medium (PGM supplemented with dexamethasone, 3-isobutyl-1-methylxanthine, indomethacin and h-insulin; PT-9502, Lonza). ADSCs were incubated with differentiation medium for 10 days. Finally, cells were washed twice with PBS, and the differentiation medium was replaced with PGM overnight. Adipogenesis was monitored and quantified by morphological examination of the cellular accumulation of lipid droplets by Oil Red O staining (234117, Sigma-Aldrich, St. Louis, MO, USA; Fig A in S1 File) and by spectrophotometric determination of washed Oil Red O staining (Fig B in S1 File). All treatments were performed on differentiated adipocytes on day 10.

Catalase activity assay

Human differentiated adipocytes were incubated in the presence or absence of 3-AT (2 mM and 10 mM) for 24 h, and the catalase activity was determined in cell lysates using a colorimetric assay (K033-H1, Arbor assays, Michigan, USA). Briefly, the cells were harvested, lysed with protein lysis buffer (PLB) containing 10 mM Tris-HCl (pH 7.5), 150 mM NaCl, 2 mM EDTA, 1% Triton X-100, 10% glycerol and protease inhibitor cocktail (Thermo Scientific, Massachusetts, USA), and placed on ice for 20 min. Then, the cell lysates were centrifuged (30 min, 13000 \times g,

4°C), and the supernatants were used to determine the protein concentrations with the Protein Assay Kit II (Bio-Rad Laboratories, California, USA), which was performed according to the manufacturer's instructions. A bovine catalase standard was used to generate a standard curve for the assay. Next, hydrogen peroxide was added to the supernatants, and they were incubated at room temperature for 30 min. The HRP reacts with the substrate in the presence of hydrogen peroxide to convert the colorless substrate into a pink-colored product. All samples were compared to the standard curve, and the activity of catalase in each sample was calculated after making the appropriate corrections for dilutions, using the software available with the plate reader. The results were presented as units of catalase activity per mg protein. Sensitivity was determined to be 0.052 U/mL, and the limit of detection was determined to be 0.062 U/mL.

Intracellular H₂O₂ determination

The generation of intracellular H₂O₂ in the presence or absence of 3-AT (2 mM and 10 mM) for 24 h by adipocytes was measured in cell lysates using the OxiSelect fluorometric assay (Cell Biolabs, San Diego, CA, USA). Cell lysates were incubated, and the fluorescence was measured with a microplate reader in standard 96-well fluorescence black microtiter plates using an excitation wavelength of 530 nm and a detection wavelength of 590 nm. Intracellular H₂O₂ results were expressed as μM of H₂O₂.

Superoxide dismutase and glutathione peroxidase activity assays

SOD and GPX activities were determined spectrophotometrically in cell lysates of adipocytes in the presence or absence of 3-AT (10 mM) for 24 h using two commercial kits (K028-H1 for SOD, Arbor assays, Michigan, USA; 703102 for GPX, Cayman Chemical, Michigan, USA). Samples were harvested with PLB, diluted in the buffer diluents and then added to the wells with the rest of the reagents. The SOD activity assay was performed according to the manufacturer's instructions. The absorbance was measured at 450 nm, and the results were expressed in terms of the units of SOD activity per mg protein. Sensitivity was determined to be 0.044 U/mL, and the limit of detection was determined to be 0.0625 U/mL. GPX activity was measured indirectly by a coupled reaction with glutathione reductase (GR). Oxidized glutathione (GSSG), which is produced upon reduction of cumene hydroperoxide by GPX, is recycled to its reduced state by GR and NADPH. The oxidation of NADPH to NADP⁺ is accompanied by a decrease in absorbance at 340 nm. Thus, the rate of decrease is directly proportional to the GPX activity in the sample. The results were expressed in nmol/min/mg protein. Sensitivity was determined to be 0.02 of decreased absorbance per minute, and the limit of detection was determined to be 50 nmol/min/mL.

GSH/GSSG ratio detection assay

Reduced and oxidized glutathione GSH/GSSG ratio of cell lysates was measured with a fluorometric kit (ab138881, Abcam, Cambridge, UK). GSH and total glutathione were determined by changes in fluorescence intensity, and GSSG concentration was calculated using total glutathione-GSH. The results were expressed as GSH/GSSG ratios in the presence or absence of 3-AT (10 mM) for 24 h in human differentiated adipocytes.

Lipolysis assay

The total glycerol release, the final product of lipolysis, was measured in cell supernatants using a colorimetric assay (Free Glycerol Reagent, F6428, Sigma, St. Louis, MO, USA). The cells were treated with 3-AT (10 mM) for 24 h, and the cell supernatants were harvested. Then, the cell supernatants were incubated in the reagent at room temperature for 15 min in a

96-well plate, and the optical density at 550 nm was measured using a microplate reader (Bio-Tek HTX, Fischer Scientific, USA).

RNA isolation and qRT-PCR

Total RNA was extracted from cells using the PeqGOLD HP Total RNA kit (Peqlab, Germany). Isolated RNA was treated with Turbo DNase (Ambion, Life Technologies, Carlsbad, CA, USA). The final RNA concentration and quality were determined using a NanoDrop2000 (NanoDrop Technologies, Winooski, Vermont, USA). Total RNA (500 ng) was transcribed into cDNA using the iScript cDNA Synthesis Kit (Bio-Rad Laboratories, California, USA). Differential gene expression levels of *CAT*, hormone sensitive lipase (*HSL*), adipose triglyceride lipase (*ATGL*), *PPAR γ* , adipocyte fatty acid-binding protein (*FABP4*), and perilipin (*PLIN*) were determined by qPCR using specific primer sequences. Glyceraldehyde 3-phosphate dehydrogenase (*GAPDH*) was used as a reference gene for the differentiation experiments, while hypoxanthine-guanine phosphoribosyltransferase-1 (*HPRT1*) was used for 3-AT treatment experiments as *GAPDH* is not a suitable reference gene when glucose metabolism is altered. The specific primer sequences were designed using Primer3 (<http://bioinfo.ut.ee/primer3-0.4.0/>, Table 1). Primers for *GLUT4*, *IL-6*, *TNF- α* , *NFKB2*, tumor necrosis factor receptor superfamily, member 1A (*TNFRSF1A*), glutathione peroxidase 4 (*GPX4*), peroxiredoxin 1 (*PRDX1*), peroxiredoxin 3 (*PRDX3*), peroxiredoxin 5 (*PRDX5*), catenin beta 1 (*CTNNB1*), *FOXO1*, *NRF2* and superoxide dismutase 1, soluble (*SOD1*) were obtained from Bio-Rad Laboratories, California, USA. The qPCR was performed with an ABI Prism 7900 instrument (Applied Biosystems, Foster City, CA, USA) using SYBR Green PCR Master Mix (Applied Biosystems, Foster City, CA, USA). Quantification was performed using the Pfaffl method [27]. Compliance with the minimum information for publication of quantitative real-time PCR experiments (MIQE) was made possible using Bio-Rad's PrimePCR assays. Statistical validation of the stability of the reference genes was calculated in each sample. Bio-Rad recommends using a <0.5 value, which is the most stable expression in the tested samples. The results are expressed as fold-change calculated using the $2^{-\Delta\Delta C_t}$ method.

Western blot assays

Protein samples from cell lysates containing 2.5 μ g of protein were mixed with 3X SDS-PAGE sample buffer (100 mM Tris-HCl, pH 6.8, 25% SDS, 0.4% bromophenol blue, 10% β -

Table 1. Forward and reverse primer sequences used in the qPCR assays.

Gene	Primer sequence		Size (bp)
	Forward	Reverse	
<i>CAT</i>	5'-GCCTGGGACCCAATTATCTT-3'	5'-GAATCTCCGCACTTCTCCAG-3'	203
<i>HSL</i>	5'-CTTCTGGAAGCCTTCTGGAACATCACCGA-3'	5'-CTGAGCTCCTCACTGTCCTGCCTTCCAC-3'	249
<i>ATGL</i>	5'-GACGAGCTCATCCAGGCCAATGTCTG-3'	5'-GATGGTGTTCTTAAGCTCATAGAGTGGCAGG-3'	141
<i>PPARγ</i>	5'-CTCGAGGACACCGGAGAGG-3'	5'-CACGGAGCTGATCCCAAAGT-3'	121
<i>FABP4</i>	5'-GCTTTTGTAGGTACCTGGAAACTT-3'	5'-ACACTGATGATCATGTTAGGTTTGG-3'	125
<i>PLIN</i>	5'-CTCTCGATACACCGTGCAGA-3'	5'-tggtcctcatgatcctcctc-3'	207
<i>GAPDH</i>	5'-GAGTCAACGGATTTGGTCGT-3'	5'-TTGATTTTGGAGGGATCTCG-3'	238
<i>HPRT1</i>	5'-GAGATGGGAGGCCATCACATTGTAGCCCTC-3'	5'-CTCCACCAATTACTTTTATGTCCCTGTTGACTGGTC-3'	76

CAT, Catalase; *HSL*, Hormone sensitive lipase; *ATGL*, Adipose triglyceride lipase; *PPAR γ* , Peroxisome proliferator-activated receptor gamma; *FABP4*, Fatty acid binding protein 4, adipocyte; *PLIN*, Perilipin; *GAPDH*, Glyceraldehyde 3-phosphate dehydrogenase; *HPRT1*, Hypoxanthine-guanine phosphoribosyltransferase-1.

doi:10.1371/journal.pone.0152550.t001

mercaptoethanol and 2% glycerol), separated via SDS-PAGE using a TGX Any kD gel (Bio-Rad Laboratories, California, USA) and transferred to a nitrocellulose membrane (Bio-Rad Laboratories, California, USA). After incubation in blocking buffer [5% non-fat milk and 1% Tween 20 in Tris-buffered saline (TBS)], the membranes were probed with one of the following antibodies: anti-catalase (1:2000 in 5% non-fat milk), anti-GLUT4 (1:100 in 5% non-fat milk), anti-adiponectin (1:500 in 5% bovine serum albumin, BSA), anti-PPAR γ (1:1000 in 5% BSA), anti-TNF α (1:100 in 5% BSA), anti-phospho-NF-kB p65 (Ser536) (1:500 in 5% BSA), anti-total AMPK α , anti-phosphorylated AMPK α (phospho-AMPK α T172) (both 1:1000 in 5% BSA) and anti- α -tubulin (internal control, 1:4000 in 5% non-fat milk). Immunoreactive signals were detected via enhanced chemiluminescence (Super-Signal West Dura Chemiluminescent Substrate, 34075, Thermo Scientific, Europe). The membrane images were digitally captured and the densitometric analyses were conducted using ImageJ software. The results were expressed as the fold-change in expression relative to the control.

Intracellular IL-6 protein levels

The intracellular IL-6 levels were determined in cell lysates in the presence or absence of 10 mM 3-AT for 24 h. Samples were harvested with PLB, diluted in the buffer diluents and then added to the wells with the rest of the reagents. IL-6 was determined using a MILLIplexTM kit (HADK2MAG-61K-05) with the Luminex 200 multiplex assay system built on xMAP technology (Millipore, USA). The results were calculated as pg per mg protein, and the bars were represented as units of IL-6 adjusted to control, taken as %.

Glucose uptake assays

Glucose uptake was determined using a colorimetric assay kit (MAK083, Sigma-Aldrich, St. Louis, MO, USA). Briefly, ADSCs were differentiated in 12-well plates as described in the "Cell culture and incubation" section. Differentiated adipocytes were washed twice with PBS and then starved overnight in serum-free medium. Then, the cells were washed 3 times with PBS and glucose starved by incubating for 40 min in KRPH buffer (5 mM Na₂HPO₄, 20 mM HEPES, pH 7.4, 1 mM MgSO₄, 1 mM CaCl₂, 137 mM NaCl and 4.7 mM KCl) containing 2% BSA. Glucose uptake was assessed in the presence or absence of 10 mM 3-AT for 24 h with 1 mM 2-deoxy-D-glucose in KRPH for 20 min at 37°C and 5% CO₂. As a positive control, the cells were stimulated with insulin (1 μ M) for 20 min in the presence or absence of 3-AT. Glucose uptake levels were expressed in pmol/well.

Protein kinase A (PKA) activity assay

Human differentiated adipocytes were incubated in the presence or absence of 10 mM 3-AT for 24 h, and cell lysates were obtained with PLB as previously described. Then, Protein kinase A (PKA) activity was determined using the PKA activity kit (ADI-EKS-390A, Enzo Life Science, Switzerland) after incubating the cell lysates with or without cAMP (0.1 mM) for 15 min.

Statistical analysis

All experiments were repeated at least three times. In each independent experiment, two replicates were performed. The data are expressed as the mean \pm standard error of the mean (SEM). Significant differences in the levels of *CAT* expression during the adipogenic differentiation, catalase activity, intracellular H₂O₂, SOD activity, GPX activity, gene expression, protein expression, lipolysis and glucose uptake were determined using the non-parametric Mann-

Whitney U test. Statistical significance was defined as $*P < 0.05$ and $**P < 0.01$. Statistical analyses were performed using SPSS version 22 for Windows (SPSS, Chicago, IL, USA).

Results

CAT expression during adipogenic differentiation

First, we tested *CAT* expression in human ADSCs and differentiated adipocytes by analyzing gene and protein expression on different days during adipogenic differentiation. As expected, we found that *CAT* gene expression and protein levels were significantly up-regulated on days 5, 9 and 12 compared with day 0 (Figs A and B in S2 File, respectively). Moreover, *CAT* activity was significantly increased during adipogenic differentiation on days 5, 9 and 12 compared with day 0 (Fig C in S2 File).

Inhibition of catalase activity by 3-amino-1,2,4-triazole (3-AT)

To characterize the toxicity of 3-AT in human differentiated adipocytes, we monitored the cellular viability in adipocytes exposed to increasing concentrations of 3-AT (0, 2, 6, 10, 50 and 100 mM) for 24 h using a Neubauer chamber and trypan blue (4%). No toxicity was observed for the tested range of 3-AT (S3 File). Then, taking into consideration this information as well as the available literature [28, 29, 30], we chose the concentrations of 2 mM and 10 mM 3-AT to test their effects on catalase activity in human differentiated adipocytes. 3-AT significantly inhibited catalase activity in a dose-dependent manner, producing an analogous increase in H_2O_2 levels (Fig 1A and 1B, respectively). However, 10 mM 3-AT generated a significantly higher increase in H_2O_2 than 2 mM 3-AT. According to these results, the final chosen condition for the following experiments was 10 mM 3-AT for 24 h.

Effects of 3-AT treatment on the intracellular antioxidant system in human adipocytes

GPX activity, which is responsible for H_2O_2 degradation, decreased by 28% (Fig 2A; $P = 0.001$) in human adipocytes treated with 3-AT. Moreover, SOD activity, an enzyme that generates

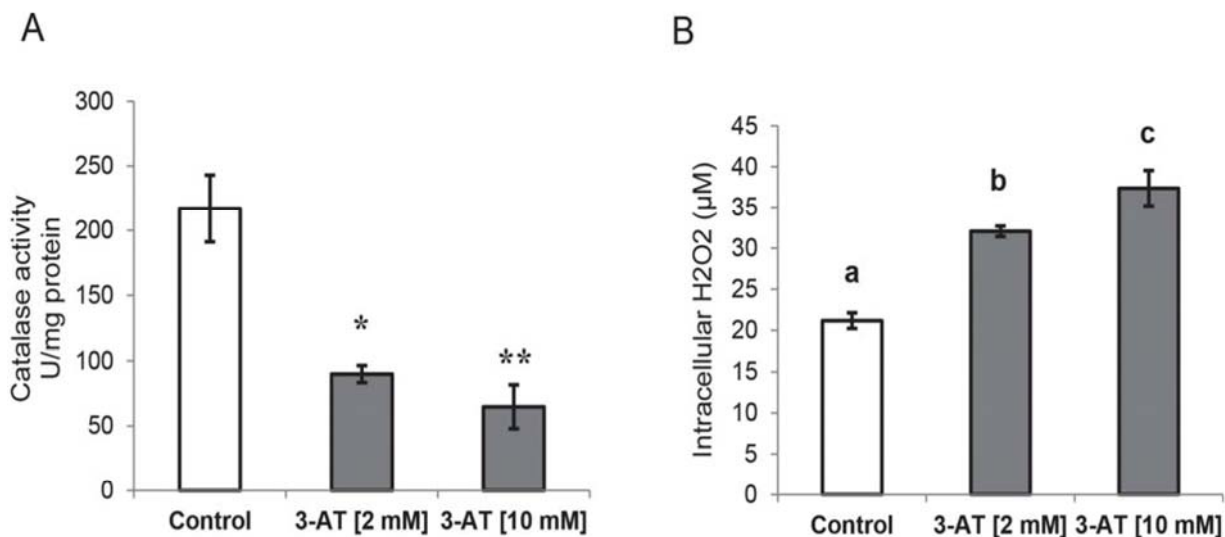


Fig 1. Catalase activity (U/mg protein) (A) and intracellular H_2O_2 levels (μM) (B) in differentiated adipocytes. Differentiated adipocytes at day 10 were treated with 2 mM and 10 mM 3-amino-1,2,4-triazole (3-AT) for 24 h. Significant differences were identified by Mann-Whitney U test. The data are expressed as the mean \pm SEM. * $P < 0.05$ vs. control; ** $P < 0.01$ vs. control. Different letters indicate significant differences ($P < 0.05$).

doi:10.1371/journal.pone.0152550.g001

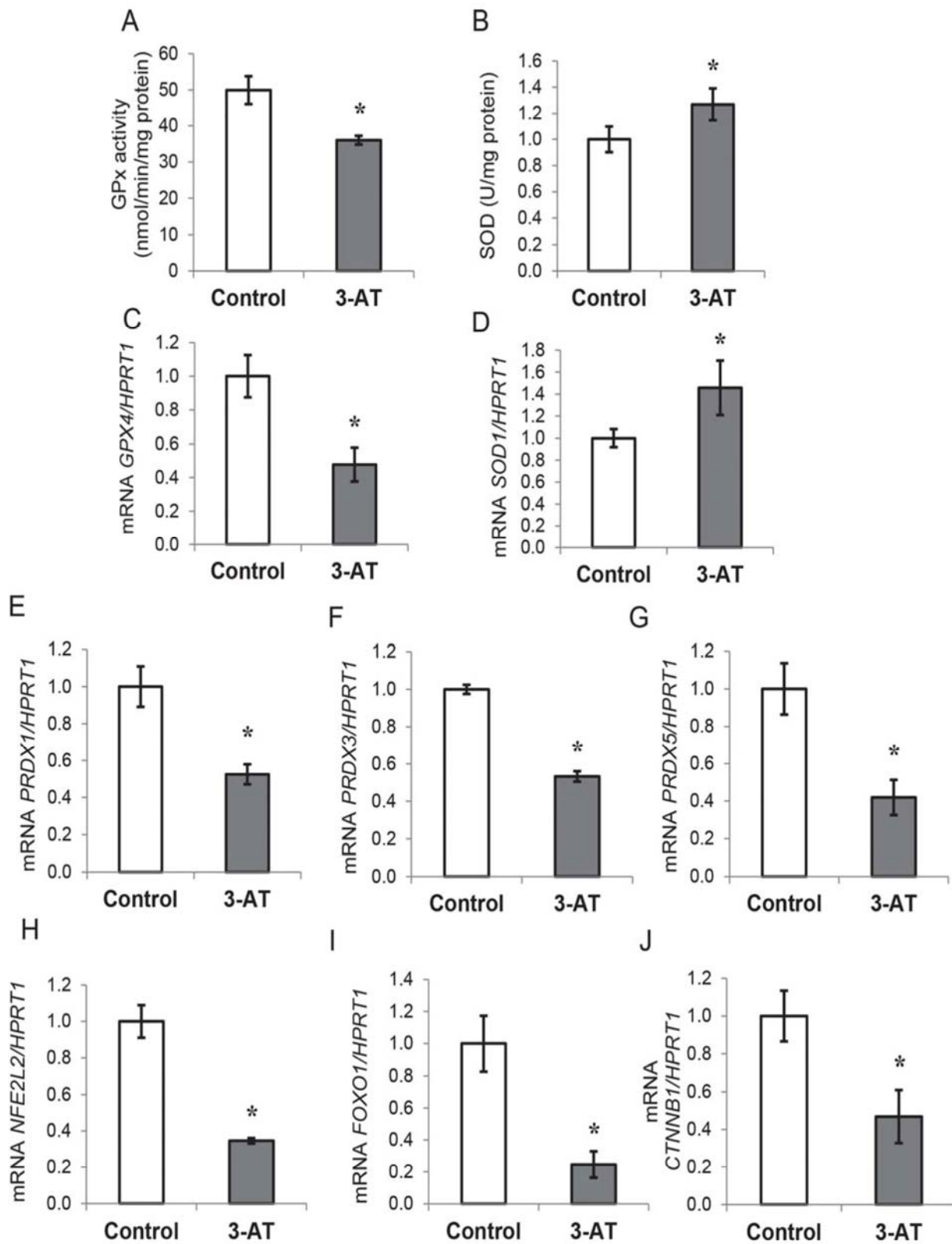


Fig 2. Effects of 3-amino-1,2,4-triazole (3-AT) on the antioxidant system in human differentiated adipocytes. A: Superoxide dismutase activity (SOD) expressed as U/mg protein in the presence or absence of 3-AT. B: mRNA expression of *SOD1* normalized to hypoxanthine-guanine phosphoribosyltransferase-1 (*HPRT1*) mRNA levels. C: Glutathione peroxidase (GPX) activity expressed as nmol/min/mg protein in the presence or absence of 3-AT. D: mRNA expression of glutathione peroxidase 4 (*GPX4*) normalized to *HPRT1* mRNA levels. E-G: mRNA expression of peroxiredoxin 1, 3 and 5 (*PRDX1*, *PRDX3*, and *PRDX5*) normalized to *HPRT1* mRNA levels in the presence or absence of 3-AT. H-J: mRNA expression of nuclear factor, erythroid 2-like 2 (*NRF2*), forkhead box O1 (*FOXO1*) and catenin beta 1 (*CTNNB1*) normalized to *HPRT1* mRNA levels in the presence or absence of 3-AT. The fold-changes from three independent experiments were calculated using the Pfaffl method. The data are presented as the means \pm SEM of three independent experiments. Significant differences were identified using the Mann-Whitney U test; * $P < 0.05$.

doi:10.1371/journal.pone.0152550.g002

H_2O_2 from the degradation of superoxide anion, was significantly higher in 3-AT-treated adipocytes (Fig 2B). Similarly, *GPX4* gene expression was significantly inhibited, whereas *SOD1* expression was increased ($P < 0.05$) after 3-AT treatment (Fig 2C and 2D, respectively). Interestingly, the gene expression levels of *PRDX1*, *PRDX3* and *PRDX5*, enzymes involved in H_2O_2 degradation, were all significantly reduced in 3-AT treated cells (Fig 2E, 2F and 2G, respectively). In addition, we observed a decrease in the gene expression levels of *NRF2*, *FOXO1* ($P < 0.05$), (Fig 2E and 2F, respectively) and *CTNNB1* (Fig 2J).

Effects of 3-AT treatment on inflammation in adipocytes

Next, we determined whether 3-AT-treated adipocytes displayed signs of inflammation by analyzing NF- κ B activation and pro-inflammatory marker expression and synthesis. Interestingly, adipocytes treated with 3-AT had higher levels of the phosphorylated NF- κ B p65 subunit (Fig 3A). In addition, the treatment of adipocytes with 3-AT significantly increased *TNF* and *IL-6* gene expression levels (FC (fold-change) = 1.93, $P = 0.03$; FC = 2.77, $P = 0.037$, respectively) (Fig 3B and 3C, respectively). Moreover, TNF- α and IL-6 protein levels were significantly increased upon 3-AT treatment in human adipocytes (Fig 3D and 3E, respectively). However, the mRNA levels of *NFKB2* and *TNFRSF1A* did not change after treatment with 3-AT (data not shown).

Effects of 3-AT on adipocyte metabolism

To characterize the underlying regulation of these findings, we analyzed the gene and protein expression levels of *PPAR γ* , which is involved in both lipid and glucose metabolism, and we found that they were down-regulated after 3-AT treatment (Fig 4A and 4B, respectively).

Glucose metabolism. Basal glucose uptake was significantly inhibited by approximately 40% in human differentiated adipocytes after treatment with 3-AT (Fig 5A). However, insulin-stimulated glucose uptake did not change between conditions. This decrease in basal glucose uptake levels was accompanied by significantly lower *GLUT4* gene and protein expression after 3-AT treatment (Fig 5B). Moreover, the intracellular levels of adiponectin were also significantly lower in 3-AT-treated adipocytes compared with untreated cells (Fig 5C).

Lipid metabolism. Regarding lipid metabolism, 3-AT-treated adipocytes exhibited reduced lipolysis as observed by decreased extracellular glycerol levels (Fig 6A). In addition, the expression levels of the lipases *HSL* and *ATGL* were significantly down-regulated upon 3-AT treatment (Fig 6B and 6C, respectively). The expression of *FABP4* was also significantly inhibited at both the mRNA and protein levels (31% \downarrow , $P = 0.037$; 55% \downarrow , $P = 0.014$, respectively). However, there were no significant differences in *PLIN* expression between 3-AT-treated and untreated adipocytes (Fig 6D).

Moreover, PKA activity was determined in the presence or absence of 3-AT (10 mM for 24 h) and cAMP (0.1 mM) in the differentiated adipocytes. Although 3-AT showed a tendency toward lower PKA activity when cAMP was added, the change was not statistically significant.

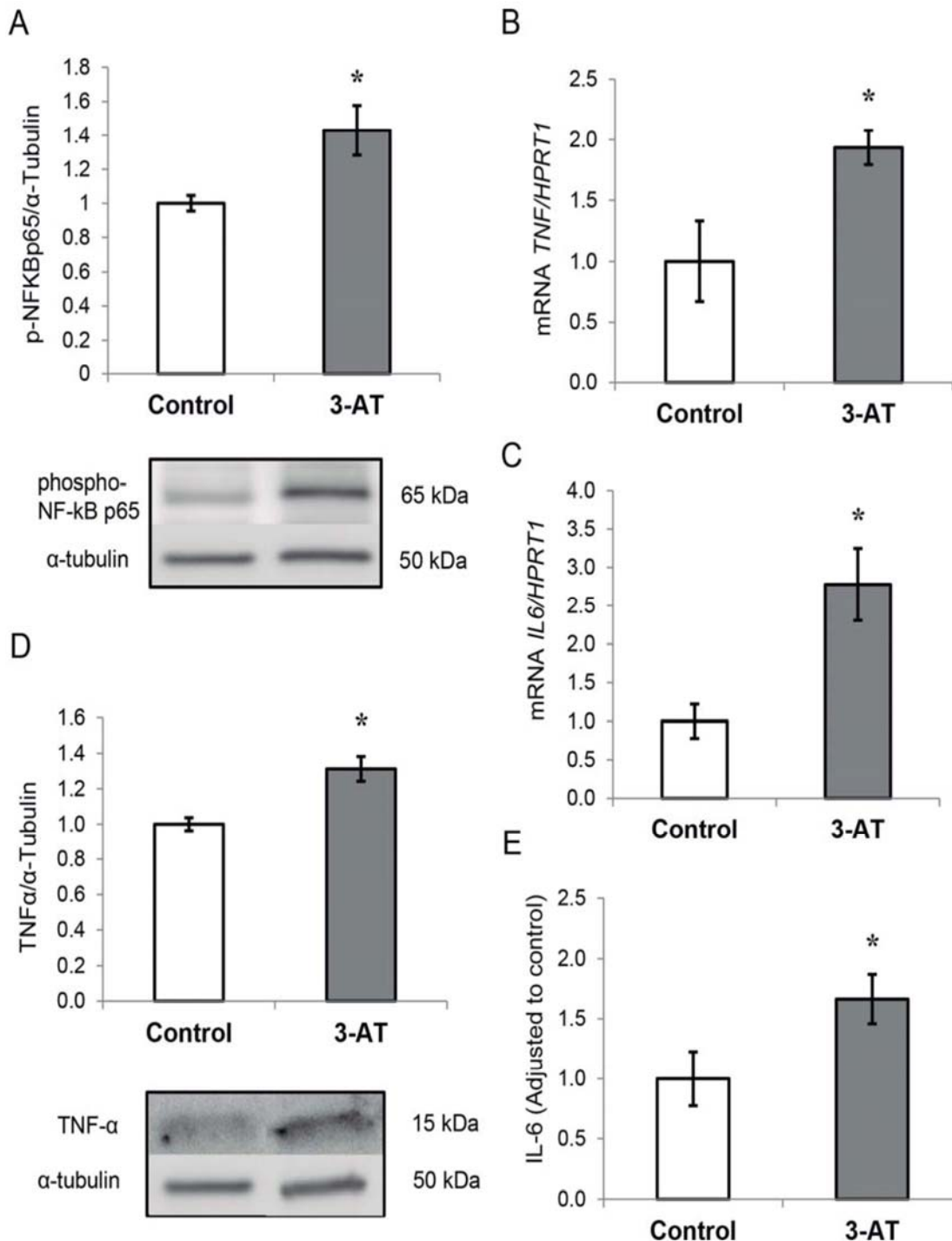


Fig 3. Effect of 3-amino-1,2,4-triazole (3-AT) treatment on inflammation in adipocytes. A: phospho-NF κ B p65 protein levels analyzed by western blot. B: mRNA expression of tumor necrosis factor- α (*TNFA*) normalized to hypoxanthine-guanine phosphoribosyltransferase-1 (*HPRT1*) mRNA levels. C: mRNA expression of interleukin 6 (*IL-6*) normalized to *HPRT1* mRNA levels. The fold-changes from three independent experiments were calculated using the Pfaffl method. D: TNF- α protein levels analyzed by western blot using a specific antibody, normalized to α -tubulin. E: IL-6 protein levels analyzed by XMap technology (Luminex) as indicated in the methods section. The data from three independent experiments are presented as the means \pm SEM. Significant differences were identified using the Mann-Whitney U test; * $P < 0.05$.

doi:10.1371/journal.pone.0152550.g003

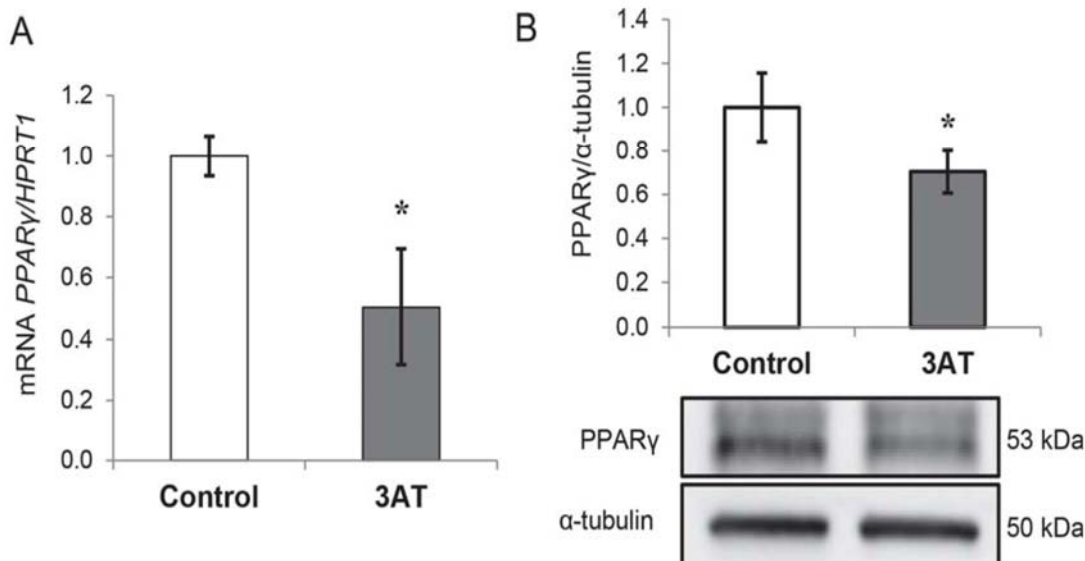


Fig 4. Effects of 3-amino-1,2,4-triazole (3-AT) on peroxisome proliferator-activated receptor gamma (PPAR γ) expression. A: mRNA expression of PPAR γ in human differentiated adipocytes. The mRNA levels were normalized to those of hypoxanthine-guanine phosphoribosyltransferase-1 (HPRT1) and the fold-changes from three independent experiments were calculated using the Pfaffl method. B: Protein expression of PPAR γ analyzed by western blot as described in the Methods section. Protein levels were normalized to the internal control α -tubulin and expressed as fold-changes. The data are presented as the means \pm SEM of three independent experiments. Significant differences were identified using the Mann-Whitney U test; * $P < 0.05$, ** $P < 0.01$.

doi:10.1371/journal.pone.0152550.g004

Finally, total AMPK α (catalytic subunit alpha) and phosphorylated AMPK α (Thr 172) were determined by western blot in the presence or absence of 3-AT. The ratio of phosphorylated AMPK α to total AMPK α was significantly lower after treatment (Fig 6F).

Discussion

Aiming to replicate the conditions observed in obesity, where CAT is inhibited, we intended to elucidate the degree to which catalase activity is responsible for the alterations found in obese adipose tissue using the inhibitor 3-AT in human adipocytes. The present study shows that the 10 mM 3-AT (24 h) treatment lowered CAT activity to 30% of the activity of control cells, doubled the content of cellular H₂O₂ and triggered inflammation while affecting antioxidant enzyme expression and lipid and glucose metabolism (Fig 7).

3-AT-treated adipocytes present an impaired antioxidant defense system

Activity and expression of antioxidant enzymes. The mechanisms involved in H₂O₂ synthesis and degradation were affected in 3-AT-treated adipocytes. We observed higher SOD activity, responsible for the conversion of superoxide ions into H₂O₂, and significantly lower GPX activity, and both events were paralleled by analogous changes in *SOD1* and *GPX4* gene expression. These results are in line with those of Than *et al.* [31] who found lower GPX and CAT protein expression levels in the presence of TNF- α -induced ROS in human adipocytes. The divergent results regarding SOD and GPX activities may seem counterintuitive. However, SOD appears to be the first line of defense against ROS in cells because it has been found augmented in different situations as a mechanism of protection [32,33,34], even along with lower CAT activity [35]. Other studies have also observed similar results where SOD activity was increased, while CAT [36,37] and GPX [37] activities were decreased. Moreover, SOD

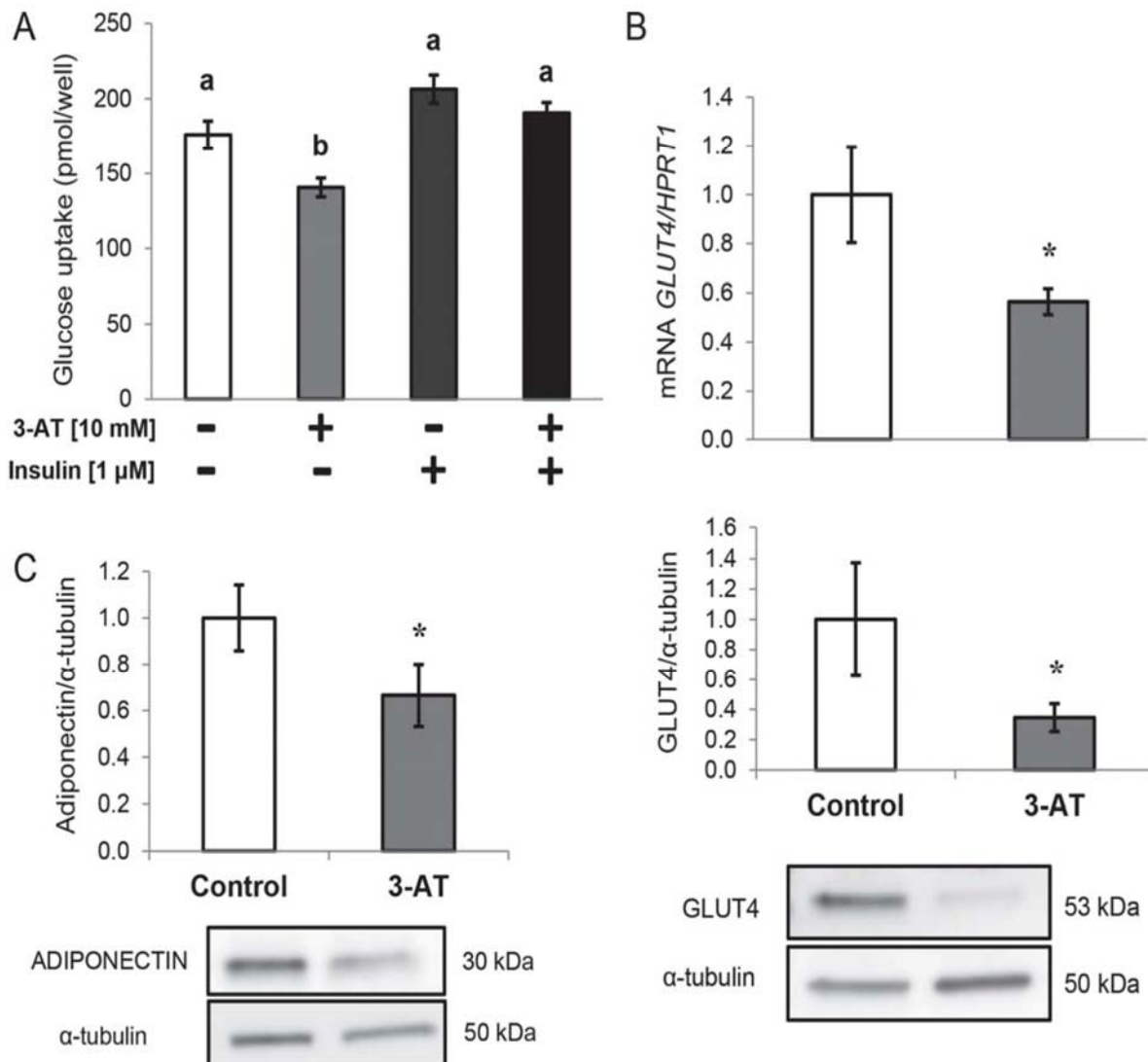


Fig 5. Effects of 3-amino-1,2,4-triazole (3-AT) on glucose metabolism in human differentiated adipocytes. A: Basal and insulin-stimulated glucose uptake levels in human differentiated adipocytes with or without 10 mM 3-AT and 1 μM insulin. Significant differences were identified using the Kruskal-Wallis test. B: mRNA and protein levels of glucose transporter 4 (*GLUT4*) in the presence or absence of 3-AT (10 mM, 24 h). The mRNA levels were normalized to those of hypoxanthine-guanine phosphoribosyltransferase-1 (*HPRT1*). The results are presented as fold-changes, which were calculated using the Pfaffli method. Protein expression of *GLUT4* analyzed by western blot as described in the Methods section. Protein levels were normalized to the internal control (α -tubulin) and expressed as fold-changes. The data from three independent experiments are presented as the means \pm SEM. Significant differences were identified using the Mann-Whitney U test. * $P < 0.05$.

doi:10.1371/journal.pone.0152550.g005

expression has been observed to be increased by $\text{TNF-}\alpha$ in a mechanism involving $\text{NF-}\kappa\text{B}$ activation [38]. Although we cannot rule out the possibility of partial inhibition of GPX by 3-AT [39], most of the studies using 3-AT report a specific inhibition of catalase [40,41]. Additionally, the expression levels of *PRDX1*, *PRDX3* and *PRDX5*, which are enzymes that are also involved in H_2O_2 clearance, were significantly reduced after treatment with 3-AT, which could contribute to increase H_2O_2 levels. Indeed, *PRDX3* is expressed in mature adipocytes and has been observed to be decreased in obesity [42,43]. In fact, Huh *et al.*, 2012 demonstrated that *PRDX3* deficiency leads to impaired glucose metabolism and decreased adiponectin levels.

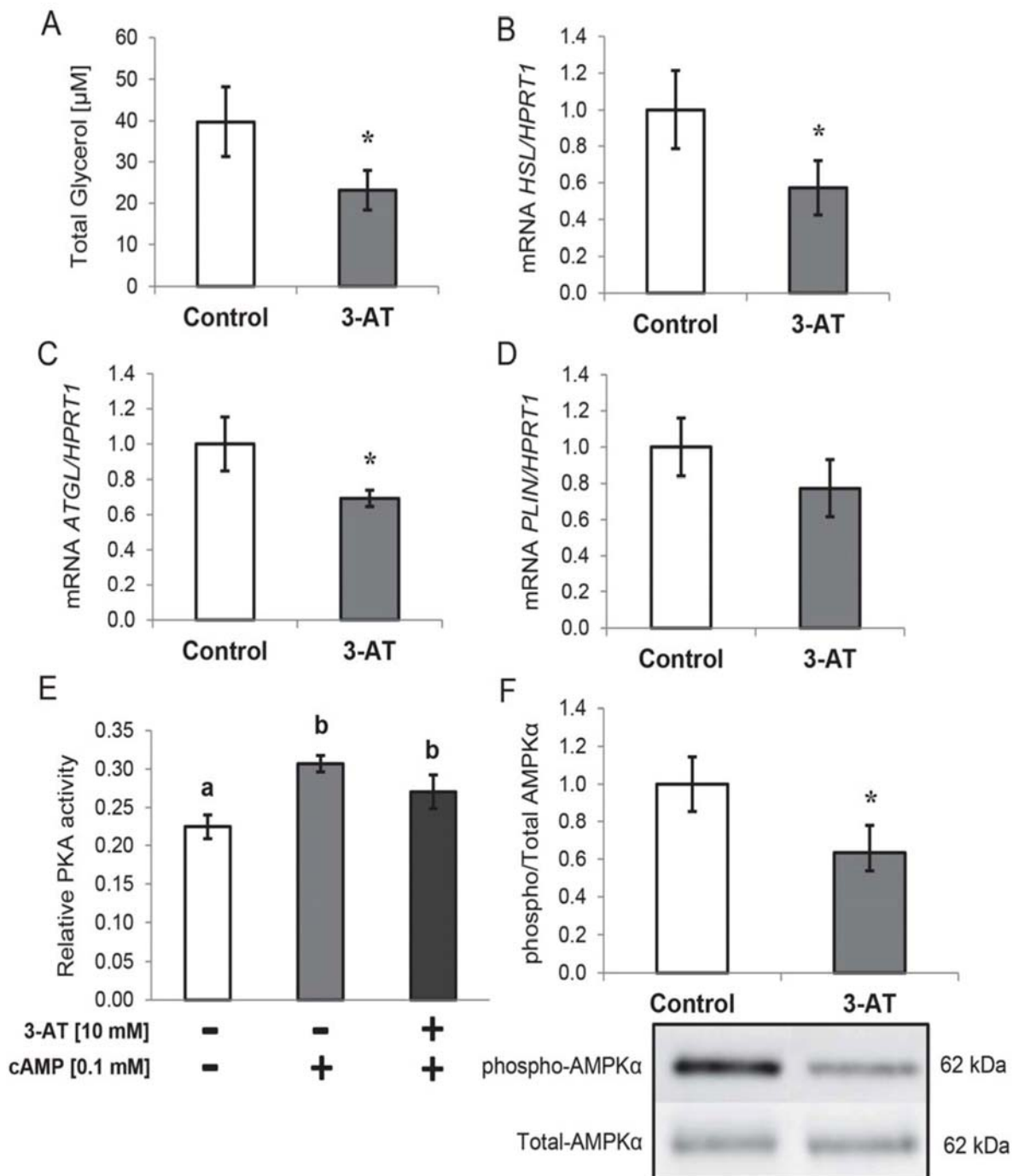


Fig 6. Effects of 3-amino-1,2,4-triazole (3-AT) on lipid metabolism. A: Glycerol levels (μM) in cell supernatants after treatment with 3-AT (10 mM, 24 h). B: Hormone sensitive lipase (*HSL*) gene expression. C: Adipose triglyceride lipase (*ATGL*) gene expression. D: Perilipin (*PLIN*) gene expression. The mRNA levels were normalized to those of hypoxanthine-guanine phosphoribosyltransferase-1 (*HPRT1*), and data from three independent experiments are presented as the means \pm SEM of the fold-changes calculated using the Pfaffl method. E: Protein Kinase A (PKA) activity in the cell lysates of adipocytes treated with or without 3-AT (10 mM, 24 h) and 0.1 mM cAMP. F: 5'-AMP-activated protein kinase catalytic subunit alpha (AMPK α) protein levels. The cell lysates were prepared and then analyzed by western blot using specific antibodies against total AMPK α and phospho-AMPK α (Thr172) as described in the Methods section. The data are presented as the ratio of phosphor-AMPK α /total-AMPK α to no treatment fold-change, and the bars represent the means \pm SEM of three separate experiments. Significant differences were identified using the Mann-Whitney U test; * $P < 0.05$, ** $P < 0.01$.

doi:10.1371/journal.pone.0152550.g006

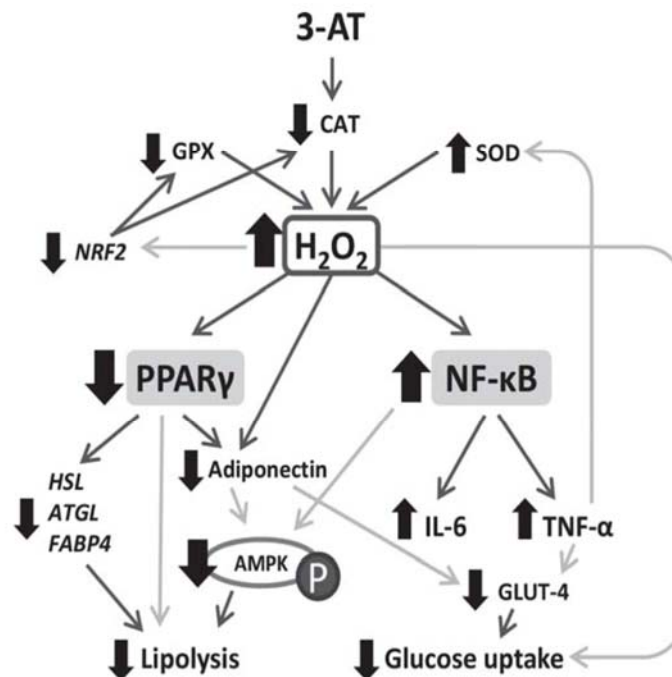


Fig 7. Diagram of the conditions observed in 3-AT-treated adipocytes. The increased hydrogen peroxide production leads to lower *PPAR* γ expression and *NF- κ B* activation, while decreasing the expression of important enzymes in metabolism, all of which finally reduce glucose uptake and lipolysis. AMPK: 5'-AMP-activated protein kinase; ATGL: adipose triglyceride lipase; CAT: catalase; FABP4: fatty-acid binding protein 4; GLUT4: glucose transporter type 4; GPX: glutathione peroxidase; HSL: hormone sensitive lipase; IL-6: interleukin 6; NRF2: nuclear factor, erythroid 2-like 2; *NF- κ B*: nuclear factor of kappa light polypeptide gene enhancer in B-cells 2; P: enzyme phosphorylation; *PPAR* γ : peroxisome proliferator-activated receptor gamma; SOD: superoxide dismutase; *TNF- α* : tumor necrosis factor alpha. The black arrows indicate an increase or decrease in activity, expression or protein levels. The bold arrows indicate causal relationships between findings, and the light grey arrows indicate potential relationships according to the revised literature.

doi:10.1371/journal.pone.0152550.g007

Transcription factors involved in the protection against oxidative stress. To elucidate the cause of the general decrease in antioxidant enzyme gene expression, we studied Nrf2 and FOXO1, two transcription factors responsible for the maintenance of redox homeostasis [44,24], as well as β -catenin, which is involved in oxidative stress responses [45]. Interestingly, we found that their expression levels were inhibited in 3-AT-treated adipocytes. First, our results agree with a recent study that found that H_2O_2 lowers *NRF2* expression [46]. Moreover, the inflammatory response present in adipocytes treated with 3-AT could also explain the reduced *NRF2* expression because it has been widely demonstrated that Nrf2 and *NF- κ B* behave antagonistically [47]. Indeed, a similar situation is observed in chronic kidney disease in which Nrf2 is inactive, while *NF- κ B* triggers inflammation [48]. Additionally, the lack of Nrf2 in obese mice resulted in severe metabolic syndrome [49]. The reduced *NRF2* expression could explain the lower mRNA levels of the antioxidant enzymes *GPX4*, *CAT*, and *PRDXs*, which are under transcriptional control by Nrf2 [44,23]. Regarding *SOD1*, its transcription is also regulated by other factors, which include *TNF- α* [38], as mentioned above, and could be increased as a mechanism of protection against 3-AT-induced oxidative stress. Second, the lower FOXO1 mRNA levels could also explain the inhibition of the gene expression of antioxidant enzymes that is observed in 3-AT-treated adipocytes [24]. Moreover, the gene expression of β -Catenin (*CTNNB1*), necessary for FOXO1 transcriptional activation [50], was inhibited by 3-AT treatment. A similar situation was observed in a previous study, which showed that ROS

inhibits the Wnt/ β -Catenin pathway and that this effect can be repaired by *CTNNB1* overexpression [45]. Interestingly, *CTNNB1* expression is also inhibited in mesenchymal stem cells from infants born to obese mothers [51].

3-AT treatment triggers inflammation and lowers *PPAR* γ expression in adipocytes

The oxidative stress derived from 3-AT treatment led to two main events that could be the cause of the effects found in the present study. On one hand, 3-AT treatment triggered inflammation. On the other hand, the generated oxidative stress affected *PPAR* γ expression, a transcription factor with important regulatory functions in oxidative stress and adipocyte metabolism.

Regarding inflammation, the oxidative stress caused by 3-AT led to the activation of NF- κ B and to the subsequent increase in transcription and protein synthesis of *TNF- α* and *IL-6*, which is in agreement with previous studies [15]. Indeed, it has been shown that there is a relationship between *TNF- α* , oxidative stress and insulin resistance [52].

Regarding *PPAR* γ , we found its expression and protein levels to be significantly reduced after 3-AT treatment. In line with this finding, a previous study showed that H_2O_2 treatment significantly decreased the mRNA abundance of *PPAR* γ in adipocytes, even suggesting that *PPAR* γ could mediate the actions of H_2O_2 [19]. Similarly, ROS exposure led to lower *PPAR* γ expression in murine adipocytes [4], and treatment with *PPAR* γ agonists increased CAT protein levels in adipose tissues of obese individuals [21] and in 3T3-L1 cells [20].

Both inflammation and inhibition of *PPAR* γ expression derived from the 3-AT treatment had a clear impact on the adipocyte's metabolism, approaching to the situation found in obese adipose tissue.

Effects of 3-AT treatment on glucose metabolism

We observed a significantly lower basal glucose uptake in 3-AT-treated adipocytes, which was accompanied by lower *GLUT4* gene and protein expression. However, the insulin-stimulated glucose uptake results indicate that insulin resistance is not present in the studied conditions. Nevertheless, our results are in line with those of Rudich *et al.*, who observed that *GLUT4* translocation was inhibited by ROS in 3T3-L1 murine adipocytes [6]. Furthermore, it has been shown that impaired *PPAR* γ action is associated with insulin resistance [53]. Additionally, adiponectin, the insulin-sensitizing adipokine found at low circulating levels in obesity [54] that has been observed to increase *GLUT4* expression [55,56], was found at lower levels in 3-AT treated cells. Because adiponectin expression is enhanced by *PPAR* γ agonists [57], the decreased *PPAR* γ gene expression and the increased H_2O_2 concentrations could partially explain the lower adiponectin and glucose uptake levels observed in the 3-AT-treated cells. Indeed, similar results from other studies have shown that oxidative stress decreases the secretion of adiponectin [6,31,58,59]. However, another cause for the reduced glucose uptake could be *TNF- α* because it has been observed to cause a reduction in *GLUT4* expression in 3T3-L1 adipocytes [60]. In fact, artificially induced oxidative stress increased *TNF- α* production and provoked insulin resistance through reduced *GLUT4* expression in adipocytes [17]. Moreover, CAT prevented *TNF- α* -induced insulin resistance in 3T3-L1 adipocytes [61].

Effects of 3-AT treatment on lipid metabolism. We observed reduced lipolysis in 3-AT-treated adipocytes. To fully characterize the agents involved in regulation of lipolysis, PKA activity, AMPK activation and expression of lipase genes were determined. It has been shown that H_2O_2 oxidizes PKA cysteine residues, interfering with cAMP activation of the enzyme and thus reducing lipolysis [62,14]. However, we did not find differences in cAMP-stimulated PKA

activity between control and 3-AT-treated adipocytes. In contrast, the reduced AMPK activation is in agreement with our lipolysis results. In fact, the decreased AMPK activation could actually be due to the existing inflammation [63] and to the lower adiponectin and lipolysis levels, which lead to AMPK phosphorylation [64,22]. In addition, the reduced lipolysis could also be derived from the lower gene expression levels of lipases *HSL* and *ATGL*. This could be explained by the lower *PPAR γ* expression because *HSL* [65] and *ATGL* [66] are two of its transcriptional targets. Indeed, in a similar study, *PPARG2* knockout adipocytes were shown to exhibit reduced lipolysis [67]. Finally, although our results contradict with previous studies in which *TNF- α* has been shown to activate lipolysis [18], this could be due to inflammation being at early stages because we did not observe changes in *NFKB2* and *TNFRSF1A* expression in 3-AT-treated adipocytes [68].

Conclusions

The present study shows that CAT activity is important for the metabolic homeostasis of adipocytes. In adipocytes, 3-AT treatment inhibited catalase activity and generated oxidative stress and inflammation while decreasing *PPAR γ* expression, which led to lower glucose uptake and lipolysis. Our findings suggest an important role of catalase in the protection of adipocytes against the oxidative stress and metabolic complications observed in obesity through the regulation of H_2O_2 levels, which exerts complex signaling functions.

Finally, we have shown that the compound 3-AT can be successfully used to inhibit CAT activity in adipocytes *in vitro* as a tool for the study of ROS in metabolic alterations associated with obesity. Further research is needed to better understand the metabolic effects of catalase in adipose tissue in the presence of obesity *in vivo*.

Limitations

We are aware of several limitations of the present study. In particular, the use of differentiated adipocytes from human ADSCs is not the same as the use of adipose tissues or mature adipocytes. Moreover, the degree to which we inhibited CAT (by approximately 70%) is higher than the inhibition of CAT activity observed in obese individuals (approximately 42%) [11]. Finally, the effects of 3-AT on the actions of insulin or other hormones upon other metabolic parameters and cellular responses was not fully elucidated in the present study, and thus, requires further research.

Supporting Information

S1 File. Oil Red O staining of human adipose-derived stem cells at day 0 (d0) and during the adipogenic differentiation at days 5, 9 and 12 (d5, d9 and d12). Fig A: Optical microscopy images. Fig B: Quantification of lipid content from Oil Red O staining (absorbance at 520 nm). All values are expressed as the means \pm SEM of three independent experiments. Significant differences were identified using the non-parametric Mann-Whitney U test; * $P < 0.05$; * $P < 0.01$.
(PDF)

S2 File. Catalase expression during the adipogenic differentiation. Fig A: Catalase (*CAT*) mRNA levels normalized to those of glyceraldehyde 3-phosphate dehydrogenase (*GAPDH*) and presented as fold-change, calculated using the Pfaffl method. Fig B: *CAT* protein levels from cell lysates analyzed by western blot using a specific antibody against *CAT*, normalized to the internal control (α -tubulin) and expressed as fold-change. Fig C: *CAT* activity of cell lysates during adipogenic differentiation. All values are expressed as the means \pm SEM of three

independent experiments. Significant differences were identified using the non-parametric Mann-Whitney U test; * $P < 0.05$.

(PDF)

S3 File. Effects of increasing concentrations of 3-amino-1,2,4-triazole (3-AT) on cell viability after a 24-h incubation. Cell viability was determined using a Neubauer chamber and trypan blue (4%).

(PDF)

Acknowledgments

This paper will be part of Francisco Javier Ruiz-Ojeda's doctorate, which is being completed as part of the "Nutrition and Food Sciences Program" at the University of Granada, Spain.

Author Contributions

Conceived and designed the experiments: AIR CGL CMA AG. Performed the experiments: FJRO AIR. Analyzed the data: FJRO AIR CGL CMA AG. Wrote the paper: FJRO AIR.

References

1. Ng M, Fleming T, Robinson M, Thomson B, Graetz N, Margono C, et al. Global, regional, and national prevalence of overweight and obesity in children and adults during 1980–2013: a systematic analysis for the Global Burden of Disease Study 2013. *Lancet*. 2014; 384(9945): 766–81. doi: [10.1016/S0140-6736\(14\)60460-8](https://doi.org/10.1016/S0140-6736(14)60460-8) PMID: [24880830](https://pubmed.ncbi.nlm.nih.gov/24880830/)
2. Tilg H, Moschen AR. Inflammatory mechanisms in the regulation of insulin resistance. *Mol Med* 2008; 14(3–4): 222–231. doi: [10.2119/2007-00119.Tilg](https://doi.org/10.2119/2007-00119.Tilg) PMID: [18235842](https://pubmed.ncbi.nlm.nih.gov/18235842/)
3. Masoodi M, Kuda O, Rossmeisl M, Flachs P, Kopecky J. Lipid signaling in adipose tissue: Connecting inflammation & metabolism. *Biochim Biophys Acta* 2015; 1851(4): 503–518. doi: [10.1016/j.bbaliip.2014.09.023](https://doi.org/10.1016/j.bbaliip.2014.09.023) PMID: [25311170](https://pubmed.ncbi.nlm.nih.gov/25311170/)
4. Furukawa S, Fujita T, Shimabukuro M, Iwaki M, Yamada Y, Nakajima Y, et al. Increased oxidative stress in obesity and its impact on metabolic syndrome. *J. Clin. Invest.* 2004; 114(12): 1752–1761. PMID: [15599400](https://pubmed.ncbi.nlm.nih.gov/15599400/)
5. Anderson EJ, Lustig ME, Boyle KE, Woodlief TL, Kane DA, Lin CT, et al. Mitochondrial H₂O₂ emission and cellular redox state link excess fat intake to insulin resistance in both rodents and humans. *Journal of Clinical Investigation*. 2009; 119(3): 573–81. doi: [10.1172/JCI37048](https://doi.org/10.1172/JCI37048) PMID: [19188683](https://pubmed.ncbi.nlm.nih.gov/19188683/)
6. Rudich A, Tirosh A, Potashnik R, Hemi R, Kanety H, Bashan N. Prolonged oxidative stress impairs insulin-induced GLUT4 translocation in 3T3-L1 adipocytes. *Diabetes*. 1998; 47(10): 1562–9. PMID: [9753293](https://pubmed.ncbi.nlm.nih.gov/9753293/)
7. Rupérez AI, Gil A, Aguilera CM. Genetics of oxidative stress in obesity. *International Journal of Molecular Sciences*. 2014; 15(2): 3118–3144. doi: [10.3390/ijms15023118](https://doi.org/10.3390/ijms15023118) PMID: [24562334](https://pubmed.ncbi.nlm.nih.gov/24562334/)
8. Walton PA, Pizzitelli M. Effects of peroxisomal catalase inhibition on mitochondrial function. *Frontiers in physiology*. 2012 (3): 108.
9. Truong TH, Carroll KS. Redox regulation of protein kinases. *Critical reviews in Biochemistry and Molecular Biology*. 2013; 1549–7798
10. Chen B, Wei J, Wang W, Cui G, Zhao Y, Zhu X, et al. Identification of signaling pathways involved in aberrant production of adipokines in adipocytes undergoing oxidative stress. *Arch Med Res* 2009; 40(4): 241–248. doi: [10.1016/j.arcmed.2009.03.007](https://doi.org/10.1016/j.arcmed.2009.03.007) PMID: [19608012](https://pubmed.ncbi.nlm.nih.gov/19608012/)
11. Amirkhizi F, Siassi F, Djalali M, Shahraki SH. Impaired enzymatic antioxidant defense in erythrocytes of women with general and abdominal obesity. *Obes Res Clin Pract*. 2014; 8(1): 26–34.
12. Rupérez AI, Olza J, Gil-Campos M, Leis R, Mesa MD, Tojo R, et al. Are Catalase -844A/G Polymorphism and Activity Associated with Childhood Obesity? *Antioxid Redox Signal*. 2013; 19(16): 1970–1975. doi: [10.1089/ars.2013.5386](https://doi.org/10.1089/ars.2013.5386) PMID: [23641975](https://pubmed.ncbi.nlm.nih.gov/23641975/)
13. Shin MJ, Park E. Contribution of insulin resistance to reduced antioxidant enzymes and vitamins in non-obese Korean children. *Clin Chim Acta*. 2006; 365(1–2): 200–205. PMID: [16154553](https://pubmed.ncbi.nlm.nih.gov/16154553/)
14. Vázquez-Meza H, Zentella de Piña M, Pardo JP, Riveros-Rosas H, Villalobos-Molina R, Piña E. Non-steroidal anti-inflammatory drugs activate NADPH oxidase in adipocytes and raise the H₂O₂ pool to

- prevent cAMP-stimulated protein kinase a activation and inhibit lipolysis. *BMC Biochemistry*. 2013; 14:13. doi: [10.1186/1471-2091-14-13](https://doi.org/10.1186/1471-2091-14-13) PMID: [23718778](https://pubmed.ncbi.nlm.nih.gov/23718778/)
15. Barnes PJ, Karin M. Nuclear Factor- κ B—a pivotal transcription factor in chronic inflammation diseases. *N Engl J Med*. 1997; 336(15): 1066–1071. PMID: [9091804](https://pubmed.ncbi.nlm.nih.gov/9091804/)
 16. Sasaki CY, Barberi TJ, Ghosh P, Longo DL. Phosphorylation of RelA/p65 on serine 536 defines an I κ B independent NF- κ B pathway. *J Biol Chem*. 2005; 280(41):34538–47. PMID: [16105840](https://pubmed.ncbi.nlm.nih.gov/16105840/)
 17. Yang ZC, Wang KS, Wu Y, Zou XQ, Xiang YY, Chen XP, et al. Asymmetric Dimethylarginine Impairs Glucose Utilization via ROS/TLR4 Pathway in Adipocytes: an Effect Prevented by Vitamin E. *Cell Physiol Biochem* 2009; 24(1–2): 115–124. doi: [10.1159/000227819](https://doi.org/10.1159/000227819) PMID: [19590199](https://pubmed.ncbi.nlm.nih.gov/19590199/)
 18. Chen X, Xun K, Chen L, Wang Y. TNF- α , a potent lipid metabolism regulator. *Cell Biochem Funct*. 2009; 27(7): 407–16. doi: [10.1002/cbf.1596](https://doi.org/10.1002/cbf.1596) PMID: [19757404](https://pubmed.ncbi.nlm.nih.gov/19757404/)
 19. Chen B, Lam KS, Wang Y, Wu D, Lam MC, Shen J, et al. Hypoxia dysregulates the production of adiponectin and plasminogen activator inhibitor-1 independent of reactive oxygen species in adipocytes. *Biochem Biophys Res Commun*. 2006; 341(2): 549–56. PMID: [16427606](https://pubmed.ncbi.nlm.nih.gov/16427606/)
 20. Okuno Y, Matsuda M, Kobayashi H, Morita K, Suzuki E, Fukuhara A, et al. Adipose expression of catalase is regulated via a novel remote PPAR γ -responsive region. *Biochem Biophys Res Commun*. 2008; 366(3): 698–704. PMID: [18073138](https://pubmed.ncbi.nlm.nih.gov/18073138/)
 21. Ahmed M, Neville MJ, Edelmann MJ, Kessler BM, Karpe F. Proteomic analysis of human adipose tissue after rosiglitazone treatment shows coordinated changes to promote glucose uptake. *Obesity*. 2010; 18(1): 27–34. doi: [10.1038/oby.2009.208](https://doi.org/10.1038/oby.2009.208) PMID: [19556978](https://pubmed.ncbi.nlm.nih.gov/19556978/)
 22. Gauthier MS, Miyoshi H, Souza SC, Cacicedo JM, Saha AK, Greenberg AS, et al. AMP-activated Protein Kinase is activated as a consequence of lipolysis in the adipocyte: potential mechanism and physiological relevance. *J Biol Chem*. 2008; 283(24): 16514–16524. doi: [10.1074/jbc.M708177200](https://doi.org/10.1074/jbc.M708177200) PMID: [18390901](https://pubmed.ncbi.nlm.nih.gov/18390901/)
 23. Kim J, Cha YN, Surh YJ. A protective role of nuclear factor-erythroid 2-related factor-2 (Nrf2) in inflammatory disorders. *Mutat Res*. 2010; 690(1–2): 12–23. doi: [10.1016/j.mrfmmm.2009.09.007](https://doi.org/10.1016/j.mrfmmm.2009.09.007) PMID: [19799917](https://pubmed.ncbi.nlm.nih.gov/19799917/)
 24. Higuchi M, Dusting GJ, Peshavariya H, Jiang F, Hsiao ST, Chan EC, et al. Differentiation of human adipose-derived stem cells into fat involves reactive oxygen species and Forkhead box O1 mediated upregulation of antioxidant enzymes. *Stem Cells Dev*. 2013; 22(6): 878–88. doi: [10.1089/scd.2012.0306](https://doi.org/10.1089/scd.2012.0306) PMID: [23025577](https://pubmed.ncbi.nlm.nih.gov/23025577/)
 25. Korswagen HC. Regulation of the Wnt/ β -catenin pathway by redox signaling. *Dev Cell*. 2006; 10(6):687–8. PMID: [16740470](https://pubmed.ncbi.nlm.nih.gov/16740470/)
 26. Margoliash E, Novogrodsky A, Schejter A. Irreversible reaction of 3-amino-1,2,4-triazole and related inhibitors with the protein of Catalase. *Biochem J*. 1960; 74: 339–350. PMID: [13848609](https://pubmed.ncbi.nlm.nih.gov/13848609/)
 27. Pfaffl MW. A new mathematical model for relative quantification in real-time RT-PCR. *Nucleic Acids Res*. 2001; 29(9): e45. PMID: [11328886](https://pubmed.ncbi.nlm.nih.gov/11328886/)
 28. Mukherjee SP, Mukherjee C. Similar activities of nerve growth factor and its homologue proinsulin in intracellular hydrogen peroxide production and metabolism in adipocytes. Transmembrane signalling relative to insulin-mimicking cellular effects. *Biochem Pharmacol* 1982; 31(20): 3163–3172. PMID: [7150345](https://pubmed.ncbi.nlm.nih.gov/7150345/)
 29. May JM. The effect of insulin-stimulated pentose phosphate cycle activity on cellular glutathione content in rat adipocytes. *Horm Metabol Res* 1982; 14: 634–637.
 30. Kumar N, Solt LA, Wang Y, Rogers PM, Bhattacharyya G, Kamenecka TM, et al. Regulation of adipogenesis by natural and synthetic REV-ERB ligands. *Endocrinology*. 2010; 151(7):3015–25. doi: [10.1210/en.2009-0800](https://doi.org/10.1210/en.2009-0800) PMID: [20427485](https://pubmed.ncbi.nlm.nih.gov/20427485/)
 31. Than A, Zhang X, Leow MK, Poh CL, Chong SK, Chen P. Apelin attenuates oxidative stress in human adipocytes. *J Biol Chem*. 2014; 289(6): 3763–74. doi: [10.1074/jbc.M113.526210](https://doi.org/10.1074/jbc.M113.526210) PMID: [24362107](https://pubmed.ncbi.nlm.nih.gov/24362107/)
 32. Andreeva ER, Lobanova MV, Udartseva OO. Response of Adipose Tissue Derived Stromal Cells in Tissue-Related O₂ Microenvironment to Short-Term Hypoxic Stress. *Cells Tissues Organs* 2014; 200(5): 307–315. doi: [10.1159/000438921](https://doi.org/10.1159/000438921) PMID: [26407140](https://pubmed.ncbi.nlm.nih.gov/26407140/)
 33. Adachi T, Toishi T, Wu H, Kamiya T, Hara H. Expression of extracellular superoxide dismutase during adipose differentiation in 3T3-L1 cells. *Redox Rep*. 2009; 14(1): 34–40. doi: [10.1179/135100009X392467](https://doi.org/10.1179/135100009X392467) PMID: [19161676](https://pubmed.ncbi.nlm.nih.gov/19161676/)
 34. Barbosa DS, Cecchini R, El Kadri MZ, Rodríguez MA, Burini RC, Dichi I. Decreased oxidative stress in patients with ulcerative colitis supplemented with fish oil omega-3 fatty acids. *Nutrition*. 2003; 19(10): 837–42. PMID: [14559317](https://pubmed.ncbi.nlm.nih.gov/14559317/)

35. Comim CM, Cassol OJ Jr, Constantino LC, Constantino LS, Petronilho F, Tuon L, et al. Oxidative variables and antioxidant enzymes activities in the mdx mouse brain. *Neurochem Int.* 2009; 55(8): 802–5. doi: [10.1016/j.neuint.2009.08.003](https://doi.org/10.1016/j.neuint.2009.08.003) PMID: [19682526](https://pubmed.ncbi.nlm.nih.gov/19682526/)
36. Djordjevic D, Cubrilo D, Macura M, Barudzic N, Djuric D, Jakovljevic V. The influence of training status on oxidative stress in young male handball players. *Mol Cell Biochem.* 2011; 351(1–2): 251–9. doi: [10.1007/s11010-011-0732-6](https://doi.org/10.1007/s11010-011-0732-6) PMID: [21264496](https://pubmed.ncbi.nlm.nih.gov/21264496/)
37. Sinha S, Ray US, Tomar OS, Singh SN. Different adaptation patterns of antioxidant system in natives and sojourners at high altitude. *Respiratory Physiology & Neurobiology.* 2009; 167(3): 255–260.
38. Sugino N, Karube-Harada A, Sakata A, Takiguchi S, Kato H. Nuclear factor-kappa B is required for tumor necrosis factor-alpha-induced manganese superoxide dismutase expression in human endometrial stromal cells. *J Clin Endocrinol Metab.* 2002; 87(8): 3845–50. PMID: [12161520](https://pubmed.ncbi.nlm.nih.gov/12161520/)
39. Doni MG, Piva E. Glutathione peroxidase blockage inhibits prostaglandin biosynthesis in rat platelets and aorta. *Haemostasis.* 1983; 13(4): 240–3. PMID: [6352424](https://pubmed.ncbi.nlm.nih.gov/6352424/)
40. Bhuyan KC, Bhuyan DK. Regulation of hydrogen peroxide in eye humors. Effect of 3-amino-1H-1,2,4-triazole on catalase and glutathione peroxidase of rabbit eye. *Biochim Biophys Acta.* 1977; 497(3): 641–51. PMID: [889879](https://pubmed.ncbi.nlm.nih.gov/889879/)
41. Bagnyukova TV, Vasyukov OY, Storey KB, Lushchak VI. Catalase inhibition by amino triazole induces oxidative stress in goldfish brain. *Brain Res.* 2005; 1052(2): 180–6. PMID: [16023088](https://pubmed.ncbi.nlm.nih.gov/16023088/)
42. Huh JY, Kim Y, Jeong J, Park J, Kim I, Huh KH, et al. Peroxiredoxin 3 is a key molecule regulating adipocyte oxidative stress, mitochondrial biogenesis, and adipokine expression. *Antioxid Redox Signal.* 2012; 16(3):229–43. doi: [10.1089/ars.2011.3952](https://doi.org/10.1089/ars.2011.3952) PMID: [21902452](https://pubmed.ncbi.nlm.nih.gov/21902452/)
43. Brinkmann C, Brixius K. Peroxiredoxins and sports: new insights on the antioxidative defense. *J Physiol Sci.* 2013; 63(1): 1–5. doi: [10.1007/s12576-012-0237-4](https://doi.org/10.1007/s12576-012-0237-4) PMID: [23055024](https://pubmed.ncbi.nlm.nih.gov/23055024/)
44. Kensler TW, Wakabayashi N, Biswal S. Cell survival responses to environmental stresses via the Keap1-Nrf2-ARE pathway. *Annu Rev Pharmacol Toxicol* 2007; 47: 89–116. PMID: [16968214](https://pubmed.ncbi.nlm.nih.gov/16968214/)
45. Atashi F, Modarressi A, Pepper MS. The Role of Reactive Oxygen Species in Mesenchymal Stem Cell Adipogenic and Osteogenic Differentiation: A Review. *Stem Cells and Development.* Stem Cells Dev. 2015; 24(10): 1150–63. doi: [10.1089/scd.2014.0484](https://doi.org/10.1089/scd.2014.0484) PMID: [25603196](https://pubmed.ncbi.nlm.nih.gov/25603196/)
46. Yeh CH, Ma KH, Liu PS, Kuo JK, Chueh SH. Baicalein Decreases Hydrogen Peroxide-Induced Damage to NG108-15 Cells via Upregulation of Nrf2. *J Cell Physiol* 2015; 230(8): 1840–51. doi: [10.1002/jcp.24900](https://doi.org/10.1002/jcp.24900) PMID: [25557231](https://pubmed.ncbi.nlm.nih.gov/25557231/)
47. Jin W, Wang H, Yan W, Xu L, Wang X, Zhao X, et al. Disruption of Nrf2 enhances upregulation of nuclear factor-kappaB activity, proinflammatory cytokines, and intercellular adhesion molecule-1 in the brain after traumatic brain injury. *Mediators Inflamm.* 2008; 725174. doi: [10.1155/2008/725174](https://doi.org/10.1155/2008/725174) PMID: [19190763](https://pubmed.ncbi.nlm.nih.gov/19190763/)
48. Pedruzzi LM, Stockler-Pinto MB, Leite M Jr, Mafra D. Nrf2-keap1 system versus NF-kB: The good and the evil in chronic kidney disease? *Biochimie.* 2012; 94(12): 2461–6. doi: [10.1016/j.biochi.2012.07.015](https://doi.org/10.1016/j.biochi.2012.07.015) PMID: [22874821](https://pubmed.ncbi.nlm.nih.gov/22874821/)
49. Xue P, Hou Y, Chen Y, Yang B, Fu J, Zheng H, et al. Adipose deficiency of Nrf2 in ob/ob mice results in severe metabolic syndrome. *Diabetes.* 2013; 62(3): 845–54. doi: [10.2337/db12-0584](https://doi.org/10.2337/db12-0584) PMID: [23238296](https://pubmed.ncbi.nlm.nih.gov/23238296/)
50. Essers MA, de Vries-Smits LM, Barker N, Polderman PE, Burgering BM, Korswagen HC. Functional interaction between beta-catenin and FOXO in oxidative stress signaling. *Science.* 2005; 308(5725): 1181–4. PMID: [15905404](https://pubmed.ncbi.nlm.nih.gov/15905404/)
51. Boyle KE, Patinkin ZW, Shapiro AL, Baker PR 2nd, Dabelea D, Friedman JE. Mesenchymal Stem Cells from Infants Born to Obese Mothers Exhibit Greater Potential for Adipogenesis: The Healthy Start Baby BUMP Project. *Diabetes* 2015; db150849.
52. D'Alessandro ME, Selenscig D, Illesca P, Chicco A, Lombardo YB. Time course of adipose tissue dysfunction associated with antioxidant defense, inflammatory cytokines and oxidative stress in dyslipemic insulin resistant rats. *Food Funct.* 2015; 6(4): 1299–309. doi: [10.1039/c4fo00903g](https://doi.org/10.1039/c4fo00903g) PMID: [25765549](https://pubmed.ncbi.nlm.nih.gov/25765549/)
53. Lehrke M, Lazar MA. The many faces of PPAR-gamma. *Cell.* 2005; 123(6): 993–9. PMID: [16360030](https://pubmed.ncbi.nlm.nih.gov/16360030/)
54. Han SH, Quon MJ, Kim AJ, Koh KK. Adiponectin and Cardiovascular Disease Response to Therapeutic Interventions Seung Hwan *Journal of the American College of Cardiology.* 2007; 49(5): 531–8. PMID: [17276175](https://pubmed.ncbi.nlm.nih.gov/17276175/)
55. Wu X, Motoshima H, Mahadev K, Stalker TJ, Scalia R, Goldstein BJ. Involvement of AMP-activated protein kinase in glucose uptake stimulated by the globular domain of adiponectin in primary rat adipocytes. *Diabetes* 2003; 52(6): 1355–1363. PMID: [12765944](https://pubmed.ncbi.nlm.nih.gov/12765944/)
56. Chang E, Choi JM, Park SE, Rhee EJ, Lee WY, Oh KW, et al. Adiponectin deletion impairs insulin signaling in insulin-sensitive but not insulin-resistant 3T3-L1 adipocytes. *Life Sci.* 2015; 132: 93–100. doi: [10.1016/j.lfs.2015.02.013](https://doi.org/10.1016/j.lfs.2015.02.013) PMID: [25956568](https://pubmed.ncbi.nlm.nih.gov/25956568/)

57. Stefan N, Stumvoll M. Adiponectin—its role in metabolism and beyond. *Horm Metab Res.* 2002; 34(9): 469–74. PMID: [12384822](#)
58. Soares AF, Guichardant M, Cozzone D, Bernoud-Hubac N, Bouzaïdi-Tiali N, Lagarde M, et al. Effects of oxidative stress on adiponectin secretion and lactate production in 3T3-L1 adipocytes. *Free Radical Biology and Medicine.* 2005; 38(7): 882–889. PMID: [15749384](#)
59. Monickaraj F, Aravind S, Nandhini P, Prabu P, Sathishkumar C, Mohan V, et al. Accelerated fat cell aging links oxidative stress and insulin resistance in adipocytes. *J Biosci.* 2013; 38(1): 113–22. PMID: [23385819](#)
60. Stephens JM, Lee J, Pilch PF. Tumor Necrosis Factor- α -induced Insulin Resistance in 3T3-L1 Adipocytes Is Accompanied by a Loss of Insulin Receptor Substrate-1 and GLUT4 Expression without a Loss of Insulin Receptor-mediated Signal Transduction. *J Biol Chem.* 1997; 272(2): 971–976. PMID: [8995390](#)
61. Houstis N, Rosen ED, Lander ES. Reactive oxygen species have a causal role in multiple forms of insulin resistance. *Nature.* 2006; 440(7086): 944–8. PMID: [16612386](#)
62. Little SA, de Haën C. Effects of hydrogen peroxide on basal and hormone-stimulated lipolysis in perfused rat fat cells in relation to the mechanism of action of insulin. *J Biol Chem.* 1980; 255(22): 10888–95. PMID: [6159357](#)
63. Gauthier MS, O'Brien EL, Bigornia S, Mott M, Cacicedo JM, Xu XJ, et al. Decreased AMP-activated protein kinase activity is associated with increased inflammation in visceral adipose tissue and with whole-body insulin resistance in morbidly obese humans. *Biochem Biophys Res Commun.* 2011; 404(1): 382–7. doi: [10.1016/j.bbrc.2010.11.127](#) PMID: [21130749](#)
64. Tomas E, Tsao TS, Saha AK, Murrey HE, Zhang Cc Cc, Itani SI et al. Enhanced muscle fat oxidation and glucose transport by ACRP30 globular domain: acetyl-CoA carboxylase inhibition and AMP-activated protein kinase activation. *Proc Natl Acad Sci U S A.* 2002; 99(25): 16309–13. PMID: [12456889](#)
65. Yajima H, Kobayashi Y, Kanaya T, Horino Y. Identification of peroxisome-proliferator responsive element in the mouse HSL gene. *Biochem Biophys Res Commun.* 2007; 352(2): 526–31. PMID: [17134676](#)
66. Kershaw EE, Schupp M, Guan HP, Gardner NP, Lazar MA, Flier JS. PPAR- γ regulates adipose triglyceride lipase in adipocytes in vitro and in vivo. *Am J Physiol Endocrinol Metab.* 2007; 293(6): 1736–45.
67. Rodriguez-Cuenca S, Carobbio S, Vidal-Puig A. Ablation of Pparg2 impairs lipolysis and reveals murine strain differences in lipolytic responses. *FASEB J.* 2012; 26(5): 1835–1844. doi: [10.1096/fj.11-193631](#) PMID: [22319009](#)
68. Sethi JK, Xu H, Uysal KT, Wiesbrock SM, Scheja L, Hotamisligil GS. Characterisation of receptor-specific TNF α functions in adipocyte cell lines lacking type 1 and 2 TNF receptors. *FEBS Lett.* 2000; 469(1): 77–82. PMID: [10708760](#)

Discussion

Discussion

Firstly, the adipogenic differentiation was checked by Oil Red O staining assay from ADSCs into adipocytes at the different days (d0, d5, d9 and d12). We observed a significant increased of lipid accumulation from d0 to d12, and the d10 was selected for the subsequent experiments. According to previous reports (Wu *et al.* 1999, Vater *et al.* 2011), gene expression of adipogenic markers such as *LEP*, *ADIPOQ* and *PPAR-γ* were up-regulated significantly during the adipogenic differentiation (Supplementary figure S1). Moreover, we tested *NPR3* and *CAT* expression in human ADSCs and differentiated adipocytes by analyzing gene and protein expression on different days during adipogenic differentiation. As expected, we found that *NPR3* (Supplementary figure S2) and *CAT* (Supplementary figure S5) gene expression and protein levels were significantly up-regulated on d5, d9 and d12 compared with day 0.

Analogue to atrial natriuretic peptide (C-ANP₄₋₂₃) effects on adipocyte metabolism

Maack *et al.* 1987 was the first to describe C-ANP₄₋₂₃ as a specific peptide for NPR3 with no affinity for NPR1 or NPR2 (Maack *et al.* 1987, Li *et al.* 2014). To this date, the main reported relevance of C-ANP₄₋₂₃ has been the improvement of endothelial migration, proliferation and angiogenesis in bovine and human endothelial cells (Almeida *et al.*, 2014, Li *et al.*, 2014). Anand-Srivastava *et al.* showed that NPR3 was coupled to adenylyl cyclase activity via inhibitory guanine nucleotide regulatory proteins (Gi) (Anand-Srivastava *et al.* 2005). Two different subtypes of NPR3 with molecular mass of 67 and 77 kDa have been

identified. The 77-kDa protein is implicated in ligand internalization as a clearance receptor, endocytosis and degradation; whereas the 67-kDa protein is coupled to adenylyl cyclase system (Anand Srivastava *et al.* 2005). Anand-Srivastava demonstrated the inhibition of adenylate cyclase by C-ANP₄₋₂₃ in rat cells (1990). However, Sellitti *et al.* (2001) reported the possibility that the binding of C-ANP₄₋₂₃ to NPR3 activates rather than inhibits the adenylyl cyclase system. This was explained by the hypothesis that NPR3 coupling to adenylate cyclase (inhibition vs stimulation) might be restricted to certain cell types, possibly because some cells express enzymes (e.g., kinases) that are capable of modifying the intracellular NPR3 domain (Sellitti *et al.* 2001). Our results show that the intracellular cAMP levels increase rather than decrease in human adipocytes after treatment with C-ANP₄₋₂₃. Indeed, the adenylyl cyclase inhibitor SQ22536 suppressed the C-ANP₄₋₂₃-induced increase in the cAMP levels.

On one hand, it has been demonstrated that elevated intracellular cAMP levels in rat cultured adipocytes stimulate AMPK activity, which plays an important role in the regulation of glucose uptake (Omar *et al.* 2009, Bolsoni-lobes *et al.* 2014). Upon activation, AMPK promotes GLUT4 expression and translocation to the plasma membrane and glucose uptake independent of insulin (Govers *et al.* 2014, Bolsoni-lobes *et al.* 2014). Correspondingly, we observed significantly higher levels of activated AMPK (phospho-AMPK α -Thr172) after treatment with C-ANP₄₋₂₃. Indeed, we have found that C-ANP₄₋₂₃ increases glucose uptake by 2-fold in adipocytes and up-regulates *GLUT4* gene and protein expression. Importantly, such increase in GLUT4 protein expression and activation of AMPK induced by C-ANP₄₋₂₃, was prevented by inhibition of

adenylate cyclase systems with SQ22536. Although many of the downstream effects of cAMP are mediated by PKA, exchange proteins directly activated by cAMP have been shown to mediate signals downstream of cAMP independent of PKA (Omar *et al.* 2009). The exact mechanism by which C-ANP₄₋₂₃ increases glucose uptake in human differentiated adipocytes was not completely elucidated here, however, our findings suggested that this effect is mediated by cAMP/AMPK activation.

On the other hand, it has been reported that catecholamines stimulate the adenylylase system/cAMP and inhibit glucose uptake in adipocytes through the dissociation of mTOR complex. However, this fact is due to products of lipolysis which inhibit glucose uptake (Mullins *et al.* 2014). As we have shown, incubation with C-ANP₄₋₂₃ did not increase the lipolysis levels in adipocytes neither the intracellular cGMP levels, in agreement with previous studies showing that C-ANP₄₋₂₃ does not increase cGMP levels (Anand Srivastava *et al.* 1990, Skowronska *et al.* 2010). In contrast, ANP increased cGMP and lipolysis levels acting *via* NPR1 (Potter *et al.* 2006, Moro *et al.* 2013, Kumar *et al.* 1997).

Additionally, a relationship between NPs and inflammation in adipose tissue has been reported. Adipocytes secrete adipokines and cytokines that are implicated in the chronic low-grade inflammation and insulin resistance associated with obesity, and ANP inhibits the secretion of factors involved in inflammation (Moro *et al.* 2006). We explored whether C-ANP₄₋₂₃ affects the inflammatory pathway in human adipocytes by analysing the expression of different genes involved in the inflammatory system, such as interleukin 1- β (*IL1B*), caspase 1 (*CASP1*), nuclear factor of kappa light polypeptide gene

enhancer in B-cells 2 (p49/p100) (*NFKB2*), toll interacting protein (*TOLLIP2*), tumour necrosis factor receptor superfamily, member 1A (*TNFRSF1A*) and interleukin-1 receptor-associated kinase 4 (*IRAK4*). We found that *IL1B* and *CASP1* were significantly down-regulated after C-ANP₄₋₂₃ treatment. However, we were unable to determine the protein levels of these two genes in the cell lysates. The NLRP3 inflammasome controls the activation of CASP1 and promotes the maturation of IL-1 β (Haneklaus *et al.* 2015, Schroder *et al.* 2010). Therefore, C-ANP₄₋₂₃ might be involved in the inflammatory process independent of glucose metabolism by inhibiting the inflammasome in adipocytes. Further studies are needed to fully characterise the role of C-ANP₄₋₂₃ in the inflammatory process in adipocytes.

Catalase activity and 3-AT-treated adipocytes effects on adipocyte metabolism

The mechanisms involved in H₂O₂ synthesis and degradation were affected in 3-AT-treated adipocytes. We observed higher SOD activity, responsible for the conversion of superoxide ions into H₂O₂, and significantly lower GPX activity, and both events were paralleled by analogous changes in *SOD1* and *GPX4* gene expression. These results are in line with those of Than *et al.* 2014 who found lower *GPX* and *CAT* protein expression levels in the presence of TNF- α -induced ROS in human adipocytes. The divergent results regarding SOD and GPX activities may seem counterintuitive. However, SOD appears to be the first line of defense against ROS in cells because it has been found augmented in different situations as a mechanism of protection (Andreeva *et al.* 2014, Adachi *et al.* 2009, Barbosa *et al.* 2003), even along with lower CAT activity (Comim *et al.* 2009).

Other studies have also observed similar results where SOD activity was increased, while CAT (Djordjevic *et al.* 2011) and GPX (Sinha *et al.* 2009) activities were decreased. Moreover, SOD expression has been observed to be increased by TNF- α in a mechanism involving NF- κ B activation (Sugino *et al.* 2002). Although we cannot rule out the possibility of partial inhibition of GPX by 3-AT (Doni *et al.* 1983), most of the studies using 3-AT report a specific inhibition of catalase (Bhuyan *et al.* 1977, Bagnyukova *et al.* 2005). Additionally, the expression levels of *PRDX1*, *PRDX3* and *PRDX5*, which are enzymes that are also involved in H₂O₂ clearance, were significantly reduced after treatment with 3-AT, which could contribute to increase H₂O₂ levels. Indeed, *PRDX3* is expressed in mature adipocytes and has been observed to be decreased in obesity (Huh *et al.* 2012, Brinkmann *et al.* 2013). In fact, Huh *et al.*, 2012 demonstrated that *PRDX3* deficiency leads to impaired glucose metabolism and decreased adiponectin levels.

To elucidate the cause of the general decrease in antioxidant enzyme gene expression, we studied Nrf2 and FOXO1, two transcription factors responsible for the maintenance of redox homeostasis (Kensler *et al.* 2007, Higuchi *et al.* 2013), as well as β -catenin, which is involved in oxidative stress responses (Atashi *et al.* 2015). Interestingly, we found that their expression levels were inhibited in 3-AT-treated adipocytes. First, our results agree with a recent study that found that H₂O₂ lowers *NRF2* expression (Yeh *et al.* 2015). Moreover, the inflammatory response present in adipocytes treated with 3-AT could also explain the reduced *NRF2* expression because it has been widely demonstrated that Nrf2 and NF- κ B behave antagonistically (Jin *et al.* 2008). Indeed, a similar situation is observed

in chronic kidney disease in which Nrf2 is inactive, while NF- κ B triggers inflammation (Pedruzzi *et al.* 2012). Additionally, the lack of Nrf2 in obese mice resulted in severe metabolic syndrome (Xue *et al.* 2013). The reduced *NRF2* expression could explain the lower mRNA levels of the antioxidant enzymes *GPX4*, *CAT*, and *PRDXs*, which are under transcriptional control by Nrf2 (Kensler *et al.* 2007, Kim *et al.* 2010). Regarding *SOD1*, its transcription is also regulated by other factors, which include TNF- α (Sugino *et al.* 2002), as mentioned above, and could be increased as a mechanism of protection against 3-AT-induced oxidative stress. Second, the lower *FOXO1* mRNA levels could also explain the inhibition of the gene expression of antioxidant enzymes that is observed in 3-AT-treated adipocytes (Higuchi *et al.* 2013). Moreover, the gene expression of β -Catenin (*CTNNB1*), necessary for FOXO1 transcriptional activation (Essers *et al.* 2005), was inhibited by 3-AT treatment. A similar situation was observed in a previous study, which showed that ROS inhibits the Wnt/ β -Catenin pathway and that this effect can be repaired by *CTNNB1* overexpression (Atashi *et al.* 2015). Interestingly, *CTNNB1* expression is also inhibited in mesenchymal stem cells from infants born to obese mothers (Boyle *et al.* 2015).

The oxidative stress derived from 3-AT treatment led to two main events that could be the cause of the effects found in the present study. On one hand, 3-AT treatment triggered inflammation. On the other hand, the generated oxidative stress affected *PPAR γ* expression, a transcription factor with important regulatory functions in oxidative stress and adipocyte metabolism

Regarding inflammation, the oxidative stress caused by 3-AT led to the activation of NF- κ B and to the subsequent increase in transcription and protein synthesis of *TNF- α* and *IL-6*, which is in agreement with previous studies (Barnes et al. 1997). Indeed, it has been shown that there is a relationship between TNF- α , oxidative stress and insulin resistance (D'Alessandro et al. 2015).

Regarding PPAR γ , we found its expression and protein levels to be significantly reduced after 3-AT treatment. In line with this finding, a previous study showed that H₂O₂ treatment significantly decreased the mRNA abundance of *PPAR γ* in adipocytes, even suggesting that PPAR γ could mediate the actions of H₂O₂ (Chen et al. 2006). Similarly, ROS exposure led to lower *PPAR γ* expression in murine adipocytes (Furukawa et al. 2004), and treatment with PPAR γ agonists increased CAT protein levels in adipose tissues of obese individuals (Ahmed et al. 2010) and in 3T3-L1 cells (Okuno et al. 2008).

Both inflammation and inhibition of *PPAR γ* expression derived from the 3-AT treatment had a clear impact on the adipocyte's metabolism, approaching to the situation found in obese adipose tissue.

We observed a significantly lower basal glucose uptake in 3-AT-treated adipocytes, which was accompanied by lower *GLUT4* gene and protein expression. However, the insulin-stimulated glucose uptake results indicate that insulin resistance is not present in the studied conditions. Nevertheless, our results are in line with those of Rudich et al., who observed that GLUT4 translocation was inhibited by ROS in 3T3-L1 murine adipocytes (Rudich et al. 1998). Furthermore, it has been shown that impaired PPAR γ action is associated

with insulin resistance (Lehrke *et al.* 2005). Additionally, adiponectin, the insulin-sensitizing adipokine found at low circulating levels in obesity (Han *et al.* 2007) that has been observed to increase *GLUT4* expression (Wu *et al.* 2003, Chang *et al.* 2015), was found at lower levels in 3-AT treated cells. Because adiponectin expression is enhanced by PPAR γ agonists (Stefan *et al.* 2002), the decreased PPAR γ gene expression and the increased H₂O₂ concentrations could partially explain the lower adiponectin and glucose uptake levels observed in the 3-AT-treated cells. Indeed, similar results from other studies have shown that oxidative stress decreases the secretion of adiponectin (Rudich *et al.* 1998, Than *et al.* 2014, Soares *et al.* 2005, Monickaraj *et al.* 2013). However, another cause for the reduced glucose uptake could be TNF- α because it has been observed to cause a reduction in *GLUT4* expression in 3T3-L1 adipocytes (Stephens *et al.* 1997). In fact, artificially induced oxidative stress increased TNF- α production and provoked insulin resistance through reduced *GLUT4* expression in adipocytes (Yang *et al.* 2009). Moreover, CAT prevented TNF- α -induced insulin resistance in 3T3-L1 adipocytes (Houstis *et al.* 2006).

We observed reduced lipolysis in 3-AT-treated adipocytes. To fully characterize the agents involved in regulation of lipolysis, PKA activity, AMPK activation and expression of lipase genes were determined. It has been shown that H₂O₂ oxidizes PKA cysteine residues, interfering with cAMP activation of the enzyme and thus reducing lipolysis (Little *et al.* 1980, Vázquez-Meza *et al.* 2013). However, we did not find differences in cAMP-stimulated PKA activity between control and 3-AT-treated adipocytes. In contrast, the reduced AMPK activation is in agreement with our lipolysis results. In fact, the decreased AMPK activation

could actually be due to the existing inflammation (Gauthier *et al.* 2011) and to the lower adiponectin and lipolysis levels, which lead to AMPK phosphorylation (Tomas *et al.* 2002, Gauthier *et al.* 2008). In addition, the reduced lipolysis could also be derived from the lower gene expression levels of lipases *HSL* and *ATGL*. This could be explained by the lower *PPAR γ* expression because *HSL* (Yajima *et al.* 2007) and *ATGL* (Kershaw *et al.* 2007) are two of its transcriptional targets. Indeed, in a similar study, *PPARG2* knockout adipocytes were shown to exhibit reduced lipolysis (Rodriguez-Cuenca *et al.* 2012). Finally, although our results contradict with previous studies in which TNF- α has been shown to activate lipolysis (Chen *et al.* 2009), this could be due to inflammation being at early stages because we did not observe changes in *NFKB2* and *TNFRSF1A* expression in 3-AT-treated adipocytes (Sethi *et al.* 2000).

Conclusions

Conclusions

1-Human adipose-derived stem cells (ADSCs) are fully differentiated into mature adipocytes and the adipogenic differentiation has been validated by Oil Red O staining assay and *PPAR-γ*, *leptin* and *adiponectin* gene expression at different times (day 0, day 5, day 9 and day 12).

2-The analogue to atrial natriuretic peptide (C-ANP₄₋₂₃), which is specific for natriuretic peptide receptor 3 (NPR3), enhances glucose metabolism in human differentiated adipocytes. These effects were mediated by the intracellular cyclic adenosine monophosphate (cAMP) increased levels, the up-regulation of glucose transporter 4 (GLUT4) and 5'-AMP-activated protein kinase (AMPK) activation.

3-The catalase (CAT) activity is important for the redox homeostasis of human differentiated adipocytes. Thus, the 3-amine-1,2,4-triazole (3-AT) treatment lowered CAT activity, increased intracellular hydrogen peroxide (H₂O₂) levels significantly and antioxidant enzymes such as glutathione peroxidase *GPX* and peroxiredoxins (1, 3 and 5) were also inhibited in the adipocytes. Additionally, nuclear factor-(erythroid-derived-2)-like-2 (*Nrf2*) and Forkhead box protein O1 (*FOXO1*) mRNA levels, which are involved in redox homeostasis, were also down-regulated in the 3-AT-treated cells.

4-The 3-AT treatment leads to nuclear factor kappa-light-chain-enhancer or activated B cells (NF-κB) activation and increases tumor necrosis factor(TNF)-α and interleukin(IL)-6 protein and gene expression levels, while lowering peroxisome proliferator-activated receptor(*PPAR*)-γ mRNA and protein levels,

which led to lower glucose uptake and lipolysis. These findings suggest an important role of CAT in the protection of adipocytes against the oxidative stress and metabolic complications observed in obesity through the regulation of H₂O₂ levels, which exerts complex signaling functions.

General conclusion

Our results indicate that *NPR3* and *CAT* genes are extensively involved in the adipocyte metabolism and its derived complications. Thus, C-ANP₄₋₂₃ enhances glucose metabolism through the GLUT4 up-regulation and AMPK activation; and the CAT activity plays a significant role in the metabolic homeostasis of adipocytes due to impair on the antioxidant defense system, initiate inflammation and glucose and lipid metabolism alterations observed in the 3-AT-treated cells. These findings support the role of several genes in the adipocyte metabolism and its putative association with obesity.

Conclusiones

Conclusiones

1-Las células madre mesenquimales derivadas de tejido adiposo humano (ADSCs) se diferencian completamente hasta adipocitos maduros. La diferenciación adipogénica se validó mediante la tinción con *Oil Red O* y mediante la expresión génica de *PPAR-γ*, *leptina* y *adiponectina* en diferentes tiempos (día 0, día 5, día 9 y día 12).

2-El análogo al péptido natriurético atrial (C-ANP₄₋₂₃), que es específico para el receptor 3 de los péptidos natriuréticos (NPR3), mejora el metabolismo glucídico en adipocitos humanos diferenciados. Estos efectos fueron mediados a través del aumento de los niveles de AMP cíclico, la sobreexpresión del transportador de glucosa 4 (GLUT4) y la activación de la proteína quinasa activada por AMP (AMPK).

3-La actividad de la catalasa (CAT) es importante para la homeostasis redox de adipocitos humanos diferenciados. De este modo, el tratamiento con el 3-amino-1,2,4-triazol (3-AT) disminuye la actividad de CAT, aumenta los niveles de peróxido de hidrógeno de forma significativa y enzimas antioxidantes como son la glutatión peroxidasa y peroxirredoxinas (1, 3 y 5) son inhibidas en los adipocitos. Además, los niveles de expresión génica de factores de transcripción involucrados en la homeostasis redox, como el *Nrf2* y el *FOXO1*, se encuentran también disminuídos en las células tratadas con 3-AT.

4-El tratamiento con 3-AT conlleva la activación del factor nuclear potenciador de las cadenas ligeras kappa de las células B activas (NF-κB) y aumento del factor de necrosis tumoral (TNF)-α e interleucina 6 (IL-6), mientras

que disminuye la expresión del *PPAR-γ*, el cual a su vez, produce una menor captación de glucosa y menor lipólisis. Estos hallazgos sugieren un papel importante de la CAT en la protección de los adipocitos contra el estrés oxidativo y complicaciones metabólicas en la obesidad a través de la regulación de los niveles de H_2O_2 , que ejerciendo funciones de señalización complejas.

Conclusión general

Nuestros resultados indican que los genes *NPR3* y *CAT* están inmensamente involucrados en el metabolismo del adipocito y sus complicaciones derivadas. Así, C-ANP₄₋₂₃ mejora el metabolismo glucídico a través del aumento del GLUT4 y la activación de la AMPK; y la actividad de CAT juega un papel significativo en la homeostasis metabólica de los adipocitos debido al daño en el sistema de defensa antioxidante, el inicio de inflamación y las alteraciones en el metabolismo glucídico y lipídico observadas en las células tratadas con 3-AT. Estos hallazgos apoyan la función de los genes *NPR3* y *CAT* en el metabolismo del adipocito y su posible asociación con la obesidad.

Future perspectives

Future perspectives

Currently, we are working with others candidate genes associated with obesity in human differentiated adipocytes such as tenomodulin (*TNMD*) and calcitonin receptor like-receptor (*CALCRL*). *TNMD* was found to be up-regulated in obese children; however, *CALCRL* gene expression was confirmed to be down-regulated (Aguilera *et al.* 2015). We have previously shown that *TNMD* expression is higher during the adipogenic differentiation human adipose-derived tissue stem cells (ADSCs). Recently, it has been reported that *TNMD* promotes adipocyte differentiation in 3T3-L1 cells (Senol-Cosar *et al.* 2016). Therefore, our main objective is elucidating the putative role of *TNMD* on adipogenesis, glucose and lipid metabolism in the human differentiated adipocytes from ADSCs.

Additionally, a collaboration with the Prof. Dr. Mariana Fátima Fernández is going on to assess the impact of low levels of bisphenol A (BPA), as well as its proposed substitutes bisphenol F (BPF) and bisphenol S (BPS) on adipogenic differentiation and lipid metabolism of human adipose-derived stem cells (ADSCs). Preliminary results were presented in the 2nd Paris Workshop on Endocrine Disruptors Effects on Wildlife and Human Health, Paris, France. The communication were “entitled Bisphenol A and congeners proposed as substitutes promote adipogenesis of human ADSC at environmentally relevant doses”.

Finally, I will apply for a post-doctoral fellowship.

References

References

Adachi T, Toishi T, Wu H, Kamiya T, Hara H. Expression of extracellular superoxide dismutase during adipose differentiation in 3T3-L1 cells. *Redox Rep.* **2009**; 14(1): 34-40.

Aguilera C, Gomez-Llorente C, Tofe I, Gil-Campos M, Cañete R, Gil A. Genome-wide expression in visceral adipose tissue from obese prepubertal children. *Int J Mol Sci* **2015**; 16,7723e7737.

Ahmed M, Neville MJ, Edelman MJ, Kessler BM, Karpe F. Proteomic analysis of human adipose tissue after rosiglitazone treatment shows coordinated changes to promote glucose uptake. *Obesity* **2010**; 18(1):27–34.

Almeida SA, Cardoso CC, Orellano LA, Reis AM, Barcelos LS, Andrade SP. Natriuretic peptide clearance receptor ligand (C-ANP₄₋₂₃) attenuates angiogenesis in a murine sponge implant model. *Clin. Exp. Pharmacol. Physiol* **2014**; 41, 691e697.

Amirkhizi F, Siassi F, Djalali M, Shahraki SH. Impaired enzymatic antioxidant defense in erythrocytes of women with general and abdominal obesity. *Obes Res Clin Pract* **2014**; 8(1): 26–34.

Anand-Srivastava MB, Sairam MR, Cantin M. Ring-deleted analogs of atrial natriuretic factor inhibits adenylate cyclase/cAMP system. Possible coupling of clearance atrial natriuretic factor receptors to adenylate cyclase/cAMP signal transduction system. *J Biol Chem* **1990**; 265, 8566e8572.

Anand-Srivastava MB. Natriuretic peptide receptor-C signaling and regulation. *Peptides* **2005**; 26:1044–1059.

Anderson EJ, Lustig ME, Boyle KE, Woodlief TL, Kane DA, Lin CT, et al. Mitochondrial H₂O₂ emission and cellular redox state link excess fat intake to insulin resistance in both rodents and humans. *Journal of Clinical Investigation* **2009**; 119(3):573–81.

Andreeva ER, Lobanova MV, Udartseva OO. Response of Adipose Tissue Derived Stromal Cells in Tissue-Related O₂ Microenvironment to Short-Term Hypoxic Stress. *Cells Tissues Organs* **2014**; 200(5): 307–315.

Atashi F, Modarressi A, Pepper MS. The Role of Reactive Oxygen Species in Mesenchymal Stem Cell Adipogenic and Osteogenic Differentiation: A Review. *Stem Cells and Development. Stem Cells Dev.* **2015**; 24(10): 1150-63.

Bagnyukova TV, Vasylykiv OY, Storey KB, Lushchak VI. Catalase inhibition by amino triazole induces oxidative stress in goldfish brain. *Brain Res.* **2005**; 1052 (2): 180-6.

Baraban E, Chavakis T, Hamilton BS, Sales S, Wabitsch M, Bornstein SR, Ehrhart-Bornstein M. Anti-inflammatory properties of bone morphogenetic protein 4 in human adipocytes. *International Journal of Obesity* **2016**; 40, 319–327.

Baranova A, Collantes R, Gowder SJ, Elariny H, Schlauch K, Younoszai A, et al. Obesity-related differential gene expression in the visceral adipose tissue. *Obes Surg* **2005**; 15, 758e765.

Barbosa DS, Cecchini R, El Kadri MZ, Rodríguez MA, Burini RC, Dichi I. Decreased oxidative stress in patients with ulcerative colitis supplemented with fish oil omega-3 fatty acids. *Nutrition* **2003**; 19(10): 837-42.

Bhuyan KC, Bhuyan DK. Regulation of hydrogen peroxide in eye humors. Effect of 3-amino-1H-1,2,4-triazole on catalase and glutathione peroxidase of rabbit eye. *Biochim BiophysActa*. **1977**; 497(3): 641-51.

Bolsoni-lobes A, Festuccia WT, Chimin P, Farias TS, Torres-Leal FL, Cruz MM et al. Palmitoleic acid (n-7) increases white adipocytes GLUT4 content and glucose uptake in association with AMPK activation. *Lipids Health Dis*. **2014**; 13: 199.

Bordicchia M, Liu D, Amri EZ, Ailhaud G, Dessi-Fulgheri P, Zhang C, et al. Cardiac natriuretic peptides act via p38 MAPK to induce the brown fat thermogenic program in mouse and human adipocytes. *J Clin Invest* **2012**; 122, 1022e1036.

Boyle KE, Patinkin ZW, Shapiro AL, Baker PR 2nd, Dabelea D, Friedman JE. Mesenchymal Stem Cells from Infants Born to Obese Mothers Exhibit Greater Potential for Adipogenesis: The Healthy Start Baby BUMP Project. *Diabetes* **2015**; db150849.

Bradley D, Conte C, Mittendorfer B, Eagon JC, Varela JE, Fabbrini E, Gastaldelli A, Chambers KT, Su X, Okunade A, Patterson BW, Klein S. Gastric bypass and banding equally improve insulin sensitivity and β cell function. *J Clin Invest*. **2012**; 122(12):4667-74.

Brinkmann C, Brixius K. Peroxiredoxins and sports: new insights on the antioxidative defense. *J Physiol_Sci*. **2013**; 63(1):1-5.

Chang E, Choi JM, Park SE, Rhee EJ, Lee WY, Oh KW, et al. Adiponectin deletion impairs insulin signaling in insulin-sensitive but not insulin-resistant 3T3-L1 adipocytes. *Life Sci*. **2015**; 132: 93-100.

Chen B, Lam KS, Wang Y, Wu D, Lam MC, Shen J, et al. Hypoxia dysregulates the production of adiponectin and plasminogen activator inhibitor-1 independent of reactive oxygen species in adipocytes. *Biochem Biophys Res Commun* **2006**; 341(2):549–56.

Choe SS, Huh JY, Hwang IJ, Kim JI, Kim JB. Adipose tissue remodeling: its role in energy metabolism and metabolic disorders. *Front Endocrinol (Lausanne)* **2016**; 7:30. .

Coate KC, Huggins KW. Consumption of a high glycemic index diet increases abdominal adiposity but does not influence adipose tissue pro-oxidant and antioxidant gene expression in C57BL/6 mice. *Nutr Res*. **2010**; 30(2):141-50.

Comim CM, Cassol-Jr OJ, Constantino LC, Constantino LS, Petronilho F, Tuon L, et al. Oxidative variables and antioxidant enzymes activities in the mdx mouse brain. *Neurochem Int*. **2009**; 55(8): 802-5.

Cordero P, Li J, Oben JA. Epigenetics of obesity: beyond the genome sequence. *Curr Opin Clin Nutr Metab Care* **2015**; 18(4): 361-6.

Crilley C, Garcia R. Effects of atrial natriuretic factor on glucose metabolism in isolated adipocytes. *Regul Pept* **1997**; 68(2):125-30.

- D'Alessandro ME, Selenscig D, Illesca P, Chicco A, Lombardo YB. Time course of adipose tissue dysfunction associated with antioxidant defense, inflammatory cytokines and oxidative stress in dyslipemic insulin resistant rats. *Food Funct.* **2015**; 6(4):1299-309.
- Dessi-Fulgheri P, Sarzani R, Tamburrini P, Moraca A, Espinosa E, Cola G, et al. Plasma atrial natriuretic peptide and natriuretic peptide receptor gene expression in adipose tissue of normotensive and hypertensive obese patients. *J Hypertens* **1997**; 15,1695e1699.
- Djordjevic D, Cubrilo D, Macura M, Barudzic N, Djuric D, Jakovljevic V. The influence of training status on oxidative stress in young male handball players. *Mol Cell Biochem.* **2011**; 351(1-2): 251-9.
- Dominici M, LeBlanc K, Mueller, I, Slaper-Cortenbach I, Marini F, Krause D, et al. Minimal criteria for defining multipotent mesenchymal stromal cells. The International Society for Cellular Therapy position statement. *Cytotherapy* **2006**; 8(4), 315-317.
- Doni MG, Piva E. Glutathione peroxidase blockage inhibits prostaglandin biosynthesis in rat platelets and aorta. *Haemostasis.* **1983**; 13(4): 240-3.
- Essers MA, de Vries-Smits LM, Barker N, Polderman PE, Burgering BM, Korswagen HC. Functional interaction between beta-catenin and FOXO in oxidative stress signaling. *Science.* **2005**; 308(5725): 1181-4.
- Fall T, Ingelsson E. Genome-wide association studies of obesity and metabolic syndrome. *Mol Cell Endocrinol* **2014**; 382: 740–757.
- Furukawa S, Fujita T, Shimabukuro M, Iwaki M, Yamada Y, Nakajima Y, et al. Increased oxidative stress in obesity and its impact on metabolic syndrome. *J Clin Invest* **2004**; 114(12): 1752–1761.
- Gauthier MS, Miyoshi H, Souza SC, Cacicedo JM, Saha AK, Greenberg AS, et al. AMP-activated Protein Kinase is activated as a consequence of lipolysis in the adipocyte: potential mechanism and physiological relevance. *J Biol Chem* **2008**; 283(24): 16514–16524.
- Gauthier MS, O'Brien EL, Bigornia S, Mott M, Cacicedo JM, Xu XJ, et al. Decreased AMP-activated protein kinase activity is associated with increased inflammation in visceral adipose tissue and with whole-body insulin resistance in morbidly obese humans. *Biochem Biophys Res Commun.* **2011**; 404(1): 382-7.
- Gómez-Ambrosi J, Catalán V, Diez-Caballero A, Martínez-Cruz LA, Gil MJ, García-Foncillas J, et al. Gene expression profile of omental adipose tissue in human obesity. *FASEB J* **2004**; 18, 215e217.
- Gough, D.R.; Cotter, T.G. Hydrogen peroxide: a Jekyll and Hyde signalling molecule. *Cell Death Dis* **2011**; 2:e213.
- Govers R. Molecular mechanisms of GLUT4 regulation in adipocytes. *Diabetes Metab* **2014**; 40: 400-410.
- Gower WR Jr1, Carter GM, McAfee Q, Solivan SM. Identification, regulation and anti-proliferative role of the NPR-C receptor in gastric epithelial cells. *Mol Cell Biochem.* **2006**; 293(1-2): 103-18

Gruden G, Landi A, Bruno G. Natriuretic peptides, heart, and adipose tissue: new findings and future developments for diabetes research. *Diabetes Care* **2014**; 37, 2899e2908.

Han SH, Quon MJ, Kim AJ, Koh KK. Adiponectin and Cardiovascular Disease Response to Therapeutic Interventions Seung Hwan *Journal of the American College of Cardiology*. **2007**; 49(5): 531-8.

Haneklaus M, O' Neill LA. NLRP3 at the interface of metabolism and inflammation. *Immunol Rev* **2015**; 265: 53-62.

Harms M, Seale P. Brown and beige fat: development, function and therapeutic potential. *Nat Med* **2013**; 19(10):1252e63.

Appleman D, Heim Wg, Pyfrom Ht. Effects of 3-amino-1, 2, 4-triazole (AT) on catalase and other compounds. *Am J Physiol*. **1956**; 186(1):19-23.

Higuchi M, Dusting GJ, Peshavariya H, Jiang F, Hsiao ST, Chan EC, et al. Differentiation of human adipose-derived stem cells into fat involves reactive oxygen species and Forkhead box O1 mediated upregulation of antioxidant enzymes. *Stem Cells Dev* **2013**; 22(6): 878–88.

Hirosumi J, Tuncman G, Chang L, Gorgun CZ, Uysal KT, Maeda K, et al. A central role for JNK in obesity and insulin resistance. *Nature* **2002**; 420:333–6. doi:10.1038/nature01137.

Houstis N, Rosen ED, Lander ES. Reactive oxygen species have a causal role in multiple forms of insulin resistance. *Nature*. **2006**; 440(7086): 944-8.

Huh JY, Kim Y, Jeong J, Park J, Kim I, Huh KH, et al. Peroxiredoxin 3 is a key molecule regulating adipocyte oxidative stress, mitochondrial biogenesis, and adipokine expression. *Antioxid Redox Signal*. **2012**; 16(3):229-43.

Hunt SC, Hasstedt SJ, Xin Y, et al. Polymorphisms in the NPY2R gene show significant associations with BMI that are additive to FTO, MC4R, and NPF2R2 gene effects. *Obesity (Silver Spring)* **2011**; 19:2241–2247.

Hutchinson DS, Chernogubova E, Dallner OS, Cannon B, Bengtsson T. Beta-adrenoceptors, but not alpha-adrenoceptors, stimulate AMP-activated protein kinase in brown adipocytes independently of uncoupling protein-1. *Diabetologia* **2005**; 48(11):2386-95.

Ibrahim MM. Subcutaneous and visceral adipose tissue: structural and functional differences. *Obes Rev*. **2010**; 11(1):11-8.

Jernas M, Palming J, Sjöholm K, Jennische E, Svensson PA, Gabrielsson BG, et al. Separation of human adipocytes by size: hypertrophic fat cells display distinct gene expression. *FASEB J* **2006**; 20:1540–2.

Jin W, Wang H, Yan W, Xu L, Wang X, Zhao X, et al. Disruption of Nrf2 enhances upregulation of nuclear factor-kappaB activity, proinflammatory cytokines, and intercellular adhesion molecule-1 in the brain after traumatic brain injury. *Mediators Inflamm*. **2008**; 725174.

Jung UJ, Choi MS. Obesity and its metabolic complications: the role of adipokines and the relationship between obesity, inflammation, insulin resistance, dyslipidemia and nonalcoholic fatty liver disease. *Int J Mol Sci.* **2014**; 15(4):6184-223.

Kensler TW, Wakabayashi N, Biswal S. Cell survival responses to environmental stresses via the Keap1-Nrf2-ARE pathway. *Annu Rev Pharmacol Toxicol* **2007**; 47: 89-116.

Kershaw EE, Schupp M, Guan HP, Gardner NP, Lazar MA, Flier JS. PPAR- γ regulates adipose triglyceride lipase in adipocytes in vitro and in vivo. *Am J Physiol Endocrinol Metab.* **2007**; 293(6): 1736-45.

Kershaw, E.E.; Flier, J.S. Adipose tissue as an endocrine organ. *J. Clin. Endocrinol. Metab.* **2004**, 89, 2548–2556.

Kim J, Cha YN, Surh YJ. A protective role of nuclear factor-erythroid 2-related factor-2 (Nrf2) in inflammatory disorders. *Mutat Res* **2010**; 690(1–2): 12–23.

Kim JI, Huh JY, Sohn JH, Choe SS, Lee YS, Lim CY, et al. Lipid-overloaded enlarged adipocytes provoke insulin resistance independent of inflammation. *Mol Cell Biol* **2015**; 35:1686–99.

Korswagen HC. Regulation of the Wnt/beta-catenin pathway by redox signaling. *Dev Cell* **2006**; 10 (6):687–8.

Kumar N, Solt LA, Wang Y, Rogers PM, Bhattacharyya G, Kamenecka TM, et al. Regulation of adipogenesis by natural and synthetic REV-ERB ligands. *Endocrinology* **2010**; 151(7):3015–25.

Kumar R, Cartledge WA, Lincoln TM, Pandey KN. Expression of guanylyl cyclase-A/atrial natriuretic peptide receptor blocks the activation of protein kinase C in vascular smooth muscle cells. Role of cGMP and cGMP-dependent protein kinase. *Hypertension* **1997**; 29: 414-421.

Lanthier N, Leclercq IA. Adipose tissues as endocrine target organs. *Best Pract Res Clin Gastroenterol.* **2014**; 28(4):545-58.

Lavie CJ, Sharma A, Alpert MA, De Schutter A, Lopez-Jimenez F, Milani RV, Ventura HO. Update on Obesity and Obesity Paradox in Heart Failure. *Prog Cardiovasc Dis.* **2016**;58(4):393-400.

Lee, M.J; Fried, S.K. Optimal Protocol for the Differentiation and Metabolic Analysis of Human Adipose Stromal Cells. *Methods Enzymol.* **2014**, 538, 49–65.

Lehrke M, Lazar MA. The many faces of PPAR- γ . *Cell.* **2005**; 123(6): 993-9.

Levin ER. Natriuretic peptide C-receptor: more than a clearance receptor. *Am J Physiol* **1993**; 264 (4 Pt 1), E483eE489.

Lewandowska E, Zieliński A. White adipose tissue dysfunction observed in obesity. *Pol Merkur Lekarski.* **2016**; 40(239):333-6.

Li Y, Madiraju P, Anand-Srivastava MB. Knockdown of natriuretic peptide receptor-A enhances receptor C expression and signalling in vascular smooth muscle cells. *Cardiovasc Res.* **2012**; 93: 350-359.

Li Y, Sarkar O, Brochu M, Anand-Srivastava MB. Natriuretic peptide receptor-C attenuates hypertension in spontaneously hypertensive rats: Role of nitroxidative stress and Gi proteins. *Hypertension* **2014**; 63: 846–855.

Lijnen H.R., Van Hul M., Hemmeryckx B. Caloric restriction improves coagulation and inflammation profile in obese mice. *Thromb. Res.* **2012**; 129:74–79.

Little SA, de Haën C. Effects of hydrogen peroxide on basal and hormone-stimulated lipolysis in perfused rat fat cells in relation to the mechanism of action of insulin. *J Biol Chem.* **1980**; 255(22): 10888-95.

Locke AE, Kahali B, Berndt SI, Justice AE, Pers TH, Day FR, Powell C, Vedantam S, Buchkovich ML, Yang J, et al. Genetic studies of body mass index yield new insights for obesity biology. *Nature.* **2015**; 518(7538):197-206.

Lu Y, Day FR, Gustafsson S, Buchkovich ML, Na J, Bataille V, Cousminer DL, Dastani Z, DrongAW, EskoT. New loci for body fat percentage reveal link between adiposity and cardiometabolic disease risk. *Nat Commun.* **2016**; 7:10495.

Maack T, Suzuki M, Almeida FA, Nussenzveig D, Scarborough RM, McEnroe GA et al. Physiological role of silent receptors of atrial natriuretic factor. *Science* **1987**; 238:675–678.

Margoliash E, Novogrodsky A. A study of the inhibition of catalase by 3-amino-1,2,4-triazole. *Biochem J.* **1958**; 68(3):468-75.

Margoliash E, Novogrodsky A, Schejter A. Irreversible reaction of 3-amino-1,2,4-triazole and related inhibitors with the protein of Catalase. *Biochem. J.* **1960**; 74: 339-350.

Matsukawa N, Grzesik WJ, Takahashi N, Pandey KN, Pang S, Yamauchi M, et al. The natriuretic peptide clearance receptor locally modulates the physiological effects of the natriuretic peptide system. *Proc Natl Acad Sci USA* **1999**; 96, 7403e7408.

May JM. The effect of insulin-stimulated pentose phosphate cycle activity on cellular glutathione content in rat adipocytes. *Horm Metabol Res* **1982**; 14: 634–637.

Monickaraj F, Aravind S, Nandhini P, Prabu P, Sathishkumar C, Mohan V, et al. Accelerated fat cell aging links oxidative stress and insulin resistance in adipocytes. *J Biosci.* **2013**; 38(1): 113-22.

Morigny P, Houssier M, Mouisel E, Langin D. Adipocyte lipolysis and insulin resistance. *Biochimie.* **2016**; 125: 259-66.

Moro C, Lafontan M. Natriuretic peptides and cGMP signaling control of energy homeostasis. *Am J Physiol Heart Circ Physiol* **2013**; 304, H358eH368.

Moro C, Polak J, Hejnova J, Klimcakova E, Crampes F, Stich V et al. Atrial natriuretic peptide stimulates lipid mobilization during repeated bouts of endurance exercise. *Am J Physiol Endocrinol Metab.* **2006**; 290 : E864–E869.

- Mukherjee SP, Mukherjee C. Similar activities of nerve growth factor and its homologue proinsulin in intracellular hydrogen peroxide production and metabolism in adipocytes. Transmembrane signaling relative to insulin-mimicking cellular effects. *Biochem Pharmacol* **1982**; 31(20): 3163–3172.
- Mullins GR, Wang L, Rajea V, Sherwooda SG, Rebecca C. Catecholamine-induced lipolysis causes mTOR complex dissociation and inhibits glucose uptake in adipocytes. *PNAS* **2014**; (111):17450–17455.
- Okuno Y, Matsuda M, Kobayashi H, Morita K, Suzuki E, Fukuhara A, et al. Adipose expression of catalase is regulated via a novel remote PPARgamma-responsive region. *Biochem Biophys Res Commun* **2008**; 366(3): 698–704.
- Olza J, Gil-Campos M, Leis R, Rupérez AI, Tojo R, Cañete R, Gil A, Aguilera CM. A gene variant of 11 β -hydroxysteroid dehydrogenase type 1 is associated with obesity in children. *Int J Obes (Lond)*. **2012**; 36(12):1558-63.
- Omar B, Zmuda-Trzebiatowska E, Manganiello V, Göransson O, Degerman E., Regulation of AMP-activated protein kinase by cAMP in adipocytes: roles for phosphodiesterases, protein kinase B, protein kinase A, Epac and lipolysis. *Cell Sig.* **2009**; 21, 760e766.
- Ortego J, Coca-Prados M. Functional expression of components of the natriuretic peptide system in human ocular nonpigmented ciliary epithelial cells. *Biochem Biophys Res Commun.* **1999**; 258(1): 21-8
- Pedruzzi LM, Stockler-Pinto MB, Leite M Jr, Mafra D. Nrf2-keap1 system versus NF-kB: The good and the evil in chronic kidney disease? *Biochimie.* **2012**; 94(12): 2461-6.
- Petersen RK, Madsen L, Pedersen LM, Hallenborg P, Hagland H, Viste K, et al. Cyclic AMP (cAMP)-mediated stimulation of adipocyte differentiation requires the synergistic of Epac- and cAMP-dependent protein kinase-dependent processes. *Mol Cell Biol.* **2004**; 28(11), 3804-3816.
- Pfaffl MW. A new mathematical model for relative quantification in real-time RT-PCR. *Nucleic Acids Res* **2001**; 29(9): e45.
- Pivovarova O, Gögebakan Ö, Klötting N, Sparwasser A, Weickert MO, Haddad I, et al. Insulin up-regulates natriuretic peptide clearance receptor expression in the subcutaneous fat depot in obese subjects: a missing link between CVD risk and obesity? *J. Clin. Endocrinol. Metab* **2012**; 97, 731e739.
- Potter LR, Abbey-Hosch S, Dickey DM. Natriuretic peptides, their receptors, and cyclic guanosine monophosphate-dependent signaling functions. *Endocr Rev* **2006**; 27, 47e72.
- Racette SB, Deusinger SS, Deusinger RH. Obesity: overview of prevalence, etiology, and treatment. *Phys Ther.* **2003**33(3):276-88.
- Rindler PM, Plafker SM, Szweda LI, Kinter M. High dietary fat selectively increases catalase expression within cardiac mitochondria. *J Biol Chem* **2013**, 288, 1979–1990.
- Rodriguez-Cuenca S, Carobbio S, Vidal-Puig A. Ablation of Pparg2 impairs lipolysis and reveals murine strain differences in lipolytic responses. *FASEB J.* **2012**; 26(5): 1835-1844.

Rosen ED, Spiegelman BM. Molecular regulation of adipogenesis. *Annu Rev Cell Dev Biol* **2000**; 16: 145-171.

Rudich A, Tirosh A, Potashnik R, Hemi R, Kanety H, Bashan N. Prolonged oxidative stress impairs insulin-induced GLUT4 translocation in 3T3-L1 adipocytes. *Diabetes* **1998**; 47(10): 1562–9.

Rupérez AI, Gil A, Aguilera CM. Genetics of Oxidative Stress in Obesity. *Int J Mol Sci* **2014**, 15, 3118-3144.

Rupérez AI, Olza J, Gil-Campos M, Leis R, Mesa MD, Tojo R, Cañete R, Gil A, Aguilera CM. Are Catalase -844A/G Polymorphism and Activity Associated with Childhood Obesity? *Antioxid Redox Signal* **2013**, 19, 1970–1975.

Rupérez AI, Olza J, Gil-Campos M, Leis R, Mesa MD, Tojo R, Cañete R, Gil Á, Aguilera CM. Association of genetic polymorphisms for glutathione peroxidase genes with obesity in Spanish children. *J Nutrigenet Nutrigenomics*. **2014**; 7(3):130-42.

Rutherford RA, Matsuda Y, Wilkins MR, Polak JM, Wharton J. Identification of renal natriuretic peptide receptor subpopulations by use of the non-peptide antagonist, HS-142-1. *Br J Pharmacol*. **1994**; 113(3):931-9.

Rutkowski JM, Stern JH, Scherer PE. The cell biology of fat expansion. *J Cell Biol* **2015**; 208:501–12.

Santangelo C, Vari R, Scazzocchio B, Filesi C, D'Archivio M, Giovanni C, et al. CCAAT/enhancer-binding protein- β participates in oxidized LDL-enhanced proliferation in 3T3-L1 cells. *Biochimie* **2011**; 93, 1510e1519.

Sarzani R, Dessì-Fulgheri P, Paci VM, Espinosa E, Rappelli A. Expression of natriuretic peptide receptors in human adipose and other tissues. *J. Endocrinol. Invest.* **1996**; 19, 581e585.

Sasaki CY, Barberi TJ, Ghosh P, Longo DL. Phosphorylation of RelA/p65 on serine 536 defines an I κ B independent NF- κ B pathway. *J Biol Chem*. **2005**; 280(41):34538–47.

Schenk DB, Phelps MN, Porter JG, Fuller F, Cordell B, Lewicki JA. Purification and subunit composition of atrial natriuretic peptide receptor. *Proc Natl Acad Sci USA* **1987**; 84, 1521e1525.

Schlueter N, de Sterke A, Willmes DM, Spranger J, Jordan J, Birkenfeld A. Metabolic actions of natriuretic peptides and therapeutic potential in the metabolic syndrome. *Pharmacol Ther* **2014**; 144, 12e27.

Schroder K, Tschopp J. The inflammasomes. *Cell* **2010**; 140:821– 832.

Sellitti DF, Perrella G, Doi SQ, Curcio F. Natriuretic peptides increase cAMP production in human thyrocytes via the natriuretic peptide clearance receptor (NPR-C). *Regul. Pept.* **2001**; 97, 103e109.

Sengenès C, Moro C, Galitzky J, Berlan M, Lafontan M. Natriuretic peptides: a new lipolytic pathway in human fat cells. *Med Sci Paris* **2005**; 21, 29e33.

Sethi JK, Xu H, Uysal KT, Wiesbrock SM, Scheja L, Hotamisligil GS. Characterisation of receptor-specific TNF α functions in adipocyte cell lines lacking type 1 and 2 TNF receptors. *FEBS Lett.* **2000**; 469(1): 77-82.

Shin MJ, Park E. Contribution of insulin resistance to reduced antioxidant enzymes and vitamins in non obese Korean children. *Clin Chim Acta.* **2006**; 365(1–2): 200–205.

Shungin D, Winkler TW, Croteau-Chonka DC, Ferreira T, Locke AE, Mägi R, Strawbridge RJ, Pers TH, Fischer K, Justice AE, et al. New genetic loci link adipose and insulin biology to body fat distribution. *Nature.* **2015**; 518(7538):187-96.

Sinha S, Ray US, Tomar OS, Singh SN. Different adaptation patterns of antioxidant system in natives and sojourners at high altitude. *Respiratory Physiology & Neurobiology* **2009**; 167(3): 255-260.

Skowronska, M., Zielinska, M., Albrecht, J. Stimulation of natriuretic peptide receptor C attenuates accumulation of reactive oxygen species and nitric oxide synthesis in ammonia-treated astrocytes. *J. Neurochem* **2010**; 115 (4), 1068e1076.

Soares AF, Guichardant M, Cozzone D, Bernoud-Hubac N, Bouzaïdi-Tiali N, Lagarde M, et al. Effects of oxidative stress on adiponectin secretion and lactate production in 3T3-L1 adipocytes. *Free Radical Biology and Medicine.* **2005**; 38(7): 882–889.

Spiegelman BM, Flier JS. Obesity and the regulation of energy balance. *Cell* **2001**; 104:531–43.

Stefan N, Stumvoll M. Adiponectin - its role in metabolism and beyond. *Horm Metab Res.* **2002**; 34(9): 469-74.

Stephens JM, Lee J, Pilch PF. Tumor Necrosis Factor- α -induced Insulin Resistance in 3T3-L1 Adipocytes Is Accompanied by a Loss of Insulin Receptor Substrate-1 and GLUT4 Expression without a Loss of Insulin Receptor-mediated Signal Transduction. *J Biol Chem.* **1997**; 272(2): 971–976.

Sugino N, Karube-Harada A, Sakata A, Takiguchi S, Kato H. Nuclear factor-kappa B is required for tumor necrosis factor-alpha-induced manganese superoxide dismutase expression in human endometrial stromal cells. *J Clin Endocrinol Metab.* **2002**; 87(8): 3845-50.

Than A, Zhang X, Leow MK, Poh CL, Chong SK, Chen P. Apelin attenuates oxidative stress in human adipocytes. *J Biol Chem.* **2014**; 289(6): 3763-74.

Tomas E, Tsao TS, Saha AK, Murrey HE, Zhang CcCc, Itani SI et al. Enhanced muscle fat oxidation and glucose transport by ACRP30 globular domain: acetyl-CoA carboxylase inhibition and AMP-activated protein kinase activation. *Proc Natl Acad Sci U S A.* **2002**; 99(25): 16309-13.

Trayhurn P. Hypoxia and adipose tissue function and dysfunction in obesity. *Physiol Rev* **2013**; 93:1–21.

Vater, C., Kasten, P., Stiehler, M.,. Culture media for the differentiation of mesenchymal stromal cells. *Acta Biomater* **2011**; 7, 463e477.

Vázquez-Meza H, Zentella de Piña M, Pardo JP, Riveros-Rosas H, Villalobos-Molina R, Piña E. Non steroidal anti-inflammatory drugs activate NADPH oxidase in adipocytes and raise the H₂O₂ pool to prevent cAMP-stimulated protein kinase a activation and inhibit lipolysis. *BMC Biochemistry*. **2013**; 14:13

Volz AC, Huber B, Kluger PJ. Adipose-derived stem cell differentiation as a basic tool for vascularized adipose tissue engineering. *Differentiation*. **2016**; 92(1-2):52-64.

Wang QA, Scherer PE, Gupta RK. Improved methodologies for the study of adipose biology: insights gained and opportunities ahead. *Journal of Lipid Research*. **2014**; 55, 605-624.

Wang TJ, Larson MG, Keyes MJ, Levy D, Benjamin EJ, Vasan RS. Association of plasma natriuretic peptide levels with metabolic risk factors in ambulatory individuals. *Circulation* **2007**; 115, 1345e1353.

Wheeler E, Huang N, Bochukova EG, et al. Genome-wide SNP and CNV analysis identifies common and low-frequency variants associated with severe early-onset obesity. *Nat Genet* **2013**; 45:513–517.

Wu J, Bostrom P, Sparks LM, Ye L, Choi JH, Giang AH, Khandekar M, Virtanen KA, Nuutila P, Schaart G. et al. Beige adipocytes are a distinct type of thermogenic fat cell in mouse and human. *Cell* **2012**; 150, 366–376.

Wu X, Motoshima H, Mahadev K, Stalker TJ, Scalia R, Goldstein BJ. Involvement of AMP-activated protein kinase in glucose uptake stimulated by the globular domain of adiponectin in primary rat adipocytes. *Diabetes* **2003**; 52 (6) 1355–1363.

Wu, Z., Rosen, E.D., Brun, R., Hauser, S., Adelmant, G., Troy, A.E., et al. Crossregulation of C/EBP α and PPAR γ controls the transcriptional pathway of adipogenesis and insulin sensitivity. *Mol. Cell*. **1999**; 151e158.

Xu S, Chen P, Su L. Regulatory networks of non-coding RNAs in brown/beige adipogenesis. *Biosci Rep* **2015**; 35, e00262.

Xue P, Hou Y, Chen Y, Yang B, Fu J, Zheng H, et al. Adipose deficiency of Nrf2 in ob/ob mice results in severe metabolic syndrome. *Diabetes*. **2013**; 62(3): 845-54.

Yajima H, Kobayashi Y, Kanaya T, Horino Y. Identification of peroxisome-proliferator responsive element in the mouse HSL gene. *BiochemBiophys Res Commun*. **2007**; 352(2): 526-31.

Yeh CH, Ma KH, Liu PS, Kuo JK, Chueh SH. Baicalein Decreases Hydrogen Peroxide-Induced Damage to NG108-15 Cells via Upregulation of Nrf2. *J Cell Physiol* **2015**; 230(8): 1840-51.

Yin W, Mu J, Birnbaum MJ. Role of AMP-activated protein kinase in cyclic AMP-dependent lipolysis in 3T3-L1 adipocytes. *J Biol Chem* **2003**; 278, 43074e43080.

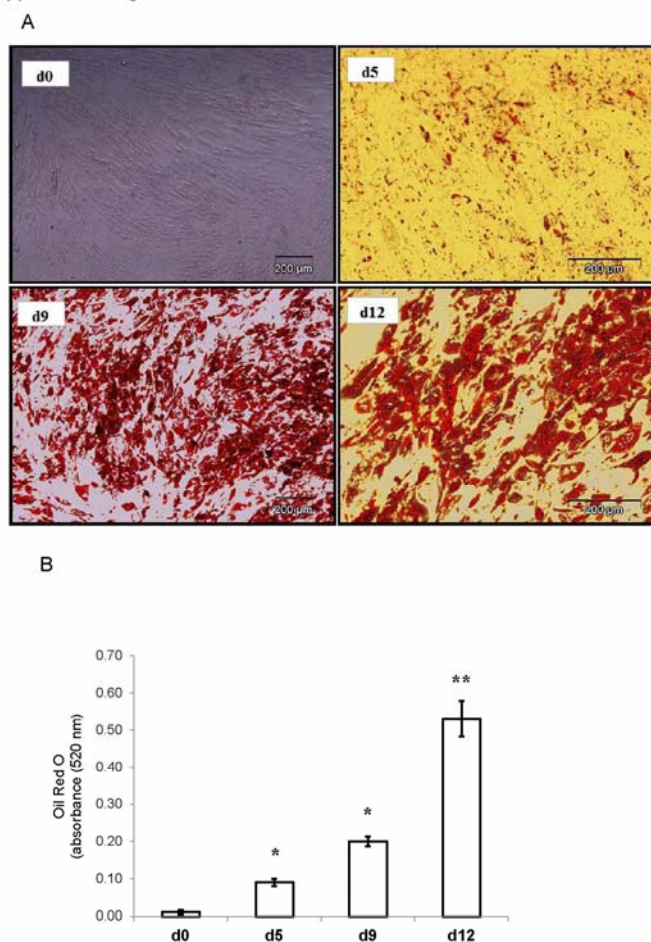
Zhang JW, Klemm DJ, Vinson C, Lane MD. Role of CREB in transcriptional regulation of CCAAT/enhancer-binding protein beta gene during adipogenesis. *J Biol Chem* **2004**; 279(6), 4471-4478.

Zhang M, Tang H, Shen G, Zhou B, Wu Z, Peng Z, et al. Atrial natriuretic peptide induces an acrosome reaction in giant panda spermatozoa and enhances their penetration of salt-stored porcine oocytes. *Theriogenology*. **2005**; 64(6): 1297-308.

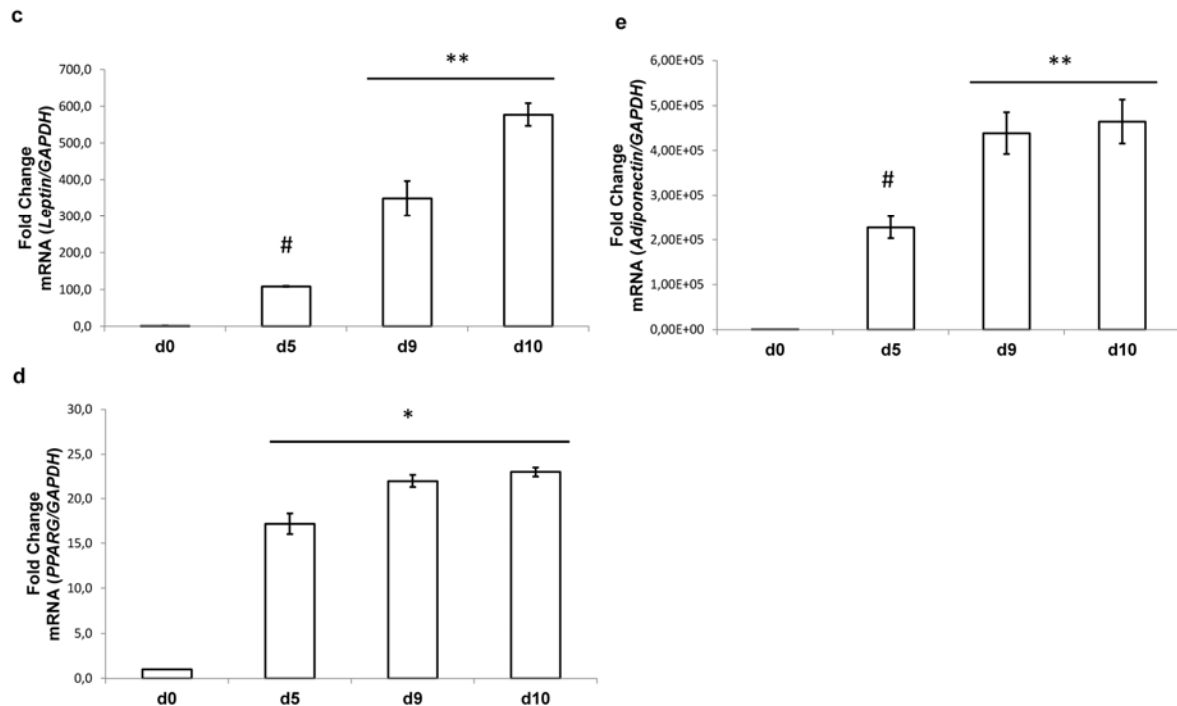
Appendix

Supplementary data

Supplemental Figure 1

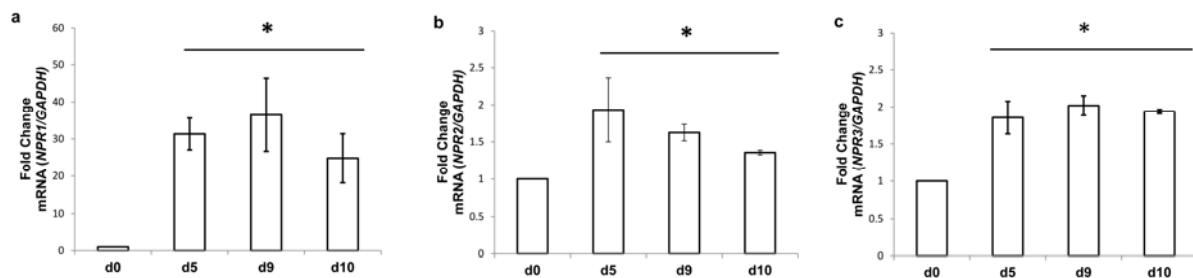


Supplementary Figure S1. Oil Red O staining of human adipose-derived stem cells at day 0 (d0) and during the adipogenic differentiation at days 5, 9 and 12 (d5, d9 and d12). **(a)** Optical microscopy images. **(b)** Quantification of lipid content from Oil Red O staining (absorbance at 520 nm). All values are expressed as means \pm SEM of three independent experiments. Significant differences were identified using the non-parametric Mann-Whitney U test; * $P < 0.05$; ** $P < 0.01$.



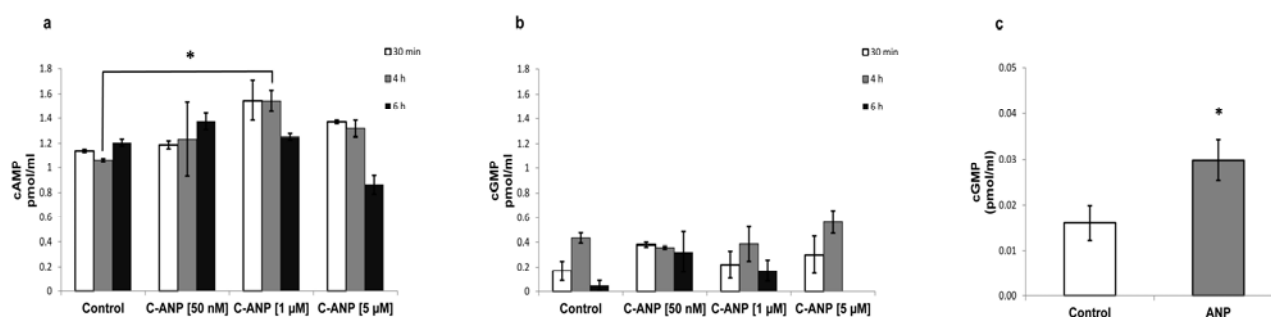
(c, d, e) *Leptin (LEP)*, *peroxisome proliferator-activated receptor gamma (PPARG)* and *adiponectin (ADIPOQ)* expression during adipogenic differentiation. The *LEP*, *PPARG* and *ADIPOQ* mRNA levels were normalised to those of *glyceraldehyde 3-phosphate dehydrogenase (GAPDH)*, and the data from three independent experiments are presented as the fold-change, which was calculated using the Pfaffl method. The white bars represent the ADSCs at day 0 (d0) and during the adipogenic differentiation at days 5, 9 and 10 (d5, d9 and d10). All values are expressed as means \pm s.e.m. of three independent experiments. Significant differences were analysed using the Mann-Whitney U test; d0 vs d9 and d10 $*P < 0.05$; d0 vs d5 $\#P < 0.05$; d0 vs d9 and d10 $**P < 0.01$.

Supplementary Figure S2



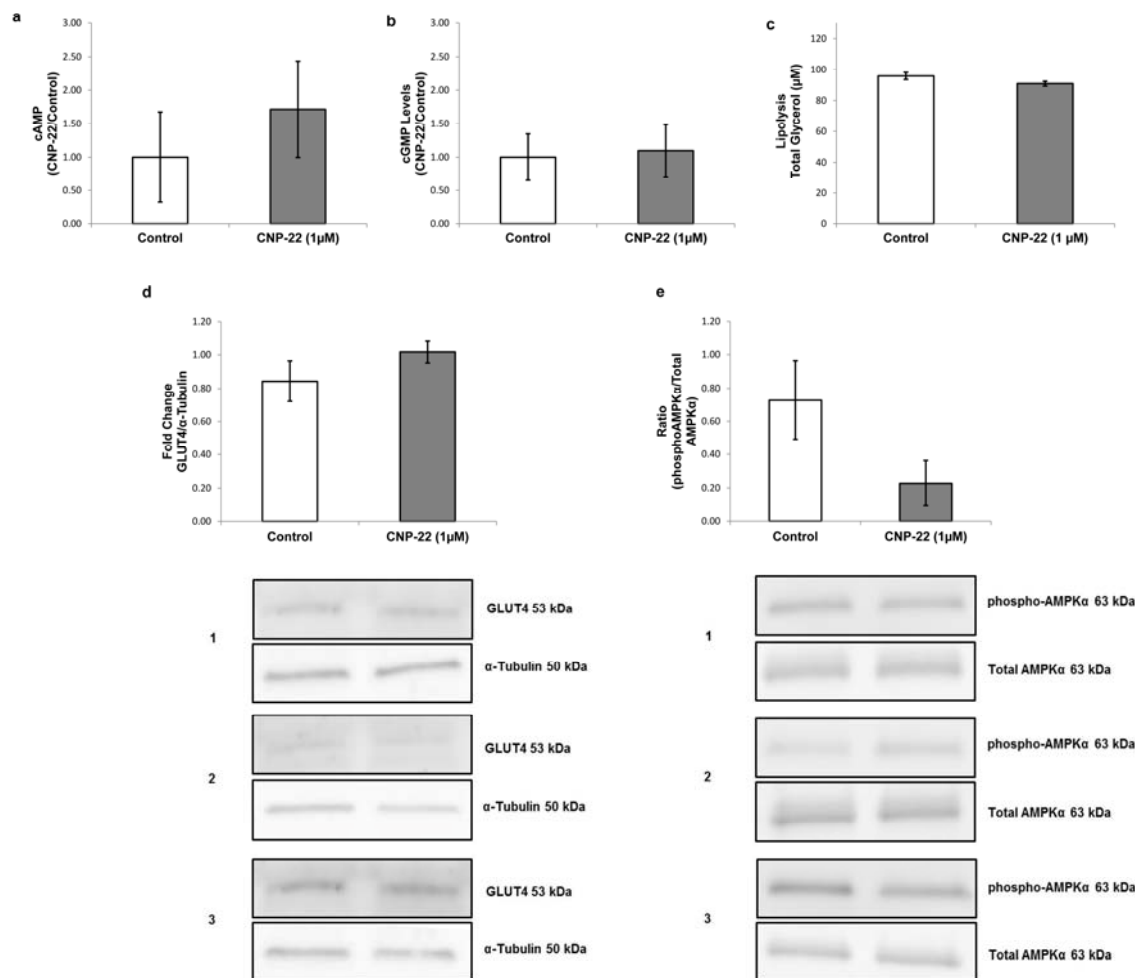
Supplementary Figure S2. Natriuretic peptide receptor 1 (*NPR1*), natriuretic peptide receptor 2 (*NPR2*) and natriuretic peptide receptor 3 (*NPR3*) expression during adipogenic differentiation. **(a)** The *NPR1* mRNA levels were normalised to those of *glyceraldehyde 3-phosphate dehydrogenase (GAPDH)*, and the data from three independent experiments are presented as the fold-change, which was calculated using the Pfaffl method. **(b)** The *NPR2* mRNA levels were normalised to those of *GAPDH*, and the data from three independent experiments are presented as the fold-change, which was calculated using the Pfaffl method. **(c)** The *NPR3* mRNA levels were normalised to those of *GAPDH*, and the data from three independent experiments are presented as the fold-change, which was calculated using the Pfaffl method. The white bars represent the human adipose-derived stem cells (ADSCs) at day 0 (d0) and during the adipogenic differentiation at days 5, 9 and 10 (d5, d9 and d10). Significant differences were analysed using the Mann-Whitney U test. The data are presented as the means \pm s.e.m.; $*P < 0.05$.

Supplementary Figure S3



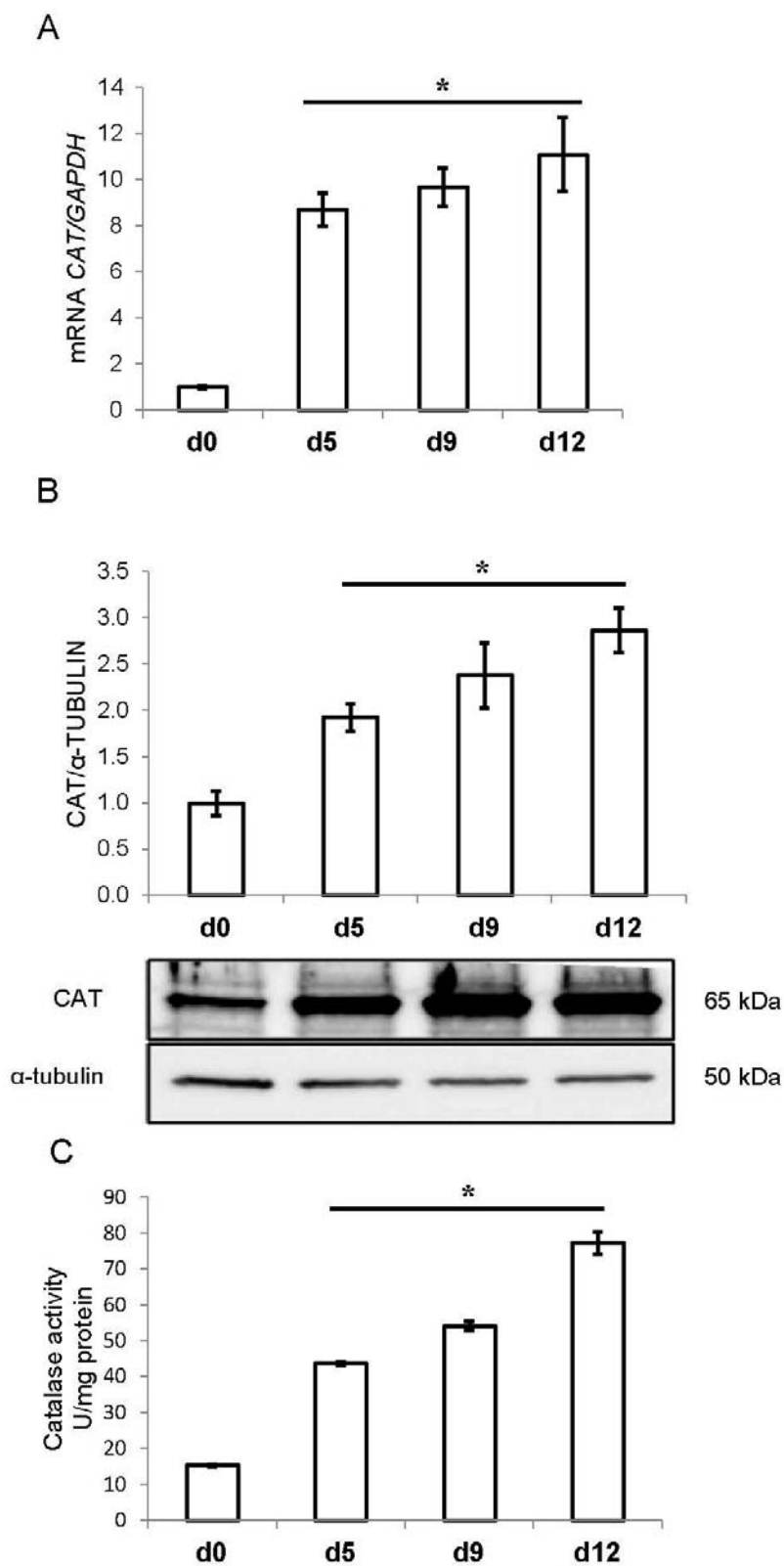
Supplementary Figure S3. Effects of C-atrial natriuretic peptide (C-ANP₄₋₂₃) on the intracellular cyclic adenosine monophosphate (cAMP), on the intracellular cyclic guanosine monophosphate (cGMP) levels and effects of atrial natriuretic peptide (ANP) on cGMP levels in human differentiated adipocytes at day 10. **(a)** Intracellular cAMP levels at different concentrations of C-ANP₄₋₂₃ (50 nM, 1 µM and 5 µM) and incubation times (30 minutes, 4h and 6h). **(b)** Intracellular cGMP levels at different concentrations of C-ANP₄₋₂₃ (50 nM, 1 µM and 5 µM) and incubation times (30 minutes, 4h and 6h). **(c)** Intracellular cGMP levels after incubation with ANP (1 µM for 4 h). The data are presented as the mean \pm s.e.m. of three independent experiments. Significant differences were analysed using the Mann-Whitney U test; $*P < 0.05$.

Supplementary Figure S4



Supplementary Figure S4. Effects of C-type natriuretic peptide-22 (CNP-22) on intracellular cyclic adenosine monophosphate (cAMP), intracellular cyclic guanosine monophosphate (cGMP) levels, lipolysis levels, glucose transporter (GLUT4) and 5'AMP-activated protein kinase catalytic subunit alpha (AMPK α) protein expression. **(a)** Intracellular cAMP levels after the treatment with CNP-22 (1 μ M, 4 h). **(b)** Intracellular cGMP levels after the treatment with CNP-22 (1 μ M, 4 h). **(c)** Glycerol levels (μ M) in total cell supernatants after treatment with CNP-22 (1 μ M, 4 h). **(d)** GLUT4 protein levels after treatment with CNP-22 (1 μ M, 4 h). The cell lysates were prepared and then analysed by Western blot using a specific antibody against GLUT4 as described in the Methods section. **(e)** Ratio phosphor-AMPK α /total-AMPK α after treatment with CNP-22 (1 μ M, 4 h). The cell lysates were prepared and then analysed by Western blot using specific antibodies against total AMPK α and phospho-AMPK α (Thr172) as described in the Methods section. The data are presented as the relative to no treatment fold-change, and the bars represent the means \pm s.e.m. of three separate experiments. Significant differences were analysed using the Mann-Whitney U test.

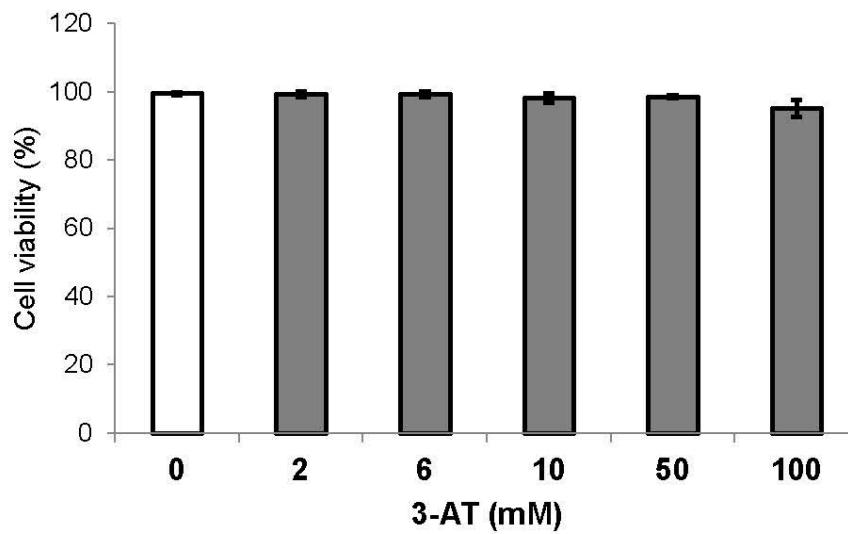
Supplementary Figure S5



Supplementary Figure S5. A: Catalase (*CAT*) mRNA levels normalized to those of glyceraldehyde 3-phosphate dehydrogenase (*GAPDH*) and presented as fold change, calculated

using the Pfaffl method. B: CAT protein levels from cell lysates analyzed by Western blot using a specific antibody against CAT, normalized to the internal control (α -tubulin) and expressed as fold change. C: CAT activity of cell lysates during adipogenic differentiation. All values are expressed as means \pm SEM of three independent experiments. Significant differences were identified using the non-parametric Mann-Whitney U test; * $P < 0.05$.

Supplementary Figure S6



Supplementary Figure S6. Effect of increasing concentrations of 3-amino-1,2,4-triazole (3-AT) on cell viability after a 24 h incubation. Cell viability was determined using a Neubauer chamber and trypan blue (4%).

Abbreviations

3-AT: 3-amino-1,2,4-triazole

ADIPOQ: adiponectin

ADSCs: Adipose-derived stem cells

AMPK: 5'-adenosin monophosphate-activated protein kinase

ANP: atrial natriuretic peptide

ATGL: adipose triglyceride lipase

BAT: brown adipose tissue

BNP: brain natriuretic peptide

C/EBP: CCAAT-enhancer binding protein

cAMP: cyclic adenosine monophosphate

C-ANP₄₋₂₃: C-atrial natriuretic peptide-(4-23)

CASP1: caspase 1

CAT: catalase

CD: cluster of differentiation

cGMP: cyclic guanosin monophosphate

CNP: C-type natriuretic peptide

CTNNB1: catenin beta 1

DMEM: Dulbecco's modified eagle medium

FABP4: fatty acid binding protein 4

FBS: fetal bovine serum

FFA: free fatty acid

FOXO1: forkhead box O 1

FTO: fat mass and obesity-associated

GAPDH: Glyceraldehyde 3-phosphate dehydrogenase

GLUT4: glucose transporter 4

GPX: glutathione peroxidases

GWAS: genetic wide association studies

HPRT1: Hypoxanthine-guanine phosphoribosyltransferase-1

HSL: hormone-sensitive lipase

IBMX: 3-isobutyl-1-methylxanthine

IL: interleukin

IL1B: interleukine 1-β

IR: insulin resistance

IRAK4: interleukin-1 receptor-associated kinase 4

LEP: leptin

LEPR: leptin receptor

MAPK: mitogen activated protein kinases

MCP-1: monocyte chemoattractant protein-1

MSC: mesenchymal stem cell

NAFLD: non-alcoholic fatty liver disease

NFKB2: nuclear factor of kappa light polypeptide gene enhancer in B-cells 2 (p49/p100)

NF-κB: nuclear factor kappa-light-chain-enhancer of activated B cells

NP: natriuretic peptide

NPR: natriuretic peptide receptor

NPR1: natriuretic peptide receptor 1

NPR2: natriuretic peptide receptor 2

NPR3: natriuretic peptide receptor 3

Nrf2: nuclear factor (erythroid 2-like 2)

PBS: phosphate buffer saline

PKA: protein kinase A

PLB: protein lysis buffer

PLIN: perilipin

PPAR- γ : peroxisome proliferator-activated receptor gamma

PRDX: peroxiredoxin

ROS: reactive oxygen species

SNP: single nucleotide polymorphism

SOD: superoxide dismutase

SREBP1c: sterol regulatory element-binding transcription factor 1c

SVF: stromal vascular fraction

TNFRSF1A: tumor necrosis factor receptor superfamily, member 1A

TNF- α : tumor necrosis factor α

TOLLIP2: Toll interacting protein

UCP-1: uncoupled protein 1

VAT: visceral adipose tissue

WAT: white adipose tissue

WHO: World Health Organization

List of figures and tables

Figure 1.A.World map of obesity prevalence in male.B.World map of obesity prevalence in female.

Figure 2.Characteristics of hypertrophic and hyperplastic adipocytes in obesity.

Figure 3.Molecular mechanism of adipogenesis and its common in vitro inducers.

Figure 4.Potential link between NPs, obesity, insulin resistance, and diabetes.

Figure 5.The natriuretic peptides exert their effects through transmembrane receptors.

Figure 6.Effects of different antioxidant enzymes on oxidative metabolism in adipocytes

Figure 7.3-amino-1,2,4-triazole (3-AT) chemical structure.

Figure 8.Diagram of Polimerase chain reaction (PCR).

Figure 9.Amplification plot and melting-dissotiation curve of a real-time PCR by using Sybr green in a ABI-7900HT instrument

Figure 10.Western blot equipment from Bio-rad

Table 1. Forward and reverse primer sequences used in the qPCR assays.

Additional Publication:

Literature review

**Effects of Probiotics and Synbiotics on Obesity,
Insulin Resistance Syndrome, Type 2 Diabetes
and Non-Alcoholic Fatty Liver Disease: A
Review of Human Clinical Trials.**

Sáez-Lara MJ, Robles-Sánchez C, Ruiz-Ojeda FJ, Plaza-Díaz J, Gil A.

International Journal of Molecular Sciences.**2016**; 17(6), 928.

Impact Factor 2015: **3,257**



Review

Effects of Probiotics and Synbiotics on Obesity, Insulin Resistance Syndrome, Type 2 Diabetes and Non-Alcoholic Fatty Liver Disease: A Review of Human Clinical Trials

Maria Jose Sáez-Lara ^{1,2}, Candido Robles-Sanchez ^{2,3}, Francisco Javier Ruiz-Ojeda ^{2,3,4}, Julio Plaza-Diaz ^{2,3,4} and Angel Gil ^{2,3,4,5,*}

¹ Department of Biochemistry & Molecular Biology I, School of Sciences, University of Granada, Granada 18071, Spain; mjsaez@ugr.es

² Institute of Nutrition and Food Technology “José Mataix”, Biomedical Research Center, University of Granada, Armilla 18100, Spain; croblesan@hotmail.com (C.R.-S.); fruizojeda@ugr.es (F.J.R.-O.); jrplaza@ugr.es (J.P.-D.)

³ Department of Biochemistry and Molecular Biology II, School of Pharmacy, University of Granada, Granada 18071, Spain

⁴ Instituto de Investigación Biosanitaria ibs, GRANADA, Complejo Hospitalario Universitario de Granada/Universidad de Granada, Granada 18014, Spain

⁵ CIBEROBN (Physiopathology of Obesity and Nutrition CB12/03/30038), Instituto de Salud Carlos III (ISCIII), Madrid 28029, Spain

* Correspondence: agil@ugr.es; Tel.: +34-958-241-000 (ext. 20307)

Academic Editor: Alejandro Cifuentes

Received: 16 April 2016; Accepted: 2 June 2016; Published: 13 June 2016

Abstract: The use of probiotics and synbiotics in the prevention and treatment of different disorders has dramatically increased over the last decade. Both probiotics and synbiotics are well known ingredients of functional foods and nutraceuticals and may provide beneficial health effects because they can influence the intestinal microbial ecology and immunity. The present study reviews the effects of probiotics and synbiotics on obesity, insulin resistance syndrome (IRS), type 2 diabetes (T2D) and non-alcoholic fatty liver disease (NAFLD) in human randomized clinical trials. Select probiotics and synbiotics provided beneficial effects in patients with obesity, mainly affecting the body mass index and fat mass. Some probiotics had beneficial effects on IRS, decreasing the cell adhesion molecule-1 levels, and the synbiotics decreased the insulin resistance and plasma lipid levels. Moreover, select probiotics improved the carbohydrate metabolism, fasting blood glucose, insulin sensitivity and antioxidant status and also reduced metabolic stress in subjects with T2D. Some probiotics and synbiotics improved the liver and metabolic parameters in patients with NAFLD. The oral intake of probiotics and synbiotics as co-adjuvants for the prevention and treatment of obesity, IRS, T2D and NAFLD is partially supported by the data shown in the present review. However, further studies are required to understand the precise mechanism of how probiotics and synbiotics affect these metabolic disorders.

Keywords: probiotics; randomized clinical trial; obesity; insulin resistance; metabolic syndrome X; type 2 diabetes; non-alcoholic fatty liver disease; synbiotics

1. Introduction

The microbiota (the full collection of microbes that naturally exist within a particular biological niche) has a profound influence on human physiology, affecting metabolism and the immune system and protecting against pathogens while modulating gastrointestinal (GI) development [1–3].

Perturbations in the composition of the microbiota may be especially important during early life, when the immune system is still developing [4].

Obesity is one of the most important public health problems worldwide, affecting both developed and emerging countries. It is characterized by an abnormal excess of white adipose tissue, which is a major risk factor for the development of diabetes, cardiovascular disease and cancer [5,6]. Among the studied potential determinants of obesity, the intestinal microbiota has been proposed to have an impact on the energy balance in humans [7–11]. Specific bacterial populations, such as *Prevotellaceae*, *Blautia coccooides*, *Eubacteria rectale* group, *Lactobacillus*, and *Bifidobacterium*, have been reported to be related to obesity. Consequently, it is believed that modulation of the intestinal microbiota toward a healthier “non-obese” profile might present a promising tool for prevention [12].

Metabolic syndrome is referred to as syndrome X or insulin resistance syndrome (IRS). Currently, the number of individuals with IRS is increasing worldwide and is primarily composed of those with abdominal obesity, glucose intolerance, dyslipidemia and high blood pressure. IRS increases cardiovascular morbidity and mortality as well as overall mortality [13]. Low insulin sensitivity, particularly in the visceral adipose tissue, leads to increased free fatty acid flux and inhibition of insulin action in insulin-sensitive tissues. Moreover, IRS is also associated with the development of diabetes mellitus [13,14].

There are about 382 million people living with diabetes in the world, and the number is expected to rise to 592 million by 2035 according to the International Diabetes Federation. The pathogenetic mechanism of type 2 diabetes (T2D) has not yet been completely elucidated. Recent evidence suggests that the intestinal microbiota composition is associated with the development of T2D [15]. A clear relationship has been demonstrated between T2D and compositional changes in the gut microbiota, with a lower relative abundance of *Firmicutes* and a higher proportion of *Bacteroidetes* and *Proteobacteria* in T2D patients [16,17].

Non-alcoholic fatty liver disease (NAFLD) is the most common type of liver disease worldwide that affects both adults and children. NAFLD encompasses a broad spectrum of diseases from simple steatosis at early stages to non-alcoholic steatohepatitis (NASH) and fibrosis, and it eventually may lead to cirrhosis. NAFLD may be caused mainly by obesity, but it can also be caused by T2D, glucocorticoids, and small bowel bacterial overgrowth (SIBO) caused by inflammatory bowel disease. Considering the intimate relationship between the intestine and the liver (called the gut-liver axis), it is becoming widely accepted that the composition of the gut microbiota is an environmental factor that affects host metabolism and contributes to the associated pathological conditions, such as obesity [18].

Probiotics are live microorganisms that confer a health benefit on the host when administered in adequate amounts [19], although dead bacteria and their components can also show probiotic properties. *Bifidobacterium* and *Lactobacillus* strains are the most widely used bacteria exhibiting probiotic properties and are included in many functional foods and dietary supplements [20]. Major mechanisms underlying the antagonistic effects of probiotics include improvement of the gut barrier function, increased competitive adherence to the mucosa and epithelium, gut microbiota modification, and regulation of the gut associated lymphoid immune system. In this sense, probiotics communicate with the host through intestinal cell pattern recognition receptors, such as toll-like receptors and nucleotide-binding oligomerization domain-containing protein-like receptors, which modulate important key signaling pathways, such as nuclear factor- κ B and mitogen-activated protein kinase, to enhance or suppress activation and influence downstream pathways [21–25].

A prebiotic is a nonviable food component that confers a health benefit on the host associated with modulation of the microbiota, they may be a fiber, but a fiber is not necessarily a prebiotic. Using prebiotics and probiotics in combination is often described as synbiotic, only if the net health benefit is synergistic [26].

Probiotics and synbiotics are consumed in many and diverse forms, such as yogurt and other fermented milks, cheese and several fermented foods, and also as prevention and treatment for different GI tract dysfunctions and other diseases like allergy [27]. However, the actual effects of probiotics to

affect intestinal ecology is still under debate because there are numerous confounding elements, such as dissimilarities in microbial strains, concentrations of viable cells and product formulations [3,28,29].

Recently, Yoo and Kim (2016) [30] have indicated that probiotics and prebiotics affect T2D and cardiovascular diseases by changing gut microbiota, regulating insulin signaling, and lowering cholesterol.

The present review was conducted to investigate the effectiveness of probiotics and synbiotics in the prevention and treatment of obesity, IRS, T2D and NAFLD in human studies designed as clinical trials.

2. Results

2.1. Effects of Probiotics and Synbiotics on Obesity

2.1.1. Probiotics

Lactobacillus salivarius Ls-33 was tested in obese adolescents to investigate its impact on fecal microbiota and anthropometric measures, biomarkers related to inflammation, carbohydrate and lipid metabolism. The ratios of *Bacteroides*, *Prevotellae*, and *Porphyromonas* group bacteria to *Firmicutes*-belonging bacteria, including *Clostridium* cluster XIV, *Blautia coccooides*, *Eubacterium rectale* group and *Roseburia intestinalis*, were significantly increased after the administration of *L. salivarius* Ls-33. However, the overall cell numbers of fecal bacteria, including the groups above as well as *Clostridium* cluster I and cluster IV, *Faecalibacterium prausnitzii*, *Enterobacteriaceae*, *Enterococcus*, *Lactobacillus* group and *Bifidobacterium* spp., were not significantly altered by intervention. Similarly, the short chain fatty acids (SCFA) remained unaffected [31]. Moreover, Gobel *et al.*, (2012) [32] carried out an intervention to study the *Lactobacillus salivarius* Ls-33 effects on some inflammation biomarkers and several parameters of metabolic syndrome in adolescents with obesity. However, they did not find changes in those parameters.

The effect of *L. gasseri* SBT2055 was examined in two studies using a cohort of Japanese adults with large visceral fat areas (VFA). The participants were randomly assigned to three groups receiving increasing colony-forming units (CFUs) of *L. gasseri* SBT2055 for 12 weeks. The results showed a reduction in body mass index (BMI), waist, abdominal VFA and hip circumferences [33,34]. Additionally, a hypocaloric diet supplemented with a probiotic-enriched cheese containing *Lactobacillus plantarum* reduced the BMI, the putrescine content and the intestinal lactobacilli in Russian adults with obesity and hypertension. Similarly, there was a reduction in the blood pressure (BP), namely a lower diastolic BP and a tendency toward lower systolic BP at the end of the intervention in the obese hypertensive patients that received the hypocaloric diet supplemented with the probiotic cheese [35].

The administration of *L. acidophilus* La5, *B. lactis* Bb12, and *L. casei* DN001 was evaluated in individuals with high BMI who were randomly assigned to three groups depending on particular intervention diets: one group was established with a regular yogurt with low calorie diet (RLCD), the second one received a probiotic yogurt with low calorie diet (PLCD) and, the third one received probiotic yogurt without low calorie diet (PWLCD) for about two months. A reduction in BMI, fat percentage, and leptin level was observed that was more obvious in groups who received the weight-loss diet including probiotic yogurt. Additionally, a reduction in the serum levels of CRP was more evident in the PWLCD group than in the PLCD and RLCD groups after the 8-week intervention. The expression of the *FOXP3*, *T-bet*, *GATA3*, *TNF- α* , *IFN- γ* , *TGF- β* , and *ROR- γ t* genes in peripheral blood mononuclear cell (PBMCs) were assessed before and after intervention. In the three groups, *ROR- γ t* expression was reduced and *FOXP3* was increased. The expression of the *TNF- α* , *TGF- β* , and *GATA3* genes did not change. Interestingly, *T-bet* gene expression was down-regulated in the PLCD and PWLCD groups. However, the *IFN- γ* expression was down-regulated in all groups. The authors suggested that weight loss diet and probiotics yogurt had effects on gene expression in PBMCs among overweight and obese individuals [36–38].

An 8-week, randomized, double-blind, placebo- and compliance-controlled parallel study in overweight and obese subjects was conducted to evaluate the effects of one strain of *E. faecium* and two strains of *S. thermophilus* [39]. The patients were randomly divided into five groups: (1) a yogurt fermented with two strains of *S. thermophilus* and two strains of *L. acidophilus*; (2) a placebo yogurt fermented with delta-acid-lactone; (3) a yogurt fermented with two strains of *S. thermophilus* and one strain of *L. rhamnosus*; (4) a yogurt fermented with one strain of *E. faecium* and two strains of *S. thermophilus*; and finally (5) two placebo pills daily [39]. After adjustment for small changes in body weight, low-density lipoprotein cholesterol (LDL-C) decreased and fibrinogen increased significantly after 8 weeks in the group that received the yogurt fermented with one strain of *E. faecium* and two strains of *S. thermophilus* compared to the group consuming chemically fermented yogurt and the placebo pill group. Additionally, after 8 weeks, the systolic BP was significantly more reduced in group 1 and the group that received the yogurt fermented with one strain of *E. faecium* and two strains of *S. thermophilus* than in group 3 [39].

The administration of capsules with bifidobacteria, lactobacilli, and *S. thermophilus* was conducted in overweight subjects. The probiotic mixture had a significant improvement in their lipid profiles, reducing total cholesterol (TC), triacylglycerols (TAG), and LDL-C levels and increasing high-density lipoprotein cholesterol (HDL-C) levels. The probiotic mixture improved insulin sensitivity and decreased C-reactive protein (CRP) [40].

On the other hand, a total of 58 obese, postmenopausal women were randomized into a single-blinded, parallel-group intervention of 6-week duration, with a daily ingestion of *L. paracasei* F19, flaxseed mucilage or placebo. The intake of *L. paracasei* F19 did not modulate any metabolic markers (homeostasis model assessment of insulin resistance (HOMA-IR), Matsuda index, CRP, and lipid profile) compared with the placebo [41]. Moreover, the intake of *L. acidophilus* La5 and *B. animalis* subsp. *lactis* Bb12 not affected the HOMA-IR, BP, heart rate or serum lipid concentrations in overweight adults [42,43].

2.1.2. Synbiotics

The impact of *L. rhamnosus* CGMCC1.3724 with oligo-fructose and inulin supplementation was investigated on weight loss and maintenance in obese men and women during 24 weeks [12].

The mean weight loss in women in the *L. rhamnosus* group was significantly higher than in women in the placebo group after the first 12 weeks, whereas it was similar in men in the two groups. The *L. rhamnosus*-induced weight loss in women was associated not only with significant reductions in fat mass and circulating leptin concentrations but also with the relative abundance of bacteria of the *Lachnospiraceae* family in the feces; this family belongs to the *Firmicutes* phylum, a taxonomic group that has previously been reported to be positively associated with obesity [12].

In obese children, two studies determined the effect of synbiotic supplementation on cardiometabolic risk factors, anthropometric measurements, serum lipid profile, and oxidative stress levels. The intake of synbiotics resulted in a significant reduction in the BMI z-score and waist circumference, as well as in some cardiometabolic risk factors, such as TC, LDL-C and TAG [36,37], and also changes in anthropometric measurements (% reduction comparing to baseline) were significantly higher in the children receiving synbiotics. After synbiotic supplementation, total oxidative stress serum levels significantly decreased [44,45].

In summary, the supplementation of selected probiotics appears to have beneficial effects on BMI, waist circumference, VFA and hip circumference in overweight or obese people. Moreover, it has been reported that some probiotic strains modulate the gene expression of specific transcription factors such as *ROR- γ t* (down-regulated) and *FOXP3* (up-regulated) in PBMCs. This was associated with beneficial effects on the immune system among overweight and obese individuals. However, no effects were observed at the level of inflammatory biomarkers in the administration of *L. paracasei* F19, and *L. acidophilus* La5 and *B. animalis* subsp. *lactis* Bb12. On the other hand, some synbiotics can reduce BMI in women, decrease fat mass and serum leptin levels and increase the levels of the

Lachnospiraceae family in the feces. Finally, synbiotic treatment would help to decrease the BMI z-score and waist circumference in children, as well as TC, LDL-C and TAG serum levels. Table 1 summarizes the studies of probiotics and synbiotics in obesity.

Table 1. Summary of randomized clinical intervention trials of probiotics and synbiotics in obesity.

Reference	Subjects	Strain/Dose	Time	Main Outcome
Probiotics				
Larsen <i>et al.</i> , 2013 [31]	50 obese adolescents	<i>L. salivarius</i> Ls-33	12 wk	Increase in the ratios of <i>Bacteroides</i> , <i>Prevotellae</i> and <i>Porphyromonas</i> .
Gobel <i>et al.</i> , 2012 [32]	50 adolescents with obesity	<i>L. salivarius</i> Ls-33, 10 ¹⁰ CFU	12 wk	No effect.
Kadooka <i>et al.</i> , 2010 [33]	87 subjects with high BMI	<i>L. gasseri</i> SBT2055, 5 × 10 ¹⁰ CFU	12 wk	Reduction in BMI, abdominal VFA. Increase in adiponectin levels.
Kadooka <i>et al.</i> , 2013 [34]	210 adults with large VFA	<i>L. gasseri</i> SBT2055, 10 ⁸ CFU	12 wk	Reduction in BMI, waist, abdominal VFA and hip circumference.
Sharafedinov <i>et al.</i> , 2013 [35]	40 adults with obesity	<i>L. plantarum</i> 1.5 × 10 ¹¹ CFU/g	3 wk	Reduction in BMI and arterial BP values.
Zarrati <i>et al.</i> , 2013a, 2013b, 2014 [36–38]	75 subjects with high BMI	<i>L. acidophilus</i> La5, <i>B. lactis</i> Bb12, and <i>L. casei</i> DN001, 10 ⁸ CFU/g	8 wk	Changes in gene expression in PBMCs as well as BMI, fat percentage and leptin levels.
Agerholm-Larsen <i>et al.</i> , 2000 [39]	70 overweight and obese subjects	<i>E. faecium</i> and two strains of <i>S. thermophilus</i>	8 wk	Reduction in body weight, systolic BP, LDL-C, and increase on fibrinogen levels.
Rajkumar <i>et al.</i> , 2013 [40]	60 overweight subjects	Bifidobacteria, lactobacilli, and <i>S. thermophilus</i>	6 wk	Improvement in lipid profile, insulin sensitivity, and decrease in CRP.
Brahe <i>et al.</i> , 2015 [41]	58 obese PM women	<i>L. paracasei</i> N19, 9.4 × 10 ¹⁰ CFU	6 wk	No effect.
Ivey <i>et al.</i> , 2014, 2015 [42,43]	156 overweight adults	<i>L. acidophilus</i> La5 and <i>B. animalis</i> subsp. <i>lactis</i> Bb12	6 wk	Reduction in fasting glucose concentration and increase in HOMA-IR.
Synbiotics				
Sánchez <i>et al.</i> , 2014 [12]	153 obese men and women	<i>L. rhamnosus</i> CGMCC1.3724, 6 × 10 ⁸ CFU, and inulin	36 wk	Weight loss and reduction in leptin. Increase in <i>Lachnospiraceae</i> .
Safavi <i>et al.</i> , 2013 [44]	70 children and adolescents with high BMI	<i>L. casei</i> , <i>L. rhamnosus</i> , <i>S. thermophilus</i> , <i>B. breve</i> , <i>L. acidophilus</i> , <i>B. longum</i> , <i>L. bulgaricus</i> , and FOS	8 wk	Decrease in BMI z-score and waist circumference.
Ipar <i>et al.</i> , 2015 [45]	77 obese children	<i>L. acidophilus</i> , <i>L. rhamnosus</i> , <i>B. bifidum</i> , <i>B. longum</i> , <i>E. faecium</i> , and FOS	4 wk	Changes in anthropometric measurements. Decrease in TC, LDL-C and total oxidative stress serum levels.

Abbreviations: BMI, body mass index; BP, blood pressure; CFU, colony-forming-unit; CRP, C-reactive protein; FOS, fructo-oligosaccharides; HOMA-IR, homeostasis model assessment of insulin resistance; LDL-C, low-density lipoprotein cholesterol; PBMC, peripheral blood mononuclear cell; PM, postmenopausal; TC, total cholesterol; VFA, visceral fat area; wk, week.

2.2. Effects of Probiotics and Synbiotics on Insulin Resistance Syndrome

2.2.1. Probiotics

The effects of *Lactobacillus casei* Shirota were evaluated in patients with IRS for studying the gut permeability, the presence of endotoxin and neutrophil function, the insulin sensitivity index, quantitative insulin sensitivity check index, insulin sensitivity by oral glucose tolerance test, HOMA-IR

and β -cell function. The gut permeability increases, but the endotoxin and neutrophil function remain unaffected [46]. The only parameter that improved after probiotic administration was insulin sensitivity index [47]. IRS in postmenopausal women is an important risk factor for cardiovascular morbidity, especially stroke and coronary heart disease and mortality. The effectiveness of *L. plantarum* or placebo was evaluated in postmenopausal women over the course of 90 days. The TC, interleukin (IL)-6 and γ -glutamyltranspeptidase (γ -GTP) levels were significantly decreased in both groups at the end of the study, whereas the LDL-C level was significantly lower in the placebo group. Glucose and homocysteine levels were significantly reduced in the *L. plantarum* group compared with the placebo group [48].

2.2.2. Synbiotics

Patients with IRS were supplemented with either synbiotic capsules containing seven strains plus fructo-oligosaccharide or placebo capsules to evaluate the insulin resistance and lipid profile. Levels of fasting blood sugar and insulin resistance were improved significantly in the synbiotic group [49].

In summary (Table 2), some probiotic strains have beneficial effects such as decreasing the cell adhesion molecule-1 levels. Moreover, in postmenopausal women, *L. plantarum* decreased TC, IL-6 γ -GTP, glucose and homocysteine levels after 90 days. Finally, synbiotic mixture improved the insulin resistance and HDL-C and reduced the TAG and TC levels in subjects with IRS.

Table 2. Summary of randomized clinical intervention trials of probiotics and synbiotics in insulin resistance syndrome.

Reference	Subjects	Strain/Dose	Time	Main Outcome
Probiotics				
Leber <i>et al.</i> , 2013 [46]	28 patients with IRS	<i>L. casei</i> Shirota, $3 \times 6.5 \times 10^9$ CFU	12 wk	No effects.
Tripolt <i>et al.</i> , 2012 [47]	30 patients with IRS	<i>L. casei</i> Shirota	12 wk	Significant reduction in the VCAM-1 level.
Barreto <i>et al.</i> , 2014 [48]	24 PM women with IRS	<i>L. plantarum</i>	12 wk	Glucose and homocysteine levels were significantly reduced.
Synbiotics				
Eslamparast <i>et al.</i> , 2014 [49]	38 subjects with IRS	<i>L. casei</i> , <i>L. rhamnosus</i> , <i>S. thermophilus</i> , <i>B. breve</i> , <i>L. acidophilus</i> , <i>B. longum</i> , <i>L. bulgaricus</i> , and FOS	28 wk	The levels of fasting blood sugar and insulin resistance improved significantly.

Abbreviations: CFU, colony-forming-unit; FOS, fructo-oligosaccharides; IRS, insulin resistance syndrome; VCAM-1, soluble vascular cell adhesion molecule-1; wk, week.

2.3. Effects of Probiotics and Synbiotics in Type 2 Diabetes

2.3.1. Probiotics

Hariri *et al.* (2015) investigated the effect of consuming probiotic soy milk containing *L. plantarum* A7 or soy milk alone. Each day, the subjects received probiotic soy milk or regular soy milk to supplement their usual diet. Probiotic soy milk significantly decreased the levels of promoter methylation in the proximal and distal *MLH1* promoter region compared with the baseline values, while the plasma concentration of 8-hydroxy-20-deoxyguanosine decreased significantly compared with the subjects receiving soy milk. Additionally, a significant increase in superoxide dismutase activity was observed in the probiotic soy milk group compared with the baseline value. However, there were no significant changes from baseline in the promoter methylation of *MSH2* within either group. Therefore, *L. plantarum* A7-inoculated soy milk can have antioxidative properties and decrease the risk of mismatched base pairs in DNA among patients with T2D [50].

L. acidophilus La-5 and *B. animalis* subsp. *lactis* BB-12 administration was evaluated on T2D patients. There was a significant difference between groups concerning mean changes in the HbA1c, TC and LDL-C levels [51]. In addition, an increase in HDL-C levels and a decrease in the LDL-C/HDL-C ratio in the intervention group [52].

Previous studies using the same strains [53,54] were carried out in T2D patients. The authors reported significantly decreased fasting blood glucose, TC, LDL-C and hemoglobin A1c levels as well as increased erythrocyte superoxide dismutase and glutathione peroxidase activity and total antioxidant status compared with the control group. They concluded that probiotic yogurt is a promising tool for diabetes management, and it may be a functional food that can exert antidiabetic and antioxidant properties [53,54].

In a double-blind, randomized study, males with T2D, impaired or normal glucose tolerance were enrolled and placed on a 4-week treatment course with either *L. acidophilus* NCFM or a placebo to investigate the effects of oral supplementation with the probiotic on insulin sensitivity and the inflammatory response [55]. After the treatment, the probiotic strain was detected in 75% of the fecal samples. Insulin sensitivity was preserved only among volunteers in the *L. acidophilus* NCFM group. Finally, baseline inflammatory markers and the systemic inflammatory response were unaffected by the *L. acidophilus* NCFM supplementation [55].

2.3.2. Synbiotics

The synbiotic supplementation was used to determine the effects on metabolic profiles, CRP and oxidative stress in T2D patients. The multispecies probiotic supplement consisted of 7 viable and freeze-dried strains and fructo-oligosaccharides. A significant increase in HOMA-IR in both groups was detected. However, the increase in the placebo group was significantly higher than that in the probiotic group. The mean changes in serum CRP were significantly lower in the experimental group. Additionally, probiotic supplementation led to a significant increase in the plasma total glutathione levels compared to the placebo [56].

A clinical trials were performed in T2D patients to examined the effects of synbiotic bread contained *L. sporogenes* and inulin. Consumption of the synbiotic bread resulted in a significant reduction in the serum insulin levels, HOMA-IR, and homeostatic model assessment- β -cell function, serum lipid profile (TAG, TC/HDL-C) and a significant increase in the serum HDL-C levels compared to the control bread [57,58].

Finally, a synbiotic shake containing *L. acidophilus*, *B. bifidum* and fructo-oligosaccharides was investigated on glycemic and cholesterol levels in elderly people with T2D. The TC, TAG, HDL-C and blood sugar levels were evaluated. The synbiotic group did not experience any reduction in total cholesterol and TAG levels, but had a significant increase in HDL-C and a significant reduction in fasting glycemia [59].

In summary (Table 3), some of the effects of probiotics in subjects with T2D included a lower fasting blood glucose level, improved insulin sensitivity and an increased antioxidant status. Some synbiotics increased the total glutathione levels, HDL-C and reduced the fasting glycemia levels and CRP. Moreover, an improved serum lipid profile was observed in patients with T2D after the consumption of synbiotics.

Table 3. Summary of randomized clinical intervention trials of probiotics and synbiotics in type 2 diabetes.

Reference	Subjects	Strain/Dose	Time	Main Outcome
Probiotics				
Hariri <i>et al.</i> , 2015 [50]	40 patients with T2D	<i>L. plantarum</i> A7	8 wk	Decreased methylation process, SOD and 8-OHDG.
Tonucci <i>et al.</i> , 2015 [51]	45 patients with T2D	<i>L. acidophilus</i> La-5 and <i>B. animalis</i> subsp. <i>lactis</i> BB-12	6 wk	Significant difference between groups concerning mean changes of HbA1c, TC and LDL-C.
Mohamadshahi <i>et al.</i> , 2014 [52]	44 patients with T2D	<i>L. acidophilus</i> La-5 and <i>B. animalis</i> subsp. <i>lactis</i> BB-12	8 wk	Increased HDL-C levels and decreased LDL-C/HDL-C ratio.
Ejtahed <i>et al.</i> , 2012 [53]	64 patients with T2D	<i>L. acidophilus</i> La5 and <i>B. lactis</i> Bb12	6 wk	Reduced fasting blood glucose and antioxidant status.
Ejtahed <i>et al.</i> , 2011 [54]	60 patients with T2D	<i>L. acidophilus</i> La5 and <i>B. lactis</i> Bb12	6 wk	TC and LDL-C improvement.
Andreasen <i>et al.</i> , 2010 [55]	45 males with T2D	<i>L. acidophilus</i> NCFM	4 wk	No effect.
Synbiotics				
Asemi <i>et al.</i> , 2013 [56]	54 patients with T2D (35–70 years)	<i>L. acidophilus</i> , <i>L. casei</i> , <i>L. rhamnosus</i> , <i>L. bulgaricus</i> , <i>B. breve</i> , <i>B. longum</i> , <i>S. thermophilus</i> , 10 ⁹ CFU, and 100 mg FOS	8 wk	Increased HOMA-IR and TGL plasma level; reduced CRP in serum.
Tajadadi-Ebrahimi <i>et al.</i> , 2014 [57]	81 patients with T2D	<i>L. sporogenes</i> , 1 × 10 ⁸ CFU and 0.07 g inulin per 1 g	8 wk	Significant reduction in serum insulin levels, HOMA-IR, and homeostatic model assessment-β-cell function.
Shakeri <i>et al.</i> , 2014 [58]	78 patients with T2D	<i>L. sporogenes</i> , 1 × 10 ⁸ CFU and 0.07 g inulin per 1 g	8 wk	Decrease in serum lipid profile (TAG, TC/HDL-C) and a significant increase in serum HDL-C levels.
Moroti <i>et al.</i> , 2012 [59]	20 patients with T2D	<i>L. acidophilus</i> 10 ⁸ CFU/mL, <i>B. bifidum</i> 10 ⁸ CFU/mL and 2 g oligofructose	2 wk	Increased HDL-C and reduced fasting glycemia.

Abbreviations: 8-OHDG; 8-hydroxy-2'-deoxyguanosine; CFU, colony-forming-unit; CRP, C-reactive protein; FOS, fructo-oligosaccharides; HDL-C, high-density lipoprotein cholesterol; HOMA-IR, homeostasis model assessment of insulin resistance; LDL-C, low-density lipoprotein cholesterol; SOD, superoxide dismutase, T2D, type 2 diabetes; TAG, triacylglycerols; TC, total cholesterol; TGL, total glutathione levels; wk, week.

2.4. Effects of Probiotics and Synbiotics in Non-Alcoholic Fatty Liver Disease

2.4.1. Probiotics

The effects of *L. bulgaris* and *S. thermophilus* were measured on different parameters of liver function and cardiovascular risk factors. This treatment revealed a decrease in alanine amino transferase (ALT), aspartate amino transferase (ASP) and γ-GTP levels as indicators of improving liver function [60].

On the other hand, in obese children with NAFLD treated with *L. rhamnosus* strain GG, presented a significant decrease in the titer of anti-peptidoglycan-polysaccharide antibodies, which are suitable as an indirect indicator of SIBO. Moreover, in this randomized clinical trial, a restoration of liver function was also observed in the probiotic group through a decrease in ALT [61].

A double-blind, randomized, controlled clinical trial was conducted using a probiotic yogurt with *L. acidophilus* La5 and *B. lactis* Bb12 for 8 weeks on patients with NAFLD. *L. acidophilus* La5 and *B. lactis* Bb12 consumption resulted in a reduction in the serum levels of ALT, ASP, TC, and LDL-C compared with the control group [62].

In another randomized study, Alisi *et al.* (2014) found a significant improvement in fatty liver severity (evaluated by ultrasound) and a significant decrease in the BMI of children with NAFLD who were treated with bifidobacteria, lactobacilli, and *S. thermophilus* strains for 4 months. These data suggest that those strains might reduce liver fat and therefore prevent the progression of NAFLD [63].

Furthermore, Alisi *et al.* (2014) [63] also evaluated glucagon-like peptide 1 (GLP-1), which is an incretin secreted by cells from the small intestine and proximal colon. GLP-1 is dependent on the presence of nutrients in the lumen of the small intestine. Its physiological effects include the activation of catabolism via an increase in insulin secretion and the suppression of glucagon secretion [63,64]. In this sense, Alisi *et al.* (2014) [63] showed that the circulating levels of the total and active forms of GLP-1 were significantly elevated in the patients after 4 months of treatment with synbiotics. Although there is not yet an adequate amount of data, in humans it has been observed that the use of probiotics improves the efficacy of lifestyle modifications in obese individuals with NAFLD, may improve conventional liver function tests, and may decrease markers of lipid peroxidation [60,61,63,65,66] and NASH [67]. This improvement in liver function could be due to a decrease in SIBO and/or dysbiosis and consequently a minor metabolic endotoxemia in the host because the restoration of normal gut microbiota might reduce intestinal permeability.

2.4.2. Synbiotics

The translocation of products derived from bacteria such as lipopolysaccharide (LPS), ethanol and SCFA leads to their arrival to the liver from the intestinal lumen. Additionally, SCFAs stimulated the synthesis and storage of hepatic triacylglycerols. This process can saturate the detoxification mechanisms of the liver, resulting in an accumulation of intrahepatic triacylglycerol (IHTG) content, thus increasing the fatty liver severity. Recently, a randomized study on the use of a synbiotic that contains five probiotics (*L. plantarum*, *L. delbrueckii* spp. *bulgaricus*, *L. acidophilus*, *L. rhamnosus*, *B. bifidum* and inulin) over 6 months in adults with NASH produced a significant decrease in IHTG [67].

On the other hand, it is well known that LPS induces pro-inflammatory cytokines, such as tumor necrosis factor (TNF)- α , which play a critical role in insulin resistance and hepatic inflammatory cell recruitment in NAFLD. In fact, the evaluation of supplementation with a synbiotic, which is a mixture of *L. casei*, *L. rhamnosus*, *S. thermophilus*, *B. breve*, *L. acidophilus*, *B. longum*, *L. bulgaricus* and fructo-oligosaccharides, in a study with 52 adults over 28 weeks, demonstrated that synbiotic supplementation inhibited NF- κ B and reduced TNF- α production [65]. These authors indicated an important limitation in their study, as they did not evaluate the gut microbiota to confirm the mechanism of action suggested. Furthermore, these results are still controversial because similar studies did not detect significant modifications in the values of TNF- α following treatment with several probiotics [60,61] and different synbiotics [63,67]. This could be explained by the large differences in several variables observed in the different studies, including the intervention period, the probiotic doses, and the bacterial strains used as well as the study subjects.

In summary (Table 4), some probiotics produced positive effects, mainly by improving liver function and decreasing SIBO. In the case of some synbiotics, the results showed a reduction in liver fat and TNF- α production to prevent NAFLD and its progression.

Table 4. Summary of randomized clinical intervention trials of probiotics and synbiotics in non-alcoholic fatty liver disease.

Reference	Subjects	Strain/Dose	Time	Main Outcome
Probiotics				
Vajro P <i>et al.</i> , 2011 [61]	20 obese children with NAFLD	<i>L. rhamnosus</i> GG, 1.2×10^9 CFU/day	8 wk	Decreased ALT and PG-PS IgAg antibodies.
Aller R <i>et al.</i> , 2011 [60]	28 adult individuals with NAFLD	<i>L. bulgaris</i> and <i>S. thermophilus</i> , 5.0×10^{11} CFU/day	12 wk	Decreased ALT and γ -GTP levels.
Nabavi <i>et al.</i> , 2014 [62]	72 patients with NAFLD	<i>L. acidophilus</i> La5 and <i>B. breve</i> subsp. <i>lactis</i> Bb12	8 wk	Reduced serum levels of ALT, ASP, TC, and LDL-C.
Alisi A <i>et al.</i> , 2014 [63]	44 obese children with NAFLD	Bifidobacteria, lactobacilli, and <i>S. thermophilus</i>	16 wk	Improved fatty liver severity, decreased BMI and increased GLP1/aGLP1.
Synbiotics				
Wong VW <i>et al.</i> , 2013 [67]	20 individuals with NASH	<i>L. plantarum</i> , <i>L. delbrueckii</i> spp. <i>bulgaricus</i> , <i>L. acidophilus</i> , <i>L. rhamnosus</i> , <i>B. bifidum</i> and inulin	26 wk	Decreased IHTG content.
Eslamparast T <i>et al.</i> , 2014 [65]	52 adult individuals with NAFLD	<i>L. casei</i> , <i>L. rhamnosus</i> , <i>S. thermophilus</i> , <i>B. breve</i> , <i>L. acidophilus</i> , <i>B. longum</i> , <i>L. bulgaricus</i> , and FOS	30 wk	Inhibition of NF- κ B and reduction of TNF- α .

Abbreviations: ALT, alanine amino transferase; ASP, aspartate amino transferase; CFU, colony-forming-unit; FOS, fructo-oligosaccharides; γ -GTP, γ -glutamyltranspeptidase; GLP1, glucagon-like peptide 1; IHTG, intrahepatic triacylglycerol; LDL-C, low-density lipoprotein cholesterol; NAFLD, non-alcoholic fatty liver disease; NF- κ B, nuclear factor κ B; TC, total cholesterol; TNF- α , tumor necrosis factor α ; wk, week.

3. Methodology

A comprehensive search of the relevant literature was performed in electronic databases, including MEDLINE (PubMed), EMBASE and Cochrane Library. MEDLINE through PubMed was searched for human clinical trial articles that were published between 2000 and 2016 in English using the MeSH terms “probiotics” and “synbiotics” combined with “obesity”, “insulin resistance”, “diabetes mellitus, type 2”, “non-alcoholic fatty liver disease” and “metabolic syndrome X”. Here, we evaluate results obtained using the following equation search: (“obesity”[All Fields] OR “insulin resistance”[All Fields] OR “metabolic syndrome X”[All Fields] OR “non-alcoholic fatty liver disease”[All Fields] OR “diabetes mellitus, Type 2”[All Fields]) AND (“probiotics”[All Fields] OR “synbiotics”[All Fields]) AND Clinical Trial[ptyp], which yielded 66 articles. Only were included the human clinical studies regarding to obesity, IRS, T2D and NAFLD participants. A total of 36 articles were selected and revised. Additionally, we searched the reference lists of the included studies for potential relevant literature.

4. Conclusions

The present review focuses on the clinical effects that support the use of probiotics as a coadjuvant strategy for the prevention and treatment of obesity, IRS, T2D and NAFLD. The current scientific evidence regarding to overweight and obese patients that received some probiotics and synbiotics shows a significant reduction in the abdominal adiposity and BMI; and also, probiotic supplementation produced an improvement in the metabolism of carbohydrates, as well as a reduction in the metabolic stress in patients with T2D and IRS. Moreover, an improved serum lipid profile was observed in patients with T2D after the consumption of synbiotics. The effects of probiotics in patients with NAFLD were primarily an improvement in the liver function and metabolic parameters. Some clinical results reported beneficial effects using both probiotic and synbiotic supplementation. However, in this review, we discussed some studies that did not show any significant effect of probiotic administration on these chronic diseases. These contradictory effects in the reported studies might be related to

inappropriate design such as diversity, the use of several strains, and the small number of individuals receiving some interventions.

Undeniably, further studies to evaluate the best dose-response effect of probiotics and synbiotics are needed, including following up with patients after the probiotic intervention to evaluate the persistence of their potential beneficial effects in obesity, IRS, T2D, and NAFLD.

Author Contributions: Maria Jose Sáez-Lara, Candido Robles-Sanchez, Francisco Javier Ruiz-Ojeda, Julio Plaza-Diaz and Angel Gil contributed to the planning of the literature search, designed the analysis and presentation of the results, created the tool for assessing the quality of the articles, and were involved in the analyses of the articles. Maria Jose Sáez-Lara, Candido Robles-Sanchez, Francisco Javier Ruiz-Ojeda, Julio Plaza-Diaz and Angel Gil wrote the draft. All authors discussed and revised all drafts and approved the final manuscript.

Conflicts of Interest: The authors declare no conflict of interest.

References

1. Backhed, F.; Ley, R.E.; Sonnenburg, J.L.; Peterson, D.A.; Gordon, J.I. Host bacterial mutualism in the human intestine. *Science* **2005**, *307*, 1915–1920. [[CrossRef](#)] [[PubMed](#)]
2. Hooper, L.V.; Midtvedt, T.; Gordon, J.I. How host-microbial interactions shape the nutrient environment of the mammalian intestine. *Annu. Rev. Nutr.* **2002**, *22*, 283–307. [[CrossRef](#)] [[PubMed](#)]
3. Plaza-Díaz, J.; Fernandez-Caballero, J.Á.; Chueca, N.; Garcia, F.; Gómez-Llorente, C.; Sáez-Lara, M.J.; Fontana, L.; Gil, A. Pyrosequencing analysis reveals changes in intestinal microbiota of healthy adults who received a daily dose of immunomodulatory probiotic strains. *Nutrients* **2015**, *7*, 3999–4015. [[CrossRef](#)] [[PubMed](#)]
4. McCoy, K.D.; Köller, Y. New developments providing mechanistic insight into the impact of the microbiota on allergic disease. *Clin. Immunol.* **2015**, *159*, 170–176. [[CrossRef](#)] [[PubMed](#)]
5. Bass, R.; Eneli, I. Severe childhood obesity: An under-recognised and growing health problem. *Postgrad. Med. J.* **2015**, *91*, 639–645. [[CrossRef](#)] [[PubMed](#)]
6. Lanthier, N.; Leclercq, I.A. Adipose tissues as endocrine target organs. *Best Pract. Res. Clin. Gastroenterol.* **2014**, *28*, 545–558. [[CrossRef](#)] [[PubMed](#)]
7. Qin, J.; Li, Y.; Cai, Z.; Li, S.; Zhu, J.; Zhang, F.; Liang, S.; Zhang, W.; Guan, Y.; Shen, D.; *et al.* A metagenome-wide association study of gut microbiota in type 2 diabetes. *Nature* **2012**, *490*, 55–60. [[CrossRef](#)] [[PubMed](#)]
8. Forslund, K.; Hildebrand, F.; Nielsen, T.; Falony, G.; Le Chatelier, E.; Sunagawa, S.; Prifti, E.; Vieira-Silva, S.; Gudmundsdottir, V.; Krogh Pedersen, H.; *et al.* Disentangling type 2 diabetes and metformin treatment signatures in the human gut microbiota. *Nature* **2015**, *528*, 262–266. [[CrossRef](#)] [[PubMed](#)]
9. Qin, J.; Li, R.; Raes, J.; Arumugam, M.; Burgdorf, K.S.; Manichanh, C.; Nielsen, T.; Pons, N.; Levenez, F.; Yamada, T.; *et al.* A human gut microbial gene catalogue established by metagenomic sequencing. *Nature* **2010**, *464*, 59–65. [[CrossRef](#)] [[PubMed](#)]
10. Karlsson, F.H.; Tremaroli, V.; Nookaew, I.; Bergström, G.; Behre, C.J.; Fagerberg, B.; Nielsen, J.; Bäckhed, F. Gut metagenome in European women with normal, impaired and diabetic glucose control. *Nature* **2013**, *498*, 99–103. [[CrossRef](#)] [[PubMed](#)]
11. Turnbaugh, P.J.; Hamady, M.; Yatsunencko, T.; Cantarel, B.L.; Duncan, A.; Ley, R.E.; Sogin, M.L.; Jones, W.J.; Roe, B.A.; Affourtit, J.P.; *et al.* A core gut microbiome in obese and lean twins. *Nature* **2009**, *457*, 480–484. [[CrossRef](#)] [[PubMed](#)]
12. Sanchez, M.; Darimont, C.; Drapeau, V.; Emady-Azar, S.; Lepage, M.; Rezzonico, E.; Ngom-Bru, C.; Berger, B.; Philippe, L.; Ammon-Zuffrey, C.; *et al.* Effect of *Lactobacillus rhamnosus* CGMCC1.3724 supplementation on weight loss and maintenance in obese men and women. *Br. J. Nutr.* **2014**, *111*, 1507–1519. [[CrossRef](#)] [[PubMed](#)]
13. Hong, H.R.; Ha, C.D.; Kong, J.Y.; Lee, S.H.; Song, M.G.; Kang, H.S. Roles of physical activity and cardiorespiratory fitness on sex difference in insulin resistance in late elementary years. *J. Exerc. Nutr. Biochem.* **2014**, *18*, 361–369. [[CrossRef](#)] [[PubMed](#)]
14. Juhan-Vague, I.; Morange, P.E.; Alessi, M.C. The insulin resistance syndrome: Implications for thrombosis and cardiovascular disease. *Pathophysiol. Haemost. Thromb.* **2002**, *32*, 269–273. [[CrossRef](#)] [[PubMed](#)]

15. Jun-Ling, H.; Hui-Ling, L. Intestinal microbiota and type 2 diabetes: From mechanism insights to therapeutic perspective. *World J. Gastroenterol.* **2014**, *20*, 17737–17745.
16. Larsen, N.; Vogensen, F.K.; van den Berg, F.W.J.; Nielsen, D.S.; Andreasen, A.S.; Pedersen, B.K.; Al-Soud, W.A.; Sørensen, S.J.; Hansen, L.H.; Jakobsen, M. Gut microbiota in human adults with type 2 diabetes differs from non-diabetic adults. *PLoS ONE* **2010**, *5*, e9085. [CrossRef] [PubMed]
17. Hulston, C.J.; Churnside, A.A.; Venables, M.C. Probiotic supplementation prevents high-fat, overfeeding-induced insulin resistance in human subjects. *Br. J. Nutr.* **2015**, *113*, 596–602. [CrossRef] [PubMed]
18. Ley, R.E.; Bäckhed, F.; Turnbaugh, P.; Lozupone, C.A.; Knight, R.D.; Gordon, J.I. Obesity alters gut microbial ecology. *Proc. Natl. Acad. Sci. USA* **2005**, *102*, 11070–11075. [CrossRef] [PubMed]
19. World Health Organization and Food & Agriculture Organization. *Guidelines for the Evaluation of Probiotics in Food*; Report of a Joint FAO/WHO Working Group on Drafting Guidelines for the Evaluation of Probiotics in Food; FAO/WHO: London, ON, Canada, 2002; Available online: <ftp://ftp.fao.org/es/esn/food/wgreport2.pdf> (accessed on 2 June 2016).
20. Plaza-Diaz, J.; Gomez-Llorente, C.; Abadia-Molina, F.; Saez-Lara, M.J.; Campaña-Martin, L.; Muñoz-Quezada, S.; Romero, F.; Gil, A.; Fontana, L. Effects of *Lactobacillus paracasei* CNCM I-4034, *Bifidobacterium breve* CNCM I-4035 and *Lactobacillus rhamnosus* CNCM I-4036 on hepatic steatosis in Zucker rats. *PLoS ONE* **2014**, *9*, e98401.
21. World Health Organization, Food and Agricultural Organization of the United Nations. *Health and Nutritional Properties of Probiotics in Food including Powder Milk with Live Lactic Acid Bacteria*; FAO Nutrition Paper; FAO: Cordoba, Argentina, 2001; Volume 85, pp. 1–33.
22. Hill, C.; Guarner, F.; Reid, G.; Gibson, G.R.; Merenstein, D.J.; Pot, B.; Morelli, L.; Canani, R.B.; Flint, H.J.; Salminen, S.; *et al.* Expert consensus document. The International Scientific Association for Probiotics and Prebiotics consensus statement on the scope and appropriate use of the term probiotic. *Nat. Rev. Gastroenterol. Hepatol.* **2014**, *11*, 506–514. [CrossRef] [PubMed]
23. Kruis, W.; Fric, P.; Pokrotnieks, J.; Lukás, M.; Fixa, B.; Kascák, M.; Kamm, M.A.; Weismueller, J.; Beglinger, C.; Stolte, M.; *et al.* Maintaining remission of ulcerative colitis with the probiotic *Escherichia coli* Nissle 1917 is as effective as with standard mesalazine. *Gut* **2004**, *53*, 1617–1623. [CrossRef] [PubMed]
24. Bermudez-Brito, M.; Plaza-Díaz, J.; Muñoz-Quezada, S.; Gómez-Llorente, C.; Gil, A. Probiotic mechanisms of action. *Ann. Nutr. Metab.* **2012**, *61*, 160–174. [CrossRef] [PubMed]
25. Fontana, L.; Bermudez-Brito, M.; Plaza-Diaz, J.; Muñoz-Quezada, S.; Gil, A. Sources, isolation, characterisation and evaluation of probiotics. *Br. J. Nutr.* **2013**, *2*, S35–S50. [CrossRef] [PubMed]
26. Pineiro, M.; Asp, N.G.; Reid, G.; Macfarlane, S.; Morelli, L.; Brunser, O.; Tuohy, K. FAO Technical meeting on prebiotics. *J. Clin. Gastroenterol.* **2008**, *42*, S156–S159. [CrossRef] [PubMed]
27. Upadhyay, N.; Moudgal, V. Probiotics: A Review. *J. Clin. Outcomes Manag.* **2012**, *19*, 76–84.
28. Kim, S.W.; Suda, W.; Kim, S.; Oshima, K.; Fukuda, S.; Ohno, H.; Morita, H.; Hattori, M. Robustness of gut microbiota of healthy adults in response to probiotic intervention revealed by high-throughput pyrosequencing. *DNA Res.* **2013**, *20*, 241–253. [CrossRef] [PubMed]
29. Ferrario, C.; Taverniti, V.; Milani, C.; Fiore, W.; Laureati, M.; de Noni, I.; Stuknyte, M.; Chouaia, B.; Riso, P.; Guglielmetti, S. Modulation of fecal Clostridiales bacteria and butyrate by probiotic intervention with *Lactobacillus paracasei* DG varies among healthy adults. *J. Nutr.* **2014**, *144*, 1787–1796.
30. Yoo, J.Y.; Kim, S.S. Probiotics and prebiotics: Present status and future perspectives on metabolic disorders. *Nutrients* **2016**, *8*, 173. [CrossRef] [PubMed]
31. Larsen, N.; Vogensen, F.K.; Gøbel, R.J.; Michaelsen, K.F.; Forssten, S.D.; Lahtinen, S.J.; Jakobsen, M. Effect of *Lactobacillus salivarius* Ls-33 on fecal microbiota in obese adolescents. *Clin. Nutr.* **2013**, *32*, 935–940. [CrossRef] [PubMed]
32. Gøbel, R.J.; Larsen, N.; Jakobsen, M.; Mølgaard, C.; Michaelsen, K.F. Probiotics to adolescents with obesity: Effects on Inflammation and metabolic syndrome. *J. Pediatr. Gastroenterol. Nutr.* **2012**, *55*, 673–678. [CrossRef] [PubMed]
33. Kadooka, Y.; Sato, M.; Imaizumi, K.; Ogawa, A.; Ikuyama, K.; Akai, Y.; Okano, M.; Kagoshima, M.; Tsuchida, T. Regulation of abdominal adiposity by probiotics (*Lactobacillus gasseri* SBT2055) in adults with obese tendencies in a randomized controlled trial. *Eur. J. Clin. Nutr.* **2010**, *64*, 636–643. [CrossRef] [PubMed]

34. Kadooka, Y.; Sato, M.; Ogawa, A.; Miyoshi, M.; Uenishi, H.; Ogawa, H. Effect of *Lactobacillus gasseri* SBT2055 in fermented milk on abdominal adiposity in adults in a randomised controlled trial. *Br. J. Nutr.* **2013**, *110*, 1696–1703. [CrossRef] [PubMed]
35. Sharafedinov, K.K.; Plotnikova, O.A.; Alexeeva, R.I.; Sentsova, T.B.; Songisepp, E.; Stsepetova, J.; Smidt, I.; Mikelsaar, M. Hypocaloric diet supplemented with probiotic cheese improves body mass index and blood pressure indices of obese hypertensive patients—A randomized double-blind placebo-controlled pilot study. *Nutr. J.* **2013**, *12*, 138. [CrossRef] [PubMed]
36. Zarrati, M.; Salehi, E.; Nourijelyani, K.; Mofid, V.; Zadeh, M.J.; Najafi, F.; Ghaflati, Z.; Bidad, K.; Chamari, M.; Karimi, M.; *et al.* Effects of probiotic yogurt on fat distribution and gene expression of proinflammatory factors in peripheral blood mononuclear cells in overweight and obese people with or without weight-loss diet. *J. Am. Coll. Nutr.* **2014**, *33*, 417–425. [CrossRef] [PubMed]
37. Zarrati, M.; Shidfar, F.; Nourijelyani, K.; Mofid, V.; Hossein zadeh-Attar, M.J.; Bidad, K.; Najafi, F.; Gheflati, Z.; Chamari, M.; Salehi, E. *Lactobacillus acidophilus* La5, *Bifidobacterium* BB12, and *Lactobacillus casei* DN001 modulate gene expression of subset specific transcription factors and cytokines in peripheral blood mononuclear cells of obese and overweight people. *Biofactors* **2013**, *39*, 633–643. [CrossRef] [PubMed]
38. Zarrati, M.; Salehi, E.; Mofid, V.; Hossein Zadeh-Attar, M.J.; Nourijelyani, K.; Bidad, K.; Shidfar, F. Relationship between probiotic consumption and IL-10 and IL-17 secreted by PBMCs in overweight and obese people. *Iran. J. Allergy Asthma Immunol.* **2013**, *12*, 404–406. [PubMed]
39. Agerholm-Larsen, L.; Raben, A.; Haulrik, N.; Hansen, A.S.; Manders, M.; Astrup, A. Effect of 8 week intake of probiotic milk products on risk factors for cardiovascular diseases. *Eur. J. Clin. Nutr.* **2000**, *54*, 288–297. [CrossRef] [PubMed]
40. Rajkumar, H.; Mahmood, N.; Kumar, M.; Varikuti, S.R.; Challa, H.R.; Myakala, S.P. Effect of probiotic (VSL#3) and Ω -3 on lipid profile, insulin sensitivity, inflammatory markers, and gut colonization in overweight adults: A randomized, controlled trial. *Mediat. Inflamm.* **2014**, *2014*, 348959. [CrossRef]
41. Brahe, L.K.; Le Chatelier, E.; Prifti, E.; Pons, N.; Kennedy, S.; Blædel, T.; Håkansson, J.; Dalsgaard, T.K.; Hansen, T.; Pedersen, O. Dietary modulation of the gut microbiota—A randomised controlled trial in obese postmenopausal women. *Br. J. Nutr.* **2015**, *114*, 406–417. [CrossRef] [PubMed]
42. Ivey, K.L.; Hodgson, J.M.; Kerr, D.A.; Lewis, J.R.; Thompson, P.L.; Prince, R.L. The effects of probiotic bacteria on glycaemic control in overweight men and women: A randomised controlled trial. *Eur. J. Clin. Nutr.* **2014**, *68*, 447–452. [CrossRef] [PubMed]
43. Ivey, K.L.; Hodgson, J.M.; Kerr, D.A.; Thompson, P.L.; Stojceski, B.; Prince, R.L. The effect of yoghurt and its probiotics on blood pressure and serum lipid profile; a randomised controlled trial. *Nutr. Metab. Cardiovasc. Dis.* **2015**, *25*, 46–51. [CrossRef] [PubMed]
44. Safavi, M.; Farajian, S.; Kelishadi, R.; Mirlohi, M.; Hashemipour, M. The effects of synbiotic supplementation on some cardio metabolic risk factors in overweight and obese children: A randomized triple-masked controlled trial. *Int. J. Food Sci. Nutr.* **2013**, *64*, 687–693. [CrossRef] [PubMed]
45. Ipar, N.; Aydogdu, S.D.; Yildirim, G.K.; Inal, M.; Gies, I.; Vandenplas, Y.; Dinleyici, E.C. Effects of synbiotic on anthropometry, lipid profile and oxidative stress in obese children. *Benef. Microbes* **2015**, *6*, 775–781. [CrossRef] [PubMed]
46. Leber, B.; Tripolt, N.J.; Blattl, D.; Eder, M.; Wascher, T.C.; Pieber, T.R.; Stauber, R.; Sourij, H.; Oettl, K.; Stadlbauer, V. The influence of probiotic supplementation on gut permeability in patients with metabolic syndrome: An open label, randomized pilot study. *Eur. J. Clin. Nutr.* **2012**, *66*, 1110–1115. [CrossRef] [PubMed]
47. Tripolt, N.J.; Leber, B.; Blattl, D.; Eder, M.; Wonisch, W.; Scharnagl, H.; Stojakovic, T.; Obermayer-Pietsch, B.; Wascher, T.C.; Pieber, T.R.; *et al.* Effect of supplementation with *Lactobacillus casei* Shirota on insulin sensitivity, β -cell function, and markers of endothelial function and inflammation in subjects with metabolic syndrome—A pilot study. *J. Dairy Sci.* **2013**, *96*, 89–95. [CrossRef] [PubMed]
48. Barreto, F.M.; Colado Simão, A.N.; Morimoto, H.K.; Batisti Lozovoy, M.A.; Dichi, I.; Helena da Silva Miglioranza, L. Beneficial effects of *Lactobacillus plantarum* on glycemia and homocysteine levels in postmenopausal women with metabolic syndrome. *Nutrition* **2014**, *30*, 939–942. [CrossRef] [PubMed]

49. Eslamparast, T.; Zamani, F.; Hekmatdoost, A.; Sharafkhah, M.; Eghtesad, S.; Malekzadeh, R.; Poustchi, H. Effects of synbiotic supplementation on insulin resistance in subjects with the metabolic syndrome: A randomised, double-blind, placebo-controlled pilot study. *Br. J. Nutr.* **2014**, *112*, 438–445. [[CrossRef](#)] [[PubMed](#)]
50. Hariri, M.; Salehi, R.; Feizi, A.; Mirlohi, M.; Ghasvand, R.; Habibi, N. A randomized, double-blind, placebo-controlled, clinical trial on probiotic soy milk and soy milk: Effects on epigenetics and oxidative stress in patients with type II diabetes. *Genes Nutr.* **2015**, *10*, 52. [[CrossRef](#)] [[PubMed](#)]
51. Tonucci, L.B.; Olbrich Dos Santos, K.M.; Licursi de Oliveira, L.; Rocha Ribeiro, S.M.; Duarte Martino, H.S. Clinical application of probiotics in type 2 diabetes mellitus: A randomized, double-blind, placebo-controlled study. *Clin. Nutr.* **2015**. [[CrossRef](#)] [[PubMed](#)]
52. Mohamadshahi, M.; Veissi, M.; Haidari, F.; Javid, A.Z.; Mohammadi, F.; Shirbeigi, E. Effects of probiotic yogurt consumption on lipid profile in type 2 diabetic patients: A randomized controlled clinical trial. *J. Res. Med. Sci.* **2014**, *19*, 531–536. [[PubMed](#)]
53. Ejtahed, H.S.; Mohtadi-Nia, J.; Homayouni-Rad, A.; Niafar, M.; Asghari-Jafarabadi, M.; Mofid, V. Probiotic yogurt improves antioxidant status in type 2 diabetic patients. *Nutrition* **2012**, *28*, 539–543. [[CrossRef](#)] [[PubMed](#)]
54. Ejtahed, H.S.; Mohtadi-Nia, J.; Homayouni-Rad, A.; Niafar, M.; Asghari-Jafarabadi, M.; Mofid, V.; Akbarian-Moghari, A. Effect of probiotic yogurt containing *Lactobacillus acidophilus* and *Bifidobacterium lactis* on lipid profile in individuals with type 2 diabetes mellitus. *J. Dairy Sci.* **2011**, *94*, 3288–3294. [[CrossRef](#)] [[PubMed](#)]
55. Andreassen, A.S.; Larsen, N.; Pedersen-Skovsgaard, T.; Berg, R.M.; Møller, K.; Svendsen, K.D.; Jakobsen, M.; Pedersen, B.K. Effects of *Lactobacillus acidophilus* NCFM on insulin sensitivity and the systemic inflammatory response in human subjects. *Br. J. Nutr.* **2010**, *104*, 1831–1838. [[CrossRef](#)] [[PubMed](#)]
56. Asemi, Z.; Zohreh, Z.; Shakeri, H.; Sima-sadat Sabihi, S.S.; Esmailzadeh, A. Effect of multispecies probiotic supplements on metabolic profiles, hs-CRP, and oxidative stress in patients with type 2 diabetes. *Ann. Nutr. Metab.* **2013**, *63*, 1–9. [[CrossRef](#)] [[PubMed](#)]
57. Tajadadi-Ebrahimi, M.; Bahmani, F.; Shakeri, H.; Hadaegh, H.; Hijjajafari, M.; Abedi, F.; Asemi, Z. Effects of daily consumption of synbiotic bread on insulin metabolism and serum high-sensitivity C-reactive protein among diabetic patients: A double-blind, randomized, controlled clinical trial. *Ann. Nutr. Metab.* **2014**, *65*, 34–41. [[CrossRef](#)] [[PubMed](#)]
58. Shakeri, H.; Hadaegh, H.; Abedi, F.; Tajadadi-Ebrahimi, M.; Mazrooi, N.; Ghandi, Y.; Asemi, Z. Consumption of synbiotic bread decreases triacylglycerol and VLDL levels while increasing HDL levels in serum from patients with type-2 diabetes. *Lipids* **2014**, *49*, 695–701. [[CrossRef](#)] [[PubMed](#)]
59. Moroti, C.; Souza Magri, L.F.; Rezende-Costa, M.; Cavallini, D.; Sivieri, K. Effect of the consumption of a new symbiotic shake on glycemia and cholesterol levels in elderly people with type 2 diabetes mellitus. *Lipids Health Dis.* **2012**, *11*, 29. [[CrossRef](#)] [[PubMed](#)]
60. Aller, R.; De Luis, D.A.; Izaola, O.; Conde, R.; Gonzalez Sagrado, M.; Primo, D.; de la Fuente, B.; Gonzalez, J. Effect of a probiotic on liver aminotransferases in nonalcoholic fatty liver disease patients: A double blind randomized clinical trial. *Eur. Rev. Med. Pharmacol. Sci.* **2011**, *15*, 1090–1095. [[PubMed](#)]
61. Vajro, P.; Mandato, C.; Licenziati, M.R.; Franzese, A.; Vitale, D.F.; Lenta, S.; Caropreso, M.; Vallone, G.; Meli, R. Effects of *Lactobacillus rhamnosus* strain GG in pediatric obesity-related liver disease. *J. Gastroenterol. Nutr.* **2011**, *52*, 740–743. [[CrossRef](#)] [[PubMed](#)]
62. Nabavi, S.; Rafraf, M.; Somi, M.H.; Homayouni-Rad, A.; Asghari-Jafarabadi, M. Effects of probiotic yogurt consumption on metabolic factors in individuals with nonalcoholic fatty liver disease. *J. Dairy Sci.* **2014**, *97*, 7386–7393. [[CrossRef](#)] [[PubMed](#)]
63. Alisi, A.; Bedogni, G.; Baviera, G.; Giorgio, V.; Porro, E.; Paris, C.; Giammaria, P.; Reali, L.; Anania, F.; Nobili, V. Randomised clinical trial: The beneficial effects of VLS#3 in obese children with non-alcoholic steatohepatitis. *Aliment. Pharmacol. Ther.* **2014**, *39*, 1276–1285. [[CrossRef](#)] [[PubMed](#)]
64. Sandoval, D.A.; D'Alessio, D.A. Physiology of proglucagon peptides: Role of glucagon and GLP-1 in health and disease. *Physiol. Rev.* **2015**, *95*, 513–548. [[CrossRef](#)] [[PubMed](#)]

65. Eslamparast, T.; Poustchi, H.; Zamani, F.; Sharafkhah, M.; Malekzadeh, R.; Hetmatdoost, A. Synbiotic supplementation in nonalcoholic fatty liver disease: A randomized, double-blind, placebo-controlled pilot study. *Am. J. Clin. Nutr.* **2014**, *99*, 535–542. [[CrossRef](#)] [[PubMed](#)]
66. Lirussi, F.; Mastropasqua, E.; Orando, S.; Orlando, R. Probiotics for non-alcoholic fatty liver disease and/or steatohepatitis. *Cochrane Database Syst. Rev.* **2007**, *1*, CD005165. [[CrossRef](#)] [[PubMed](#)]
67. Wong, V.W.; Won, G.L.; Chim, A.M.; Chu, W.C.; Yeung, D.K.; Li, K.C.; Chan, L. Treatment of nonalcoholic steatohepatitis with probiotics. A proof-of-concept study. *Ann. Hepatol.* **2013**, *12*, 256–262. [[PubMed](#)]



© 2016 by the authors; licensee MDPI, Basel, Switzerland. This article is an open access article distributed under the terms and conditions of the Creative Commons Attribution (CC-BY) license (<http://creativecommons.org/licenses/by/4.0/>).

Curriculum vitae

Curriculum vitae

Francisco Javier Ruiz Ojeda

Academic formation

-Master's degree in Human Nutrition at the University of Granada, (2011 – 2012).

-Bachelor's degree in Science and Food Technology, University of Granada, (2009 – 2011).

-Diploma of Human Nutrition and Dietetics, University of Granada, (2006 – 2009).

Professional experience

-Ph D student at the research group CTS-461 “Biochemistry of nutrition. Therapeutical implications”, Department of Biochemistry and Molecular Biology II, Faculty of Pharmacy; Institute of Nutrition and Food Technology “José Mataix”, Center of Biomedical Research, University of Granada, Granada, Spain. Supervisors: Ángel Gil and Concepción Aguilera, (2012 - present).

-Ph D student visiting at the School of Life Sciences in Medical School, The University of Nottingham. Nottingham, United Kingdom.

-Ph D student visiting at the Li Ka Shing Centre for Health Research Innovation, University of Alberta. Edmonton, Alberta, Canada. Supervisor: Spencer Proctor, (10 May 2016 – 9 August 2016).

Participation in Research Projects

-Biological implications of insulin resistance signalling, inflammation and extracellular matrix genes in culture of human adipose tissue-derived stem cells (Junta de Andalucía, P10-CTS-6770).

-Guía para la sustanciación de declaraciones de salud de alimentos: funciones inmunitaria, cognitiva y síndrome metabólico (Puleva Biosearch, 3600).

-Role of Melatonin on metabolic síndrome prevention in Zucker obese and diabetic fatty rats (University of Granada, GREIB

Scientific Publications

1. **Ruiz-Ojeda FJ**, Rupérez AI, Gomez-Llorente C, Gil A, Aguilera CM. Cell Models and Their Application for Studying Adipogenic Differentiation in Relation to Obesity: A Review. *Int. J. Mol. Sci.* 2016; 17(7), 1040.
2. **Ruiz-Ojeda FJ**, Aguilera CM, Rupérez AI, Gil Á, Gomez-Llorente C. An analogue of atrial natriuretic peptide (C-ANP₄₋₂₃) modulates glucose metabolism in human differentiated adipocytes. *Mol Cell Endocrinol.* 2016; 431:101-8.
3. **Ruiz-Ojeda FJ**, Gomez-Llorente C, Aguilera CM, Gil A, Rupérez AI. Impact of 3-Amino-1,2,4-Triazole (3-AT)-Derived Increase in Hydrogen Peroxide Levels on Inflammation and Metabolism in Human Differentiated Adipocytes. *PLoS One.* 2016; 11(3):e0152550.
4. Sáez-Lara MJ, Robles-Sanchez C, **Ruiz-Ojeda FJ**, Plaza-Diaz J, Gil A. Effects of Probiotics and Synbiotics on Obesity, Insulin Resistance Syndrome, Type 2 Diabetes and Non-Alcoholic Fatty Liver Disease: A Review of Human Clinical Trials. *Int J Mol Sci.* 2016; 17(6), 928.
5. Roman S, Agil A, Peran M, Alvaro-Galue E, **Ruiz-Ojeda FJ**, Fernández-Vázquez G, Marchal JA. Brown adipose tissue and novel therapeutic approaches to treat metabolic disorders. *Transl Rev.* 2014; 165(4):464-79.
6. Navarro-Alarcón M, **Ruiz-Ojeda FJ**, Blanca-Herrera RM, A-Serrano MM, Acuña-Castroviejo D, Fernández-Vázquez G, Agil A. Melatonin and metabolic regulation: a review. *Food Funct.* 2014; 5(11):2806-32.
7. Navarro-Alarcon M, **Ruiz-Ojeda FJ**, Blanca-Herrera RM, Kaki A, Adem A, Agil A. Melatonin administration in diabetes: regulation of plasma Cr, V and Mg in young male Zucker diabetic Fatty rats. *Food Funct.* 2014; 5(3):512-6.
8. Navarro-Alarcon M, **Ruiz-Ojeda FJ**, Blanca-Herrera RM, Agil A. Antioxidant activity of melatonin in diabetes in relation to the regulation

and levels of plasma Cu, Zn, Fe, Mn, and Se in Zucker diabetic fatty rats. *Nutrition*. 2013; 29(5):785-9.

Congress communications

Internationals

1. **Francisco J. Ruiz-Ojeda**, Concepción Aguilera-García, Carolina Gómez-Llorente, Ángel Gil y Azahara I. Rupérez-Cano. Catalase: metabolic effects in adipocytes. SLAN (*Sociedad Latinoamericana de Nutrición*). Oral communication, Punta Cana, República Dominicana. 8-12 November 2015.
2. **Francisco J. Ruiz-Ojeda**, Concepción Aguilera-García, Azahara I. Rupérez-Cano, Ángel Gil y Carolina Gómez-Llorente. C-ANP₄₋₂₃ modulates gene expression associated with signaling pathway insulin and inflammation in human adipocytes. FENS (Federation of European Nutrition Societies). Poster communication, Berlin, Germany. 20-23 October 2015.
3. Vicente Mustieles; **Francisco J. Ruiz-Ojeda**; Jose Manuel Molina Molina; Jose Maria Saenz; Juan Pedro Arrebola Moreno; Nicolas Olea Serrano; Mariana Fatima Fernandez. Bisphenol-A and other bisphenol-A congeners promotes adipogenic differentiation of human adipose stromal/stem cells. 2nd Paris Workshop on Endocrine Disruptors Effects on Wildlife and Human Health. Poster communication, Paris, France. 21-22 January 2016.

Nationals

4. Jesus R Huertas, Julio Plaza-Diaz, Jeronimo Aragon-Vela, Daniel Camiletti-Moiron, **Francisco J. Ruiz Ojeda**, Cándido Robles-Sánchez, Alberto Ruiz-Ariza, Antonio Martínez-Amat, Marina Hebberecht, Carlos Melero-Romero, Luis M Salmeron, Rafael A Casuso. Sprint interval training induces a weak oxidative-related transcriptional response within the *triceps brachii* of trained swimmers. *J Physiol Biochem* (2016) 72 (Suppl 1): S1-S111.

5. **Francisco J. Ruiz-Ojeda**, Concepción Aguilera-García, Carolina Gómez-Llorente, Ángel Gil y Azahara I. Rupérez-Cano. Efectos metabólicos de la catalase en adipocitos diferenciados. *Sociedad española de endocrinología pediátrica (SEEP)*. Oral communication. Córdoba, Spain. 27-29 April 2016.
6. **Francisco J. Ruiz-Ojeda**, Azahara I. Rupérez-Cano, Ángel Gil, Concepción Aguilera-García y Carolina Gómez-Llorente. La activación del receptor 3 de los péptidos natriuréticos aumenta los niveles de adenosín monofosfato ciclado (AMPc) en adipocitos humanos. *Federación Española de Sociedades de Nutrición, Alimentación y Dietética (FESNAD)*. Poster communication. Sevilla, Spain. 5-7 March 2015.
7. **Francisco J. Ruiz-Ojeda**, Carolina Gómez-Llorente, Azahara I. Rupérez-Cano, Ángel Gil y Concepción Aguilera-García. Estudio de la expresión del gen Tenomodulina en adipocitos diferenciados de células mesenquimales derivadas de tejido adiposo humano. *Sociedad Española de Nutrición (SEÑ)*. Poster communication. Pamplona, Spain. 3-5 July 2014.

Fundings, Scholarships and Awards

-**Ph D stipend** from the *Programa de Formación de Profesorado Universitario* (FPU), Ministry of Education, Government of Spain (B.O.E. 10/5/12); (2013 – present) at the University of Granada, Granada, Spain.

-**Sort stay stipend for Ph D students** for visiting a foreign Institution from the FPU program, Ministry of Education, Government of Spain (B.O.E. 21/11/2013). From 10 September 2014 to 10 December 2014, at The University of Nottingham, Nottingham, United Kingdom.

-**Sort stay stipend for Ph D students** for visiting a foreign Institution from the FPU program, Ministry of Education, Government of Spain (B.O.E. 05/08/2015). From 10 May 2016 to 9 August 2016 at The University of Alberta, Edmonton, Canada.

-**Full time contract** researcher at the group CTS-461, “Biochemistry of Nutrition: Therapeutic Implications” at the University of Granada, Granada,

Spain. Funded by the Network Red Samid, RETIC RD08/0072/0028. Supervisors: Ángel Gil and Concepción Aguilera.

-**Award to the best communication** at the FESNAD (*Federación Española de Sociedades de Nutrición, Alimentación y Dietética*) congress, Sevilla, Spain. 5-7 March 2015. **Francisco J. Ruiz-Ojeda**, Azahara I. Rupérez-Cano, Ángel Gil, Concepción Aguilera-García y Carolina Gómez-Llorente. La activación del receptor 3 de los péptidos natriuréticos aumenta los niveles de adenosín monofosfato ciclado (AMPc) en adipocitos humanos.

-**Award to attend to the SLAN** (*Sociedad Latinoamericana de Nutrición*) congress in Punta Cana, República Dominicana, 8 – 12 November 2015. Award was addressed for young researchers from FINUT (*Fundación Iberoamericana de Nutrición*).

-**Colaboration stipend** at the Department of Nutrition and Food Sciences, School of Pharmacy, University of Granada, Granada, Spain (2010 - 2011).

-**Scholarship student** at the Vicerrectorado de Estudiantes, at the University of Granada, Granada, Spain (2008-2009).

Teaching experience

-Biochemistry course in the Human Nutrition and Dietetics degree, Department of Biochemistry and Molecular Biology II, School of Pharmacy, University of Granada, Granada, Spain (2014 – 2016).

Courses and seminars

-Attendance to the “II FINUT Summer Course, Healthy Lifestyles” (*Fundación Iberoamericana de Nutrición*), Granada, Spain, 15 – 17 July 2015.

-Attendance to the Symposium “VII Seminario sobre Alimentación y estilos de vida saludable” organized by Alimentomica, Vitoria-Gasteiz, Spain, 1 – 3 July 2015.

-Attendance to the “I FINUT Summer Course, Energy Balance and Healthy Lifestyles” (*Fundación Iberoamericana de Nutrición*), Granada, Spain, 9 – 11 July 2014.

-Attendance to a summer research camp “IX Obesity Summer Boot Camp” (*in Recognition for Completion of the Canadian Obesity Network*) July 19-27, 2014 Kananaskis Country, Alberta, Canada.

-Attendance to II Meeting for young researchers at the University of Navarra, Pamplona, Spain. 2 July 2014.

-Attendance to III Meeting for young researchers at the University of Seville, Seville, Spain. 4 March 2015.

-Anthropometrist Accreditation for Level I of the ISAK (International Society for the Advancement of Kinanthropometry); School of Pharmacy, University of Granada, Granada, Spain. 4 – 7 March 2012.

-Attendance to a Workshop “Desafíos de la Nutrigenómica en la Obesidad”; at the School of Pharmacy, University of Granada, Granada, Spain. March 2011.

-Attendance to “Vth Conference of the EFAD/DIETS Thematic Network” (EDAF) in Barcelona, Spain. October 2011.

-President of association for young students CYTAGRA at the School of Pharmacy, University of Granada, Granada, Spain (2009 – 2012).

-Nutritional Education Workshops as nutritionist in the Granada Diabetic Association (AGRADI), 2011 – 2012.

